

**DESIGN OF VARIABLE STRUCTURE AUTOMATIC GENERATION  
CONTROLLERS FOR ELECTRICAL POWER SYSTEMS**

BY

**FRANK N. OKAFOR**  
B.Sc., M. Phil (Electrical Engr.) (Lagos)

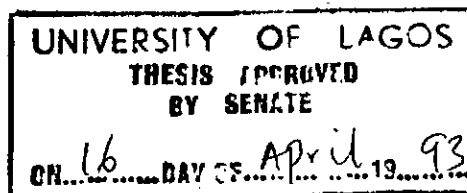
A Thesis submitted to the School of Postgraduate Studies  
University of Lagos for the award of the degree of  
Doctor of Philosophy (Ph. D)  
in Electrical Engineering

**SUPERVISORS**

**Dr. C. O. Awoşope**  
Electrical Engineering Department  
University of Lagos  
Lagos, Nigeria

**Dr. James Katende**  
Electrical Engineering Department  
Bayero University  
Kano, Nigeria

NOVEMBER 1992



SCHOOL OF POSTGRADUATE STUDIES  
UNIVERSITY OF LAGOS

CERTIFICATION

THIS IS TO CERTIFY THAT THE THESIS

DESIGN OF VARIABLE STRUCTURE AUTOMATIC  
GENERATION CONTROLLERS FOR ELECTRICAL  
POWER SYSTEMS.

SUBMITTED TO THE SCHOOL OF POSTGRADUATE STUDIES  
UNIVERSITY OF LAGOS FOR THE AWARD OF THE DEGREE OF  
DOCTOR OF PHILOSOPHY (Ph.D)

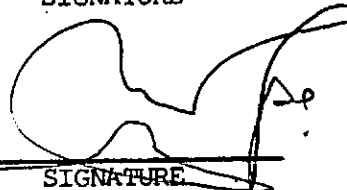
IS A RECORD OF ORIGINAL RESEARCH CARRIED OUT BY  
MR. FRANK NWOYE OKAFOR  
IN THE DEPARTMENT OF  
ELECTRICAL ENGINEERING

F. N. OKAFOR  
AUTHOR'S NAME

  
SIGNATURE

11/11/92  
DATE

C. O. A. AWOSQPE  
SUPERVISOR'S NAME

  
SIGNATURE

11/11/1992  
DATE

DR. C. C. OKORO  
INTERNAL EXAMINER'S  
NAME

  
SIGNATURE

11-11-1992  
DATE

DR J. KATENDE  
INTERNAL EXAMINER'S  
NAME

  
SIGNATURE

11/11/92  
DATE

PROF. A. J. ALOS  
EXTERNAL EXAMINER'S  
NAME

  
SIGNATURE

11-11-92  
DATE

To my entire family

ACKNOWLEDGEMENTS

It is with great pleasure that I acknowledge the guidance and encouragement given to me by my supervisors Drs. C.O.A. Awosope and J. Katende. May Almighty God reward them accordingly. My special thanks also go to Drs. O. Adegbenro, C.C. Okoro, O. Ijaola, T. A. Oduyemi, T.O.Akinbulire and Prof. R.I. Salawu, all of the Department of Electrical Engineering Unilag, for their unflinching moral support. The contribution of the non-academic staff of the Electrical Engineering Department notably, Messrs M.A.Ojo, E.A.Adeleke, A. Mustapha, N.Onike and Mrs. Amuzie to the success of this work is hereby acknowledged. Special recognition must go to Pastor Mark Anya who painstakingly typed this work.

Of course, the support of my wife Obinna and son Chibuzor could not have come at a better time. Special thanks also go to Mr. & Mrs. M.I. Uchegbu for their moral and financial support. I recognise specially the support of my mother, Mrs. C. Okafor, parents in-law, Mr & Mrs. S.C.Onuegbu as well as my brothers and sisters notably, Mr.& Mrs. B.Okafor, Chris, Tessy, Joe, Christy, Winifred, Anny and Sam. I wish also to acknowledge the concern of such families as Mr.& Mrs. Sam Egbuchunam, Chief & Mrs. P.C. Nwilo, Mr.& Mrs. Pat Uwakwe, Engr.& Mrs. S. Somolu; my neighbours Carol Nwankwo and Chimezie Okpara, Mr. Dan. Awduche, K. Achife, Chi. Uzor and others. Members of Odida Improvement Youth League, Lagos Branch, deserve special mention for their understanding and support.

## ABSTRACT

This thesis considers the automatic generation control (AGC) problem in electrical power systems. The aim is to closely regulate the mismatch between real power generation and consumption so as to maintain the frequency and/or tie-line power interchange within the scheduled values.

A review of existing literature on techniques of AGC reveals that the problem of poor transient performance in terms of large overshoots and relatively long settling time is still unresolved. In addition the existing AGC strategies are not robust in the sense that they are sensitive to parameter variations and extraneous disturbances impinging on the system.

In this thesis, a new approach to the design of automatic generation control schemes for electrical power systems is proposed. The new approach, which is based on the theory of variable structure systems (VSS), exploits the concepts of generalised eigenstructure assignment and unit vector control to synthesize a controller that guarantees asymptotically stable sliding motion with prescribed transient behaviour. Such a variable structure automatic generation control (VSAGC) scheme is inherently robust, in the sense that, when sliding, the system acquires invariance properties with respect to parameter variations and disturbances.

An interactive computer aided design software package is also developed for the implementation of the proposed AGC design approach - on an industry standard Pc-AT

microcomputer. The package is designed to provide the software part of an overall computerised scheme for the AGC of electrical power systems.

The performance of the proposed AGC strategy is illustrated by application to models of the Nigerian power system. Simulation results indicate that the VSAGC scheme yields better system performance than the existing technique.

It is concluded that the proposed VSAGC scheme provides an effective means of controlling the frequency and/or tie-line power deviations, and thus, improving the dynamic performance of electrical power systems.

TABLE OF CONTENTS

	PAGE
Dedication	ii
Acknowledgement	iii
Abstract	iv
Table of Contents	vi
List of Figures	x
CHAPTERS	
1 INTRODUCTION AND MOTIVATION	1
2. AUTOMATIC GENERATION CONTROL STRATEGIES- A REVIEW	13
2.1 Introduction	13
2.2 Proportional Control	16
2.3 Proportional Plus Integral (PI) Control	19
2.3.1 Power System Model	21
2.3.2 Method of Analysis	22
2.3.3 Assessment of the PIAGC Performance	25
2.4 Optimal Control Strategy	28
2.5 Variable Structure Control	33
2.5.1 Basic Concept of VSS	35
2.5.2 Properties of Variable Structure Systems	37
2.5.3.1 Sliding Motion	41
2.5.3.2 Invariance Properties	42
2.5.4 Existing VSAGC Design Methodology	45
2.5.4.1 The Design of the Switching Hyperplanes	46
2.5.4.2 Design of the Control Function	47
2.6 Conclusion	49
3 THE PROPOSED VSAGC DESIGN STRATEGY	52
3.1 Introduction	52
3.2 Canonical Transformation for VSCS Design	53

## TABLE OF CONTENTS (CONT'D)

	PAGE
3.3 The Design of the Switching Hyperplane	55
3.4 The Design of the Control Function	60
3.5 Application Example	66
3.5.1 Simulation Results	74
3.6 Conclusion	77
4 THE COMPUTER AIDED DESIGN (CAD) PACKAGE	83
4.1 Introduction	83
4.2 General Design Principles for the package	84
4.3 Structure and Implementation of VAGCD	88
4.4 Functions of the Modules	92
4.4.1 General Considerations	92
4.4.2 The Main Supervisor 'VAGCD'	93
4.4.3 The Input Module (INPUT)	94
4.4.4 The Hyperplane Design Module (EXIST)	97
4.4.5 The Control Functions Design Module (REACH)	101
4.4.6 The Simulation Module (SIMU)	104
4.4.7 The Output Module (OUTPUT)	107
4.4.8 The AGC Implementation Module (AGC)	108
4.5 Conclusion	114
5 APPLICATION OF THE PROPOSED VSAGC DESIGN STRATEGY TO THE MODEL OF THE NIGERIAN POWER SYSTEM	115
5.1 Introduction	115
5.2 Models of the Nigerian Power System	116
5.2.1 General Considerations	116
5.2.2 The Governing System Model	119
5.2.2.1 Dynamic Model of the Hydro-Governing Mechanism	122



## TABLE OF CONTENTS (CONT'D)

	PAGE
5.2.2.1 Speed-Governing System Model for Steam Turbine	127
5.2.3 The Turbine Dynamics Model	128
5.2.3.1 The Dynamic Model of the Hydro Turbine	129
5.2.3.2 The Steam Turbine Model	137
5.2.4 The Model of the Power Transmission System	139
5.2.4.1 The Dynamic Equations of the Transmission System	141
5.2.5 Equivalent Linear Forms of the Derived Sub-Models	146
5.2.6 Complete System Models	149
5.2.6.1 The Model of the Hydro - Dominated Single Control Area	150
5.2.6.2 The Model of a Single - Control Area Dominated by Steam - Powered Plants	150
5.2.6.3 The Model of the Two Area Interconnection	150
5.3 Synthesis of VSAGC Schemes for Models of the Nigerian Power System	152
5.3.1 VSAGC Design for a Hydro - Dominated Single Area Model	154
5.3.2 VSAGC Design for a Control Area Dominated by Steam Powered Plants	158
5.3.3 VSAGC Design for a Two Area Inter-connection	165
5.4 Simulation Results	175
5.4.1 Absence of Rate Constraints	180
5.4.2 Presence of Rate Constraints	182
5.4.3 Presence of Rate Constraints and Water Hammer	185
5.4.4 Presence of Rate Constraints and Deadband	187
5.5 Conclusion	188

## TABLE OF CONTENTS (CONT'D)

	PAGE
6 CONCLUSIONS AND RECOMMENDATIONS	192
6.1 Suggestions for Further Work	199
REFERENCES	201
APPENDIX A: Frequency and Tie-Line Power as a Function of Area Load	207
APPENDIX B: Linearization of Nonlinear Models	210
APPENDIX C: Water Hammer Effect	216
APPENDIX D: Illustration of the Effect of Deadband	219
APPENDIX E: Parameter Values of the Nigerian Power System	221
APPENDIX F: Publications	223
APPENDIX G: The Coding of VAGCD Programs	234

# LIST OF FIGURES

<u>FIGURE</u>		<u>PAGE</u>
2.1	Typical AGC Scheme For System With One Tie - Line.	14
2.2a	Zero Droop Control with Supporting Unit	18
2.2b	Generator Mw Output For Regulating Unit	18
2.3	Block Diagram of A Hydro - Dominated Area	23
2.4	Block Diagram of A Steam Dominated Area	23
2.5	Block Diagram of An Interconnected Area	24
2.6	Phase Portrait for $\psi = \alpha$	36
2.7	Phase Portrait For $\psi = \beta$	36
2.8	System With Structural Change	36
3.1	Block Diagram of A Steam - Dominated Area With VSC	68
3.2	System Responses for a 0.01pu Step Change in Load	78
3.3	System Responses for a 0.06pu Step Change in Load	79
3.4	System Responses For a 0.1 pu Step Change in Load	80
4.1	Basic Structure of VAGCD	90
5.1	Schematic Diagram of The Hydro-Governing Mechanism	120
5.2	Steam Turbine Governing System	120
5.3	Continuity Vessel	136
5.4	Caplan Turbine Runner Blade (Sectional View)	136
5.5	Block Diagram Representation of Caplan Turbine	136
5.6	Block Diagram of The Steam Turbine	145
5.7	Block Diagram of Two Area System	145
5.8	Energy Conservation Block Diagram	145
5.9a	Block Diagram of Hydro - Dominated Area	151
5.10a	Block Diagram of a Steam Dominated Area	151

## LIST OF FIGURES (CONT'D)

<u>FIGURE</u>		<u>PAGE</u>
5.11a	Block Diagram of an Interconnected Area	153
5.9b	Block Diagram of a Hydro - Dominated Area With VSC	159
5.10b	Block Diagram of a Steam - Dominated Area With VSC	159
5.12	System Responses for a Hydro Dominated Area With $D = 0.75$ , $r = 0.6$ , $R = 0.1667$	160
5.13	System Responses for a Hydro - Dominated Area with $D = 1.5$ , $r = 0.8$ and $R = 0.04$ pu	161
5.14	System Responses for a Hydro - Dominated Area with $D = 2.0$ , $r = 1.0$ and $R = 0.167$ pu	162
5.15	System Responses for an area dominated by steam powered plants: $D = 0.75$ , $R = 0.04$ pu	166
5.16	Steam - Dominated Area: $D = 1.5$ pu, $R = 0.167$ pu	167
5.17	Steam - Dominated Area: $D = 2$ pu, $R = 0.04$ pu	168
5.11b	Block Diagram of an Interconnected Area With VSC	169
5.18	System Responses in Area i For Load Variation in Area i	176
5.19	System Responses in Area j for Load Variation in Area i	177
5.20	System Responses in Area i for Load Variation in Area j	178
5.21	System Responses in Area j For Load Variation in Area j	179
5.22	System Responses in the Presence of Rate Constraints (Steam - Area Case)	183
5.23	Presence of Rate Constraints (Hydro Area Case)	184
5.24	System Responses in the Presence of Water Hammer Effect	186
5.25	System Responses in the Presence of Deadband (Hydro - Area Case)	189
5.26	System Responses in the Presence of Deadband (Steam - Area Case)	190

# LIST OF PRINCIPAL SYMBOLS

$n$	→ system order (no. of system states)
$m$	→ no. of control inputs
$p$	→ no. of disturbance inputs
$x$	→ $n$ -dimensional state vector
$u$	→ $m$ -dimensional control vector
$\xi$	→ $p$ -dimensional disturbance vector
$A$	→ $n \times n$ dimensional system matrix
$B$	→ $n \times m$ dimensional control matrix
$\Gamma$	→ $n \times p$ dimensional disturbance matrix
$\psi$	→ gain of the variable structure controller
$M$	→ $n \times n$ orthogonal transformation matrix
$C$	→ $m \times n$ sliding plane matrix
$\lambda$	→ eigenvalue spectrum
$V$	→ $n \times n$ eigenvector matrix
$\sigma$	→ sliding hyperplane
$\rho$	→ unit vector control design parameter
$\Delta P_D$	→ change in load demand (Pu)
$\Delta P_G$	→ change in generation (Pu)
$\Delta P_E$	→ Tie-line power deviation (Pu)
$\Delta f$	→ Network frequency deviation (Hz)
$\beta$	→ Area bias parameter (Mw/Hz)
ACE	→ Area control error
$\Delta P_C$	→ Power command signal deviation
$v$	→ Participation factor
$D$	→ change of load with frequency Mw/Hz
$\Delta \delta$	→ load angle deviation
$K_p$	→ gain of the power system plant (Hz/Pu Mw)
$T_p$	→ Time constant of the power system plant (seconds)
$T_{rn}$	→ reheat time constant (seconds)

$T_R$	→ dash pot relaxation time constant (seconds)
$R$	→ steady state speed regulation
$r$	→ transient speed regulation
$T_G$	→ governor time constant (seconds)
$T_w$	→ water starting time (seconds)
$s$	→ Laplace operator
$F_1$	→ reheat coefficient
$T_{ij}$	→ synchronizing coefficient of tie-line
$Int$	→ Integral controller

## CHAPTER ONE

### INTRODUCTION AND MOTIVATION

Electric power has become a basic requirement for modern life, since, most industrial and socio-economic activities, the world over, are heavily dependent on electric energy. Indeed, the availability of electricity supply in any locality signifies the first step towards its eventual industrialization. This is in addition to improving the quality of life of the people.

Electric power is obtained from generating stations which are usually remote from the consumption centre. The common generating sets utilize hydro, steam, gas or nuclear energy to produce electricity and are conventionally connected together to form what is called a power system. [1].

The primary duty of an electric power system is to supply the power demanded by all the connected loads, in the most efficient manner. Here, efficiency is a function of the economics of system operation. However, the supplied power must, in addition to continuity, conform to certain minimum requirements with regards to quality, such as constant voltage and constant frequency. This is because every electrical equipment is designed to operate at a given voltage and/or frequency within specified tolerance limits. The quality specification on contemporary power systems is made more stringent by the advent of computers and allied machinery with their tight tolerance limits. In order to derive the best service from these equipment, it is vital that the quality of power supply be maintained high.

The issue of poor quality of power supply in Nigeria has been a source of concern for some time now. Erratic power supply has been known to cause severe damages to domestic and industrial equipment as well as lead to the loss of man-hours by industries.

Table 1.1 shows the number of recorded collapses occurring in the Nigerian power system between 1985 and 1989 [2]. A partial collapse of the system means that at the grid level part of the system is totally disconnected from the grid. The disconnection creates a mismatch between real power generation and consumption. Such a mismatch results in a change in the grid frequency which if not arrested promptly may result in a total system collapse [1]. The major motivation of this work is to investigate the causes of these collapses and find solutions to the erratic power supply problem in Nigeria.

TABLE 1.1

<u>YEAR</u>	<u>TOTAL SYSTEM COLLAPSES</u>	<u>PARTIAL SYSTEM COLLAPSES</u>	<u>TOTAL NUMBER OF DISTURBANCES</u>
1985	14	34	48
1986	11	3	14
1987	20	13	33
1988	14	8	22
1989	15	9	24



The quality of power supplied by a given power system may be ensured in two ways:

- (a) The installation of several generating plants scattered all over the power system area, such that, for any fault, there still remains enough readily available generating capacity to maintain stability.
- (b) The selection of appropriate control strategy, such that any fault is arrested fast enough to forestall a sustained degradation of the nominal voltage and/or frequency.

In Nigeria, the issue of increased generating capacity has gained a lot of attention. This is evidenced by the recent commissioning of a hydro - plant at Shiroro, Niger State and a gas plant at Sapele, Bendel State. Nevertheless, the performance of the Nigerian power system has not improved much.

One likely reason for the persistent poor performance of the Nigerian power system is the near total neglect of its control structure - which is yet to benefit from the advantages of automation. A situation where the present control structure is largely manual calls for urgent steps towards formulation of a suitable automated technique. This is one of the main motives behind this thesis.

In its simplest form, the power system control problem entails finding the best way to match power generation with consumption. Since electric power is a complex quantity, studies reported in the technical literature have shown that changes in the reactive power generation of electric generators affect, essentially only the voltage, while changes in

the real power generation affect, essentially, only the system frequency [3-4]. This property has made it possible to divide the power system control problem into two separate control channels: the megavar - voltage control channel which regulates the reactive power balance and the megawatt - frequency control channel which maintains the real power balance in the system. The problem of controlling the reactive power output of electric generators so as to maintain the scheduled voltage level is often referred to as excitation control. The control of real power balance in the system so as to maintain the scheduled frequency is the subject matter of this thesis and therefore, requires further elaboration.

In the early days of power system development, each electric power generator fed an isolated load. Then the primary control action of the speed governor was sufficient to regulate the real power balance in the system and maintain the frequency constant. Later it was found that optimum economy and high reliability could be achieved by paralleling the generators into a grid network [3]. Grid operation, however, introduces more control problems, the most stringent of which is that the grid frequency be maintained at a nominal value. For example, this nominal value is 50Hz in Nigeria.

The need for frequency constancy arises simply because if the generators in a grid network operate at different frequencies, the units at higher frequencies will tend to drive the units at lower frequencies as motors. This could have consequences as severe as total system collapse.

Secondly, synchronous clocks which are connected to the system will develop time errors if the frequency deviates from the nominal value. Finally, other frequency dependent equipment such as synchronous and induction motors connected to the system will malfunction, should the frequency fluctuate. For these reasons any deviation of frequency from the nominal value must be restored as fast as possible.

However, it was found that the collective action of the speed governors of the connected generators failed to maintain the grid frequency constant [32]. Instead, whenever there existed a change in load demand, each speed governor reacted according to its droop characteristics in an attempt to restore the real power balance in the system. The result was that the system stabilized at a new frequency different from the nominal value. Thus, a secondary control action, referred to as Automatic Generation Control (AGC) or Load Frequency Control (LFC) had to be introduced to supplement the primary control action of the speed governors. In situations where two or more power systems are interconnected together via tie-lines, the AGC action is also needed to maintain the scheduled tie-line power interchange within specified limits. Equally important is the fact that decisions on unit commitment which result in economic load dispatch (ELD) are implemented by the AGC equipment [32].

Reference 1 defines automatic generation control as: "The regulation of the power output of electric generators within a prescribed area in response to changes in system frequency, tie-line loading or the relation of these to each other, so as to maintain the scheduled system frequency

and/or the established interchange with other areas within predetermined limits."

Note that in power system control terminology, a power system is referred to as a "control area". Also, throughout this thesis, AGC and LFC are used interchangeably.

Since frequency fluctuations are known to constitute a major cause of power system collapse [5], the AGC action must be fast so as to minimise frequency transients. The quantitative measure of AGC performance is in terms of the following specifications:

- (i) The static frequency error following a load change should be zero.
- (ii) The transient frequency swings should not exceed 0.05Hz from the nominal value, under normal operating conditions.
- (iii) The settling time (i.e the duration of the transient swings) should not exceed 10 seconds.

For the purposes of this thesis, two additional qualitative figures of merit are considered viz:

- (iv) The AGC scheme should be robust so as to cope with operating point variations. In other words, the AGC performance should remain acceptable in terms of the above three specifications inspite of changing system parameters.
- (v) The AGC scheme should have a simple structure. This will enhance its practical implementation and reduce its operating time which, otherwise, would increase the deadband effects in the system.

A literature survey undertaken in the course of this thesis [29-60] shows that the current AGC scheme used by industry consists of a proportional plus integral [PI] controller which has a simple structure and achieves zero static frequency deviation. With the emergence of cheap and versatile computers, a digital form of the PI controller has recently been built into a computerised control structure commonly called an energy management system (EMS) [6-7]. An EMS consists of a central control computer - usually located at the power control centre - connected to several remote terminal units linked with a supervisory control and data acquisition (SCADA) system. The EMS basically performs load-frequency control in the most efficient manner by incorporating such other functions as economic load dispatch (ELD), Optimum power flow (OPF) and security (contingency) analysis. During normal system operating state when the frequency deviation from the nominal value is small, of the order of 0.5Hz, the EMS performance is satisfactory. However, experience from prolonged use of EMS shows that it fails during emergency situations when the frequency deviation is large [69,70].

The failure of EMS during emergency has been attributed to two major reasons [69]. First, emergency situations demand for a quick and accurate decision making process and conventional EMS is not equipped with any decision making facility. Secondly, the PI action which performs the load-frequency control function is known to have poor transient performance in terms of large overshoots and relatively long settling time, of the order of 20 - 40 seconds. Due to the long settling time, the frequency fluctuations persist long

enough to energise under-frequency relays which operate to cut off some parts of the system. In consequence, loss of synchronism may occur, leading to system collapse.

The answer to the question of an intelligent EMS is currently being sought via the use of artificial intelligence (AI) techniques, especially knowledge based expert systems [69 - 72]. However, the issue of poor transient performance of PI controllers, hitherto used for AGC, still remains problematic and the need exists for more research into the possibility of developing a viable alternative AGC scheme with better performance. This is one of the major objectives of this thesis.

Studies undertaken on the Nigerian power system in the course of this research show that, the load-frequency control scheme is completely manual, [4]; relying on telephone instructions from operators at the National Control Centre (NCC) Osogbo, to others at remote generating stations. A brief description of the procedure is as follows. An operator at NCC constantly observes the grid frequency recorder. Whenever the meter records a sustained deviation from the nominal frequency of the order of 0.4Hz, the NCC operator telephones a colleague at a remote generating station asking him to change generation by a specified amount. If the known reserve capacity of one generating station is not enough to cover the required generation change, the NCC operator will telephone another generating station asking it to absorb some percentage of the change in load demand. Meanwhile the NCC operator relies solely on experience to be able to estimate the required generation change corresponding to a given

frequency deviation and thus, there could be a period of trial and error before the frequency finally returns to normal.

It is clear from the above description that the manual load-frequency control procedure is subject to human limitations with the result that it is inaccurate and open to abuse. The scheme is also subject to various time delays, including; telemetering time; time for the NCC operator to take a decision and the response time of the power station operators. Since pure time delay in a control system is known to cause severe instability, it is not surprising that the performance of the Nigerian power system is in such a poor state as shown in table 1.1. The need for improvement can, therefore, not be over-emphasized.

Given the background of poor performance of PI controllers for AGC and the dire need of the Nigerian power industry for a suitable scheme, this thesis aims at proposing a new strategy for the automatic generation control of electrical power systems. The new scheme, which derives from the theory of variable structure system (VSS), is suitable for incorporation into present day EMS design to enhance its performance during large frequency deviations.

A variable structure control system (VSCS) belongs to a class of non-linear systems with a structure that varies according to a prescribed switching logic. By so doing, it is able to adopt a certain type of motion called the sliding mode during which it acquires invariance properties to plant parameter variations and a measure of disturbance rejection

capabilities. Apart from the inherent simple structure and robustness of VSCS, its choice for AGC is further informed by the following reasons: first of all, the advent of new design techniques coupled with advances in electronics has greatly facilitated the practical realisation of sliding mode [50]. Secondly, VSCS seems to be a natural way of exploiting the use of the new power electronic components which operate in the switching mode only. Finally, the practicability of VSCS has been amply demonstrated for a wide range of industrial plants which include amongst others; robot manipulators [51 - 55], metal cutting machine tools and electrical drives [56 - 60].

The objectives of this thesis can be summarised as follows:-

- i) To propose a new strategy, based on the theory of variable structure systems, for the automatic generation control of electrical power systems, which will greatly improve on the performance of the presently used PI control scheme.
- ii) To develop a computer aided design tool for on-line synthesis of the proposed variable structure automatic generation control (VSAGC) scheme on an industrial standard PC-AT micro-computer.
- iii) To develop a digital computer simulation tool for the performance evaluation of the VSAGC scheme.
- iv) To develop an AGC model of the Nigerian power system suitable for the application of modern control theory to achieve frequency regulation.



- v) To design a VSAGC scheme for the Nigerian electric power system and evaluate its performance using digital computer simulation.
- iv) To undertake a comparative study of the VSAGC scheme and the conventional PI-AGC strategy using digital computer simulation.

This thesis is organised as follows: A review of existing and/or proposed strategies for AGC is presented in chapter two with a view to highlighting their fine qualities and setbacks. It is revealed that the VSAGC scheme is in the fore front of all the other strategies. Also presented is the basic concept of VSCS as well as its existing design techniques for automatic generation control schemes, so far reported in the technical literature. This review is necessary so as to expose the shortcomings of existing design methods for VSAGC schemes and justify the need for an alternative procedure which is proposed in this thesis. Furthermore, VSS theory is relatively new in the western literature and is not yet common in English texts.

The proposed VSAGC design procedure is outlined in chapter three where digital computer simulation studies are employed to show its superior performance. A computer aided design package for the synthesis and performance evaluation of the proposed VSAGC scheme is described in chapter four. In chapter five, three AGC models of the Nigerian electric power system are proposed, representing three possible operating strategies. Then, the proposed VSAGC strategy is synthesised for the Nigerian power system based on each of the developed models.

Simulation results are presented showing the behaviour of the system under different operating conditions. For the sake of comparison, simulation results are also presented showing the performance of the Nigerian power system under the conventional proportional plus integral automatic generation control (PIAGC) scheme. Based on the achievements of this thesis, suitable conclusions and recommendations are made in chapter six. Also included are suggestions for further work.

## CHAPTER TWO

AUTOMATIC GENERATION CONTROL STRATEGIES - A REVIEW2.1 Introduction:

The task of automatic generation control (AGC) entails the generation of an actuating (or control) signal that acts on the speed changer of electric generators, with the sole purpose of restoring the frequency and/or tie-line power interchange to the scheduled values. This is in response to signals representing frequency and/or tie-line power deviations from the nominal values.

A typical AGC channel is represented by the block diagram of Fig.2.1, for a system with one tie-line [32]. Usually a group of generating plants (4 in this case) within the power system are selected for the purposes of AGC. These plants must have their speed changers linked with the AGC equipment which is located at the power control centre. The generation commitment on such plants must also be such that they can easily take up excess load in the system, in order to offset deviations in frequency and/or tie-line power. Now, signals representing frequency and tie-line power deviations are measured and after appropriate transduction, are fed to the AGC equipment. The signals are then processed into a real-power generation - command signal which is shared among the selected plants according to a prescribed distribution logic. The nature of the distribution logic is dependent on the relative capacities of the selected plants, as well as their respective rate of change of generation. Finally, the control signal transmitter ensures that each selected plant receives

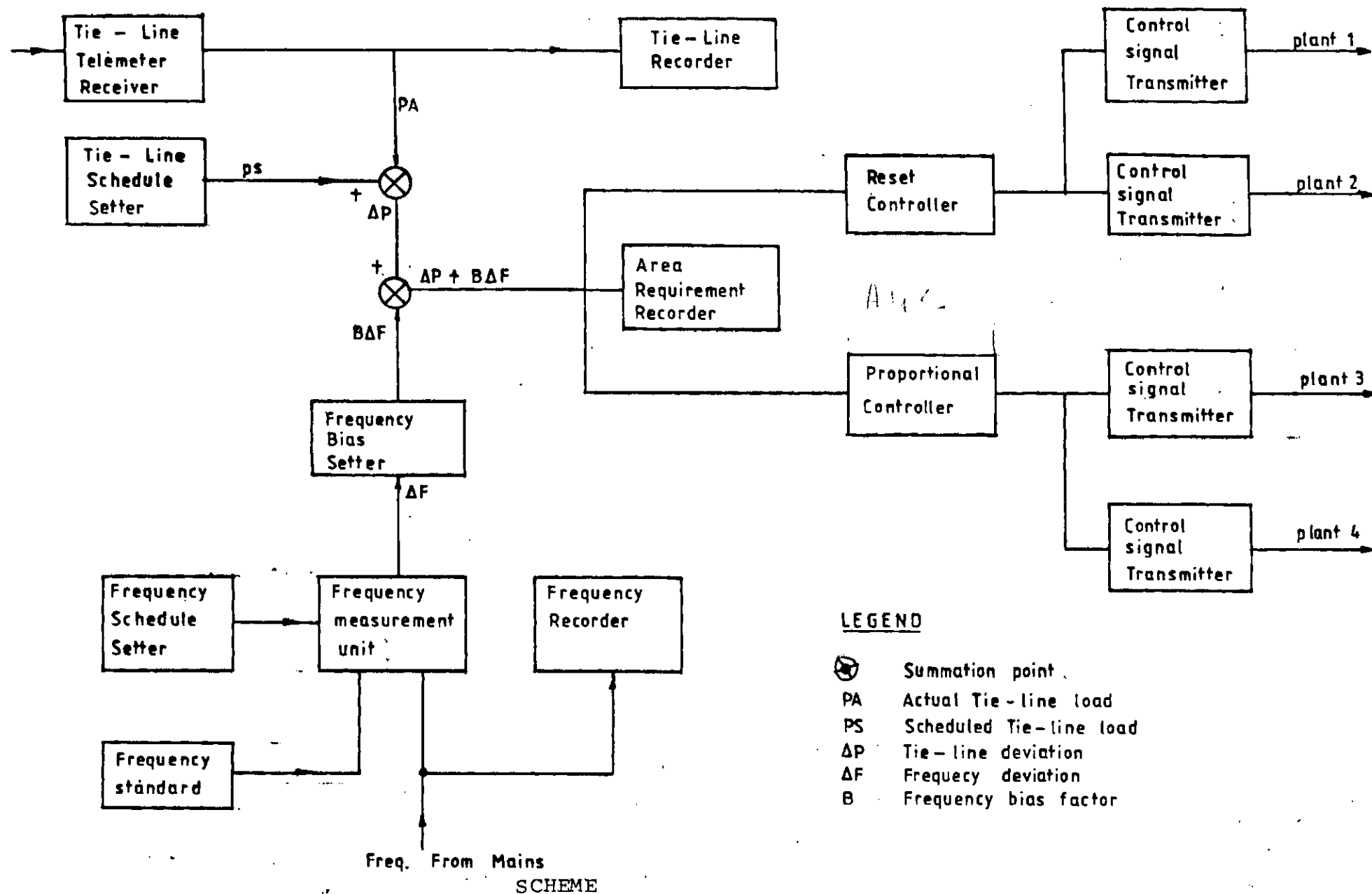


Fig.2.1: TYPICAL AGC/ FOR SYSTEM WITH ONE TIE - LINE

its own fraction of the command signal.

Based on the performance specifications listed in chapter one, the goal of any design technique for an AGC scheme, is how best to generate a command signal that gives the best frequency and/or tie-line power control performance, in terms of low overshoots, short settling time and zero steady-state error. This chapter reviews both the existing and proposed automatic generation control strategies with a view to highlighting the control principles utilized and the limitations of each scheme.

In chapter one, a manual procedure for frequency control as being practised in Nigeria and some other industrialising countries of the world is described. It is easy to see that the scheme is grossly inadequate. This necessitates the need for a strategy that is compatible with the present state of power system automation. The limitations of the manual scheme are so obvious that further review of the procedure in this chapter is unnecessary. Only the automated techniques are, therefore, reviewed.

For ease of presentation, the existing and proposed AGC schemes are classified into the following broad categories:-

- i. Proportional control
- ii. Proportional plus integral (PI) control
- iii. Optimal control and
- iv. Variable structure control

The review presented below follows the above order.

## 2.2. Proportional Control

The basic principle of proportional control action for frequency regulation is that; given a change in load demand  $\Delta P_D$  resulting in a corresponding change in frequency  $\Delta f$ , then, an actuating signal proportional to  $\Delta f$  is set up. This signal acts on the speed changer of electric generators causing a change  $\Delta P_G$  in real power generation equal to  $\Delta P_D$ . The frequency is, thus, restored to the nominal value. The total change in generation  $\Delta P_G$  required to cancel a frequency offset  $\Delta f$  is conventionally called the Area Control Error (ACE) or the Area Requirement. Expressed mathematically;

$$ACE = \Delta P_G = R \Delta f \quad (2.1)$$

where  $R = \frac{\Delta P_D}{\Delta f}$  (Megawatts/Hertz) is termed the "frequency regulating characteristic" of the power system. The actuating signal is therefore proportional to the area control error (ACE).

The initial realization of proportional control action for AGC was implemented by the use of zero - droop governors [32]. The technique is that some of the large machines in a power system are made to possess flat or isochronous load-frequency characteristics by setting their speed droops to zero. In this way the real power output of each unit will continually change in response to a frequency deviation until either the frequency is restored to nominal value or the machine reaches the high/low limit of its capacity. Generating units selected for this duty have their governors heavily damped so as to reduce their speed of response especially to

cyclic load changes.

The quality of frequency regulation with this arrangement is maintained by selecting some other suitable generating units to play a supporting role to the zero-droop machines. The speed droop on these machines is made fairly large, say 5 to 8 percent and the damping reduced as much as possible, consistent with machine stability. The support machines can, therefore, respond faster to frequency swings and thus, aid the zero - droop machines by absorbing the more rapid system load swings. Figure 2.2a shows the combined characteristics of the zero-droop and support machines while Fig.2.2b and c show their respective kilowatt records.

The above arrangement can render adequate frequency regulation provided the master machines are kept within their regulating range. This latter provision requires the operators to continually adjust the load on the other machines to prevent the zero - droop units from bumping against their high/low generation limits. Furthermore, contemporary power consumers expect a rather close control on system frequency and this may not be feasible if operators need to frequently adjust generation manually to restore the controlling machines to their regulating range. As a result of these difficulties, it was found necessary to install supplementary frequency regulating equipment as an integral part of conventional power systems [2,32].

Supplementary frequency control equipment, of the proportional type, consists of a transducer - amplifier arrangement which is capable of adjusting the real power output of

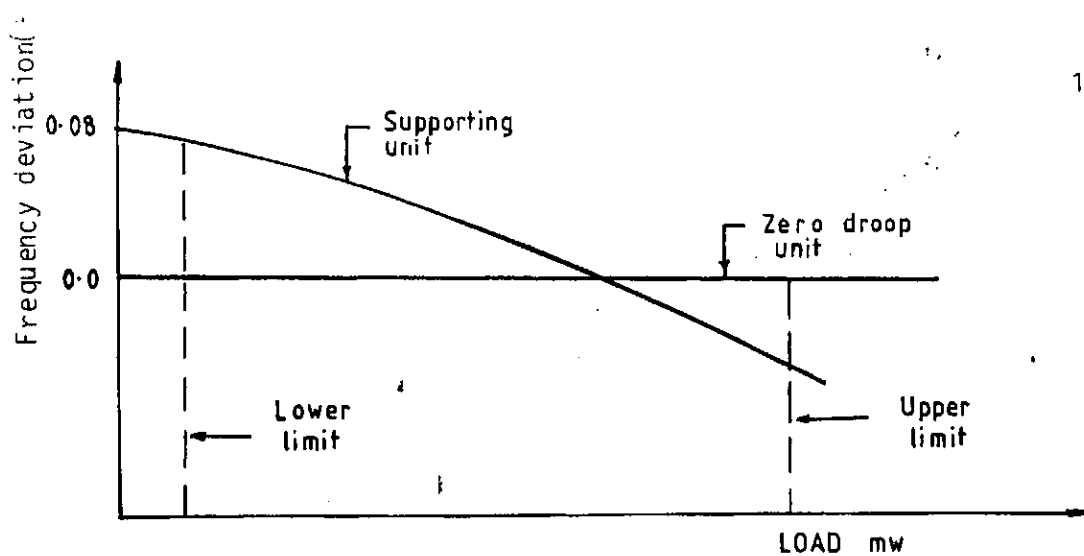


Fig. 2.2a ZERO DROOP CONTROL WITH SUPPORTING UNIT.

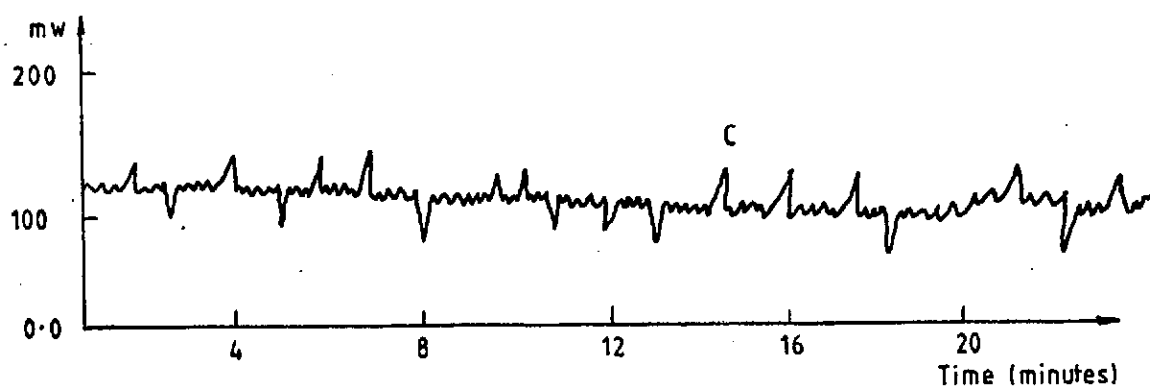
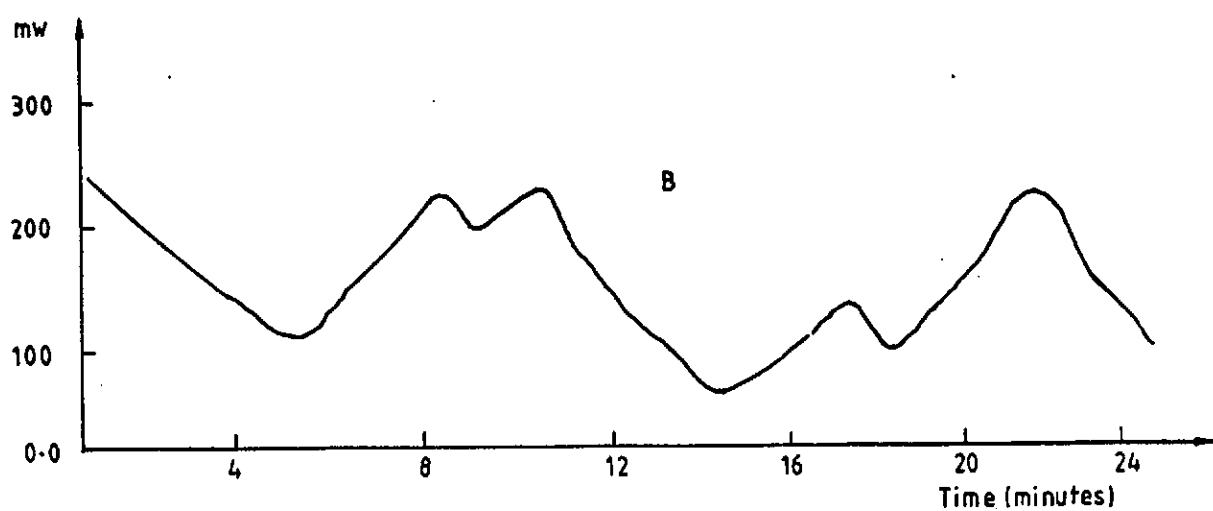


Fig. 2.2b GENERATOR MW OUTPUTS FOR REGULATING UNITS ON FREQ. CONTROL B- MASTER UNIT; C SUPPORTING UNIT WITH LARGE DROOP.



selected generating units in response to frequency deviation from the nominal value. Now, the operators need not adjust system load manually to protect the units on frequency regulation. However, the response of the proportional controller is deliberately made slow to prevent the controller from responding to cyclic load swings like switching actions, for instance. Since these load swings occur randomly throughout the day, there seems to exist intermittent intervals of frequency swings associated with proportional control schemes. This tends to undermine the integrity of the proportional control action for frequency regulation.

One other setback of the proportional control scheme is the presence of a steady-state error, which implies that the frequency cannot be restored fully to the scheduled value after a deviation. This static frequency error has been found to be responsible for large time errors in synchronous clocks and occasional malfunction of constant frequency motors [33]. The time error in a synchronous clock is known to be proportional to both the frequency error and its integral. This further explains the poor performance of the proportional control scheme. Finally, the proportional control strategy was found to be unsuitable for interconnected power systems.

In order to minimise these shortcomings, there arose the need for an alternative AGC scheme.

### 2.3 Proportional Plus Integral (PI) Control

It is well known in control systems theory that the existence of a steady-state error can be eliminated by adding

an integrator to the control loop. Therefore, in order to reduce the static frequency and tie-line power deviation to zero, there is need for an AGC scheme that generates a command signal which is proportional to the area control error (ACE) as well as its integral. Such a scheme has been developed in the form of proportional plus integral automatic generation control (PIAGC) action - [2, 21, 22, 31 - 34].

The current industrial standard for AGC is the use of a PI control scheme. Though early implementations of PI schemes for AGC were analog in form, the emergence of energy management systems [EMS] in power system operation [7], with central control computers, has forced recent PI realizations to be in digital form. In which-ever mode it appears, the basic principle is that the AGC equipment generates a control signal which is proportional to the area control error (ACE) as well as its integral. This control signal is then distributed to the speed changers of the selected generating plants, for generation adjustment.

The fundamental advantage in using PIAGC is that the static frequency error and tie-line load deviation (where applicable) following a step load change, must always reduce to zero. This is because, as long as there remains a frequency error and/or tie-line load deviation, the integrator output will continue to increase and thus, the speed changer position only attains a constant position when the ACE has been reduced to zero [31-34].

In studying the performance of power systems under PIAGC, it has become necessary to derive analytical models describing the dynamics of the power system plant. Three

models, representing different operating strategies have been widely used in the technical literature [3, 21-22, 33-34]. These are briefly described below so as to enhance the understanding of the methodology for the performance evaluation of PIAGC schemes.

### 2.3.1 The Power System Model

So far in the technical literature, three possible operating models have been assumed for a given power system viz:

- (i) single control area dominated by hydro-powered electric generators [22, 34] (See Fig.2.3)
- (ii) single control area dominated by steam-powered electric generators [21, 33-34] (See Fig.2.4)
- (iii) multiarea interconnection with each area dominated by either hydro or steam powered electric generators [21-22,33-34] (See Fig.2.5)

The purpose of the dominance assumption is to allow for a lumped circuit representation whereby a given control area is represented by an equivalent governor and turbine. In practice, a control area may consist of both hydro and steam-powered plants, although, one type may play a dominant role in the selection of suitable plants for AGC. However, comparison of simulation results with field tests [27] has confirmed that this assumption has no adverse effect on the use of these models.

In general, the power system is modelled by its power balance equation which relates the mismatch in power generation and consumption to the change in accelerating power and frequency. Each of the governor and turbine is basically represented by a single time constant  $T_G$  and  $T_t/T_\omega$  with little modifications for special applications. For instance, in Fig.2.3, the hydro-governing system has an additional time constant  $T_R$  due to the temporary droop arrangement. Alternatively, the steam turbine in Fig.2.4 has an additional time constant  $T_{rh}$  due to the reheat facility. The feedback effect of the governor is represented by the gain  $R^{-1}$ . The interconnected system, Fig.2.5, has an additional feedback signal  $\Delta P_t$  from the tie-line power deviation with the result that the area control error becomes

$$ACE = R_1 \Delta f + \Delta P_t \quad (2.2)$$

Since the authors assumed that the system is exposed to small changes in load of the order of 0.01p.u during its normal operation, the linear model will be sufficient to describe its dynamics. Also, the actual values of the parameters are dependent on the particular system under consideration.

### 2.3.2 Method of Analysis

The technique employed in evaluating the PIAGC performance involves setting up the component equations representing the transfer function of each block, on an analog or digital computer. For the single area cases, the command signal  $u$  is given by

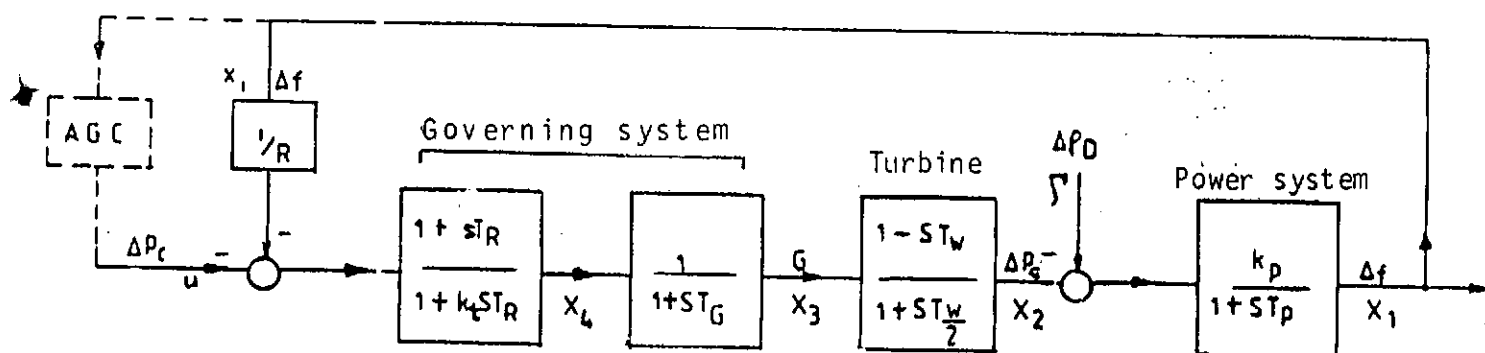


Fig. 2.3 BLOCK DIAGRAM OF A HYDRO-DOMINATED AREA

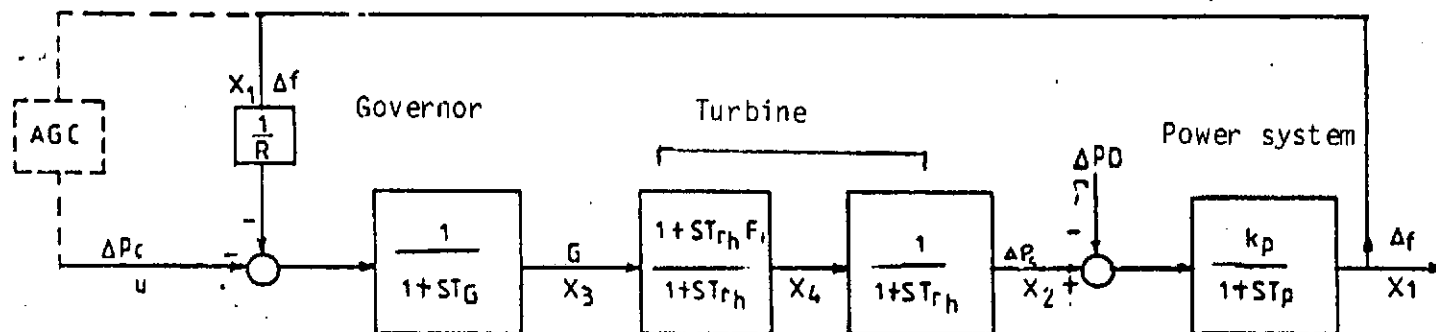


Fig. 2.4 BLOCK DIAGRAM OF A STEAM DOMINATED AREA

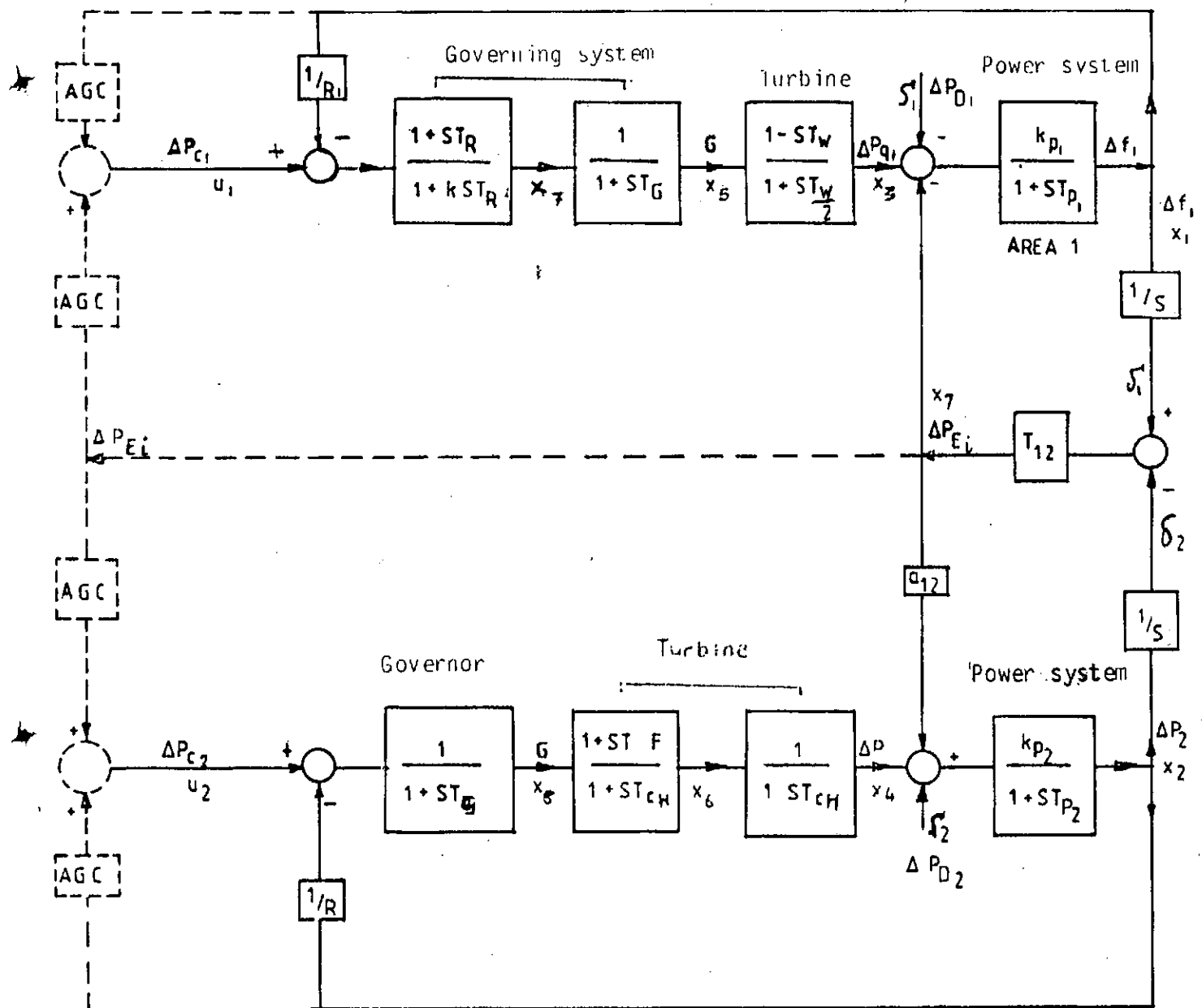


Fig. 2.5 BLOCK DIAGRAM OF INTERCONNECTED AREA

$$u(t) = -k_i \int \Delta f \, dt \quad (2.3)$$

where  $k_i$  is the integrator gain. In the case of the two area interconnection, each command signal has the general form:-

$$u_1(t) = -K_{g1} \int (\Delta P_t + \beta_1 \Delta f_1) dt \quad (2.4a)$$

$$u_2(t) = -K_{g2} \int (\Delta P_t + \beta_2 \Delta f_2) dt \quad (2.4b)$$

where  $K_g$  is the overall integrator gain and  $\beta$  is the frequency bias parameter. The value of  $\beta$  must be selected such that each area is autonomous with respect to regulating its own frequency. One of the golden rules guiding interconnected power system operation is that each area must be capable of satisfying its own load [34].

All the investigators quoted above had taken the disturbance signal to be a step change in load demand of 0.01 per unit. The choice of 0.01 p.u is informed by the fact that, under normal operations, load variation in a power system is not expected to go beyond this value. How true this assumption is in the case of the Nigerian power system will be discussed in chapter 5.

### 2.3.3 Assessment Of The PIAGC Performance

Simulation studies of the PI controller performance for AGC as applied to the three models presented earlier have been widely reported in the technical literature [21-22, 33-34, 65, 67, 73]. In reference 21, for example a two-area

interconnection consisting of steam dominated areas is considered. Reference 22 considers two types of double area interconnections, one consisting of two hydro-dominated areas while the other is made up of one steam-and one- hydro - dominated area similar to Fig.2.5. In each case, curves showing the excursions of frequency and tie-line power deviations are presented. The performance assessment is in terms of the maximum frequency and tie-line power deviations, the duration of their transients (i.e settling time) as well as their static values (i.e steady-state error).

The results show that the maximum frequency deviation following a step load change of 0.01 pu is about 0.8Hz on the average with a settling time of about forty seconds. The corresponding maximum tie-line power deviation measures about one hundred and seventy percent of the change in load demand with a settling time of sixteen seconds. The values for the frequency response are even higher for single area systems considered in references 33 and 34 using static conditions and in references 65 and 67 using dynamic state analysis. The effect of nonlinearities such as speed governor deadband [73], water hammer effect [22] and generation rate constraints [67] on PIAGC performance have also been studied. Also studied are the effects of variations in some plant parameters as well as larger load demand changes [21, 34]. The results show that the PIAGC performance deteriorates in all the cases mentioned above.

However, all the investigators agree that the static frequency and tie-line power deviation are zero. This fact, coupled with ease of practical implementation due to its



simple structure, may have informed the continued use of PIAGC in the power system industry till today.

In assessing the performance of PIAGC based on the specifications listed in chapter 1, two serious shortcomings are observed viz: large initial frequency and/or tie-line power deviations and relatively long settling time. But some of the investigators have revealed that these characteristics are proportional to the magnitude of the step change in load demand [22-23,34]. Therefore, for small change in load demand, the PIAGC renders acceptable service in regulating the frequency and tie-line power.

However, for load demand changes of the order of 0.01pu or more, the survival of the system is likely to be threatened. Take for instance, a frequency relay set at  $\pm 1.0\text{Hz}$  from the nominal value with a time delay of 10 seconds. If the magnitude of the load disturbance is higher than 0.01 pu, there is the possibility that the maximum frequency deviation will remain above 1.0Hz for up to 10 seconds, thus energising the frequency relay. Secondly, since load disturbances occur randomly, a change in load demand may occur while the frequency transient due to a previous disturbance is yet to settle. The result is a much larger frequency deviation such that can energise the frequency relay. In both cases, the consequences may be as severe as a partial or total system collapse which is undesirable.

Based on the above analysis, the need arises for an AGC scheme that can minimise significantly the shortcomings of the integral controller.

## 2.4 OPTIMAL CONTROL STRATEGY

The initial attempt at optimizing the performance of load-frequency controllers was via the so-called classical optimization scheme which sought to determine the optimum integrator gain for the area control errors and frequency bias settings [28,33]. Usually the Integral of Squared Error (ISE) criterion is used. This is defined as

$$J = \int_0^{\infty} (\Delta P_t^2 + \alpha \Delta f^2) dt \quad (2.5)$$

where  $\Delta P_t$  and  $\Delta f$  are the tie-line power and frequency deviations respectively. The parameter  $\alpha$  is a weighting factor which determines the relative penalty attached to the tie-line power error and frequency error respectively. The use of ISE necessitates that the responses  $\Delta P_t$  and  $\Delta f$  corresponding to a given pair of integrator gain  $K_g$  and bias setting  $\beta$  be found. Upon substitution into equation (2.5), the integral is evaluated to obtain a value which is a function of the parameter pair  $K_g$  and  $\beta$ . The particular values of  $K_g$  and  $\beta$  which render eqn.(2.5) a minimum represent the optimum parameter settings. In effect, the classical optimization scheme simply "fine-tunes" the PI controller for a given set of operating conditions. Should these conditions change, (and this is usual with power systems), the optimum parameters become sub-optimal or even non-conforming, resulting in poor controller performance. Furthermore, even with the optimum parameters, the performance of such a PI controller is still not very different from that

described in the last section in the sense that all the earlier listed AGC performance specifications are not met. Clearly the parameter - optimized PI controller cannot provide the much needed alternative to conventional AGC strategy. Continued interest in the dynamic aspects of load frequency control stimulated the application of modern optimal regulator theory based on state-space techniques, to the solution of the AGC problem [29,30,39 - 46]. Here, by stating the system performance specifications in terms of a quadratic cost function, a unique linear optimal feedback law could be determined which minimizes the system cost. Stated mathematically, the basic optimal regulator problem is that, given a linear time - invariant plant modelled in the state space form as:

$$\dot{x}(t) = Ax(t) + Bu(t) \quad (2.6)$$

where  $x \in \mathbb{R}^n$ ,  $u \in \mathbb{R}^m$ ; A and B are constant matrices with  $A \in \mathbb{R}^{n \times n}$  and of  $B \in \mathbb{R}^{n \times m}$ , it is required to determine a linear state feedback controller

$$u(t) = -Kx(t) \quad (2.7)$$

where K is  $m \times n$  constant optimal gain matrix, such that the integral quadratic cost function

$$J = \frac{1}{2} \int_0^{\infty} [x'(t)Qx(t) + u'(t)Ru(t)]dt \quad (2.8)$$

is minimised. Here Q is  $n \times n$  positive semi-definite symmetric state cost weighting matrix (i.e  $Q = Q' \geq 0$ ) where the superscript ' represents vector or matrix transpose and R is  $m \times m$

positive definite symmetric control cost weighting matrix (i.e.  $R = R' > 0$ ). The values of  $Q$  and  $R$  determine the relative importance of the errors in the system states and the expenditure of energy by the control signals. A finite  $J$  implies that  $x, u \rightarrow 0$  as  $t \rightarrow \infty$ . If  $K$  can be determined such that  $J$  is minimized, then the control  $u = -Kx(t)$  is optimal for any initial state  $x(0)$ . A direct method of determining  $K$  is by substituting eqn. (2.7) for  $u$  into eqns. (2.6) and (2.8) to obtain the pair

$$\dot{x} = (A - BK)x \quad (2.9)$$

$$J = \int_0^{\infty} x' (Q + K' R K) x \, dt \quad (2.10)$$

If there exists a positive definite real symmetric matrix  $V$  such that

$$x' (Q + K' R K) x = - \frac{d}{dt} [x' V x] \quad (2.11)$$

$$\text{or } x' (Q + K' R K) x = - \dot{x}' V x - x' V \dot{x} \quad (2.12)$$

then, substituting for  $\dot{x}$  from eqn. (2.9) we have that

$$x' (Q + K' R K) x = - x' [(A - BK')V + V(A - BK)]x \quad (2.13)$$

Since this equation must be true for all  $x$ , it follows that,

$$(A - BK)'V + V(A - BK) = -(Q + K' R K) \quad (2.14)$$

This is often called the Lyapunov's matrix equation or the matrix Riccati equation.

If  $(A-BK)$  is a stable matrix [4], there exists a positive definite symmetric matrix  $V$  which satisfies eqn. (2.14). By defining the matrix  $R$  as

$$R = S' S \quad (2.15)$$

where  $S$  is non-singular, eqn. (2.14) can be written as

$$(A' - B' K') V + V(A-BK) + Q + K' S' SK = 0$$

or

$$A'V + VA + [SK - (S')^{-1} B' V]' [SK - (S')^{-1} B' V] - VBR^{-1}V + Q = 0 \quad (2.16)$$

The minimization of  $J$  with respect to  $K$  requires the minimization with respect to  $K$  of the expression

$$x' [SK - (S')^{-1} B' V]' [SK - (S')^{-1} B' V] x \quad (2.17)$$

Since this value is non-negative, the minimum occurs when expression (2.17) equals zero, i.e. when

$$SK = (S')^{-1} B' V \quad (2.18)$$

Thus

$$K = S^{-1} (S')^{-1} B' V = R^{-1} B' V \quad (2.19)$$

Note that the matrix  $V$  must satisfy eqn. (2.14) or the reduced order matrix Ricatti equation

$$A'V + VA - VBR^{-1}B'V + Q = 0 \quad (2.20)$$

From the above development, it is clear that the optimal controller design procedure is very complex, requiring a lot of computer time and space. This is in contrast to the PI controller case with a simple structure. Furthermore, the parameters of the optimal controller are strongly dependent on the coefficient of the quadratic performance index. A major difficulty of the linear optimal control approach is the fact that there exists no practical guidelines for the selection of the coefficients of the performance index. Little wonder therefore, that all the proposed optimal control schemes for AGC are yet to be practically implemented. References [29,39-40] proposed a linear optimal feedback controller with infinite final time via the solution of the algebraic matrix Ricatti equation. Usually, because of the infinite final time, the system transient frequency deviation may not be effectively regulated. The use of Kalman filter to estimate some of the unmeasurable states while assuming that the load demand is constant but unknown was reported by some investigators [30,41]. In the same spirit, reference 42 replaced the Kalman filter with a Luenberger observer to avoid the necessity of specifying generally unavailable statistical data. Optimal load tracking employing aspects of stochastic control theory was also reported in reference 46. However, the problem of robustness remains unsolved, that is; how does the performance of the optimal controller remain optimum in the face of changing conditions? Since the power system is nonlinear with parameters varying with system operating conditions, it seems that optimality is a "temporary" property of the so-called optimal load-frequency controllers.

## 2.5 VARIABLE STRUCTURE CONTROL

The essential feature of a variable structure system (VSS) is the ability to assume different structures depending on the region of the state space in which the system's operating point is located. Control systems based on VSS theory are often referred to as variable structure control systems (VSCS). The nature of VSCS is such that the generally nonlinear system is provided with a means of automatically switching from one control structure to another according to a prescribed switching logic. At the point where the control function changes structure, the differential equations describing the system's dynamics have discontinuous right hand sides. This creates a discontinuity subspace of the system's state space usually referred to as a "switching manifold".

A variable structure control system may, therefore, be regarded as consisting of a set of continuous subsystems of prescribed structures, each operating in a given subspace of the entire state space. The combination of these structures according to a predetermined switching logic, ensures the exploitation of the useful properties of each of the structures and possible creation of new properties not present in any of the structures. One such new property is the sliding motion. This occurs when the system's state is constrained to move along the switching manifold because all motion in the neighbourhood of the manifold is directed inwards (i.e towards the manifold). If the control form selected is such that this motion occurs on the intersection of all the switching manifolds, the system is said to be in the sliding mode and is, then,

equivalent to a system of lower order termed the "equivalent system". Also, while sliding, the system dynamics are determined by the characteristics of the sliding subspace and are therefore, ideally insensitive to parameter variations and extraneous disturbances. As a result, variable structure systems are made to operate in the sliding mode only. Indeed, it is the deliberate introduction of a sliding mode in the system that forms the core of all the design algorithms for conventional VSS [8 - 16].

In recent times, VSC techniques have been proposed for the solution of diverse problems arising in electrical power systems [61 - 68]. References 61 to 64 dealt with the VSC approach to the excitation control problem, aimed at minimizing the adverse effect of the voltage regulator when the system operates with negative damping torque. On the other hand, the authors of references 65 to 68 proposed VSC techniques for the solution of the AGC problem. This section presents the design techniques for variable structure automatic generation control (VSAGC) schemes proposed in references 65 - 68 and reveals the qualities that place VSAGC schemes in the forefront of other AGC strategies discussed earlier. This section also highlights areas where the present design procedure for VSAGC need improvement.

In order to enhance the understanding of this presentation, a brief review of VSS theory is included. The review explains the basic concept of VSS and derives mathematical conditions for such VSS properties as sliding mode and invariance to plant parameter variations and extraneous disturbances.



### 2.5.1 Basic Concept Of VSCS

Consider a plant described in the phase canonical form as

$$\dot{x}_1 = x_2 \quad (2.21)$$

$$\dot{x}_2 = -a_2 x_2 - a_1 x_1 + u$$

where  $a_1$  and  $a_2$  are constants. Let the control function  $u$  be a piecewise linear function of  $x_1$ , i.e

$$u = \psi x_1 \quad (2.22)$$

where  $\psi$  can take on the constant values  $\alpha$  and  $\beta$  ( $\alpha \neq \beta$ ). Let the coefficient  $a_2$  be negative in eqn.(2.21);  $\alpha, \beta$  are selected such that for  $\psi = \alpha$ , the system (2.21) has complex eigenvalues while for  $\psi = \beta$ , the system (2.21) has real eigenvalues. Both structures are unstable as depicted in the phase portraits of Figs.2.6 and 2.7 respectively. Now, suppose the system structure is changed on the lines:  $x_1 = 0$  and  $\sigma = cx_1 + x_2 = 0$  ( $c > 0$ ), according to the switching logic

$$\psi = \begin{cases} \alpha & \text{if } x_1 \sigma > 0 \\ \beta & \text{if } x_1 \sigma < 0 \end{cases} \quad (2.23)$$

The coefficient  $c$  will be selected such that the straight line  $\sigma = 0$  will be between the axis  $x_1$  and the asymptote of hyperbolic trajectories associated with the structure  $\psi = \beta$ . Fig.2.8 shows the phase portrait of the system with the law of structural change given in eqn.(2.23). It is clearly seen

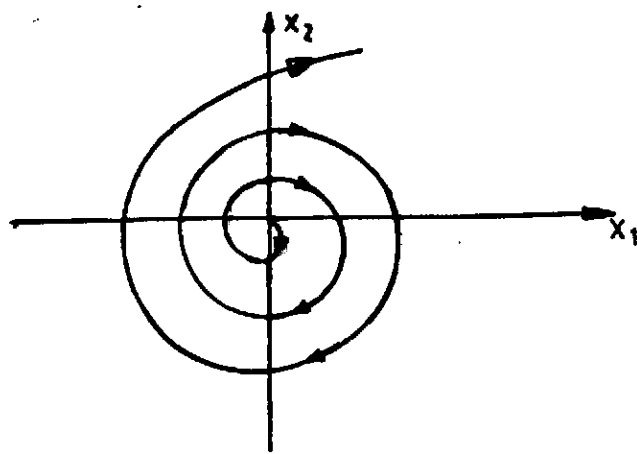


Fig. 2.6. Phase Portrait for  $\gamma = \delta$

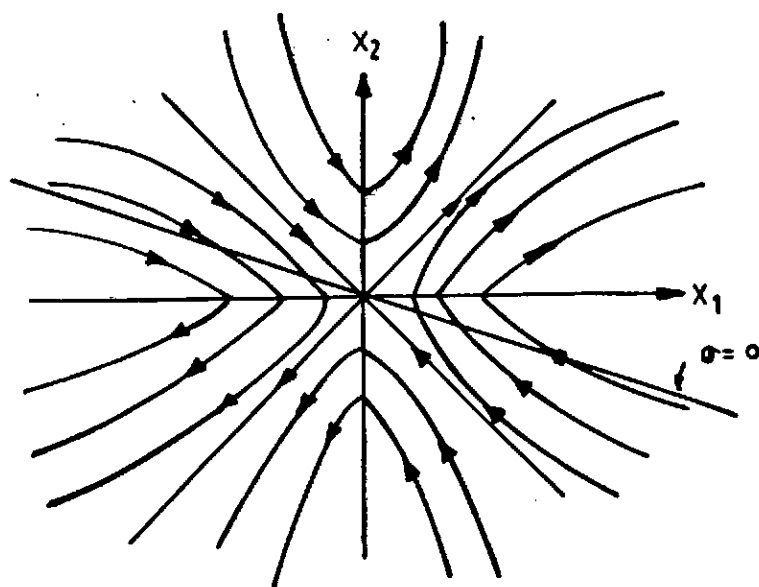


Fig. 2.7. Phase Portrait for  $\gamma = \delta$

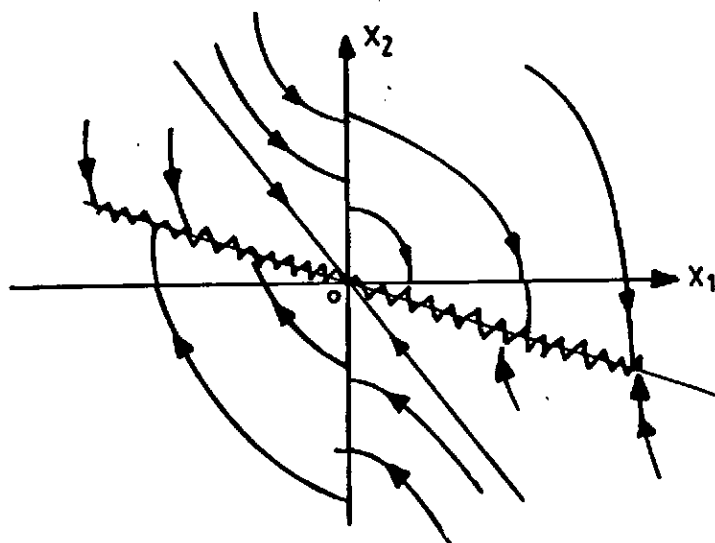


Fig. 2.8. System with Structural Change

that the system is asymptotically stable in the sense that the describing point invariably reaches the switching straight line  $\sigma = 0$  from any initial position. In the vicinity of the straight line, the trajectories of both structures are directed towards it, therefore, further motion will proceed in the sliding mode along the line  $\sigma = 0$ . While sliding, the system's describing point cannot ideally, leave any infinitesimal vicinity of the switching surface, thus, the system dynamics may be described by the lower order system;

$$c x_1 + x_2 = 0 \quad (2.24)$$

This is also called the "equivalent system". Eqn.(2.24) above can be written in the form

$$\dot{x}_1 + c x_1 = 0 \quad (2.25)$$

which is a sliding equation and is stable once  $c > 0$ . Notice that the behaviour of the equivalent system depends only on the parameter  $c$  and is independent of the plant parameters  $a_1$  and  $a_2$  and any variations there in. This is one of the good qualities of variable structure controllers.

### 2.5.2 Properties Of Variable Structure Systems

Consider a plant with variable structure control represented in the state space form as

$$\dot{x}(t) = (A + \Delta A) x(t) + Bu(t) + \Gamma \xi(t) \quad (2.26)$$

where

$x \in \mathbb{R}^n$  is the  $n$  - dimensional state vector  
 $u \in \mathbb{R}^m$  is the  $m$  - dimensional control vector  
 $\xi \in \mathbb{R}^p$  is the  $p$  - dimensional disturbance vector  
 $A \in \mathbb{R}^{n \times n}$  is the system matrix  
 $B \in \mathbb{R}^{n \times m}$  is the control matrix and  
 $\Gamma \in \mathbb{R}^{n \times p}$  is the disturbance matrix.

The triple  $(A, B, \Gamma)$  consists of known constant matrices defining the nominal linear system while the pair  $(A, B)$  is assumed to be completely controllable. The matrix function  $\Delta A(t, x(t))$  representing the internal uncertainties in the plant dynamics is assumed to be continuous with origin on the plane  $x(t) = 0$  and to satisfy the uniform Lipschitz condition

$$||\Delta A(t, x^1) - \Delta A(t, x^2)|| \leq K_f ||x^1 - x^2|| \quad (2.27)$$

for all  $(t, x^1), (t, x^2) \in \mathbb{R} \times \mathbb{R}^n$  where  $K_f \geq 0$  is a known constant. The extraneous disturbances impinging on the system are represented by the function  $\xi(t)$  which is assumed to be piece-wise continuous with known bounds on the magnitude i.e

$$||\xi(t)|| \leq k_d' \quad (2.28)$$

where  $k_d'$  is a known constant.

The assumptions in the definition of  $\Delta A(t, x(t))$  and  $\xi(t)$  have the following implications:

- (i) Since variable structure control methodology is a deterministic approach, limits must be set on the magnitudes of parameter variations and extraneous disturbances.
- (ii) The usual disturbances in interconnected power systems are changes in load demand and tie-line power which are basically step functions of varying magnitudes. They are, however, repetitive and thus, constitute a piece-wise continuous function defined by  $\xi(t)$ .

In the usual state feedback controller design for a nominal linear system without disturbances, the control  $u$  has a fixed structure defined as

$$u = K x \quad (2.29)$$

where the constant parameters of the  $m \times n$  matrix  $K$  are obtained using any of the control synthesis techniques such as those for eigenvalue/eigenstructure assignment or linear quadratic optimal control. A VSC system incorporates a state feedback regulator of the form of eqn. (2.29) with  $K$  replaced by  $\psi$  which is defined in its simplest form as

$$\psi = \hat{\psi} \text{ diag}[\text{sgn } x_1, \text{sgn } x_2, \dots, \text{sgn } x_n] \quad (2.30)$$

where

$$\hat{\psi} = [\hat{\psi}_1, \hat{\psi}_2, \dots, \hat{\psi}_m] \quad (2.31)$$

and

$$\hat{\psi} = \begin{cases} \alpha_i, & \text{for } \sigma_i(x) > 0 \\ \beta_i, & \text{for } \sigma_i(x) < 0 \end{cases} \quad (2.32)$$

$$i = 1, 2, \dots, m; \alpha_i \neq \beta_i.$$

$\hat{\psi}_i$ ,  $\alpha_i$  and  $\beta_i$  are  $n$ -vectors while  $\sigma_i(x)$  is a  $m$ -vector, all of which define a subspace of the entire state space. Equation (2.32) indicates that vector  $\hat{\psi}_i$  is discontinuous on the switching hypersurface  $\sigma_i(x) = 0$  in the  $n$ -dimensional state space. Hence the control vector  $u_i(x)$  can take on one of two structures depending on which side of  $\sigma_i(x) = 0$  the state vector  $x$  is located. In other words

$$u_i(x) = \begin{cases} u_i^+, & \text{for } \sigma_i(x) > 0 \\ u_i^-, & \text{for } \sigma_i(x) < 0 \end{cases} \quad (2.33)$$

The switching hypersurfaces are described by

$$\sigma = Cx = 0 \quad (2.34)$$

where

$$\sigma = [\sigma_1, \sigma_2, \dots, \sigma_m]^T \quad (2.35)$$

and  $C \in \mathbb{R}^{m \times n}$  with full rank  $m$ .

A state vector in the neighbourhood of the  $i$ -th switching hyperplane  $\sigma_i = 0$  (on either side of it), will be directed towards the hyperplane provided the following condition is satisfied [10]

$$\sigma_i \dot{\sigma}_i \leq 0 \quad (2.36)$$

### 2.5.3.1 Sliding Motion

Equation (2.36) also ensures sliding motion on the  $i$ -th switching hyperplane  $\sigma_i(x) = 0$ . During sliding, the system satisfies the equations

$$\sigma_i(x) = 0 \quad \text{and} \quad \dot{\sigma}_i(x) = 0 \quad (2.37)$$

Suppose sliding occurs on all the 'm' switching hyperplanes together, then, an equivalent control  $u_{eq}$  [11], is obtained by solving for  $u$  in the algebraic equation

$$\dot{\sigma} = C \dot{x} = 0 \quad (2.38)$$

By substituting  $\dot{x}$  from eqn. (2.26) into (2.38) and assuming that matrix  $(CB)$  is nonsingular so that  $(CB)^{-1}$  exists,  $u_{eq}$  is obtained as

$$u_{eq} = -(CB)^{-1} C[A + \Delta A] \dot{x}(t) - (CB)^{-1} C \Gamma \xi(t) \quad (2.39)$$

Hence for a nominal linear system without disturbances where  $\Delta A(x, t) = \xi(t) = 0$ , eqn. (2.39) becomes

$$u_{eq} = -(CB)^{-1} CAx \quad (2.40a)$$

or

$$\psi_{eq} = -(CB)^{-1} CA \quad (2.40b)$$

The dynamics of the system in the sliding mode may be obtained by substituting eqn.(2.39) for  $u_{eq}$  into eqn.(2.26) for the general system, to yield

$$\dot{x}(t) = [I - B(CB)^{-1}C][A + \Delta A]x(t) + [I - B(CB)^{-1}C]\Gamma\xi(t) \quad (2.41)$$

where  $I$  represents the unit matrix. In other words

$$\dot{x}(t) = A_{eq}x(t) + \Gamma_{eq}\xi(t) \quad (2.42)$$

where  $A_{eq} \in \mathbb{R}^{(n-m),n}$  and  $\Gamma_{eq} \in \mathbb{R}^{(n-m),n}$ , giving a lower order system.

Thus, in the sliding mode, the state vector is determined merely by the properties of the controlled plant and the orientation of the switching manifold which is characterised by the  $m \times n$  matrix  $C$ . The job of the control function  $u(t)$  is, therefore, limited to ensuring that the state vector reaches and remains within the switching manifold.

From the foregoing, the behaviour of a variable structure control system is characterised by two motions viz: a relatively fast motion bringing the state vector from any arbitrary initial condition on to the switching manifold (asymptotic stability in the large) and a slower sliding motion toward the origin  $x = 0$  (asymptotic stability in the small), during which it has invariance properties with regards to parameter variations and extraneous disturbances.

#### 2.5.3.2 Invariance Properties:

One major advantage of using VSC is that in the sliding mode, the behaviour of the system is insensitive to some



class of parameter variations and extraneous disturbances. Expanding equation (2.41) the sliding equation may be written in the form

$$\dot{x}(t) = [I - B(CB)^{-1}C]Ax(t) + [I - B(CB)^{-1}C]\Delta Ax(t) + [I - B(CB)^{-1}C]\Gamma\xi(t) \quad (2.43)$$

For total insensitivity to parameter variations, it is required that the system satisfies the condition [17]

$$[I - B(CB)^{-1}C]\Delta Ax = 0 \quad (2.44)$$

This condition will be fulfilled if all the basis vectors  $T_i$  of the subspace  $\mathbb{R}^{n-m}$  satisfy the rank relation

$$\text{rank}[B, \Delta AT_i] = \text{rank } B \quad (2.45)$$

Similarly, for total disturbance rejection, it is required (from eqn. (2.43)) that the system fulfils the condition [17]

$$[I - B(CB)^{-1}C]\Gamma = 0 \quad (2.46)$$

Equation (2.46) is satisfied for all the possible values of  $\xi$ , if all the columns of  $\Gamma$  are linear combinations of the columns of  $B$ , or mathematically

$$\text{rank } [B, \Gamma] = \text{rank } B \quad (2.47)$$

Note that even when equations (2.44) and (2.46) are satisfied, both the disturbances and parameter variations still affect

the behaviour of the system just before sliding occurs. If the preliminary part of the system motion is shortened by a suitable choice of the control function, the over-all effect of disturbances and parameter variations on the whole system motion is greatly reduced. One of the desirable properties of a VSC system, therefore, is that the state vector reaches the switching manifold in the shortest possible time.

Note also that most disturbances and parameter changes of practical importance satisfy equations (2.44) and (2.46) respectively either totally or partially [14]. Hence, a variable structure control system possesses either partial or total invariance to system parameter variations and extraneous disturbances.

Based on the fine qualities of VSS exposed above, it seems incontrovertible that the deployment of VSCS to the solution of the automatic generation control problem would yield substantial benefits. This fact is further supported by the results of comparative studies of VSAGC schemes with other strategies [65 - 68]. In references 66 and 67 for instance, a performance evaluation of the PI control scheme, optimal control scheme and VSC scheme, using digital computer simulations was presented. The results show that the VSAGC scheme is superior to the other two. Similar conclusions are reached in references 65 and 68 where only the PIAGC and the VSAGC performances are compared. Thus, in this thesis, variable structure control systems are proposed for the solution of the AGC problem.

However, the synthesis procedure for the presently proposed VSAGC schemes [65 - 68] leaves much room for improvement. This subject is discussed in more details below.

#### 2.5.4 Existing VSAGC Design Methodology

The authors of references 65 - 68 had used a model of the power system in the form of eqn. (2.26) but without parameter variation viz:

$$\dot{x}(t) = Ax(t) + Bu(t) + \Gamma\xi(t) \quad (2.48)$$

Note that any of the block diagrams of Figs. 2.3 to 2.5 can be reduced to the form of eqn. (2.48) above with  $\Delta P_c \equiv u(t)$  and  $\Delta P_D \equiv \xi(t)$ .

However in synthesizing the variable structure controller, the authors used the nominal linear system without disturbance i.e

$$\dot{x}(t) = Ax(t) + Bu(t) \quad (2.49)$$

with the hope that the controller so obtained is robust enough to function properly in the face of an extraneous disturbance  $\xi(t)$ . Thus the disturbance term is added during the simulation studies for performance evaluation.

In general, the VSC design objective is to find vectors  $\alpha_i, \beta_i$  ( $i = 1, m$ ) in eqn. (2.32) and matrix  $C$  in eqn. (2.34) such that the state vector reaches and slides on the switching hyperplane  $\sigma(x) = 0$ , toward the origin  $x = 0$ . The design may

be in two stages:

- (i) design of the switching hyperplanes through selection of the hyperplane matrix  $C$  such that the sliding mode is asymptotically stable with prescribed transients. This is often referred to as the "existence" problem and can be accomplished without a knowledge of the form of control functions.
- (ii) design of the switching control functions together with the switching logic to ensure that the state vector is steered and hastened - up to the switching hyperplanes  $\sigma = CX = 0$ . This is also referred to as the "reachability" problem.

#### 2.5.4.1 The Design Of The Switching Hyperplanes

The procedure for selecting the elements of the matrix  $C$  in references 65 and 66 involves imposing the sliding condition of eqn. (2.34) and selecting the elements of  $C$  as arbitrary real numbers. For instance, consider a single-input single - output (SISO) system of order  $n$  whereby eqn. (2.34) becomes

$$c_1 x_1 + c_2 x_2 + c_3 x_3 \dots c_n x_n = 0 \quad (2.50)$$

where  $c_i$ 's are the elements of the vector  $C$ . Now the  $c_i$ 's can be selected arbitrarily to satisfy eqn. (2.50).

It is easily observed that this is a trial and error procedure and could be very time wasting, especially if a particular transient behaviour is prescribed for the sliding motion.

As a result, the authors of reference 66 proposed a systematic approach [67] based on linear optimal control theory for the selection of the elements of the hyperplane matrix  $C$ . However, the matrix  $C$  so obtained suffers the same shortcomings as the optimal control parameters discussed in the last section, in that its elements are heavily dependent on the parameters of the quadratic cost function.

An alternative procedure based on pole-placement was proposed in reference 68. Though this procedure gives acceptable values for the elements of the matrix  $C$ , its usage is restricted to SISO systems.

Therefore, in this thesis, a technique for selecting the elements of  $C$  is proposed and is based on the generalised eigenstructure assignment. This is presented in the next chapter.

#### 2.5.4.2 Design Of The Control Function

In all the works so far reported on the application of VSC to AGC, the authors had used one form of control function [65-68]. This form is referred to as 'relays with state dependent gains' defined by

$$u = -\psi x \quad (2.51)$$

where  $\psi$  is given by eqn.(2.32). The synthesis procedure for  $\alpha_i$ 's and  $\beta_i$ 's involves satisfying the inequality constraints of eqn.(2.36), which can be written as

$$\sigma \dot{C}x \leq 0 \quad (2.52)$$

substituting for  $\dot{x}(t)$  from eqn.(2.49) yields

$$\sigma [CAx(t) + CBu(t)] \leq 0 \quad (2.53)$$

Consider, a SISO system whereby  $C$  is defined as in eqn(2.50) and  $B$  is a column vector. Then the matrix  $A$  is  $n \times n$  and the product

$$CA = [c'_1 \quad c'_2 \quad c'_3 \quad \dots \quad c'_n] \quad (2.54a)$$

while

$$CB = c_k \quad (2.54b)$$

Now substituting for  $u$  from eqn.(2.51) into eqn.(2.52) and noting that  $\psi$  is defined by eqn.(2.31), the inequality of eqn.(2.53) becomes

$$\sigma [c'_1 x_1 + c'_2 x_2 + c'_3 x_3 \dots c'_n x_n - (\psi_1 x_1 + \psi_2 x_2 + \psi_3 x_3 + \dots \psi_n x_n) c_k] \leq 0 \quad (2.55)$$

Breaking eqn.(2.55) into its components yields

$$\sigma x_1 (c'_1 - c_k \psi_1) \leq 0; \dots \sigma x_n (c'_n - c_k \psi_n) \leq 0 \quad (2.56)$$

$$\text{Hence for } \sigma x_i > 0, \quad c_i' - c_k \psi_i < 0 \text{ or } \psi_i = \alpha_i > \frac{c_i'}{c_k} \quad (2.57a)$$

$$\text{Alternatively, for } \sigma x_i < 0, \quad \psi_i = \beta_i < \frac{c_i'}{c_k} \quad (2.57b)$$

The values of  $\alpha_i$  and  $\beta_i$  ( $i = 1, \dots, n$ ) can, therefore, be selected based on the chosen values of  $c_i$ 's.

It is easily observed that the above procedure is a trial and error approach which may not necessarily yield the best control parameters. Also, since the choice of the control parameters determines how fast the system reaches the sliding plane, it is desirable to device a synthesis procedure which ensures that the sliding mode is attained in the shortest possible time.

Given the above background, this thesis has proposed a technique, based on the unit vector control concept [16], for the synthesis of variable structure control parameters. The details of this procedure is presented in chapter 3 where it is shown that faster reaching of the sliding plane is ensured.

## 2.6 CONCLUSION:

This chapter has reviewed the existing and proposed control techniques for the AGC of single and multi-area power systems. It was established that the manual load-frequency control procedure currently used by the Nigerian power supply authority (NEPA) is grossly inadequate and hence, contributes in no small measure to the poor quality of power supply in the country. The need for an alternative AGC scheme

can therefore, not be overemphasized.

The proportional plus integral (PI) controller was identified as the most widely used AGC strategy in the industry today. However, the transient performance of the PI controller was found to be unsatisfactory especially when the frequency deviation was large. Since frequency deviations are relatively large in developing countries like Nigeria, an alternative AGC technique must be sought.

Furthermore, AGC strategies based on linear optimal control theory were also considered as a feasible alternative. However, the parameters of the optimal controller were found to be heavily dependent on the coefficients of the quadratic performance index. A major difficulty of the optimal control approach was the absence of any practical guideline for the selection of the coefficients of the quadratic performance index. Added to this difficulty is the complexity of the optimal control structure both of which have rendered the practical implementation of the optimal AGC strategy rather costly.

Finally the variable structure control approach to the solution of the AGC problem was reviewed. The three properties of order - reduction, fast response and insensitivity to plant parameter variations and extraneous disturbances over wide limits, seem to make VSC scheme the best choice of AGC strategy.

However, the design techniques for contemporary VSAGC schemes proposed in the technical literature were found to be in dire need of improvement. To this end, a new design



strategy for the synthesis of VSAGC schemes is proposed in this thesis. This new approach is presented in chapter three where it is shown that it is superior to the existing techniques. Later in chapter five this proposed technique is used to synthesize a VSAGC scheme for the Nigerian electric power system.

## CHAPTER THREE

THE PROPOSED VSAGC DESIGN STRATEGY3.1 Introduction:

The last chapter reviewed the existing techniques for the automatic generation control of electrical power systems, and concluded that the deployment of variable structure controllers to solve the AGC problem held substantial promise. However, it was also revealed that the design approach to the existing variable structure automatic generation control (VSAGC) schemes suffered from severe setbacks, thus, creating the need for an improved design procedure that would eventually reduce these shortcomings to the barest minimum.

In this chapter, a new VSAGC design technique is proposed. A particular canonical transformation which is vital to the use of the proposed scheme is presented in section 2. In section 3, a systematic procedure for the computation of the hyperplane matrix  $C$  is described. This is followed in section 4, by the presentation of a technique for synthesizing the control function. A case study is presented in section 5 with the aim of revealing the superiority of the proposed VSAGC design scheme over the existing ones. This is closely followed by a few concluding remarks in section 6.

### 3.2 Canonical Transformation For VSCS Design

It is customary in control system design practice to employ some canonical transformations to convert all the defining matrices for the nominal system into the most convenient form for the chosen design method. However, since these are mere co-ordinate transformations, such properties as controllability and observability which characterise the system, are not normally affected. The transformation used here, is closely related to controllable canonical form for linear multivariable systems [19] and follows from the postulations of Utkin and Yang [13].

Consider the nominal linear system without disturbances defined by

$$\dot{x}(t) = Ax(t) + Bu(t) \quad (3.1)$$

where  $x \in \mathbb{R}^n$ ,  $u(t) \in \mathbb{R}^m$ ,  $A \in \mathbb{R}^{n \times n}$  and  $B \in \mathbb{R}^{n \times m}$  and the pair  $(A, B)$  is controllable. Let there exist a  $n \times n$  orthogonal matrix  $M$  which operates on the  $n \times m$  control matrix  $B$  such that

$$MB = \begin{bmatrix} 0 \\ \vdots \\ B_2 \end{bmatrix} \quad (3.2)$$

where  $B_2$  is  $m \times m$  and it is nonsingular. The matrix  $M$  may be obtained by inspection for simple cases. For generation control applications, a systematic method for its determination is developed here from the QU factorization procedure, whereby  $B$  is decomposed into the form

$$B = Q \begin{bmatrix} U \\ \vdots \\ 0 \end{bmatrix} \quad (3.3)$$

where  $Q$  is  $n \times n$  and orthogonal while  $U$  is  $m \times m$ , non-singular and upper - triangular. The matrix  $M$  is then determined by rearranging the rows and columns of  $Q'$ , where superscript ' denotes matrix transpose. By introducing the transformed state variable

$$y(t) = Mx(t) \quad (3.4)$$

into eqn.(3.1), the nominal system becomes

$$\dot{y}(t) = MAM' y(t) + MBu(t) \quad (3.5)$$

The sliding mode condition,  $Cx(t) = 0$ , now becomes

$$\sigma = Cx(t) = CM'y(t) = 0 \quad (3.6)$$

If the transformed state  $y(t)$  is now partitioned as

$$y' = [y_1' ; y_2']' \quad (3.7)$$

with  $y_1' \in \mathbb{R}^{n-m}$  and  $y_2' \in \mathbb{R}^m$  and the matrices  $MAM'$ ,  $MB$  and  $CM$  are correspondingly partitioned, then eqns.(3.5) - (3.6) can be rewritten in the form

$$\dot{y}_1(t) = A_{11}y_1(t) + A_{12}y_2(t) \quad (3.8a)$$

$$\dot{y}_2(t) = A_{21}y_1(t) + A_{22}y_2(t) + B_2u(t) \quad (3.8b)$$

and

$$\sigma = C_1 y_1(t) + C_2 y_2(t) = 0 \quad (3.8c)$$

where

$$MAM' = \begin{bmatrix} A_{11} & A_{12} \\ A_{21} & A_{22} \end{bmatrix} \quad (3.9a)$$

$$CM' = [C_1 \quad C_2] \quad (3.9b)$$

while  $A_{11} \in \mathbb{R}^{(n-m) \times (n-m)}$ ,  $A_{12} \in \mathbb{R}^{(n-m) \times m}$ ,  $A_{21} \in \mathbb{R}^{m \times (n-m)}$ ,  $A_{22} \in \mathbb{R}^{m \times m}$ ,  $C_1 \in \mathbb{R}^{m \times (n-m)}$  and  $C_2 \in \mathbb{R}^{m \times m}$ . Equations (3.8) and (3.9) are crucial to the proposed VSAGC design strategy which is described below.

### 3.3 The Design Of The Switching Hyperplane

The design of the switching hyperplane which yields prescribed closed-loop eigenstructure for the sliding mode is proposed. The design procedure entails the selection of suitable eigenvalues and their associated eigenvectors which combine to produce desired closed-loop system dynamics during sliding mode.

In sub-section 2.5.3, it is assumed that the product matrix  $(CB)$  is non-singular so that  $(CB)^{-1}$  exists. From the transformed matrices  $CM'$  and  $MB$  above, it can be shown that the non-singularity of  $(CB)$  implies that the  $m \times m$  matrix  $(C_2 B_2)$  is also nonsingular since;

$$|CB| = |CM' . MB| = \begin{bmatrix} C_1 \\ C_2 \end{bmatrix} \begin{bmatrix} 0 \\ B_2 \end{bmatrix} \neq 0 \quad (3.10)$$

Further simplification of eqn. (3.10) yields

$$|C_2 B_2| = |C_2| |B_2| \neq 0 \Rightarrow |C_2| \neq 0 \quad (3.11)$$

The sliding mode condition defined by eqn. (3.9) above may now be rewritten as

$$y_2(t) = -F y_1(t) \quad (3.12)$$

where  $F \in \mathbb{R}^{m \times (n-m)}$  is defined by

$$F = C_2^{-1} C_1 \quad (3.13)$$

Expression (3.12) indicates that the motion of  $y_2(t)$  in the sliding mode, is linearly related to that of  $y_1(t)$ . This is structurally similar to the conventional linear state feedback control law ( $u(t) = Kx(t)$ ); where  $K$  is a real matrix.

In order to determine the dynamics of the system in the sliding mode (i.e., the sliding equations), two known properties of variable structure systems are invoked:

- (i) During sliding motion, the order of the system is reduced from  $n$  to  $(n-m)$ . In other words, sliding mode transforms the original system into an equivalent system of lower order.
- (ii) The ideal sliding mode is independent of the control  $u$ .

From eqn.(3.8), it is easily observed that the original system of eqn.(3.1) has been decoupled into two parts; one part is of order  $(n-m)$  and is independent of the control  $u$ , while the other part is of order  $m$  and dependent on the control. The ideal sliding equation can, therefore, be written as,

$$\dot{y}_1(t) = A_{11} y_1(t) + A_{12} y_2(t) \quad (3.14)$$

$$y_2(t) = -F y_1(t) \quad (3.12)$$

which is an  $(n-m)^{th}$  order system with  $y_2(t)$  playing the role of a state feedback control function. Substituting, eqn.(3.12) in (3.14) gives the closed-loop system as;

$$\dot{y}_1(t) = (A_{11} - A_{12}F) y_1(t) \quad (3.15)$$

which shows that the design of a stable sliding mode ( $y \rightarrow 0$  as  $t \rightarrow \infty$ ) with prescribed transient behaviour requires the determination of the gain matrix  $F$  such that the matrix  $(A_{11} - A_{12}F)$  has prescribed  $(n-m)$  lefthand plane eigenvalues and associated eigenvectors. The proposed procedure for achieving this, is outlined below.

As stated in section 2.5, once the sliding motion starts on the hyperplane  $\sigma = Cx = 0$ , then, the complementary expression given by

$$C \dot{x}(t) = C[Ax + Bu(t)] = 0 \quad (3.16)$$

is also satisfied. An equivalent control,  $u_{eq}$ , can therefore,

be defined from eqn.(3.16) as

$$u_{eq} = -(CB)^{-1} C A x(t) = -Kx(t) \quad (3.17)$$

where the real matrix  $K = (CB)^{-1}CA$  is of order  $n-m$ .

Substituting for  $u_{eq}$  as defined above in eqn.(3.16) yields

$$C[A - BK] x(t) = 0 \quad (3.18)$$

For  $x(t)$  not equal to zero, the above expression reduces to

$$C[A - BK] = 0 \quad (3.19)$$

In geometrical terms, eqn.(3.19) implies that the range space of matrix  $[A-BK]$  represented by  $R([A-BK])$  is a proper subset of the null space of matrix  $C$  written as  $N(C)$ , or

$$R(A-BK) \subseteq N(C) \quad (3.20)$$

Now, let  $\{\lambda_i : i = 1, \dots, n\}$  be the eigenvalues of matrix  $[A-BK]$ , assumed distinct, while the corresponding eigenvectors are given by  $V_i$ , where  $V_i$  is a column vector of order  $n$ . Then, from theory of vector spaces [76], it follows that

$$[A-BK]V_i = \lambda_i V_i \quad (3.21)$$

from which the sliding plane condition of eqn.(3.19) can be rewritten as



$$C[A - BK]V_i = \lambda_i C V_i = 0 \quad (3.22)$$

Expression (3.22) indicates that, either  $\lambda_i = 0$  or  $V_i \in N(C)$ . Now, the matrix  $[A - BK]$  has precisely  $m$  zero valued eigenvalues. This feature is a direct consequence of the inherent order - reduction property associated with variable structure systems in the sliding mode [10]. Now, let  $(\lambda_i : i = 1, \dots, n-m)$  be the chosen non-zero eigenvalues of  $[A - BK]$ , assumed distinct. Then specifying the corresponding eigenvectors  $(V_i : i = 1, \dots, n-m)$  fixes the null space of  $C$ , since the dimension of  $N(C) = n-m$ .

Although,  $\lambda_i, V_i$  have been specified, the hyperplane matrix  $C$  obtained by solving eqn. (3.22) is not unique. This is because, the expression;

$$CV = 0 \quad (3.23)$$

$$\text{with } V = [V_1, V_2, \dots, V_{n-m}]$$

has  $m^2$  degrees of freedom. However a unique  $C$  may be obtained by defining  $n \times (n - m)$  matrix  $W$ .

$$W = MV = \begin{bmatrix} W_1 \\ \dots \\ W_2 \end{bmatrix} \quad (3.24)$$

where the partitioning of  $W$  is compatible with that of  $y_1$  (ie they must be conformable for multiplications) such that eqn. (3.24) becomes

$$CM' \cdot MV = [C_1 \mid C_2] \begin{bmatrix} W_1 \\ \vdots \\ W_2 \end{bmatrix} = C_2 [F \mid I_m] \begin{bmatrix} W_1 \\ \vdots \\ W_2 \end{bmatrix} = 0 \quad (3.25)$$

Hence, by considering eqn.(3.25) as given above and noting that  $C_2 \neq 0$ , it is easily deduced that

$$[F \mid I_m] \begin{bmatrix} W_1 \\ \vdots \\ W_2 \end{bmatrix} = 0 \Rightarrow FW_1 = -W_2 \quad (3.26)$$

Then, provided that  $W_1^{-1}$  exists, the matrix  $F$  is uniquely determined by eqn.(3.26).

Having fixed the matrix  $F$  which uniquely satisfies eqn.(3.25), it remains to determine the elements of the hyperplane matrix  $C$ . In eqn.(3.25), the matrix  $C_2$  represents an arbitrary constant matrix, such that  $C_2$  can be taken to be a unit matrix (ie  $C_2 = I_m$ ) without loss of generality. The sliding plane matrix  $C$ , can therefore, be determined from eqn. (3.25) by writing

$$C = [F \mid I_m]M \quad (3.27)$$

### 3.4 The Design Of The Control Function

The task here is to solve the reachability problem of selecting a state feedback control function  $u: \mathbb{R}^n \rightarrow \mathbb{R}^m$  which will drive the state  $x(t)$  from any initial condition  $x(t_0)$  to the sliding manifold  $Cx(t) = 0$  and thereafter maintain it within this manifold towards the origin of

ordinates i.e  $x(0) = 0$ . From the theory of vector spaces, it is evident that the sliding manifold is coincident with the null-space of matrix  $C$ , written as  $N(C)$ .

The general form of the variable structure control law consists of two parts: a linear part  $u_L$  and a non-linear component  $u_N$  which are added to form  $u$ . The linear component of the control law is a state dependent feedback controller while the nonlinear part is discontinuous with respect to the state  $x(t)$  and incorporates all the nonlinear elements of the control law.

In the existing variable structure control scheme for automatic generation control described in Chapter 2, the nonlinear part of the control law is discontinuous on the individual hyperplanes, with the result that sliding conditions are separately derived for each switching surface (eqns. 2.54 - 2.56). This often leads to a waste of control effort and an unnecessary enlargement of the control structure.

The proposed control scheme is based on a design philosophy that the individual controls are continuous except on the final intersection  $\{N(C)\}$  of the switching hyperplanes, where all the controls are discontinuous together. This approach ensures that the system motion is always towards the final target  $N(C)$ , with the advantage that the control has a simpler structure and therefore, easier to implement. In other words, the proposed approach provides a systematic method for determining the linear ( $u_L = Lx(t)$ :  $L \in \mathbb{R}^{m \times n}$ ) and nonlinear  $u_N$  components of an overall control

structure  $(u = u_L + u_N)$  such that the nominally linear controlled system has an  $(n-m)$  - dimensional asymptotically stable manifold  $\sigma = Cx(t)$ , on which motion is governed by a  $(n-m)$  - dimensional linear system with a prescribed eigenstructure spectrum. This motion must be preserved by the overall nonlinearly controlled system. In the terminology of VSS theory, the proposed approach provides a feedback control structure which guarantees the global reaching of the sliding mode and the preservation of motion on the sliding plane towards the origin of coordinates.

Following the general concept of unit vector control and considering the nominal linear system without disturbances (eqn.3.1), the nonlinear component of the proposed control law is defined as:

$$u_N = \frac{\rho}{||Hx(t)||} Gx(t), \quad (\rho > 0) \quad (3.28)$$

such that the overall control law is given by

$$u = u_L + u_N = Lx(t) + \frac{\rho}{||Hx(t)||} Gx(t) \quad (3.29)$$

where  $L, G \in \mathbb{R}^{m \times n}$  and  $H \in \mathbb{R}^{m \times n}$  are constant matrices such that  $Cx(t) \equiv Gx(t) \equiv Hx(t) \equiv 0$  (ie the null spaces  $N(C)$ ,  $N(G)$  and  $N(H)$  are coincident) and  $\rho > 0$  is a constant parameter. The elements of the matrices  $L, G$  and  $H$  are determined as follows: From the transformed state  $y$ ,

[eqn.(3.4)], a second transformation  $M_2 : \mathbb{R}^n \rightarrow \mathbb{R}^n$  is formed such that

$$Z = M_2 Y \quad (3.30)$$

where  $Z \in \mathbb{R}^n$  and

$$M_2 = \begin{bmatrix} I_{n-m} & \vdots & 0 \\ \hline F & \vdots & I_m \end{bmatrix} \quad (3.31)$$

The matrix  $F$  is as defined in eqn.(3.13), while  $I$  stands for a unit matrix. Clearly the matrix  $M_2$  is non-singular and has the inverse

$$M_2^{-1} = \begin{bmatrix} I_{n-m} & \vdots & 0 \\ \hline -F & \vdots & I_m \end{bmatrix} \quad (3.32)$$

If the transformed state variable  $Z$  in eqn.(3.30) is partitioned such that

$$Z' = [Z_1 \quad \vdots \quad Z_2]' \quad (3.33)$$

where  $Z_1 \in \mathbb{R}^{n-m}$  and  $Z_2 \in \mathbb{R}^m$ , then, substituting eqn.(3.7) for  $y'$  into eqn.(3.30) and simplifying, yields

$$z_1 = y_1 \quad (3.34a)$$

$$z_2 = Fy_1 + y_2 \quad (3.34b)$$

By comparing equations (3.34b) and (3.8c) it is easily seen that the condition  $z_2 = 0$  and  $\sigma \equiv 0$  are equivalent, in the sense that the points where  $z_2$  equals zero are precisely the same points where the original sliding manifold occurs. Now, differentiating eqns.(3.34) with respect to time and eliminating the  $y$  variables by making use of eqns. (3.8) and (3.34) gives the transformed state equations in terms of  $z$  as

$$\dot{z}_1 = \phi_1 z_1 + A_{12} z_2 \quad (3.35a)$$

$$\dot{z}_2 = \phi_2 z_1 + \phi_3 z_2 + B_2 u \quad (3.35b)$$

where  $\phi_1 = A_{11} - A_{12}F$ ;  $\phi_2 = F\phi_1 - A_{22}F + A_{21}$ ;  $\phi_3 = A_{22} + FA_{12}$

For the nominal linearly controlled system  $\dot{x}(t) = (A - BL)x(t)$  to have an asymptotically stable sliding manifold, the linear component of the control law  $u_L = Lx(t)$  must be chosen so as to force  $z_2$  and  $\dot{z}_2$  to become identically zero. A simple way to achieve this is to equate eqn.(3.35b) to zero and solve for  $u$  such that:

$$u_0 = -B_2^{-1} [\phi_2 z_1 + \phi_3 z_2] \quad (3.36)$$

However, to ensure that the motion of  $\dot{z}_2$  is asymptotically stable, the coefficient of  $z_2$  is modified so that,  $u_L$  is chosen as

$$u_L = -B_2^{-1} [\phi_2 z_1 + (\phi_3 - \phi) z_2] \quad (3.37)$$

where  $\phi$  is any  $m \times m$  matrix with left-hand half-plane eigenvalues. In this case, if a set of  $m$  eigenvalues  $(\lambda_i, i=1, m)$  have been selected such that  $[\lambda_i: \text{Re}(\lambda_i) < 0, i = 1, \dots, m]$ , then  $\phi$  may be chosen as  $\phi = \text{diag} [\lambda_i, i = 1, \dots, m]$ .

Transforming back into the original state space gives

$$L = -B_2^{-1} [\phi_2 \ ; \ \phi_3 - \phi] M_2^M \quad (3.38)$$

The linear control law only serves to drive the transformed state component  $z_2$  to zero. For the state function  $z(t)$  to attain the sliding manifold  $N(C)$  in finite time, the discontinuous control law is required. The only restriction in the choice of  $u_N$  is that  $u_N$  should be zero only when  $z_2 = 0$ , at which time it switches to another preselected value. In other words, the discontinuous control law should be selected such that the hyperplane  $z_2 = 0$  serves as the switching surface, on which sliding motion occurs. By definition  $u_N$  is continuous everywhere on the state space except on the sliding manifold where  $z_2 = 0$ . Thus, letting  $P_n$  denote the positive - definite solution of the Lyapunov equation

$$P_n \phi + \phi' P_n + I_m = 0 \quad (3.39)$$

then  $P_n z_2 = 0$  if and only if  $z_2 = 0$ . The discontinuous control law is, therefore, chosen as

$$u_N(z) = \frac{-\rho}{||P_n z_2||} B_2^{-1} P_n z_2 \quad (z_2 \neq 0) \quad (3.40)$$

where  $\rho > 0$  is a scalar parameter to be selected by the designer. When  $z_2 = 0$ ,  $u_N$  is arbitrarily chosen as a function satisfying:

$$||u_N|| \leq \rho \quad (3.41)$$

This choice has the advantage of limiting the switching time. Large switching time is known to be responsible for the chattering motion associated with variable structure systems in the sliding mode. Expressing the discontinuous control submatrices eqn. (3.28) in the x-space yields

$$G = -B_2^{-1} [0 \quad P_n] M_2^M \quad (3.42)$$

and 
$$H = [0 \quad P_n] M_2^M \quad (3.43)$$

### 3.5 Application Example

In this section, the proposed VSAGC design approach is employed to synthesize an automatic generation controller for a power system model. For ease of comparison with the existing technique, the power system model used here is the same as that employed by Chan and Hsu [67]. The model, which



is shown in Fig.3.1, represents a single area power system dominated by steam powered plants with reheat turbines. The turbine dynamics are modelled by two first order time lags with time constants  $T_{rh}$  and  $T_{ch}$ , respectively and reheat coefficient  $F_1$ . The load - frequency dynamics of the power system are modelled by a first order time lag characterised by time constant,  $T_p$ , and gain constant  $K_p$  while the time lag due to the governing system as well as its feedback effect are represented by time constant  $T_G$  and gain  $\frac{1}{R}$  respectively. The block marked  $(\frac{1}{s})$  represents an additional integrator which serves to ensure zero steady-state frequency deviation.

Finally the variable structure control block is labelled VSC and the output is the control signal  $u = \Delta P_G$ .

The system model can be written in the state variable form as:

$$\dot{x}(t) = Ax(t) + Bu(t) + \Gamma\xi(t); x(0) = -x_{ss} \quad (3.44)$$

$$\text{where } x \in \mathbb{R}^5 = (\int \Delta f . dt \quad \Delta x_e \quad \Delta f \quad \Delta P_G \quad \Delta X_r) \quad (3.45)$$

with  $x_{ss} \rightarrow$  the nominal steady - state value

- $\int \Delta f . dt \rightarrow$  load angle deviation from the nominal value
- $\Delta x_e \rightarrow$  change in turbine valve position (Pu)
- $\Delta f \rightarrow$  frequency deviation (Hz)
- $\Delta P_G \rightarrow$  change in generated power (Pu)
- $\Delta X_r \rightarrow$  Pu change in reheat output power.

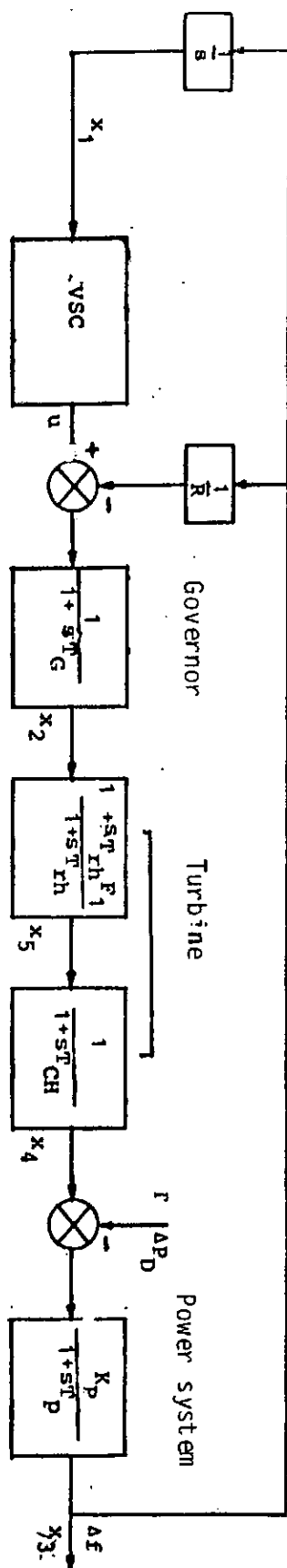


Fig.3.1 Block Diagram of a Steam - Dominated Area with VSC (67)

The control signal  $u = \Delta P_c$  is a measure of the deviation in speed changer position while the disturbance signal  $\xi(t) = \Delta P_D$  represents a step change in load demand. The system matrix  $A \in \mathbb{R}^{5 \times 5}$ , the control matrix  $B \in \mathbb{R}^{5 \times 1}$  and the disturbance matrix  $\Gamma \in \mathbb{R}^{5 \times 1}$  are defined as follows:

$$A = \begin{bmatrix} 0 & 0 & 1 & 0 & 0 \\ 0 & -\frac{1}{T_G} & -\frac{1}{T_G R} & 0 & 0 \\ 0 & 0 & -\frac{1}{T_P} & \frac{K_P}{F_1} & 0 \\ 0 & 0 & 0 & -\frac{1}{T_{ch}} & \frac{1}{T_{ch}} \\ 0 & \frac{1}{T_{rh}} - \frac{F_1}{T_G} & -\frac{F_1}{T_G R} & 0 & -\frac{1}{T_{rh}} \end{bmatrix} \quad (3.46a)$$

$$B = \begin{bmatrix} 0 & \frac{1}{T_G} & 0 & 0 & \frac{F_1}{T_G} \end{bmatrix} \quad (3.46b)$$

$$\Gamma = \begin{bmatrix} 0 & 0 & -\frac{K_P}{T_P} & 0 & 0 \end{bmatrix} \quad (3.46c)$$

The system parameter values are given as (67):

$$\begin{aligned} T_G &= 0.08 \text{ secs} & K_P &= 120 \text{ Hz/p.u. Mw} \\ T_{ch} &= 0.3 \text{ secs} \\ T_{rh} &= 10 \text{ secs} & F_1 &= 0.5 \\ T_P &= 20 \text{ secs} & R &= 2.4 \text{ Hz/p.u Mw} \end{aligned}$$

$$M_2 = \begin{bmatrix} I_4 & 0 \\ F & I_1 \end{bmatrix} = \begin{bmatrix} 1 & 0 & 0 & 0 & 0 \\ 0 & 1 & 0 & 0 & 0 \\ 0 & 0 & 1 & 0 & 0 \\ 0 & 0 & 0 & 1 & 0 \\ 5.72 & -2.25 & 5.80 & 2.92 & 1 \end{bmatrix}$$

such that

$$M_2^{-1} = \begin{bmatrix} 1 & 0 & 0 & 0 & 0 \\ 0 & 1 & 0 & 0 & 0 \\ 0 & 0 & 1 & 0 & 0 \\ 0 & 0 & 0 & 1 & 0 \\ -5.72 & 2.25 & -5.80 & -2.92 & 1 \end{bmatrix}$$

Then, the coefficients  $\phi_1$ ,  $\phi_2$ ,  $\phi_3$ ,  $A_{12}$  and  $B_2$  in eqn. (3.35) become

$$\phi_1 = \begin{bmatrix} 0 & 0 & 1 & 0 \\ 0 & -0.2 & 0 & 0 \\ 0 & 0 & -0.05 & 6 \\ 0 & 0 & 0 & -3.33 \end{bmatrix}$$

$$\phi_2 = [ 10.75 \quad -10.72 \quad 15.76 \quad 31.62 ]$$

$$\phi_3 = [ -2.23 ]$$

$$B_2 = [ 6.25 ]$$

Since the system under consideration is single-input single-output (SISO), the matrix  $\phi$  in eqn.(3.38) may be taken as any arbitrary negative scalar number. By choosing  $\phi = -1$ , the linear component of the control law defined by eqn.(3.38) reduces to

$$L = [-0.58 \quad 1.27 \quad -1.09 \quad -4.48 \quad -2.54]$$

In order to determine the nonlinear part of the proposed control law, the Lyapunov equation given by eqn.(3.39) must first be solved for the positive definite matrix  $p_n$ . However, for a SISO system, the matrix  $p_n$  becomes a scalar  $p_n$ . Substituting  $\phi = -1$  in eqn.(3.39) yields:

$$-p_n - p_n + 1 = 0 \quad (3.47)$$

or  $p_n = 0.5$

Then, eqns.(3.42) and (3.43) give the values of G and H respectively as

$$G = [-0.46 \quad 0.18 \quad -0.46 \quad -0.23 \quad -0.44]$$

$$H = [2.86 \quad -1.13 \quad 2.9 \quad 1.46 \quad 2.75]$$

The value of the parameter  $\rho$  is left for the designer

to choose. However, to ensure numerical stability, the positive constant  $\rho$  should be of the order of ten or lower. In the present case, the value of  $\rho$  is fixed at 5.0. Now, substituting for the values  $L$ ,  $G$ ,  $H$  and  $\rho$  obtained above, into eqn.(3.29) gives

$$u_L = [-0.58 \quad 1.27 \quad -1.09 \quad -4.48 \quad -2.54]x(t)$$

(3.48a)

$$u_N = \frac{5[-0.46 \quad 0.18 \quad -0.46 \quad -0.23 \quad -0.44]x(t)}{||[2.86 \quad -1.13 \quad 2.9 \quad 1.46 \quad 2.75]x(t)||} \quad \sigma \neq 0$$

(3.48b)

$$\text{OR} \quad u_N = 3 ; \quad \sigma = 0$$

### 3.5.1 Simulation Results

Experimentation with models has become a powerful tool for predicting the behaviour of designed systems under envisaged working conditions even before actual construction commences. This is because, in quite a number of cases, simulation has been found to be faster and more cost-effective than experimenting with physical components.

In this subsection, the simulation of the performance of the proposed VSAGC scheme under various working conditions

is achieved by solving eqn.(3.44) using a fourth-order Runge Kutta integration algorithm. However, the variable  $u(t)$  is replaced by the variable structure control scheme of eqn.(3.48), while  $\xi(t)$  is taken to be a step change in load demand which results in frequency fluctuation about the nominal value.

For the sake of comparison, the performance of the VSAGC strategy proposed by Chan and Hsu [67] is also presented. In this case, the hyperplane matrix  $C$  is given by

$$C = [100 \quad -0.0355 \quad 11.7 \quad 11 \quad 1.07]$$

The control function is of the form described in sub-section 2.5.4.2 with the result that the control parameters are given as;

$$\psi_1 = \begin{cases} \alpha_1 = 100 & \text{if } x_1\sigma > 0 \\ \beta_1 = -100 & \text{if } x_1\sigma < 0 \end{cases}$$

$$\psi_3 = \begin{cases} \alpha_3 = 100 & \text{if } x_3\sigma > 0 \\ \beta_3 = -100 & \text{if } x_3\sigma < 0 \end{cases}$$

$$\psi_2 = \psi_4 = \psi_5 = 0$$

For ease of comparison, the curves showing the performance of the proposed VSAGC scheme are superimposed on the curves showing the response of the existing strategy to the same

change in load. Figures 3.2 to 3.4 depict the responses of both systems to step changes in load demand of magnitudes 0.01, 0.06 and 0.1 pu respectively. In Fig.3.2 representing normal system operation, whereby load changes are not expected to vary beyond 0.01 pu, the responses of both systems are acceptable. However, the proposed scheme shows superior performance, in the sense that the existing scheme exhibits higher frequency deviation and longer settling time for the transient generation change. Specifically, the transient response of the change in power generation settled at 1.6 seconds for the proposed scheme, and 5.2 seconds for the existing scheme.

The superiority of the proposed scheme becomes clearer as the magnitude of the load demand grows higher. For  $\Delta P_D = 0.06$  pu, (Fig.3.3) representing moderate abnormal situation, the frequency transient of both schemes still remain acceptable, though the response of the existing scheme is characterised by relatively higher overshoots. However the transient of the generated power remains for more than 10 seconds for the existing scheme while that of the proposed scheme settled after about 2 seconds. An even worse situation is depicted in Fig.3.4 for  $\Delta P_D = 0.1$  pu which represents a serious abnormal operating condition. Here both the frequency and generated power transients for the existing technique are unacceptable due to their continuous oscillation which can trigger-off large amplitude swings of the entire power system. It is observed however, that the response of the proposed scheme still remained acceptable since the resulting vibrations due to the large



change in load demand settled in about 2.5 seconds.

Now, the simulation results discussed above had assumed that the power system possesses the extra capacity to take up the load increase and there is no constraint on the rate at which the extra capacity is made available. In practical power systems however, there exists a rate of change of generation which must be known. For power systems dominated by steam power plants, like the system under consideration, the rate of generation varies between 0.01 and 0.1 pu per minute [36]. Figure 3.5 depicts simulation results for a 0.01 pu change in load demand where a 0.1 pu per minute rate of change of generation has been imposed. It is observed that the system transients still settled at about 3.5 seconds for the proposed scheme while it is not so for the existing strategy. Of particular importance is that the generated power transient for the existing VSAGC scheme persists for a long time. This has the potential danger of triggering wide system oscillations leading to possible system collapse. Such a situation is very undesirable.

### 3.6 Conclusion

This chapter has presented a new systematic procedure, for the synthesis of variable structure automatic generation controllers. The proposed design scheme utilizes a particular canonical transformation which decouples the state space and facilitates the easy determination of the sliding mode - condition. The equations of sliding motion so

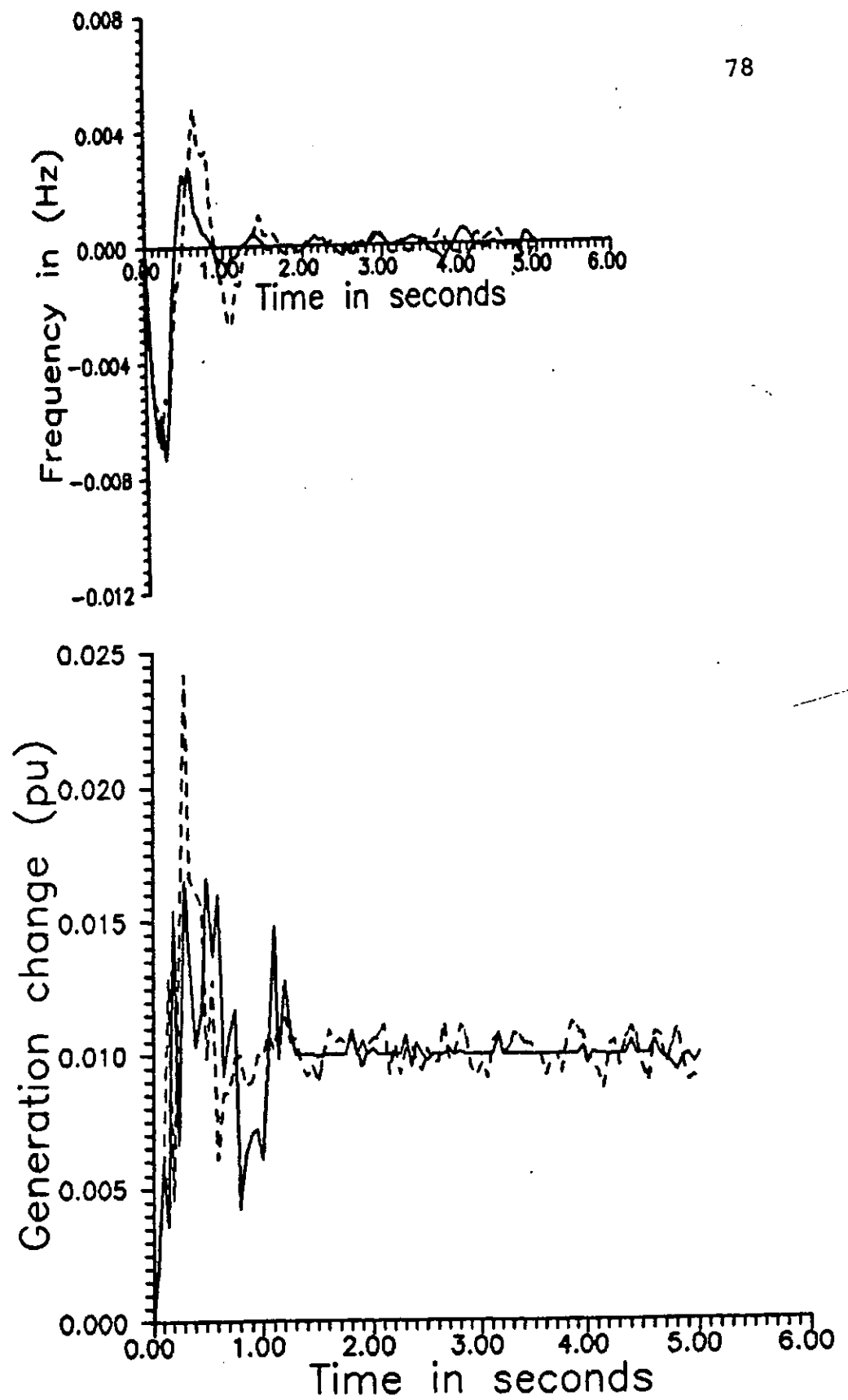
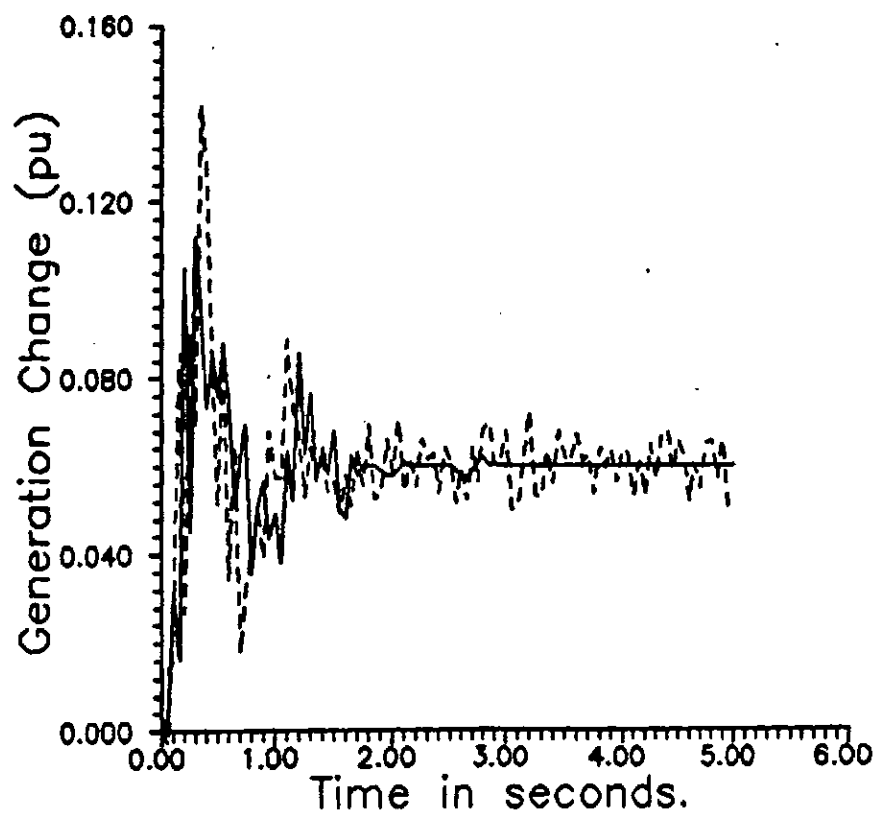
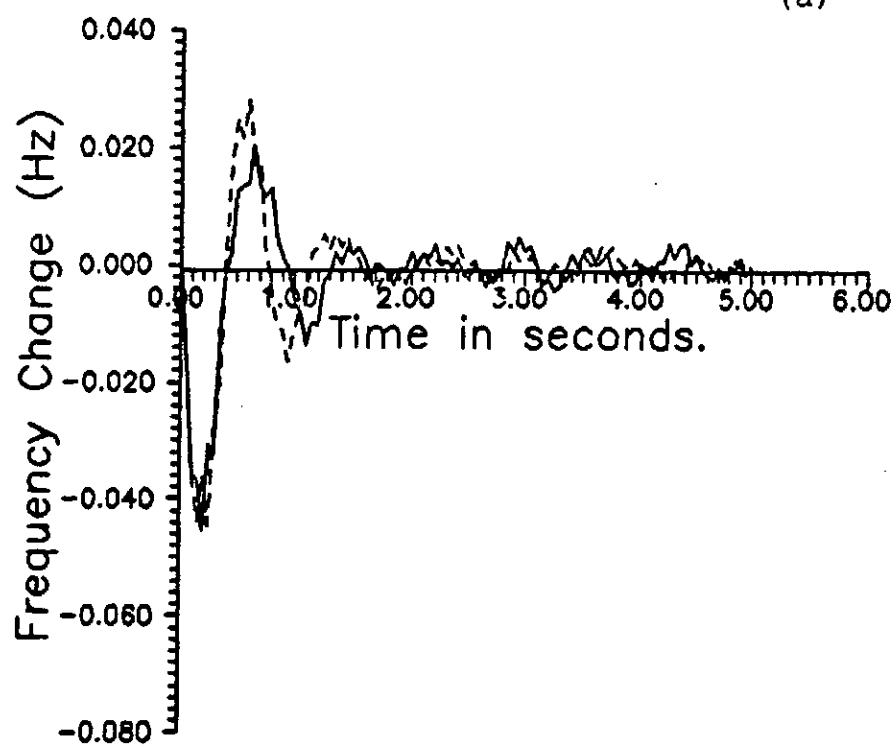


Fig.3.2: System Responses for 0.01 pu Step Change in Load  
(a) Frequency Change (b) Generation Change  
— Proposed Scheme; ---- Existing Scheme



(a)



(b)

Fig.3.3: System Response for a 0.06 pu Step Change in Load  
 (a) Generation Change (b) Frequency Change  
 —Proposed Scheme;---- Existing Scheme

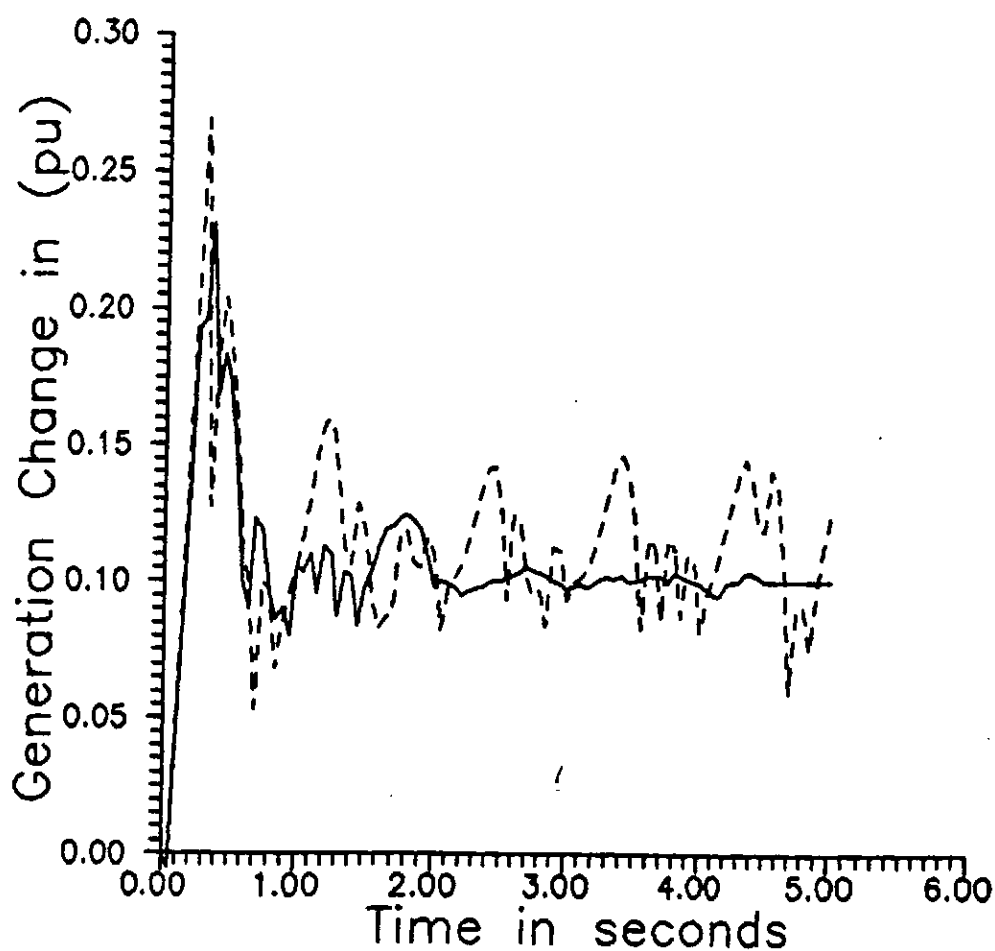
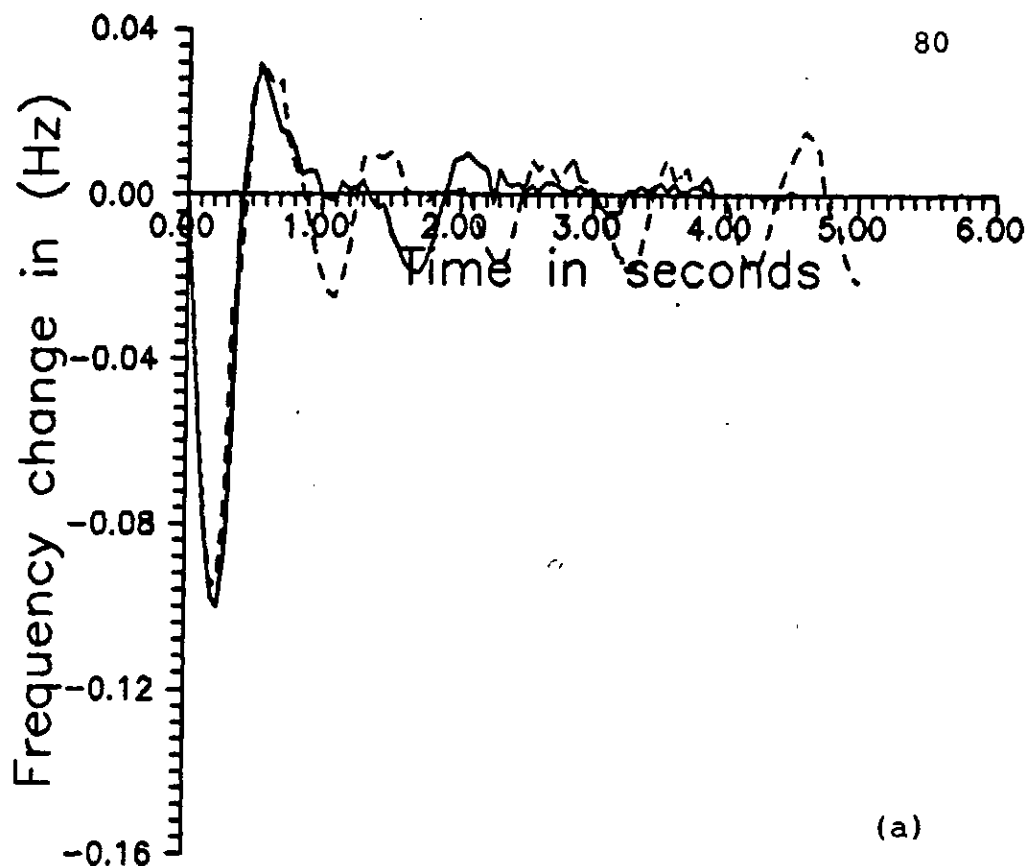


Fig.3.4 : System Responses for 0.1 pu Step Change in Load  
 (a) Frequency Change (b) Generation Change  
 — Proposed Scheme ----- Existing Scheme

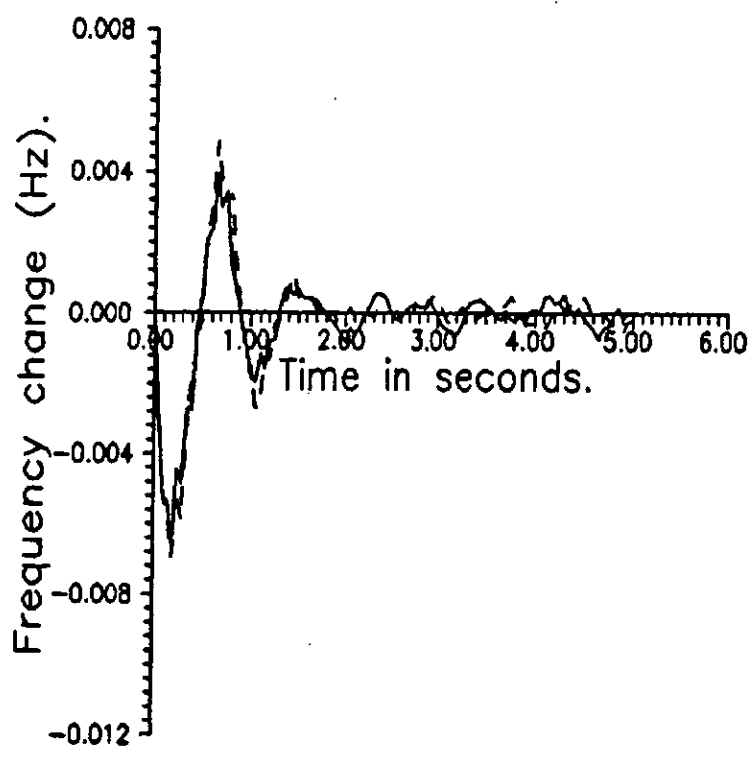
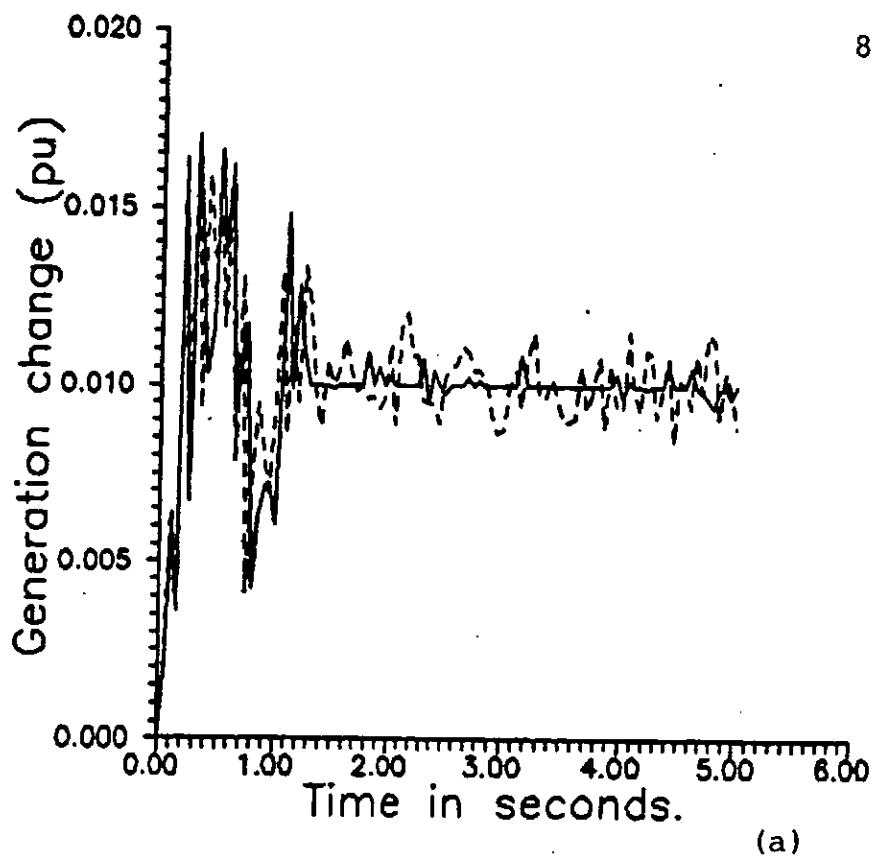


Fig.3.5: System Responses for a 0.01 pu Step Change in Load-  
with Generation Rate Constraint. (a) Generation  
Change (b) Frequency Change .  
——Proposed Scheme, ---- Existing Scheme.

determined are seen to be structurally similar to the linear regulator problem which suggests that a modified form of the conventional eigenstructure assignment technique can be employed for the computation of the hyperplane matrix  $C$ .

The synthesis of the proposed control function similarly follows a systematic procedure based on the unit vector control design approach. The resulting control function guarantees asymptotically stable sliding motion as well as ensures faster reaching of the sliding plane; in the sense that the frequency and generated power transients following a step load change settles faster than for the existing VSAGC scheme. It also has the advantage of simpler structure since only one switching action is required as opposed to the control function for VSAGC so far used in the technical literature which has the form of relays with state dependent gains. In that case, the number of switchings corresponds to the number of states, that is, the system order.

Finally, by employing a model of the power system commonly used in the technical literature, comparative simulation studies were performed to show the superiority of the proposed scheme.

In the next chapter, a computer aided design (CAD) package for the synthesis and performance evaluation of the VSAGC scheme is presented.

## CHAPTER 4

THE COMPUTER AIDED DESIGN (CAD) PACKAGE4.1 Introduction:

In the last chapter, a systematic procedure for the synthesis of variable structure automatic generation control (VSAGC) schemes was proposed and simulation results were presented to show that the controller so designed gave superior performance when compared with existing VSAGC schemes.

However, the current trend in power system control is towards computerised control. To this end, the proposed VSAGC scheme must be implementable on a dedicated and/or general purpose digital computer so as to form part of present day energy management systems (EMS) as well as serve for education/research.

This chapter presents a computer aided design (CAD) software package for the synthesis and performance evaluation of VSAGC schemes on a general purpose, Pc-AT micro-computer. The package named "The Variable Structure Automatic Generation Control Design Package" (VAGCD), is designed such that it can be used on-line in a power control centre - environment as well as for education and/or research. It is for this latter reason that VAGCD also incorporates other design techniques for VSAGC currently existing in the technical literature.

The general design principles for VAGCD are discussed in section 2 while its structure and implementation are presented in section 3. In section 4, the functions of the various subroutines as well as their sequence of execution are described. Also included is a summary of VAGCD's data requirement which is closely followed by a few concluding remarks in section 5. The flow charts for the coding of the computer programs are presented in appendix G

#### 4.2 General Design Principles for The Package

Several factors affect the design of an efficient software package. For instance the influence on a good choice of programming language of such specifications as portability, interactive capability, core algorithm selection, graphics requirement and model description is well discussed by Astrom, Martin and others [77 - 79]. On the other hand, Denham [80], has identified the pertinent design issues for any computer aided control system design package to include the following, among others:

- (i) its objectives
- (ii) its functions and
- (iii) the best way to realise these functions.

In developing VAGCD, the objectives have been to:

- Provide a tool which will enable the contemporary power system control engineer efficiently implement automatic generation control action on a general purpose PC-AT microcomputer.



- allow the VSAGC designer to fully display his intuition, skill and experience while still making use of powerful theoretical tools.
- improve the quality of continuing education in the power system industry by enhancing the learning ability of the practising engineer through exposure to theoretical models of the problems emanating from his industry.
- harness the manipulative power of the computer to minimise the level of detail with which the user (especially the technician at the power control centre) has to contend.

Therefore, the design principles for VAGCD can be summarised as follows:

- ease of use (interactiveness)
- application of graphics
- flexibility, modularity and portability
- usability in industry, education and research environments.

The package is fully interactive so as to serve a cross-section of users. Wieslander [81] classifies the users of an interactive program into four categories:-

- (i) the experienced user
- (ii) the casual user
- (iii) the beginner user and
- (iv) the batch user

The package has been designed for the first three groups of users. These user groups are known to make conflicting demands on a given package, particularly on the man-machine interface and hence, it is difficult to design an all purpose CAD tool. However the user - interface of VAGCD fulfils the following:

- the user commands the system and not vice-versa
- the software is transparent to the user
- the system commands are control engineering not computer - oriented
- all the error messages are explained in terms of what might have gone wrong and what may be done next.
- the results are expressed graphically whenever desired.

Thus each main module in the package can be executed in the 'non-expert' or 'expert' mode. On entering any of the main modules, the function of the module is summarised in one sentence, followed by the question:

Expert mode?

If the answer to this question is 'YES' or simply 'Y', the user - computer interaction is reduced to the barest minimum to save time. In the non-expert mode, the novice user is gently led to the solution of his problem.

Initially the computer has the initiative which it gradually transfers to the novice as he becomes more proficient. The expert user, on the other hand, retains the initiative and can only obtain help or advice when he so wishes.

Nevertheless, the primary design goal for VAGCD is to develop tools for the expert while a secondary goal is to make the tools usable by the novice with minimum effort.

In general, the package is designed to be run interactively on a question - and - answer basis, with intelligible prompts for all inputs required and the trapping of all unacceptable responses. Most detectable errors lead to an attempt to try the erroneous operation again, hoping for a correction (the major exception to this rule being the transfer of data to and from files). In quite a number of cases, a message indicating the nature of the error is displayed followed by an advice on what corrective measures to take. Messages in response to an error are prefixed with a three-character string which takes one of the following forms:

```
* * * Non - Fatal    error
! ! ! Fatal    error
```

A non-fatal error (\*\*\*) will lead to the repetition of the operation causing the error - usually this should mean a request to re-enter a response. On the other hand a fatal error (! ! !) will cause the termination of the program in as tidy a manner as possible.

At each point of program execution, the minimum of information is accepted in response to a prompt: for instance, single letters - usually the starting letters- are sufficient whenever non-numeric input is required.

In order to make for faster and easier execution of the programs as well as reduce the risk of typing errors, the free format input is adopted for all numerical input. Most operations may be abandoned by responding to a prompt with the escape "ESC" key; this causes the control of the program to move back a stage, (in some cases after checking that this is the intention). It follows that entering the escape - 'ESC' - key in response to successive prompts, eventually returns the user to the main menu. The only exception to this rule (for reasons of the logical structure of the program) is any question requiring a 'YES' or 'NO' answer. If the 'ESC' key is entered at this point, a message of the form

You must enter 'YES' or 'NO'

will be displayed, followed by a repetition of the question.

#### 4.3 Structure And Implementation of VAGCD

A modular structure is adopted for the package whereby there is only one main program called the "main supervisor" or "monitor" while others exist as sub-routines (submonitors) at different levels arranged in a hierarchical manner. Related subroutines at different levels are grouped to form a module which can act as a stand - alone system. Each module therefore consists of a submonitor at the highest level while other subroutines follow in the hierarchy. The main advantage of this

structure is that it allows for the use of the link-overlay technique where a module may be executed independent of others. Since only this module needs be loaded into the computer random access memory (RAM), the working core requirement of the package is drastically reduced.

The general structure of the package is shown in Fig.4.1 and consists of the main supervisor (VAGCD) and the following six modules:

1. INPUT - performs the major input functions
2. EXIST - solves the existence problem
3. REACH - solves the reachability problem
4. SIMU - evaluates the performance of the  
designed system using time domain simulation
5. AGC - implements the automatic generation  
control action
6. OUTPUT - performs the major output functions.

It is easily seen in Fig.4.1 that all the modules are at the same level in the hierarchy so that the main supervisor can access any module on an equal basis.

VAGCD is currently implemented on an industry standard, IBM-AT compatible microcomputer with an 80286 processor, 640 kilobytes RAM and 20 megabytes hard disk, under the DOS operating system version 3.2 and other latter versions. The choice of a microcomputer environment for implementing VAGCD is informed by the fact that microcomputers are comparatively cheap and are always available.

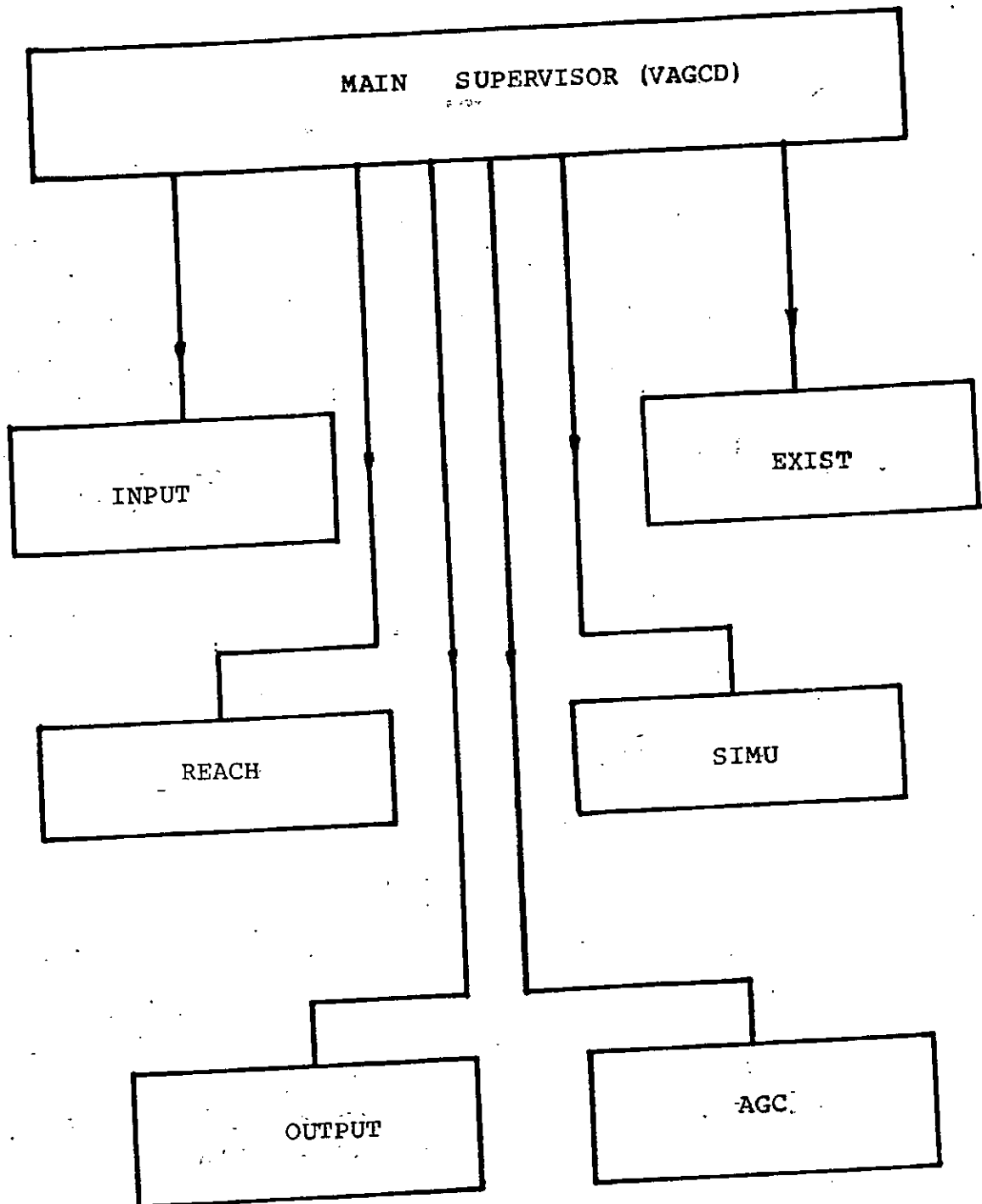


FIG.4.1: BASIC STRUCTURE OF VAGCD

The major part of the package is coded in FORTRAN-77 programming language; the only exception being the screen design which is coded in more versatile C language. The programs are thus, very portable and are made to be efficient so as to enhance the speed of computation - the particular computer currently being used runs at 10 megaHertz. It is, however, recommended that, the availability of faster machines (25 - 33 MHz) in the market should be considered in future implementations of VAGCD. This will enhance greatly, the use of the package for on-line power system control problems in the industry without any considerable increase in the system deadband.

One vital aspect of VAGCD's implementation is the flexibility of the modules. Thus, a user - owned subroutine may be added to any of the modules to effect the solution of a specific problem not strictly included in the original package design. At the monitor level, more modules can be added to the existing six in order to expand the scope of the package. For instance, an economic load-dispatch 'ELD' module may be added to compute the unit commitment of all the generators based on the fuel cost and transmission line losses. The flexibility of VAGCD also allows the user to run some commercially available application programs; though in some cases the user may need to create a batch file.

Finally, VAGCD runs in two modes: the 'Research mode' and the 'Industry mode', which is decided by the user at the monitor level. The basic difference is that the

research mode is off-line while the industry mode is on-line. In addition the AGC module does not run in the research mode for reasons which are explained in section 5.4.5. It is part of the logical design of the package that results from each mode are saved in different files for future access. There is a 'HELP' facility in each module which can be invoked to explain the required steps to run a module.

#### 4.4 Functions Of The Modules

##### 4.4.1 General Considerations

The package VAGCD is basically started in two ways depending on whether the computer used is dedicated or otherwise. On a dedicated system, the main supervisor is automatically loaded and run as soon as the computer is booted from the hard drive. On a general purpose system, VAGCD is invoked by typing the word "VAGCD" while in the subdirectory named VAGCD. Note that commands can be in either capital or lower case letters.

There is a text file named "README. Txt" located in the VAGCD subdirectory, which contains a summary of how to run the package. It is advised that users should first go through this file either on the screen or by obtaining a hard copy, before attempting to run VAGCD.

In a purely research/education environment, the research version of VAGCD which is executed by selecting the option "Research Mode" is sufficient to perform all



the necessary functions. However, the industry version runs faster since it eliminates all the interactive prompts. A detailed description of the package is given below, starting from the main supervisor.

#### 4.4.2 The Main Supervisor 'VAGCD'

The main supervisor is the overall driving routine to which control ultimately returns. It determines which part of the design process will be done next, and controls certain input and output functions.

As soon as the execution of the main supervisor starts, the screen is cleared and the user is welcomed to the package followed by the statements:

'Enter the mode please'

'D'..... Industry mode

'R'..... Research mode.

If 'D' is selected above, the existence and reachability modules are automatically executed and the results are saved in a file which is accessible to the AGC module for purposes of implementing the load-frequency control action. Note that this process assumes that all the necessary input data are in the files. If this is not so, the execution terminates with the message:

'Run the INPUT module first'

and control is returned to the monitor. If the execution is successfully completed, a message is returned to say so. To exit to the operating system, the ESC key is pressed.

On the other hand, if 'R' is chosen, the screen clears again followed by the question,

"Do you want a display of the menu?"

If the answer is 'YES' or a mere carriage return, the main menu, which consists of the list of the modules, is displayed followed by the statement:

'Enter your choice'

Otherwise, the above statement calling for choice is shown on the screen without a display of the main menu. Execution now continues by the user choosing any of the available options. Note that the INPUT module must be run first unless the input data have been entered earlier. Otherwise no other module can run successfully. As soon as the execution of any chosen module ends, control returns to the main supervisor.

#### 4.4.3 The Input Module (INPUT)

The INPUT module allows the user to enter the necessary input data for running the package. It is invoked at the monitor level by entering the word 'INPUT' or simply the letter 'I'. Two types of input data are required by the package. First is the generator data which include its unit number, the maximum generating capacity, the base generation, the maximum rate of change of real power generation etc. This set of data is required for implementing AGC and is discussed in detail

in section 4.4.5. The other set of data can be referred to as the system data and includes among others, the elements of the system, control and disturbance matrices etc. These are needed for the VSAGC design process.

As soon as the module is invoked, the INPUT sub-monitor is executed, the screen is cleared and the message:

'INPUT STAGE'

appears on the screen followed by a display of the options:

PUT - input data  
ALTER - alter existing data  
SAVE - save data in a file.

If the option 'PUT' is selected, the screen clears again and the question:

"Is data to be read from a file?"

is asked. This refers to a file in which the user has typed (on separate lines) the number of states  $n$ , the number of controls  $m$ , the rows of the system matrix  $A$ , the rows of the transposed interface matrix  $B$  and the rows of the transposed disturbance matrix  $\Gamma$ . This file must have been saved from a previous run of the package. If the user responds 'YES' to the above question, the program requests for the identity of the file with the prompt:

"Enter data file name":

The data file may have any legal file name and when this is entered, the program reads the data from the file,

displays it for the user to check and updates the working file. The working file is where the other modules which need the data will pick it up and is normally overwritten by any new set of input data. On the other hand, a response of 'NO' to the above question leads to the user being prompted to input data from the keyboard. As the data is entered, it is automatically written in the working data file in such a way as to overwrite whatever data exists there. On entry, the matrix B is checked to ensure that it is of full rank  $m$ . If it is found to be rank deficient, it must be amended before the program can continue. This process is carried out interactively and allows the user to either re-enter the entire B matrix and simply change some elements.

Once B is known to be of full rank  $m$ , the controllability of the system is tested. If  $(A,B)$  is found to be uncontrollable, the system must be altered, either by altering A or B (or both) via the use of the ALTER option. The ALTER option also incorporates the rank and controllability tests mentioned above such that after each amendment the tests are repeated until acceptable A and B matrices are obtained. The alterations mentioned here usually involve exchange of rows and columns or addition of small positive numbers. They are designed to ensure that numerical problems do not occur in subsequent stages of the design.

Finally the 'SAVE' option is used to save the data in a file where it cannot be overwritten by a future set of input data. This is necessary only in cases where it

is desired to preserve the configuration of a given system. In all cases free format input is used.

#### 4.4.4 The Hyperplane Design Module (EXIST)

The hyperplane design stage is entered when the option 'EXIST' is selected at the monitor level. The entry to the hyperplane submonitor is announced by clearing the screen and output of the message

##### HYPERPLANE DESIGN STAGE

followed by the display of the options:

```
MOD1      - system transformation
EGENS     - Eigenstructure assignment method
QUAD      - Quadratic minimization method
COMP      - Computation of C matrix from F.
```

Please enter your choice:

If this is the first time of attempting to run the 'EXIST' module for the current system, then, MOD1 must be run first. MOD1 loads the model matrices A and B into the working memory. Then it computes the  $n \times n$  transformation matrix M using either the QU algorithm or elementary matrices as explained in section 3.2. It tests for the validity of M by computing the product MB and ascertaining that the  $B_2$  is of dimension  $m \times m$  and it is nonsingular. For an acceptable M, the program then computes the product MAM' and prompts the user:

```
DISPLAY M and MAM'?
```

A 'YES' response to the above question leads to the display of both matrices, which are now saved in a file in component form (i.e,  $A_{11}$  ,  $A_{12}$ ,  $A_{21}$  and  $A_{22}$ ), and the control returns to the submonitor.

In order to determine the matrix F, either EGENS or QUAD is used. If EGENS is chosen, the screen is cleared and the heading:

'Eigenstructure Assignment Method'

is printed. Then the program invokes the subroutine CANON which converts the matrix pair ( $A_{11}$ ,  $A_{12}$ ) into controllable canonical form and displays the results on request. Then, subroutining SPEC computes the eigenvalues of matrix A and prompts the user:

Display Spectrum of A?

The user needs to know the eigenvalue spectrum of matrix A because the program will not allow the specification of any of these values as the sliding mode eigenvalues.

Having printed the spectrum of A (if requested), the program requests the sliding mode eigenvalues to be entered with a prompt for the number of complex values viz:

"Enter the no.of complex conjugate eigenvalues":

This number must be an integer between 0 and  $(n-m)/2$  inclusive. If the response is an integer within this range,

then the real and imaginary values of each pair of complex conjugate eigenvalues should be entered (each pair on one line) in response to the prompt:

"Give the real and imaginary parts of each pair":

The first figure on a row is expected to be the real part followed by the imaginary part while the second row is expected to be their conjugate pairs. The validity of the figures are correspondingly tested. If the total number of complex eigenvalues is less than the reduced system order ' $n-m$ ', a prompt is printed calling for the number of real eigenvalues followed by row-wise entering of the figures.

Now, if the system is scalar controlled, there is no freedom to assign eigenvectors. In this case, the program performs pole placement for scalar systems and returns the control to the sub-monitor. The vector  $F$  so determined can be displayed if desired.

However, if  $m > 1$ , then there is freedom to partially assign the eigenvector spectrum as described in section 3.3. Here the program prompts the user to partially assign the eigenvector spectrum for each selected eigenvalue. The eigenvector matrix so obtained is used to compute the matrix  $F$  according to the algorithm presented in section 3.3. At the end of the process, control is returned to the sub-monitor.

On the other hand, if the matrix  $F$  is to be determined using the quadratic minimization method, the screen clears and the message:

"Quadratic minimization method"

is written. Then the program calls the attention of the user to the fact that:

The form of the cost integrand is:

$\langle x, Qx \rangle$  (sliding plane penalty only).

This is followed by a prompt to enter the matrix  $Q$ . Usually  $Q$  is a diagonal matrix and the input procedure is faster if the user responds YES to the prompt:

Is the matrix  $Q$  diagonal?

In this case only one figure is expected in a row and this figure represents the diagonal element. If the response to the above question is 'NO',  $n$  elements must be entered in a row. In either case the matrix  $Q$  is tested for positive definiteness. If this test fails, a message is displayed signifying the termination of the program;

" $Q$  must be positive Definite"

followed by a prompt to enter another matrix. The procedure described in reference 68 is now followed to find the matrix  $F$  and control passes back to the sub-monitor.

Having obtained the  $F$  matrix, it remains to compute the hyperplane matrix  $C$  using the procedure of section 3.3. Now the subroutine COMP is selected at the sub-monitor level and the following prompt appears after the screen is cleared:



"Do you wish to specify CB?"

If the answer is YES, the next prompt:

"Enter the values of CB"

follows. The matrix CB will be  $m \times m$  and hence  $m$  rows are expected to be entered. If the answer to the question is 'NO', then  $CB = I_m$  as explained in section 3.3 and the matrix C is determined. At the end of this process, the matrix C is displayed with a prompt to press ESC if you want to exit. Note that in the industry mode, only the eigenstructure assignment method is executed. The selected eigenvalue spectrum must have been previously entered by the control centre personnel on duty, using the INPUT module.

#### 4.4.5 The Control Functions Design Module (REACH)

This module should be selected only after the hyperplane module 'EXIST' must have been run. This is because, the module 'REACH' makes use of the matrix F or C determined in EXIST. Once the REACH sub-monitor is being entered, it automatically searches the relevant file for matrices F and C. Failure to find these matrices leads to the message

'Matrices F and C not found;

Run EXIST first'.

Otherwise, the screen clears and the message

CONTROL DESIGN STAGE

is printed followed by the display of two available options as follows:

The following control schemes are available:

Linear Feedback + Scaled unit Vector (UVF)

Linear Feedback + relays (hierarchical) (HRC)

Please enter your choice.

On entering the word UVF, the screen clears again and the following message is displayed:

Unit Vector Control Design.

Then the program automatically runs the subroutine MOD2 which computes the second transformation matrix  $M_2$  together with matrices  $\phi_1 - \phi_3$ . Then it prompts the user for eigenvalue spectrum of the matrix  $\phi$  which is expected to be diagonal. One value must be entered in a row. Then the coefficient matrix  $L$  of the linear control law  $Lx$  is computed as described in section 3.4. In order to compute the nonlinear control law, (see section 3.4) the program invokes subroutine 'LYP' to solve the Lyapunov equation and determine the positive definite matrix  $V$  in section 3.4. Then, the program prompts for the design parameter  $\rho$  by the message

Enter the design parameter  $\rho$ .

The value of  $\rho$  must be greater than zero and any value entered must be tested for validity. Having entered a valid  $\rho$ , the non-linear gain matrix  $G$  and the non-linear factor matrix  $H$  are then determined. If the response to

the offer of a display is 'YES'; the program displays the coefficient matrices L, G and H and returns control to the submonitor.

On the other hand, if the option 'HRC' is selected at the submonitor level, the screen clears and the message

#### CONTROL HIERARCHY METHOD

is printed. The control hierarchy algorithm is outlined in appendix F and requires the selection of both the hierarchy of hyperplanes and the hierarchy of controls. For a scalar controlled case, the control hierarchy algorithm reduces to relays with state - dependent gains which is explained in chapter 2.

Now the user must select the order in which the hyperplanes are to be hit by entering a permutation of the integers 1 to m (where m is the number of controls) in response to the request

Specify the hierarchy of hyperplanes  $P(j)$ ,  $j = 1, \dots, m$ .

Next, the user must determine the order in which the control functions should be introduced in response to the prompt

Select the Control Hierarchy  $q(j)$ ,  $j = 1, \dots, m$ .

This should be another (not necessarily different) permutation of the integers 1 to m. Occasionally the control hierarchy may not be possible for a given hyperplane hierarchy and the program gives the prompt;

Invalid permutation of hierarchy given:  
followed by the request

Select a different control hierarchy  $q(j)$ ,  $j = 1, \dots, m$ .

If it is desired to alter the hyperplane hierarchy as well, the escape 'ESC' key is used to return control to the sub-monitor and the process resumed afresh. Having obtained the hierarchies  $p$  and  $q$ , the program prompts another request:

Give  $m$  positive design parameters  $\text{GAMMA}$  which determine the rate of approach to the switching surfaces and the size of the chattering motion. If valid selections are made for these parameters, the computation of the control is completed and the program offers to display the control design by the prompt

Display Control design?

If the response is 'YES', the screen is cleared, the heading 'Control Design' is printed, followed by the hyperplane hierarchy  $P(j)$ , the control hierarchy  $q(j)$  and the bounds on the parameters  $\alpha_1$  and  $\beta_1$  which satisfy the sliding plane condition  $\sigma \dot{\sigma} \leq 0$  on each of the sliding surfaces. Control is then returned to the sub-monitor. In either of the cases, the computed parameters are saved in a working file to be used by the simulation module SIMU.

#### 4.4.6 The Simulation Module SIMU

This module is used to perform a time simulation of the designed VSAGC scheme under various operating conditions. This implies that the other three modules (INPUT, EXIST and REACH) must have been executed before SIMU since they have to provide the data required.

The simulation module solves the state equation representing the power system model eqn.(3.1) using a fourth-order Runge Kutta integration algorithm. It also implements the controller (either the unit vector control scheme or the hierarchical control scheme), incorporates the system disturbance function and plots the results if desired. The user is expected to interactively enter some of the necessary parameters like, initial conditions, step magnitude of the load demand function, starting time, time step size and stopping time.

As soon as the SIMU sub-monitor is being entered, it automatically checks for all the necessary data. If any one of them is unavailable, the program gives the following prompt:

(Name of data) Not Available:

and returns control to the main monitor for the user to run the relevant module before coming back to SIMU. However, if every data is available, the screen is cleared and the heading

#### SIMULATION STAGE

is printed followed by the request and explanation:

Please Nominate the Output Device:

(Enter \* or 5 for screen or any other number  
for line printer)

If the screen is chosen, the results are displayed on the screen and not saved in any file. A choice of line printer causes the results to be saved in a named file, in

response to the prompt

Enter File Name:

The file name to be entered could be any legal file name. Having entered a valid file name, the program loads the A, B, T and C matrices as well as the coefficient matrices of the control law. It then prompts the user for the step size of the load demand;

Enter the step Magnitude of the Load Demand:

This value is measured in per unit and hence must be less than unity. After a successful validity test, the program prompts for the initial time, the time step size and the final time in that order. Then it prompts for the initial condition vector by:

Enter The Initial Condition Vector (one row).

Having entered valid initial condition values, the program calls subroutine RUNG to implement the 4th-order Runge Kutta integration algorithm. During this execution, subroutine DIST is called to implement the disturbance function. The user is also prompted to select the control function:

Enter The Choice Of Controls:

- 1 - Unit vector control
- 2 - Hierarchical Control

A valid choice of the control function leads to the completion of the SIMU module and the control returns to the main monitor. The results are now stored in a file

for the use of the output module. If screen display had been selected, the results scroll on the screen, one page at a time. At the end of each page the user is expected to press the 'enter' key for the scrolling to continue until the last line is displayed when control returns to the main supervisor.

#### 4.4.7 The Output Module (OUTPUT)

The function of this module is to produce a hard copy of the design and simulation results. On entering the OUPUT sub-monitor, the screen clears and a heading:

OUTPUT STAGE

appears on the screen followed by the prompt

Enter The File Name.

Having entered a valid file name, the program responds with the prompt:

Do you wish to plot the Data?

If the answer is 'NO', the program assumes that the user wants a hard copy of the data contained in the file and then responds with the following prompt:

Enter The Format Specification:

The format specification may include identification headings, but it must be a valid format specification. On receiving the format, the program transfers the data to the printer buffer for the production of the hard copy.

On the other hand, if it is desired to plot the data, the program quickly invokes the application program GRAPHER - for the production of the plots. The user can then specify the size of the plot, the range of data to be used, the y and x-axes labels, the graph heading etc. These specifications are entered interactively and a view of the current configuration is possible at any stage. When a satisfactory plot is viewed on the screen, the program invokes the plot subroutine to produce a hard copy.

#### 4.4.8 The Automatic Generation Control Implementation

##### Module (AGC)

The AGC module implements a closed loop control scheme which regulates the frequency and tie-line power interchange deviations (where applicable) within specified tolerance limits. In general, the supervisory control and data acquisition (SCADA) system scans the current network frequency  $f$  and tie - line power interchange  $P_{ti}$  ( $i = 1, 2$ , where  $2$  is the number of ties) and compares them with their respective scheduled values,  $f_0$  and  $P_{ti0}$ . At a given sampling interval  $kT_s$ , (where  $T_s$  is the sampling period and  $k = 1, 2, \dots$ ), the frequency and tie-line power deviations  $\Delta f$  and  $\Delta P_{ti}$  respectively are fed to the AGC module which then, computes the area control error (ACE). The ACE is then processed by the control algorithm into a power command signal representing the total extra power needed to be generated. This command signal is distributed



according to a distribution logic to all the generators participating in the AGC action, so as to increase the real power generation.

The AGC module is invoked by choosing the 'AGC' option at the monitor level. Then, the screen clears and the computer prints the message;

----AGC IMPLEMENTATION STAGE ----

Enter The Desired Mode:

- 1 - Single area control;
- 2 - Multiarea control;

The basic difference between the two modes is that, while mode 1 only regulates the frequency deviation, mode 2, in addition, incorporates tie - line power control. Assuming that the general case of mode 2 is selected, the screen clears again and the message:

MULTIAREA CONTROL

is printed followed by the question:

Have you updated the power system data?

If the answer to this question is 'NO', the computer prints the message:

Run INPUT in the Industry Mode First!

after which the program exits to the main monitor. The user then selects the INPUT module and enters the power system data. The types of data required are listed at the end of this section. However, if the answer is YES, the execution proceeds in the following steps:

### Step 1:

The deviation in frequency  $\Delta f$  and tie-line power interchange  $\Delta P_{Ei}$  ( $i = 1, \ell$ ) are scanned at the output of the SCADA system. Four samples of each are taken and the mean is computed after a validity check. The validity check compares each sample with the preceeding one and also each mean value with the mean value of the previous group of samples. If the measurand is overranged in several consecutive scanning intervals, a message is output which requires the control centre operator to take appropriate action. If, however, the validity check is successful, the mean values of the measurands are reserved for step 2.

### Step 2:

Since each area control is autonomous, the program first checks if the load variation is in its own area. If it is not, the program terminates with the message:

Load Variation In Neighbouring Area!

Otherwise the area control error (ACE) is computed using the formular

$$ACE = \sum_{i=1}^{\ell} \Delta P_{Ei} + \beta \Delta f \quad (4.1)$$

where

$\Delta P_{Ei}$  - tie line power deviation in tie-line  $i$  (Mw)

$\Delta f$  - network frequency deviation (Hz)

$\beta$  - Area bias (Mw/Hz)

The technique employed here to determine in which area the load varied is shown in appendix A.

Step 3:

The control algorithm is now implemented by solving for  $u$  in the variable structure control law, [eqn. (3.29)] with the state vector  $x$  replaced by ACE

$$u_k = L[ACE]_j + \frac{\rho G[ACE]_j}{||H[ACE]_j||} \quad (4.2)$$

where the subscript  $k$  denotes the  $k^{\text{th}}$  sampling period while  $[ACE]_j$  represents the value of ACE during the  $j$ -th period;  $L$ ,  $G$  and  $H$  are the coefficient matrices of the control law while  $\rho$  is a design parameter as defined in section 3.4. The replacement of the state vector  $x$  by the ACE is justified by practical considerations since only the two state  $\Delta f$  and  $\Delta P_t$  are available for measurement at the power control centre.

Step 4:

Having obtained the total power command signal  $u_k$  at the  $k$ -th sampling period, the next logical step is to share the signal among all the generators participating in the AGC scheme. If the number of participating generators is  $m$ , then, a participation factor  $\gamma_i$  may be defined such that;

$$\sum_{i=1}^m \gamma_i = 1 \quad (4.3)$$

where  $\gamma_i$  is the fraction of the total power command signal to be sent to the  $i$ -th generating unit. Therefore, the control signal  $\Delta P_{ci}$  sent to the  $i$ -th generating unit at the  $k$ -th sampling period is given by

$$\Delta P_{ci} = \gamma_i u_k \quad (4.4)$$

The power allocation to generator  $i$  must respect the static and dynamic limits of the generating unit concerned. Observance of the static limit is ensured by comparing the total power command signal going into generator  $i$  (ie  $\Delta P_{ci} + P_{ci}$ ; where  $P_{ci}$  is the command signal for base load) with the specified static limit of generator  $i$ , so that the absolute power command signal is clamped at the static limit. In the case of dynamic limits, a software gradient limiter is used to prevent the induced rate of change of generation from bumping beyond the limit set for generator  $i$ . In addition, the power allocation formula (4.4), should satisfy the dictates of AGC and to a reasonable extent, those of economic load dispatch (ELD).

#### Step 5:

At the end of the computations, the program offers to display the current real power generation set points of all the generators participating in the AGC scheme by the question:

Display power generation set points?

If the answer to the above question is YES, the screen clears and the heading:

----- Current Power Generation Set Points -----

is printed, followed by a page by page listing of the set points.

Note that the AGC module can be run automatically whenever the control computer scans a frequency and/or tie-line power deviation beyond a specified threshold value. Due to the peculiarities of the Nigerian power system, this threshold value is currently set at 0.1Hz. In order to enhance the on-line use of the VSAGC scheme, the following power system data must be updated at the beginning of each day

1. Total number of generators on AGC (m)
2. Nominal frequency  $f_0$  (Hz)
3. Scheduled Interchange power with area i  $P_{ti}$  (Mw)
4. Estimated Spinning reserve required (Mw)
5. Total power available for network control (Mw)
6. Area bias (Mw/Hz)

For each generating unit on AGC the following data are required:

7. Unit number (numerical identification number)
8. Type (Hydro, steam or gas)
9. Base load ( $P_{ci}$ )
10. Participation factor ( $\gamma$ )
11. Required rate of change of load (Mw/seconds)

12. Rate of load change limit (Mw/Sec.)
13. Required generating capacity (Mw)
14. Maximum generating capacity (Mw)
15. Minimum generating capacity (Mw)

#### 4.5 Conclusion

This chapter has presented a computer aided design software package for the synthesis of VSAGC schemes on a general purpose, industry standard PC - AT microcomputer. It was shown that the package could implement automatic generation control action in a power control centre environment, provided that an adequate supervisory control and data acquisition (SCADA) system is available. Performance evaluation of VSAGC schemes was also shown to be easily undertaken by the use of this package to such a level that both hard copy and screen plots of the relevant data could be obtained.

In the next chapter, this package will be employed to synthesize VSAGC schemes for the Nigerian power system based on three proposed operating models.

## CHAPTER FIVE

APPLICATION OF THE PROPOSED VSAGC STRATEGY TO THE MODEL OF  
THE NIGERIAN POWER SYSTEM.5.1 Introduction

The last chapter presented a computer aided design (CAD) package for the synthesis, performance evaluation and implementation of a proposed variable structure automatic generation control (VSAGC) strategy. The package named 'VAGCD' was shown to be fully interactive and capable of on-line usage in a power control centre environment.

In this chapter, the package 'VAGCD' is deployed to synthesize VSAGC schemes for models of the Nigerian power system. Three analytical models of the Nigerian power system are proposed, each representing a different but possible operating strategy as will be shown in section two.

The performance of the Nigerian power system under variable structure control is also investigated for different working conditions, using digital computer simulation. In order to enhance the applicability of the results so obtained, certain linear and non-linear phenomena which exist in practical power systems are simulated in the study. These phenomena include amongst others; the effect of changes in the inherent system load-frequency characteristics; the effect of changes in the temporary and permanent droop settings as well as the washout time constant; the effect of water compressibility commonly called the water hammer

effect; deadband effects and constraints on the rate of change of generation. The chapter ends with a discussion of the results, followed by a few concluding remarks.

## 5.2 Models Of The Nigerian Power System

### 5.2.1 General Considerations

In order to design a controller for a given dynamical plant, the control engineer first captures the salient features of the plant dynamics in an abstraction - called a mathematical model. Modern control theory, where the subject matter of this thesis belongs, presents this plant model as a system of first order vector - matrix differential equations known as the state-space or state-variable representation. The main objective of this section therefore, is to develop mathematical models of the megawatt - frequency dynamics of the Nigerian electric power system suitable for the application of modern control theory to achieve automatic generation control.

It is standard practice in conventional power system operation, to control the real power balance in the system by controlling the driving torques of the individual turbines via the speed governing mechanism. The load-frequency dynamics (often called the megawatt - frequency dynamics) of a typical power system, can, therefore be characterised by the interaction of three closely related subsystems viz:

- The governing mechanism
- The turbine dynamics and
- The grid network - frequency dynamics.



How these subsystems can be represented analytically has attracted a lot of interest over the past three decades [21 - 28]. In each case, the accuracy of the model so derived depends on the problem the author has set out to solve and the use for which the results are meant. For instance, if the aim is purely academic, a simplified linear model suffices [28], quite unlike when a real life engineering problem is to be solved. However, a typical power system is non-linear with parameters varying with system operating point.

Furthermore, the structure of any power system is unique. The uniqueness stems from such factors as generation mix (ie, the percentage of hydro, steam and gas plants etc), their relative locations in the defined region (country, state, district etc) and the individual design of the power equipments in use. The Nigerian power system consists of hydrogenerating plants at Kainji, Jebba and Shiroro and Fossil - fueled steam and gas plants scattered in the southern parts of the country, notably - Egbin, Afam and Sapele. These generating plants feed a single grid network and are assumed to form a coherent group characterised by a nominal frequency of 50Hertz. In other words, the current operating strategy of the Nigerian power system is that the whole country is regarded as a single control area with a power control centre at Oshogbo. A map of the Nigerian grid system is shown in Fig. 5.1A [82].

For reasons such as rate of change of generation, it is standard practice to employ hydrogenerating units with adjustable blades (where available) for the control of

# MAP OF NIGERIA SHOWING NEPA GRID SYSTEM 1990

118

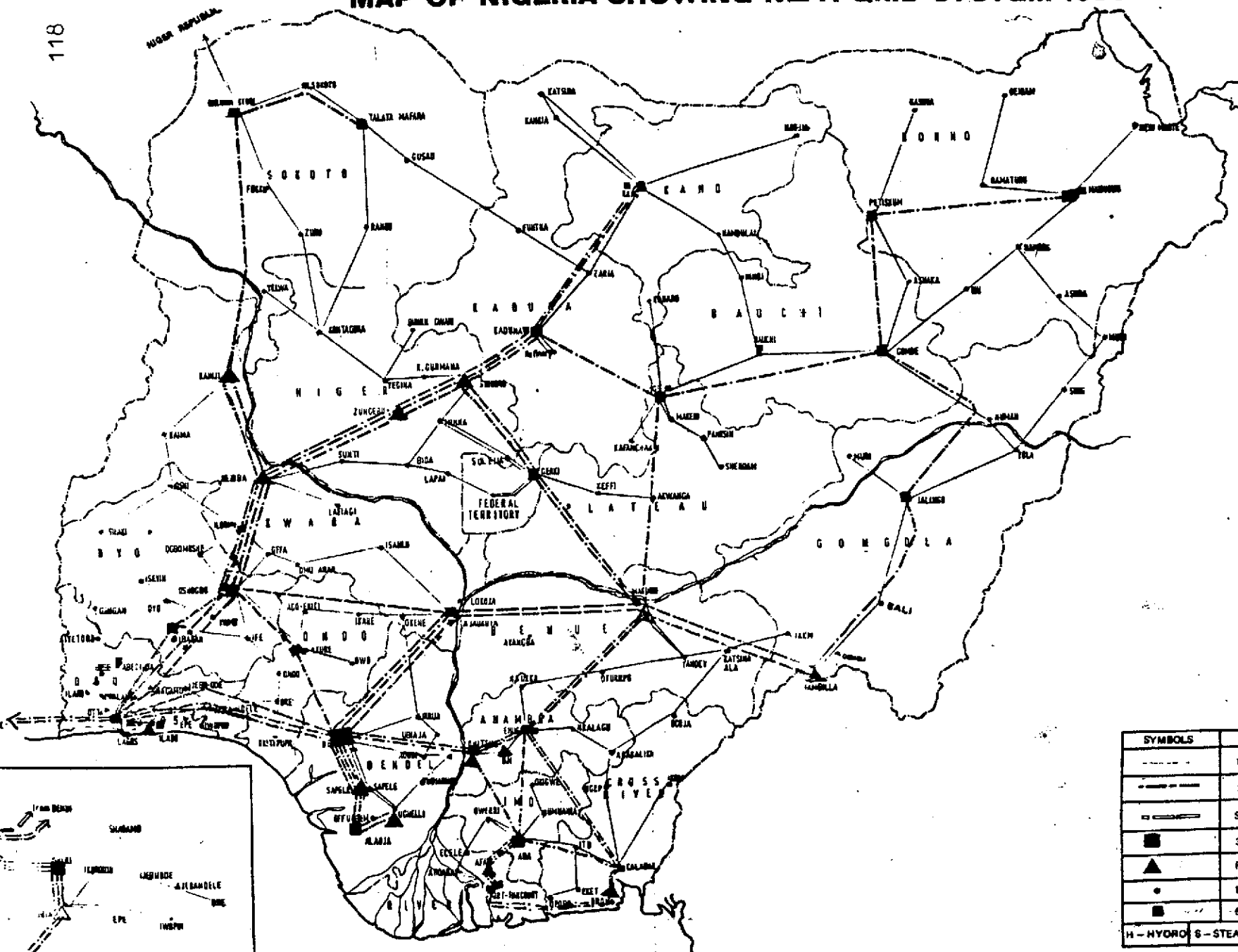


Fig. 5.1a

SYMBOLS	LEGEND
---	132KV LINES
----	330KV LINES
=====	SUPER GRID LINES
■	330KV SUBSTATION
▲	POWER STATION
●	132KV SUBSTATION
■	STATE CAPITALS
H - HYDRO	S - STEAM
G - GAS	C - COAL

LAGOS METROPOLITAN AREA

sustained load changes and steam/gas units for cyclic load changes. Consequently two hydro units with adjustable blades at Kainji and the steam plants at Egbin - for their high capacity - have been selected in this thesis for the purposes of deriving an automatic generation control (AGC) model of the Nigerian power system.

However, due to the co-ordination problem that arises in power system modelling for AGC studies [21, 25-30], it is conventional to assume that a given control area (like Nigeria for instance) consists of either predominantly hydro or steam/gas generating plants. Based on this assumption, three AGC models are proposed for the Nigerian power system representing three possible operating strategies -viz:

- (i) As a single control area consisting of predominantly hydro-generating plants
- (ii) As a single control area consisting of predominantly steam/gas generating plants
- (iii) As two interconnected areas with one area consisting of predominantly hydro plants while the other area consists of steam/gas plants.

In the technical literature so far, most investigators into the application of modern control theory to the AGC problem have assumed first order load perturbations. Therefore, they limited their simulations to the incremental linear model dynamics of the power system load-frequency interaction [28 - 30]. Given the observed characteristics (wide variations in load/generation demand) of the Nigerian

power system, results based on the incremental linear models may prove unsatisfactory for purposes of sound engineering decisions. The models developed here are non-linear so as to represent as closely as possible the actual system dynamics.

In developing the proposed models, the procedure adopted is to first derive the governing system and turbine dynamic equations for the hydro and steam generating units respectively. Each pair is then merged with the load - frequency dynamics model of the grid network to complete the desired analytical representation of the entire system. Therefore, sub-section 5.2 presents the derivation of the nonlinear hydro-governing equations as well as the necessary modifications to obtain the equations for the steam equivalent. This is followed by the derivation of the turbine dynamic equations and those of the load-frequency interaction of the grid network. The three sub-models are then, combined to obtain the complete analytical model for the AGC of the Nigerian electric power system.

#### 5.2.2 The Governing System Model

The model of the governor developed here is based on the linkage equations of a stabilized hydraulic amplifier. In order to improve on the accuracy of the model, the following nonlinear effects have been considered:

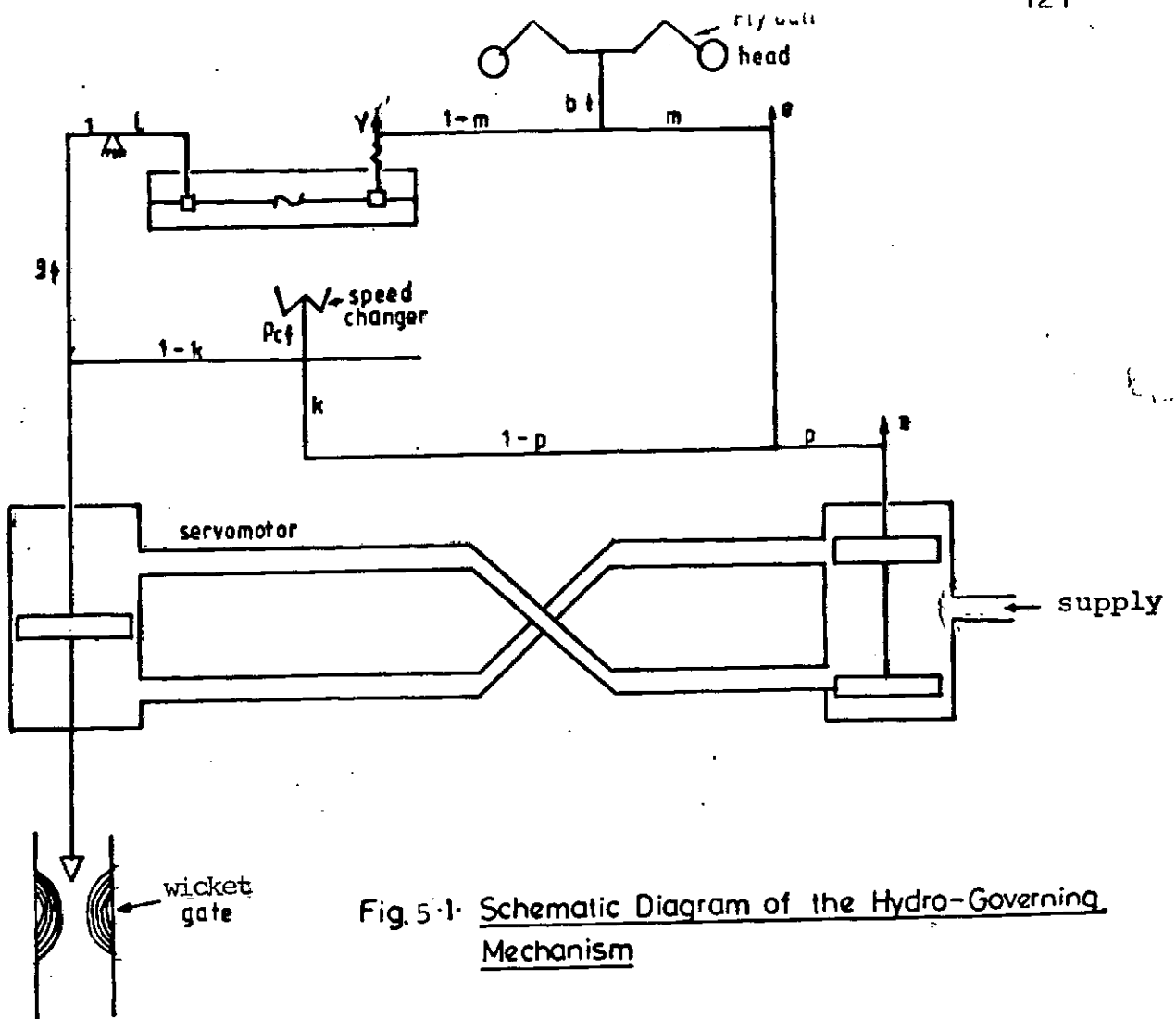


Fig. 5-1. Schematic Diagram of the Hydro-Governing Mechanism

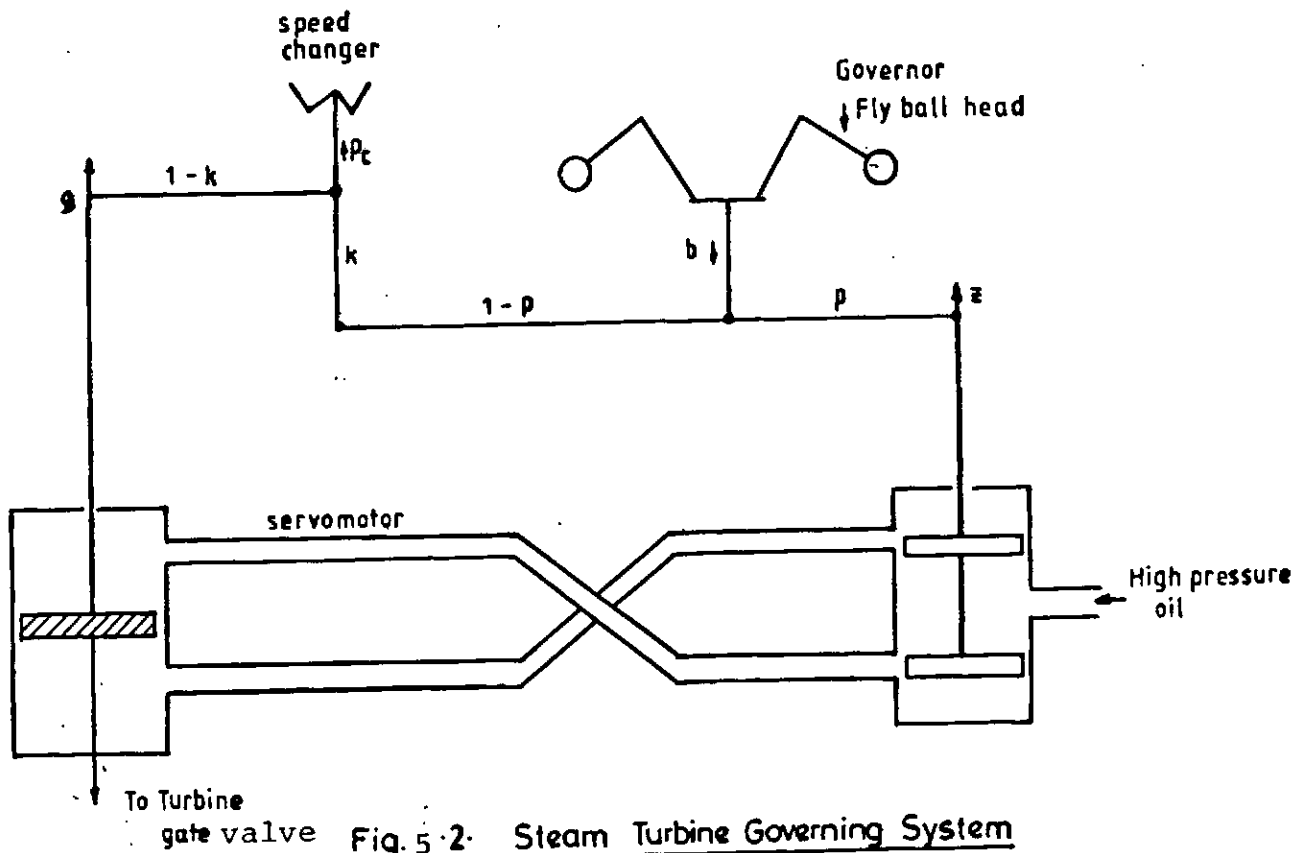


Fig. 5-2. Steam Turbine Governing System

- I. Finite gain constraints of the combined pilot valve and servo valve.
- II. Constraints of the gate servo-motor velocity and position
- III. Variation of turbine characteristics with turbine operating point (within the normal operating range)
- IV. Deadband effects including telemetering time.

A generalised linkage system is shown in Fig. 5.1.

It is assumed that all uncertain phenomena within the turbine have negligible effect on its response as detected by the governing system. This implies that the boiler produces enough steam in a steam powered generator or that enough water is in the reservoir of a hydro - generating unit to allow a desired steady state operating point for the turbine.

It is also assumed that the turbine torque at rated speed and head/steam pressure is directly proportional to gate/valve sensor reading from no load gate/valve position to full load opening. Note that at no load, the gate/valve is not fully closed (due to friction and windage losses), just as it is not completely open at full load. The implication of the above assumption is that the gate/valve position sensor - reading in per unit (on a base of fully opened gate/valve to fully closed gate/valve) must be corrected to conform with plant dynamics within the linear range. Finally the linkage rods are assumed inelastic.

Within the framework of the above assumptions, dynamic equations for the governing mechanism are derived below for

both the hydro and steam generating sets.

#### 5.2.2.1 Dynamic Model of The Hydro - Governing Mechanism

The diagram of Fig.5.1 is a typical linkage arrangement for a hydro - governing system. The feedback arm linking the speed changer, controls the permanent droop setting of the generating set while the second arm via the dash-pot, fixes the temporary droop characteristics. The phenomenon of 'temporary droop' is peculiar to hydro-generating units. It is introduced to counter the destabilizing effect of the water inertia during transient operation [24,34]. The water inertia tends to initially increase generation in response to a 'decrease generation' command and vice versa.

Neglecting the time of action of the pilot valve of the hydraulic servomotor, the linkage relations are derived by considering the final effects of a given perturbation. For instance, if the system has experienced a frequency dip, necessitating a command for increased generation, the fly ball link rod is moved in the direction -b; (Fig.5.1). From perturbation theory and superposition principle, the displacements y and e are related to b as follows:-

$$-b = \left. \frac{\partial b}{\partial y} \right|_e y + \left. \frac{\partial b}{\partial e} \right|_y e \quad (5.1)$$

where, from similar triangles,

$$\left. \frac{\partial b}{\partial y} \right|_e = m \quad \text{and} \quad \left. \frac{\partial b}{\partial e} \right|_y = 1 - m \quad (5.2)$$

and  $b$  is the per unit value of the final flyball link rod displacement while  $e$  and  $y$  are the corresponding normalized displacements of other link rods (see Fig.5.1). Hence, from eqns.(5.1) and (5.2)

$$-b = (1 - m)e + my \quad (5.3)$$

Similarly, displacements  $g$ ,  $e$  and  $z$  are related by

$$e = (1 - p)z + kpg \quad (5.4)$$

where  $k$  and  $p$  are as shown in Fig.5.1. Since the aim is to obtain an expression relating the input  $b$  (representing either a 'raise generation command' or 'lower generation command') and  $g$  representing the movement of the wicket gates,  $e$  may be eliminated from eqn.5.3 to yield:

$$-b = (1-m)pkg + (1-m)(1-p)z + my \quad (5.5)$$

The expression for permanent droop  $R$  may be obtained by imposing the condition for stationary wicket gates in which case  $z = y = 0$ , so that eqn.(5.5) reduces to

$$-b = (1-m)kpg \quad (5.6)$$

or



$$R = \frac{-b}{g} = (1-m)kp \quad (5.7)$$

Similarly, to derive an expression for the temporary droop  $r$ , the dash pot is locked solid so that  $y = \ell g$  in Fig.5.1 and the speed changer is unperturbed. In other words, the feedback link for the permanent droop setting is assumed non-existent so that  $k$  vanishes in eqn.5.5 while  $z = 0$ , giving:

$$-b = my = m\ell g \quad (5.8)$$

or

$$r = \frac{-b}{g} = m\ell \quad (5.9)$$

For a given perturbation, the dashpot displacement may be represented as  $y = \ell g$  while the dashpot dynamics are given by

$$T_R(\dot{y} - \ell \dot{g}) = -y \quad (5.10)$$

where  $T_R$  is the dashpot time constant and  $y$  is proportional to force. Using eqn.(5.9) in eqn.(5.10) gives the dashpot differential equation as:

$$T_R(\dot{y} - \frac{r}{m} \dot{g}) = -y \quad (5.11)$$

Now, by solving eqn.(5.3) for  $y$  and substituting in eqn.(5.11) gives  $\dot{y}$  as

$$\dot{y} = \frac{1}{T_R} \left[ \frac{b}{m} + \frac{(1-m)e}{m} \right] + \frac{r}{m} \dot{g} \quad (5.12)$$

Then, differentiating eqn. (5.3) with respect to time and substituting for  $\dot{y}$  given above yields

$$\dot{e} = -\frac{1}{1-m} \dot{b} - \frac{r}{1-m} \dot{g} - \frac{e}{T_R} - \frac{b}{(1-m)T_R} \quad (5.13)$$

When the governor opens the turbine gates in Fig. 5.1, the water column is allowed to hit the turbine blades. It follows that the link between the governor, the water column and the turbine is provided by the motion  $g$  of the wicket gates produced by the servomotor. Hence, the governor linkage differential equation is related to the equations for the turbine and water column by the servomotor equation

$$\dot{g} = f_n(k_h z, g, \dot{g}) \quad (5.14)$$

where  $f_n(\cdot)$  stands for 'function of' and  $k_h$  is an equivalent small signal gain relating servomotor velocity to the displacement  $z$  when the pilot actuator valve is assumed to act instantaneously. By substituting for  $z$  from eqn. (5.4) and using eqn. (5.7), the servomotor equation (5.14) transforms to:

$$\dot{g} = f_n \left[ k_h \left( \frac{e}{1-p} - \frac{R g}{(1-m)(1-p)} \right), g, \dot{g} \right] \quad (5.15)$$

Let  $C_h$  and  $\phi_h$  be defined by

$$C_h = \frac{\Delta}{\omega_n} e(1-m) \quad (5.16a)$$

$$\phi_h \triangleq \frac{k_h}{(1-m)(1-p)} \quad (5.16b)$$

Then substituting eqn. (5.16) into (5.15) yields the following governing system equations:

$$\dot{c}_h = -\dot{b} - rg - \frac{1}{T_R} (c_h + b) \quad (5.17)$$

$$\dot{g} = f_n [\phi_h (c_h - Rg), g, \dot{g}] \quad (5.18)$$

Note that the signal  $P_c$  from the AGC equipment is applied to the speed changer of the governing system. This causes a change in generation resulting to a change in frequency which is feedback via the governing mechanism. Therefore the final flyball motion  $b$  is proportional to the interaction between the AGC signal  $P_c$  and the frequency feedback signal  $\Delta f$  ie

$$b = P_c - k_t \Delta f \quad (5.19)$$

where  $k_t$  is a constant representing the transducer gain. In practice,  $k_t$  is equal to the reciprocal of the permanent speed regulation 'R'.

It is also to be noted however that the explicit form of the functional relation of eqn. (5.18) is dependent on the constraints imposed on  $g$  and  $\dot{g}$  by the design of the governor and servomotors. Such constraints include the maximum gate opening and closing velocities, the degree of damping etc. At an instant when none of the constraints exists, eqn. (5.18) reduces to

$$\dot{g} = \phi_h (c_h - Rg) \quad (5.20)$$

This form is utilised in Appendix B for deriving an equivalent linear model for the hydro governing system.

#### 5.2.2.2 Speed - Governing System Model For Steam Turbine

The basic difference between the hydro - governing mechanism and its steam counter - part is the absence of the dashpot component in the latter, due to the relatively low inertia of the pressurised steam. The linkage diagram of a typical speed governing mechanism for a steam turbine is shown in Fig.5.2.

Following the same reasoning as in the hydro - governing case, if a 'raise generation' command is applied to the governor, the flyball link moves a vertical distance  $b$  in the direction shown. The linkage relation for this motion is obtained as

$$b = (1 - p)z + kpg \quad (5.21)$$

As in the previous sub-section, the permanent droop' expression is derived by equating  $z = 0$  in eqn.(5.21) to obtain

$$R = \frac{b}{g} = kp \quad (5.22)$$

Imposing the assumption that the boiler produces enough steam at the required pressure, the relationship between the governor linkage differential equation and the turbine dynamics can be expressed by the nonlinear servomotor

equation viz:

$$\dot{g} = f_n(k_s z, \dot{g}, g) \quad (5.23)$$

where all the parameters are as defined in section 5.2.2.1 and subscript 's' stands for steam - plant. By making use of eqns. (5.21) and (5.22) to eliminate  $z$  in eqn. (5.23) and letting

$$\phi_s = \frac{k_s}{1-p} \quad (5.24)$$

eqn. (5.23) can be written in the form

$$\dot{g} = f_n[\phi_s(b - Rg), g, \dot{g}] \quad (5.25)$$

At the instant when none of the constraints exists, the explicit form of eqn. (5.25) takes the following form

$$\dot{g} = \phi_s(p_c - \frac{1}{R} \Delta f - Rg) \quad (5.26)$$

where eqn. (5.19) has been used to eliminate  $b$ .

### 5.2.3 The Turbine Dynamics Model

The basic principle behind the derivation of the dynamic equations for the turbine is the relationship between the turbine flow and the rate of change of fluid weight. This is expressed in the familiar continuity equation given by;

$$\frac{dW}{dt} = Q_{in} - Q_{out} \quad (5.27)$$

where  $W$  is the weight of fluid (water or steam or gas) in kilogram - force (kgf) and  $Q$  is the turbine flow in kilogram-force per second. Figure 5.3 illustrates the above relationship for an unconstrained flow case.

However, for effective control, the turbine gate is valved and the flow is sometimes subjected to an intermediate reheat arrangement like in some steam turbines. Some hydro-turbines like the Kaplan type also employ a mechanical follow-up servo to adjust the angle of position of the runner blades as the gate opening varies, for increased efficiency. Therefore, the turbine dynamic equations derived in this section for both the hydro and steam plants are much more complex than the continuity relation of eqn. (5.27), since all the additional components are considered.

#### 5.2.3.1 The Dynamic Model Of The Hydro - Turbine

The hydro turbines installed in the generating units of interest at Kainji hydrostation are of the 'KAPLAN' type. Their most distinguishing feature from the conventional hydro-turbines is that both the wicket gates and the runner blades are under servomotor control - the latter via a mechanical follow-up type servo - for improved efficiency. Dynamic equations for a conventional hydro-turbine have been derived by Undrill and Woodward [24]. The analysis outlined below is specifically adapted to the Kaplan turbine which is perturbed by a signal applied to the speed changer

of the governing mechanism.

Figure 5.4 represents the sectional view of a typical Kaplan turbine runner blade where the arrow-heads point to the directions of positive motion.  $V_i$  and  $V_e$  are the velocities of the runner blade at the effective moment arms at the inlet and outlet respectively. For the assumed lossless case,  $V_i$  is the inlet water velocity relative to a stationary reference frame while  $V_e$  is the exit water velocity relative to a reference frame attached to the runner blade as shown in Figure 5.4.  $V_{ti}$  and  $V_{te}$  are the tangential components of the water velocity at the inlet and exit respectively while  $V_{zi}$  and  $V_{ze}$  are the corresponding downward flow components. Finally  $V_{ni}$  and  $V_{ne}$  are the velocities of the centre of mass of the blade at the inlet and exit respectively. All quantities are in per unit of rated values. Under rated operating conditions; we have

$$V_{ni} = V_{ne} = N \quad (5.28)$$

where  $N$  is the rated blade velocity in per unit.

The velocities of the runner blade  $V_i$  and  $V_e$  can be expressed as

$$V_i = R_i N \quad (5.29a)$$

$$\text{and } V_e = R_e N \quad (5.29b)$$

If the moment arms  $R_i$  and  $R_e$  are defined as the reference lengths then for simplicity, we can write

$$R_i = R_e = 1 \text{ pu} \quad (5.30a)$$

giving  $V_i = V_e = N$  (5.30b)

The downward flow components are given by

$$V_{zi} = Q/A_i \text{ and } V_{ze} = Q/A_e \quad (5.31)$$

where  $A_i$  and  $A_e$  are the effective flow areas respectively and  $Q$  is the turbine flow in per unit. Assuming  $A_i = A_e$ , equation (5.31) becomes

$$V_z = V_{zi} = V_{ze} = Q/A \quad (5.32)$$

The inlet water velocity can be obtained from the flow and fractional gate opening 'G' as

$$V_{ti} = \frac{Q}{A_G G} \quad (5.33)$$

where  $A_G$  is the flow area at 100% gate opening.

By Newton's second law, the hydraulic force 'F' acting on the runner is given by

$$F = \frac{d}{dt} (M\Delta V) = \frac{d}{dt} M(V_{ti} - V_{te}) \quad (5.34)$$

where  $M$  is the mass of water and  $\Delta V$  is the change in velocity. Under steady-state flow conditions (i.e no turbulence)

$$\frac{d}{dt} (V_{ti} - V_{te}) = 0 \text{ and } \frac{dM}{dt} = Q; \text{ such that}$$

$$F = Q(V_{ti} - V_{te}) \quad (5.35)$$



When this is combined with eqn. (5.30a), the hydraulic torque is given by

$$T_n = FR_1 = Q(V_{ti} - V_{te}) \quad (5.36)$$

For a given blade angle  $\phi_B$  (Fig. 5.4), it can be shown that

$$V_{te} = V_{ne} - V_z \cot \phi_B = N - V_z \cot \phi_B \quad (5.37)$$

Using equations (5.32), (5.33) and (5.37) in (5.36) yields

$$T_n = Q \left( \frac{Q}{A_G} + \frac{Q}{A} \cot \phi_B - N \right) \quad (5.38a)$$

or

$$T_n = Q \left( k_1 \frac{Q}{G} + k_2 Q \cot \phi_B - N \right) \quad (5.38b)$$

where  $k_1 = \frac{1}{A_G}$  and  $k_2 = 1/A$

The hydraulic power  $P_m$  by definition is given by

$$P_m = NT_n = NQ \left( k_1 \frac{Q}{G} + k_2 Q \cot \phi_B - N \right) \quad (5.39)$$

and since  $P_m = H_T Q$ , where  $H_T$  is the effective head acting on the runner, then

$$H_T = N \left( k_1 \frac{Q}{G} + k_2 Q \cot \phi_B - N \right) \quad (5.40)$$

The water passage dynamics are given by the familiar continuity equation

$$H_R - H_T = T_\omega \frac{dQ}{dt} \quad (5.41a)$$

where  $H_R$  is the static head and  $T_w$  is the water starting time in seconds defined by [23,27]

$$T_w = \frac{\sum_i^3 L_i v_i}{g_v H_R} \quad (5.41b)$$

where  $\sum L_i$  is the total length of the water passage which includes turbine intake + scroll case + draft tube,  $v_i$  is the instantaneous rated velocity of water in these sections and  $g_v$  is the acceleration due to gravity.

The efficiency  $\eta$  of the system is defined as

$$\eta = \frac{H_T Q}{H_R Q} \quad (5.42)$$

and if  $H_T$  in eqn. (5.40) is used in eqn. (5.42), the result is

$$\eta = \frac{1}{H_R} (k_1 \frac{Q}{G} + k_2 Q \cot \phi_B - N) \quad (5.43)$$

On differentiating  $\eta$  in eqn. (5.43) partially with respect to  $G$  and  $\phi_B$  respectively, we have

$$\frac{\partial \eta}{\partial G} = - \left( \frac{k_1 Q}{H_R} \right) \frac{1}{G^2} \quad (5.44)$$

$$\frac{\partial \eta}{\partial \phi_B} = \left( \frac{k_2 Q}{H_R} \right) \left( - \frac{1}{\sin^2 \phi_B} \right) \quad (5.45)$$

The relationship between the gate opening  $G$  and blade

angle  $\phi_B$  can be obtained using the principle of equal incremental cost. Hence, equating (5.44) to (5.45) and simplifying yields:

$$\phi_B = \sin^{-1} \left\{ G \sqrt{\frac{k_2}{k_1}} \right\} \quad (5.46)$$

Due to difficulties in measuring  $A$  and  $A_G$ , the constants  $k_1$  and  $k_2$  can be obtained from the blade angle and gate opening at rated output as follows:

From eqn. (5.46)

$$k_2 = \left\{ \frac{\sin(\phi_B \text{ rated})}{G \text{ rated}} \right\}^2 k_1 \quad (5.47)$$

Under rated conditions  $H_T = Q = N = 1$  p.u and eqn. (5.40) becomes;

$$1 = \frac{k_1}{G_{\text{rated}}} + k_2 \cot(\phi_B \text{ rated}) - 1 \quad (5.48)$$

Substituting for  $k_2$  from eqn. (5.47) and simplifying gives

$$k_1 = \frac{4 G^2}{2G + \sin 2\phi_B} \quad (5.49)$$

Figure 5.5 shows a block diagram representation of the Kaplan turbine link equations where the blade servo has been modelled as a rate limited first order lag with a time constant  $T_B$ , ie

$$\phi_{B_{\text{ref}}} - \phi_B = T_B \frac{d\phi_B}{dt} \quad (5.50)$$

where  $T_B$  depends on the servomotor design.



### 5.2.3.2 The Steam Turbine Model

Steam turbines may, in general, be classified into three groups [25] namely:

- (i) The non-reheat turbines
- (ii) The single-stage reheat turbines and
- (iii) The double-stage reheat turbines.

The turbines at the Egbin generating station are of the single - stage reheat type. For such turbines, the process of extracting mechanical energy of rotation from pressurised steam - flow occurs in three stages viz, at the high pressure chamber, at the intermediate pressure chamber and at the low pressure chamber as shown in figure 5.6.

The goal of modelling the steam turbine is to obtain an expression relating the change in valve position to the corresponding change in shaft input power (or mechanical output power  $P_m$ ). The steam chest (which lies between the governor - controlled valves and the high pressure turbine) together with the inlet piping to the first turbine cylinder, the reheater and the crossover piping downstream all introduce time delays which the model must account for.

From the continuity relation (eqn.5.27), it is easily seen that any steam flow through a given chamber can be modelled by a corresponding time constant. Hence, the flow through the steam chest and high pressure piping may be modelled by a time constant  $T_{CH}$ , the reheater by a time constant  $T_{rh}$  while the crossover piping is accounted for by  $T_{co}$ . From figure 5.6, let  $P_H$ ,  $P_I$  and  $P_L$  represent the steam flow in Joules per second at the indicated locations, then

$$P_m = F_1 P_H + F_2 P_I + F_3 P_L \quad (5.51)$$

where  $F_1 P_H$ ,  $F_2 P_I$ ,  $F_3 P_L$  are the respective fractions of the total mechanical output power developed in the high pressure, intermediate pressure and low pressure sections of the turbine respectively.  $F_1$ ,  $F_2$  and  $F_3$  are measures of the output efficiencies in the respective sections and they have been normalised such that:

$$F_1 + F_2 + F_3 = 1 \quad (5.52)$$

If, for simplicity, it is assumed that  $T_{co} = 0$  then,  $P_I = P_L$  in Fig.5.6 and eqn.(5.51) reduces to

$$P_m = F_1 P_H + (1 - F_1) P_I \quad (5.53)$$

The effect of this assumption is of no serious consequence for the reason that,  $T_{co}$  is very small usually of the order of 0.3 to 0.5 seconds [25], so also is the contribution of  $F_3 P_L$  to the total mechanical power output. By substituting for  $P_H$  and  $P_I$  from Fig.5.6, eqn.(5.53) now becomes

$$P_m = F_1 P_H + \frac{1 - F_1}{1 + sT_{rh}} P_H = \left( \frac{1 + F_1 sT_{rh}}{(1 + sT_{rh})(1 + sT_{ch})} \right) P_H$$

or

$$P_m = \frac{1 + F_1 sT_{rh}}{(1 + sT_{rh})(1 + sT_{ch})} G \quad (5.54a)$$

where 's' is the Laplace operator and G is the fractional

valve opening. Typical value of  $F_1$  is about 0.5 [25]. The mechanical output power  $P_m$  is exerted on the rotor of the synchronous machine to generate electrical power  $P_G$ . For constant excitation, the generated electrical power is directly proportional to  $P_m$  such that for any increase in valve opening  $\Delta G$  necessitating an increase in generated power  $\Delta P_G$ , the steam - turbine response is given by

$$\Delta P_G = \frac{1 + F_1 s T_{rh}}{(1 + s T_{rh})(1 + s T_{ch})} \Delta G \quad (5.54b)$$

#### 5.2.4 The Model Of The Power Transmission System

The basic principle of conservation of energy is employed in the modelling of the power transmission system since the total energy generated must equal the energy consumed.

The conventional power system operating strategy is characterised by a group of generators, usually of different kinds, which are connected by relatively strong tie lines. In the event of any disturbance resulting in power swings, the group swings in unison. This coherency property allows the group not only to be characterised by the same nominal frequency but also by the same frequency deviation ( $\Delta f$ ) whenever there exists a real power imbalance in the system. Such a strongly tied group constitutes a 'control area' under one AGC scheme and can cover a whole

country (in the case of Nigeria for instance) or a small percentage of a country (such as in the United States of America).

Furthermore, each control area is interconnected with other control areas via relatively weak tie lines such that each area swings against the other in the event of a disturbance. These inter-area ties could be within a country (like in the USA) or across national boundaries (like the one between England and Scotland for instance). The inter-ties should permit the flow of power in either direction to allow for the borrowing of power from a sister area in the event of one area failing to satisfy her demand; to this extent, the present link between Nigeria and the Niger Republic is NOT an intertie. It is a case of a source feeding a sink. Figure 5.7 represents schematically a multi-area system operation consisting of two control areas which are characterised by different frequency deviations ( $\Delta f_i$ ,  $\Delta f_j$ ) resulting from a disturbance in one area. Now, if the load deviation, usually random, are assumed to be step functions whose magnitudes fall within the mathematical definition of first order perturbations, then the real power - frequency control channel and the reactive power-voltage control channel are decoupled. This is the standard industry practice so far as the control of real power imbalance is concerned [34,32].

Given the background above, the model of the transmission system suitable for AGC is limited to the dynamic equations governing the real power - frequency interaction. The



equations are derived below using an incremental (piece-wise linear) approach based on the principle of energy conservation.

#### 5.2.4.1 The Dynamic Equations Of The Transmission System

Suppose there occurs a step change in real power demand  $\Delta P_{Di}$  in area  $i$  resulting in a change in the generated power  $\Delta P_{Gi}$ , then, neglecting losses, the surplus power  $\Delta P_{Gi} - \Delta P_{Di}$  can be absorbed by the system in three possible ways viz:

- (i) by changing the area kinetic energy  $\omega_k$
- (ii) by a change in load consumption and
- (iii) by the export of power  $\Delta P_{Ei}$  via the inter ties

i. The area kinetic energy varies as the square of frequency  $f_i$ , or expressed mathematically

$$\omega_{ki} = \left(\frac{f_i}{f_o}\right)^2 \omega_{kio} \quad (5.55)$$

where  $\omega_{kio}$  is the kinetic energy, measured at the nominal frequency  $f_o$  (Hz), while  $f_i$  is the instantaneous frequency of the control area. Since  $f_i = f_o + \Delta f_i$  and  $\Delta f_i$  is small by assumption, then eqn. (5.55) can be written as

$$\omega_{ki} = \left(\frac{f_o + \Delta f_i}{f_o}\right)^2 \omega_{kio} \approx \left(1 + 2 \frac{\Delta f_i}{f_o}\right) \omega_{kio} \quad (5.56)$$

where  $\left(\frac{\Delta f_i}{f_0}\right)^2$  has been neglected.

The rate of change of kinetic energy may then be written as

$$\frac{d}{dt} \omega_{ki} = \frac{2\omega_{kio}}{f_0} \frac{d}{dt} \Delta f_i \quad (5.57a)$$

In per unit of area capacity  $P_{ri}$ , eqn. 5.56 can be rewritten as

$$\frac{1}{P_{ri}} \frac{d}{dt} \omega_{ki} = \frac{2\omega_{kio}}{f_0 P_{ri}} \frac{d}{dt} \Delta f_i = \frac{2H_i}{f_0} \frac{d}{dt} \Delta f_i \quad (5.57b)$$

where  $H_i \approx \frac{\omega_{kio}}{P_{ri}}$  is the per unit inertia constant in seconds while  $P_{ri}$  is the total mega-watt rating of the area. Typical values of  $H$  are between 2 - 8 seconds and are independent of area size.

ii. Due to the dominance of motor loads, all typical loads experience a change in power consumption in the event of fluctuations in frequency. Defining the parameter  $D_i = \partial P_D / \partial f_i$ , the portion of the surplus power lost due to increased load consumption is given by

$$\Delta P_{Dm} = \frac{\partial P_D}{\partial f_i} \Delta f_i = D_i \Delta f_i \quad (5.58)$$

The  $D_i$  parameter (Mw/Hz) is determined empirically and studies have shown [33] that for an average load which consists of 60% induction motors, 20% synchronous motors and 20% other 'ingredients'  $D_i = 1.0$ .

iii. The total incremental tie-line megawatt power exported from area i equals the sum of the out-flowing incremental powers in all the tie lines connected to area i: for a two-area system (Figure 5.7)  $\Delta P_{Ei} = \Delta P_{Ei-j}$ .

However, since both areas swing against each other, the net export of power out of area i is a function of the difference between the nominal load angles of the two areas ( $\delta_{i0} - \delta_{j0}$ ) as well as the incremental load angle changes. Expressed mathematically, this becomes

$$\Delta P_{Ei-j} = \frac{\partial P_{ijm}}{\partial (\delta_i - \delta_j)} \sin(\delta_{i0} - \delta_{j0}) [\Delta \delta_i - \Delta \delta_j] \quad (5.59)$$

or

$$\Delta P_{Ei-j} = P_{ijm} \cos(\delta_{i0} - \delta_{j0}) [\Delta \delta_i - \Delta \delta_j] \quad (5.60)$$

giving

$$\Delta P_{Ei-j} = T_{ijo} (\Delta \delta_i - \Delta \delta_j) \quad (5.61)$$

where  $P_{ijm}$  (Mw) is the static transmission capacity of the tie line,  $\delta_{i0}$  (radians) is the nominal operating load angle in area i and  $T_{ijo}$  (Mw/rad) is the synchronizing coefficient or electrical 'stiffness' of the tie line.

Now  $\Delta \delta_i$  is related to  $\Delta f_i$  by the integration of the latter viz:

$$\Delta \delta_i - \Delta \delta_j = 2\pi \int [\Delta f_i - \Delta f_j] dt \quad (5.62)$$

On changing the megawatt values to per unit of area 'i' capacity ( $P_{ri}$ ) such that

$$\Delta P_{Eij} \triangleq \frac{2\pi T_{ij0} [\int \Delta f_i dt - \int \Delta f_j dt]}{P_{ri}}$$

$$= T_{ij} [\int \Delta f_i dt - \int \Delta f_j dt] \quad (5.63)$$

$$\text{where } T_{ij} = \frac{2\pi T_{ij0}}{P_{ri}}$$

then, the energy conservation equation can be written as

$$\Delta P_{Gi} - \Delta P_{Di} = \frac{2H_i}{f_o} \frac{d}{dt} \Delta f_i + D_i \Delta f_i + T_{ij} [\int \Delta f_i dt - \int \Delta f_j dt] \quad (5.64)$$

In the Laplace domain, Eqn.(5.64) becomes

$$\Delta P_{Gi}(s) - \Delta P_{Di}(s) = \frac{2H_i}{f_{io}} s \Delta F_i(s) + D_i \Delta F_i(s) + \frac{T_{ij}}{s} [\Delta F_i(s) - \Delta F_j(s)] \quad (5.65)$$

which can also be written as

$$[\Delta P_{Gi}(s) - \Delta P_{Di}(s) - \Delta P_{Ei}(s)] G_{Pi}(s) = \Delta F_i(s) \quad (5.66)$$

where

$$G_{Pi}(s) = \frac{k_{Pi}}{1 + sT_{Pi}}$$

$$K_{Pi} = \frac{1}{D_i} \text{ Hz/Pu Mw}$$

and

$$T_{Pi} = \frac{2H_i}{f_o D_i} \text{ seconds}$$

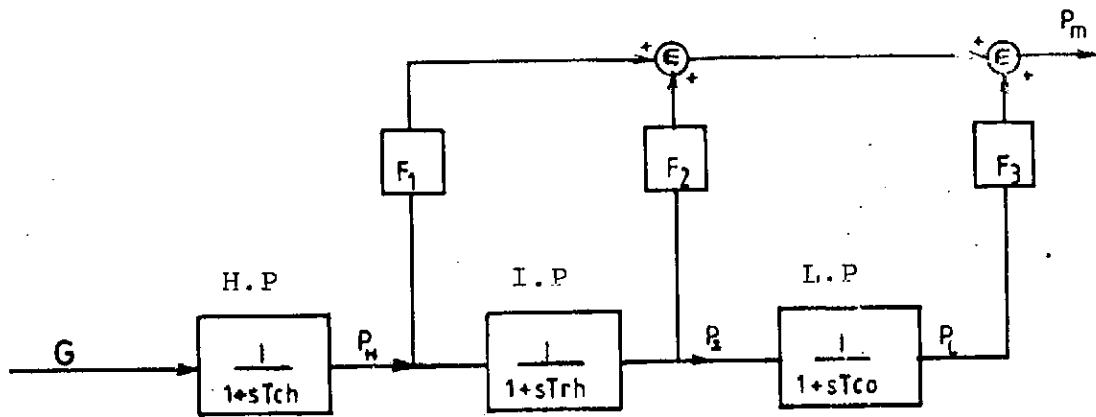


Fig. 5.6 Block Diagram of the System Turbine

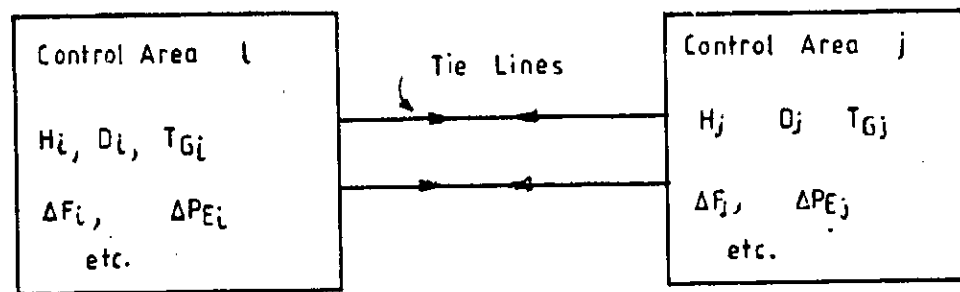


Fig. 5.7 Block Diagram of Two Area System

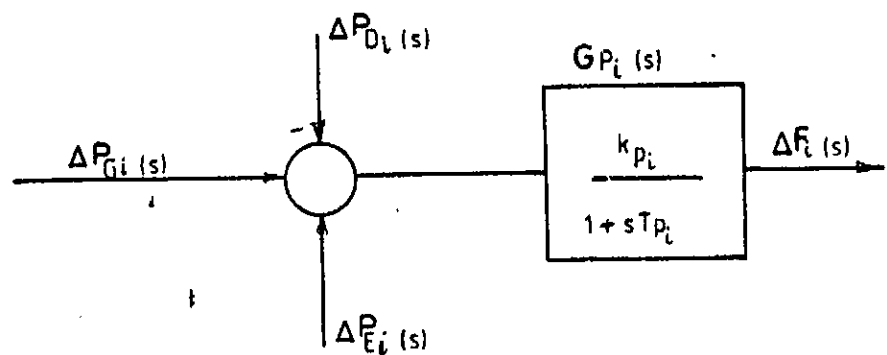


Fig. 5.8 Energy Conservation Block Diagram

The transmission system model can therefore be represented by the block diagram of figure 5.8 for a two-area inter-connection.

Note that for a single area,  $\Delta P_{Ei} = 0$  in eqn. (5.66).

### 5.2.5 Equivalent Linear Forms Of The Derived Sub-models

In order to synthesize a variable structure automatic generation control (VSAGC) scheme for each of the three different models of the Nigerian power system, the linear forms of the derived equations are needed. These linearised equations are presented below as component transfer functions.

#### ° Hydro Governing System.

If in section 5.2.2.1, the hydro generating unit is operating at a given steady-state condition below the rated output and the change in load demand is assumed to be small so that the constraints on gate opening position  $g$  and its velocity  $\dot{g}$  do not exist, then, an incremental change  $\Delta G$  in the governor - controlled gate position will result. Starting from eqn. (5.20) and using incremental analysis, it is shown in appendix B that the relationship between the speed changer signal  $\Delta P_c$ , the frequency feedback signal  $\Delta f$  and the change in gate position  $\Delta G$  is given by the transfer function

$$\Delta G = \frac{s T_R + 1}{(s T_G + 1) \left( \frac{r}{R} s T_R + 1 \right)} \left( \Delta P_c - \frac{1}{R} \Delta f \right) \quad (5.67)$$

where

- $\Delta G \rightarrow$  change in governor controlled gate position
- $T_G \rightarrow$  governor time constant
- $R \rightarrow$  steady - state speed regulation.
- $r \rightarrow$  transient speed regulation
- $\Delta P_c \rightarrow$  change in the speed changer (AGC) signal.

#### ° Steam Governing System

By following similar arguments as above and starting from eqn.(5.26), it is also shown in appendix B that the linearised model of the steam governing mechanism is given as

$$\Delta G = \frac{1}{sT_G + 1} \left( \Delta P_c - \frac{1}{R} \Delta f \right) \quad (5.68)$$

where all the parameters are as defined above.

#### ° Hydro - turbine Dynamics

In deriving the linearised model of the hydro - turbine dynamics, the effect of servo control on the turbine blades is neglected and the turbine is assumed to be operating within the linear range so that neither turbulence nor compressibility exists. Then, starting from the continuity equation of eqn. 5.27 ,the linearised model of the hydro-turbine dynamics is derived in appendix B as

$$\Delta P_G = \frac{-s T_w + 1}{s(T_w/2) + 1} \Delta G \quad (5.69)$$

where

$\Delta P_G \rightarrow$  change in generated power proportional to turbine power

$\Delta G \rightarrow$  change in governor controlled gate position

$T_w \rightarrow$  water starting time in seconds.

° Steam-Turbine Dynamics

The model of the steam turbine dynamics derived in section 5.2.3.2 is already linearised as shown in eqn. (5.54b). It is therefore used directly.

° Power Transmission System Model.

The linearised model of the power transmission system is given by eqn. (5.66).

° Power System Stabilizer.

It is conventional in power system operations to feedback a signal proportional to the integral of the frequency deviation for the purposes of zeroing the frequency error [68]. Usually, this signal is fed to the secondary control equipment. In this thesis, the above condition is achieved by passing the frequency error signal through an ideal integrator having a normalised gain of unity. If the resulting signal is represented by  $\Delta P_z$ , then it follows that

$$\Delta P_z = \frac{1}{s} \Delta f \quad (5.70)$$

where 's' is Laplace operator.



For an interconnected power system, the integral of the tie-line power error signal is also added, hence

$$\Delta P_z = \frac{1}{s} [k_f \Delta f + \Delta P_E] \quad (5.71)$$

where  $\Delta P_E$  is the tie-line power deviation and  $k_f$  is the frequency bias.

#### 5.2.6 Complete System Models

In this subsection, the corresponding component equations derived above are appropriately combined to form each of the proposed AGC models of the Nigerian power system. Each model is represented by a state equation of the general form,

$$\dot{x}(t) = Ax(t) + Bu(t) + \Gamma \xi(t) \quad (5.72)$$

where  $x \in \mathbb{R}^n$ ,  $u \in \mathbb{R}^m$ ,  $\xi \in \mathbb{R}^p$ ,  $A \in \mathbb{R}^{n \times n}$ ,  $B \in \mathbb{R}^{n \times m}$  and  $\Gamma \in \mathbb{R}^{n \times p}$ . The vector  $x$  represents the  $n$ -states of the system,  $u$  is an  $m$ -vector of control inputs while  $\xi$  is a  $p$  - vector of disturbances. The constant matrices  $A$ ,  $B$  and  $\Gamma$ , which define the nominal linear system, represent the  $n \times n$  system matrix, the  $n \times m$  control matrix and the  $n \times p$  disturbance matrix respectively. The elements of the matrices  $A$ ,  $B$  and  $\Gamma$  are computed from the known characteristics of the power system.

#### 5.2.6.1 The Model of The Hydro-Dominated Single Control Area

The complete power system model for the hydro - dominated single control area is obtained by combining eqn.(5.67) for the hydro - governing mechanism with eqn. (5.69) for the hydro-turbine dynamics, eqn.(5.66) for the power transmission network (where  $\Delta P_E = 0$ ) and eqn.(5.70) for the power system stabilizer. The result of this combination is represented in the block diagram of Fig.5.9a.

#### 5.2.6.2 The Model of A Single - Control Area Dominated By Steam - Powered Plants.

Similar to the above procedure, equation (5.68) representing the governing system dynamics for the steam plant is combined with eqn.(5.54b) for the steam - turbine, eqn.(5.66) for the power transmission network and eqn.(5.70) for the power system stabilizer to obtain the complete system model for a single control area dominated by steam-powered generators. The block diagram of Fig.5.10a shows clearly the result of this combination.

#### 5.2.6.3 The Model of The Two-Area Interconnection

The two-area interconnection described here, consists of one hydro - dominated area and another area which is dominated by steam - powered generating plants. Thus, the model of the interconnected area is obtained by combining the two single - area models derived above such that  $\Delta P_E$  is

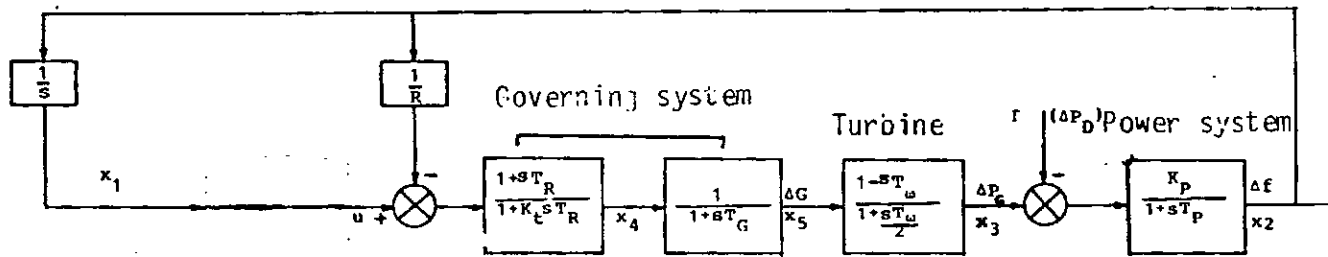


Fig. 5.9a - Block Diagram of A Hydro - Dominated Area with Integral Controller

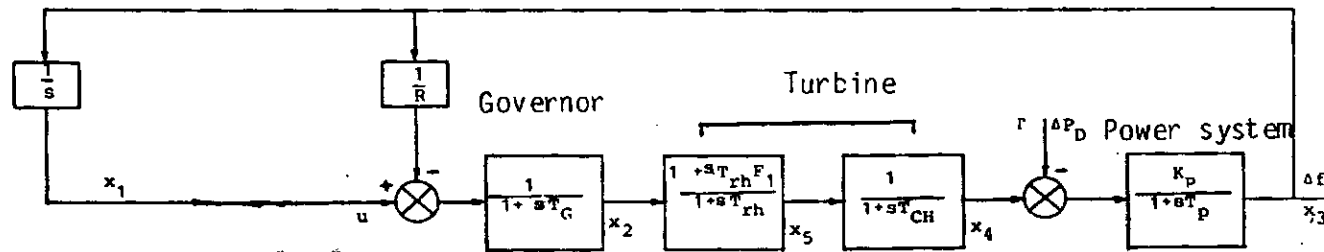


Fig.5.10a - Block Diagram of a Steam - Dominated Area with Integral Controller

retained in eqn.(5.66) for the power transmission system while eqn.(5.71) is inserted to represent the power system stabilizer. The resulting block diagram representation of the model is depicted in Fig.5.11a.

In the next section, the models of Figs.5.9a 5.10a and 5.11a are respectively utilised for synthesizing appropriate VSAGC schemes for the Nigerian power system.

### 5.3 Synthesis Of VSAGC Schemes For Models Of The Nigerian Power System

Three analytical models of the Nigerian power system representing different operating strategies were proposed in the last section. The aim was to develop models that could be used for the application of modern control theory based on state space techniques to achieve generation control.

In this section, variable structure automatic generation control (VSAGC) schemes are synthesized for each of the proposed AGC models of the Nigerian power system. The performance of the system under variable structure control is also investigated using digital computer simulation.

The implementation of the synthesis and simulation processes presented here is achieved using the VSAGC design package described in chapter four. The design procedure follows strictly the steps outlined in chapter 3 which were clearly demonstrated in the application example.

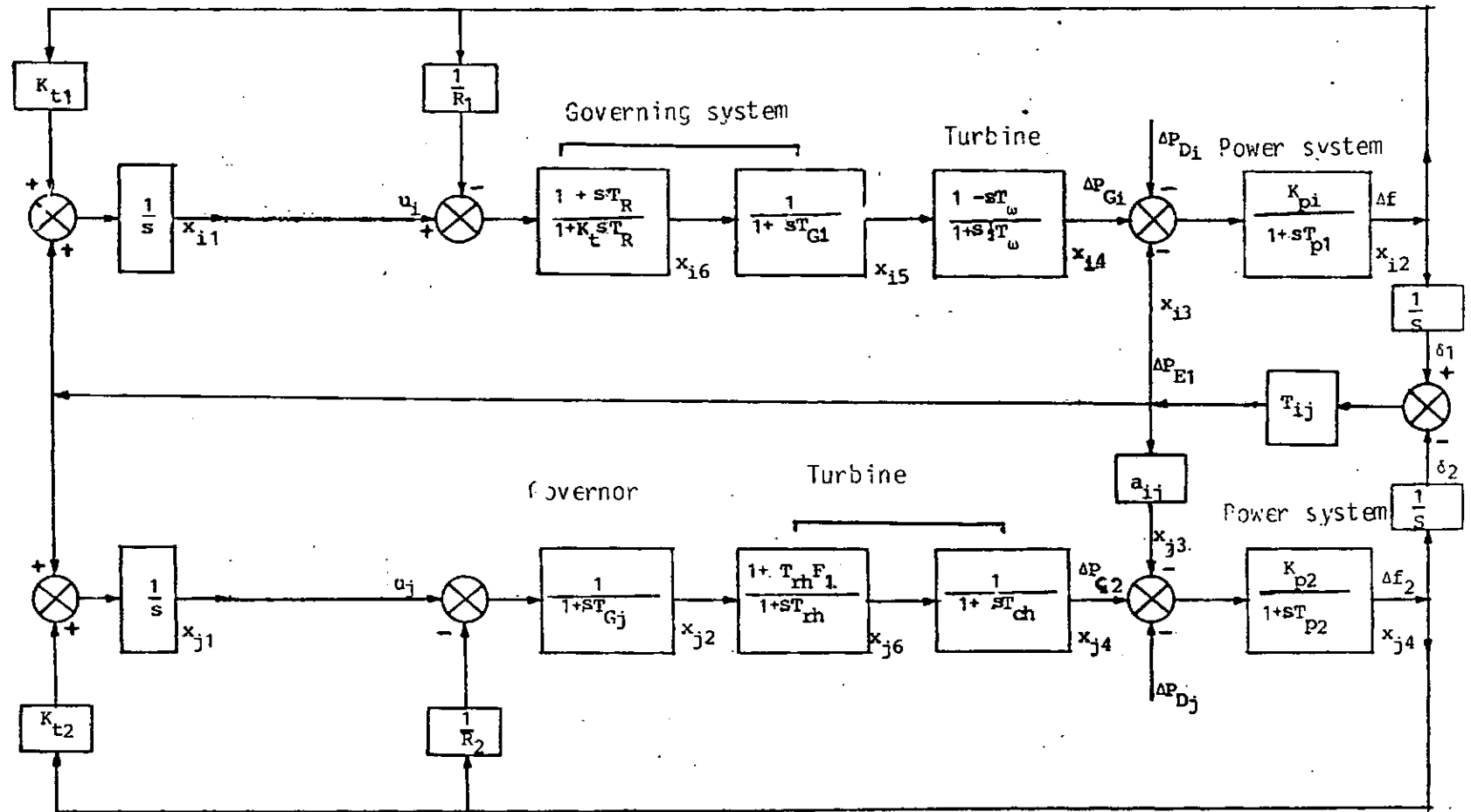


Fig: 5.11a: - Block Diagram of an Interconnected Area with Integral Controller

### 5.3.1 VSAGC Design For A Hydro - Dominated Single Area Model

The block diagram representation of a single control area dominated by hydro - generating plants and which is under variable structure control is depicted in Fig.5.9b. The block labelled 'VSC' performs the synthesis of the variable structure control signal 'u' which acts on the speed changer of electric generators to effect automatic generation control (AGC).

The system of Fig.5.9b can be represented in the state space form of eqn.(5.72) if:

$$A = \begin{bmatrix} 0 & 1 & 0 & 0 & 0 \\ 0 & -\frac{1}{T_p} & \frac{K_p}{T_p} & 0 & 0 \\ 0 & 0 & -\frac{2}{T_\omega} & -\frac{2}{T_G} & \frac{2}{T_\omega} + \frac{2}{T_G} \\ 0 & \frac{1}{K_t RT_p} - \frac{1}{K_t RT_R} & -\frac{K_p}{K_t RT_p} & -\frac{1}{K_t T_R} & 0 \\ 0 & 0 & 0 & \frac{1}{T_G} & -\frac{1}{T_G} \end{bmatrix} \quad (5.73)$$

$$B = \begin{bmatrix} 0 & 0 & 0 & \frac{1}{K_t T_R} & 0 \end{bmatrix}^T \quad (5.74)$$

$$\Gamma = \begin{bmatrix} 0 & -\frac{K_p}{T_p} & 0 & \frac{K_p}{K_t RT_p} & 0 \end{bmatrix}^T \quad (5.75)$$

The superscript ' represents vector or matrix transpose. By substituting for the parameter values of the Nigerian power system (see appendix E), eqns. 5.72 - 5.74. become

$$A = \begin{bmatrix} 0 & 1 & 0 & 0 & 0 \\ 0 & -1415 & 4.7169 & 0 & 0 \\ 0 & 0 & -0.5 & -3.33 & 3.83 \\ 0 & 6.925 & -4.718 & 0 & -0.0209 \\ 0 & 0 & 0 & 1.667 & -1.667 \end{bmatrix} \quad (5.76)$$

$$B = [0 \quad 0 \quad 0 \quad 0.0209 \quad 0]^T \quad (5.77)$$

$$T = [0 \quad -4.7169 \quad 0 \quad 4.7169 \quad 0]^T \quad (5.78)$$

Now invoking the EXIST module of the computer aided design package VAGCD to solve the existence problem, the transformation matrix M is selected as;

$$M = \begin{bmatrix} 1 & 0 & 0 & 0 & 0 \\ 0 & 1 & 0 & 0 & 0 \\ 0 & 0 & 1 & 0 & 0 \\ 0 & 0 & 0 & 0 & 1 \\ 0 & 0 & 0 & 1 & 0 \end{bmatrix}$$

such that the transformed A matrix becomes

$$\begin{bmatrix} 0 & 1 & 0 & 0 & 0 \\ 0 & -0.1415 & 4.7269 & 0 & 0 \\ 0 & 0 & -0.5 & 3.83 & -3.33 \\ 0 & 0 & 0 & -1.667 & 1.667 \\ 0 & 6.925 & -4.718 & 0 & -0.0209 \end{bmatrix} = \begin{bmatrix} A_{11} & A_{12} \\ \vdots & \vdots \\ A_{21} & A_{22} \end{bmatrix}$$

Closed-loop system poles are selected so as to ensure system stability and fast transient response. Stability is ensured when the poles are in the left-half s-plane. For a fast transient response, the poles should be located far from the origin of the s-plane, however, they should not be too large so as to avoid excessive control effort. From simulation, a suitable choice of closed-loop poles is -3, -4, -5 and -6. The corresponding reduced order vector F is computed to be

$$F = (5.721 \quad -2.250 \quad 5.80 \quad 2.923)$$

thus giving the sliding plane vector C as

$$C = (5.721 \quad -2.250 \quad 5.80 \quad 1.0 \quad 2.923)$$

Note that the model parameter values of eqns. (5.76) to (5.78) strictly represent the case where the inherent load-frequency characteristics of the system (D) equals 1.5 p.u while the temporary and permanent droop settings (r and R) are 1.0 and 0.04 pu respectively.

When these parameters change, the model parameter values change correspondingly resulting in different values for the elements of the sliding plane vector C. For instance, when  $D = 2.0$  pu,  $r = 0.6$  pu and  $R = 0.157$  p.u, the elements of the sliding plane vector are determined as;

$$C = (-13.35 \quad -2.81 \quad 17.92 \quad 1.0 \quad 10.77).$$



Simulation results are presented later to show the effect of variations in parameters  $D$ ,  $r$  and  $R$  on the system.

In order to compute the unit vector control parameters the module REACH of the computer aided design package VAGCD is invoked to solve the reachability problem. The unit vector control law is defined by eqn.(3.29) and the design problem involves computing the elements of the control vectors  $L$ ,  $G$ , and  $H$ . Using the module REACH, the second transformation matrix  $M_2$  is selected as

$$M_2 = \begin{bmatrix} I_4 & 0 \\ F & I_1 \end{bmatrix} = \begin{bmatrix} 1 & 0 & 0 & 0 & 0 \\ 0 & 1 & 0 & 0 & 0 \\ 0 & 0 & 1 & 0 & 0 \\ 0 & 0 & 0 & 1 & 0 \\ 5.721 & -2.25 & 5.80 & 2.923 & 1 \end{bmatrix}$$

where the vector  $F$  has been determined above.

Then by choosing the scalar  $\phi$  interactively as  $-1$ , the linear control vector  $L$  is obtained as

$$L = [82.645 \quad -26.91 \quad 70.27 \quad 53.74 \quad -13.44]$$

Now, with the choice of  $\phi = -1$ , the solution to the Lyapunov equation [eqn.(3.39)] becomes  $P_n = 0.5$  with the result that the control vectors  $G$  and  $H$  are obtained as:

$$G = [57.21 \quad -22.5 \quad 58.0 \quad 10.0 \quad 29.23]$$

$$H = [2.86 \quad -1.125 \quad 2.9 \quad 0.50 \quad 1.46]$$

Figure 5.12 to 5.14 below show the performance of the system under the above controller for different values of  $D$ ,  $r$  and  $R$ . The exercise is partly informed by the need to investigate the robustness of the variable structure control scheme.

### 5.3.2 VSAGC Design For A Control Area Dominated By Steam Powered Plants

The block diagram of a single control area dominated by steam - powered electric generators is shown in Fig.5.10b. This system can be modelled in the state variable form of eqn.5.17, if:

$$A = \begin{bmatrix} 0 & 0 & 1 & 0 & 0 \\ 0 & -\frac{1}{T_G} & -\frac{1}{T_G R} & 0 & 0 \\ 0 & 0 & -\frac{1}{T_P} & \frac{K_P}{T_P} & 0 \\ 0 & 0 & 0 & -\frac{1}{T_{ch}} & \frac{1}{T_{ch}} \\ 0 & \frac{1}{T_{rh}} - \frac{F_1}{T_G} & \frac{-F_1}{T_G R} & 0 & \frac{1}{T_{rh}} \end{bmatrix} \quad (5.79)$$

$$B = \begin{bmatrix} 0 & \frac{1}{T_G} & 0 & 0 & \frac{F_1}{T_G} \end{bmatrix}' \quad (5.80)$$

$$\Gamma = \begin{bmatrix} 0 & 0 & \frac{K_P}{T_P} & 0 & 0 \end{bmatrix}' \quad (5.81)$$

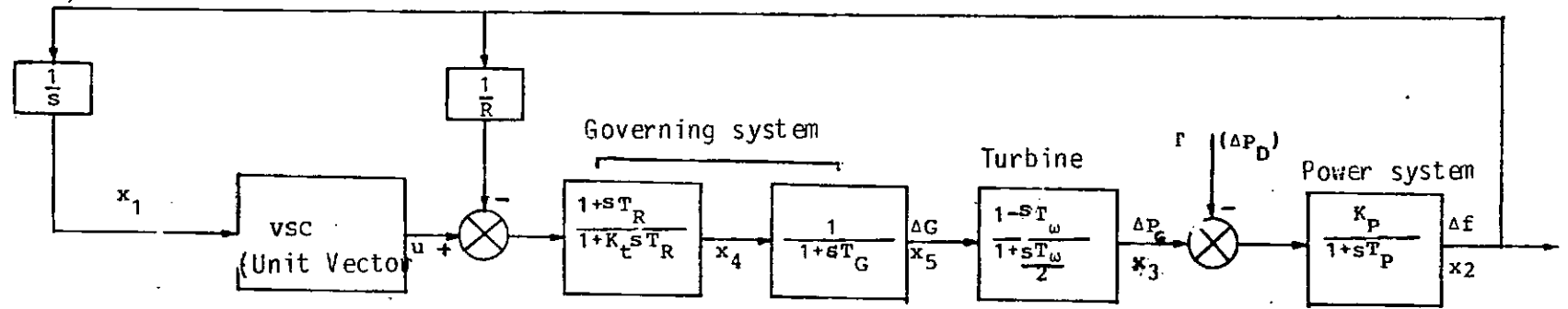


Fig. 5.9b - Block Diagram of A Hydro - Dominated Area with Unit Vector VSC

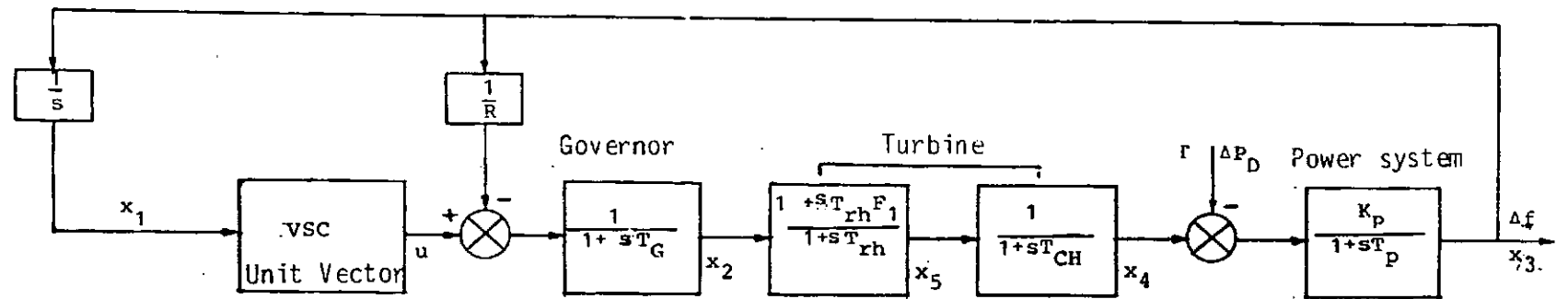


Fig. 5.10b - Block Diagram of a Steam - Dominated Area with Unit Vector VSC

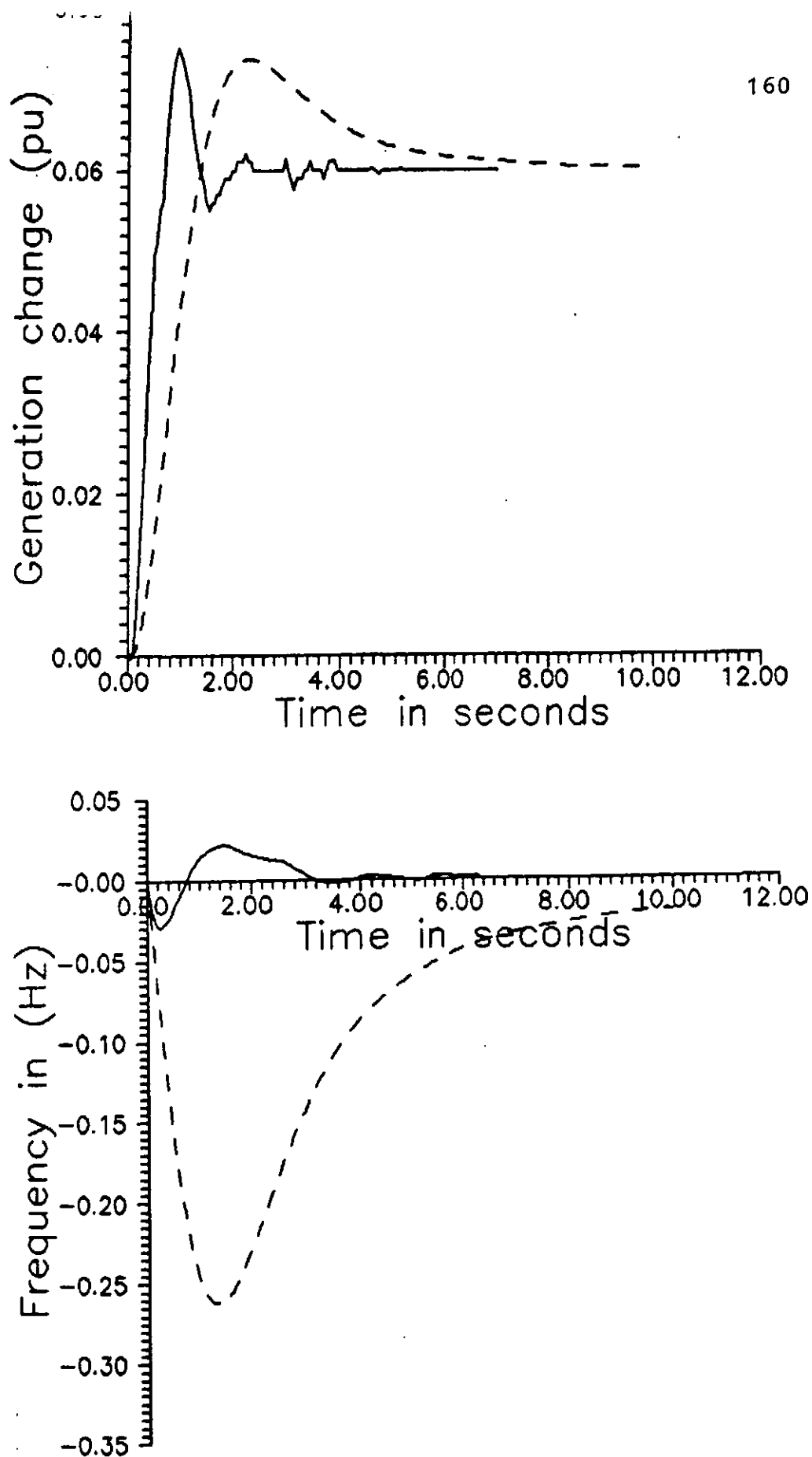


Fig.5.12 System Responses for a hydro - dominated area with  
 $D = 0.75$ ,  $r = 0.6$ ,  $R = 0.1667$  pu — VSAGC;  
---- Int. Controller.

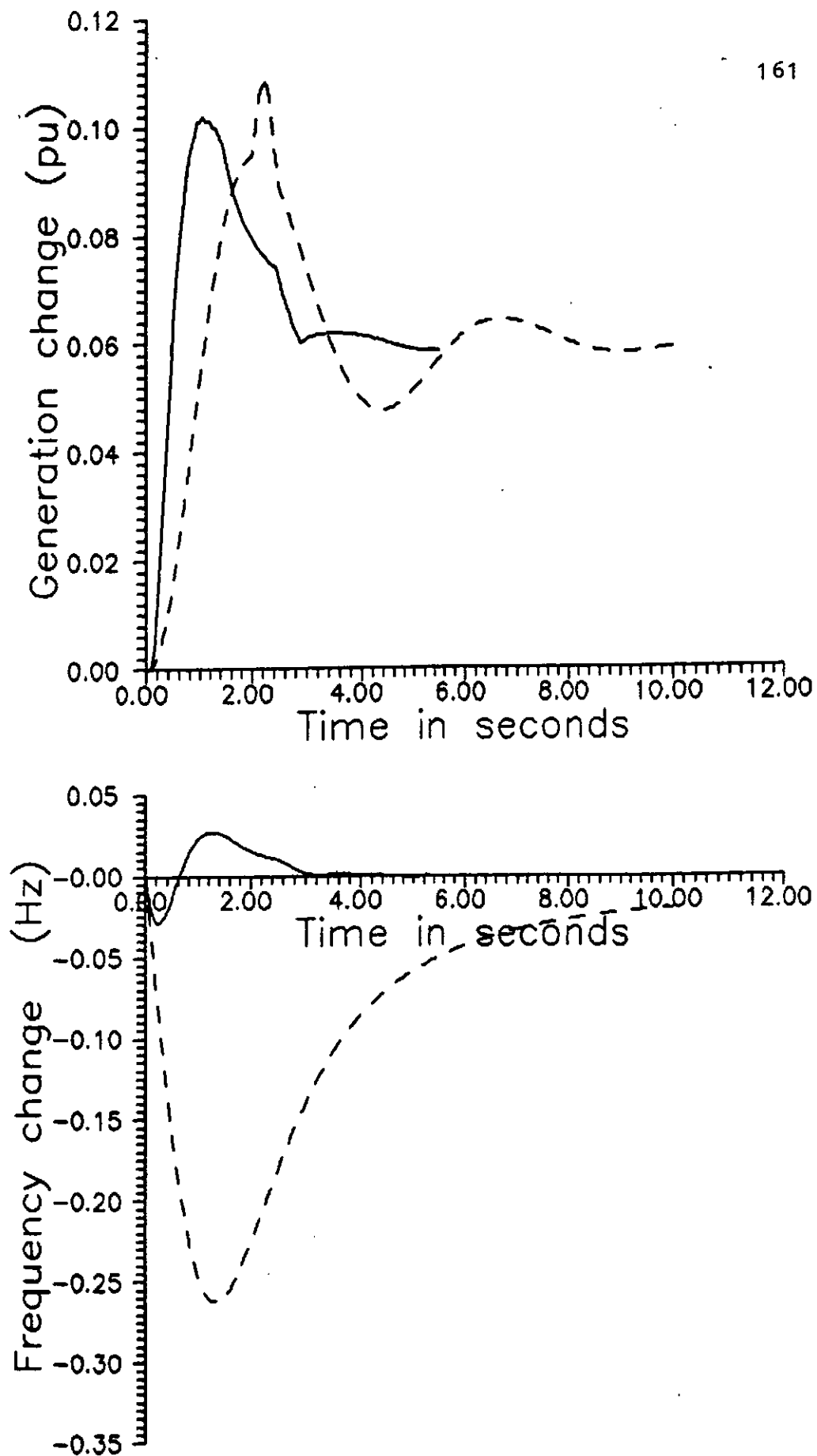


Fig.5.13 System responses for a hydro - dominated area  
with  $D = 1.5$ ,  $r = 0.8$  and  $R = 0.04$  pu;  
— VSAGC ; ---- Int. controller.

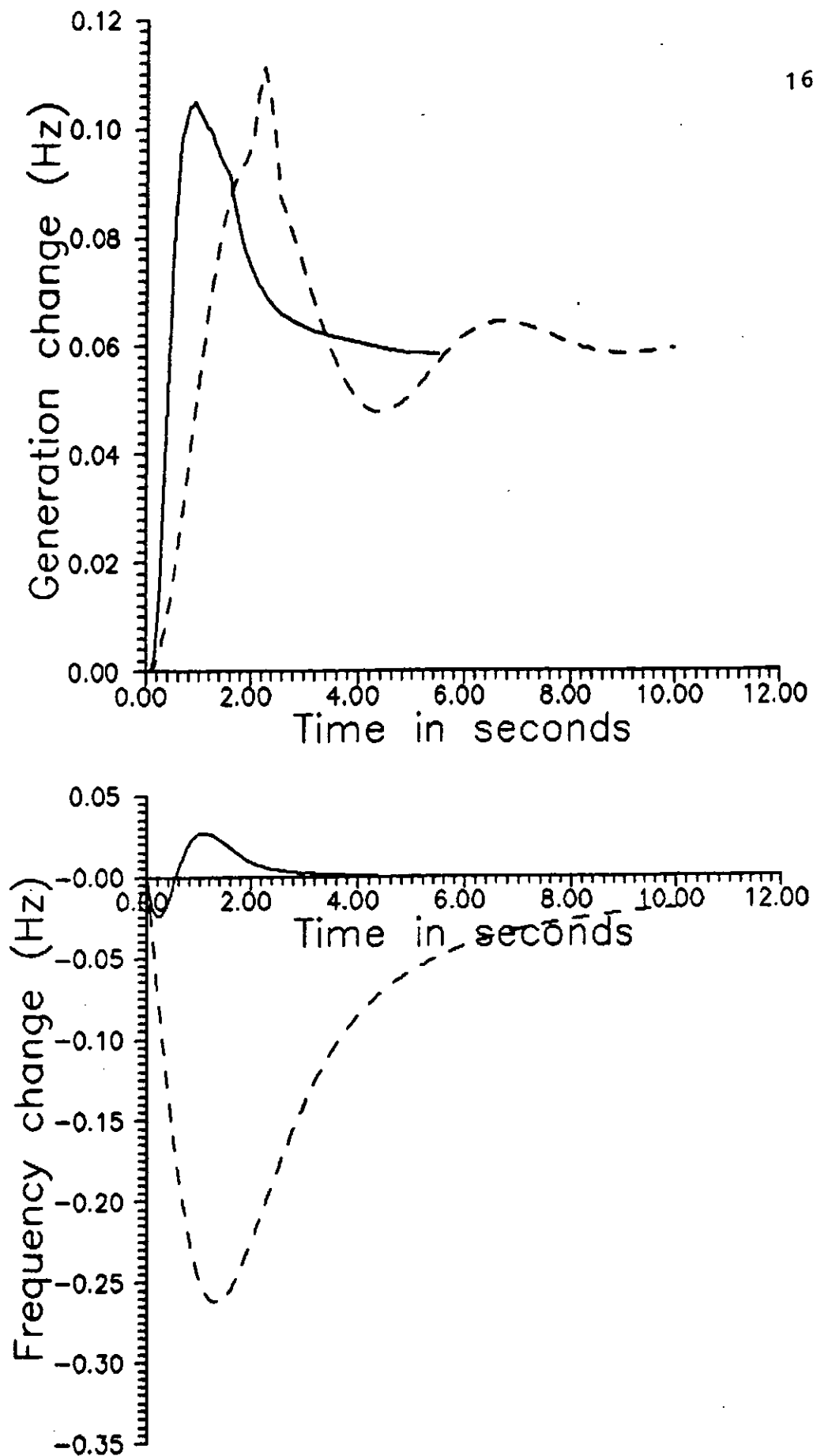


Fig.5.14 System responses for a hydro - dominated area  
with  $D = 2.0$ ,  $r = 1.0$  and  $R = 0.167$  pu  
—— VSAGC ; ----- Int. Controller.

Now, substituting for the parameter values of the Nigerian power system (see Appendix E), eqns. (5.79) to (5.81) reduce to

$$A = \begin{bmatrix} 0 & 0 & 1 & 0 & 0 \\ 0 & -10. & -5. & 0 & 0 \\ 0 & 0 & -0.07 & 4.717 & 0 \\ 0 & 0 & 0 & -3.846 & 3.846 \\ 0 & -4.9 & -2.5 & 0 & -0.1 \end{bmatrix}$$

$$B = [ 0 \quad 10 \quad 0 \quad 0 \quad 5 ]'$$

$$\Gamma = [ 0 \quad 0 \quad -4.717 \quad 0 \quad 0 ]'$$

By invoking the EXIST module of the computer aided design package VAGCD, and following the procedure of the last section, the nxn transformation matrix M is selected as;

$$M = \begin{bmatrix} 1 & 0 & 0 & 0 & 0 \\ 0 & 1 & 0 & 0 & -2 \\ 0 & 0 & 1 & 0 & 0 \\ 0 & 0 & 0 & 1 & 0 \\ 0 & 0 & 0 & 0 & 1 \end{bmatrix}$$

such that the transformed A matrix becomes

$$MAM^{-1} = \left[ \begin{array}{cccc|c} 0 & 0 & 1 & 0 & 0 \\ 0 & -10. & -5. & 0 & -0.02 \\ 0 & 0 & -0.142 & 4.718 & 0 \\ 0 & 0 & 0 & -3.846 & 3.846 \\ \hline 0 & -4.9 & -2.5 & 0 & 0.11 \end{array} \right]$$

By placing the closed loop poles of the system arbitrarily at  $-1.5$ ,  $-2.0$  and  $-2.5 \pm j1.5$ , the reduced order vector  $F$  is determined as

$$F = [0.041 \quad 4.98 \quad 2.62 \quad -1.79]$$

thus giving the sliding plane vector  $C$  as

$$C = [0.0414 \quad 4.98 \quad 2.61 \quad -1.79 \quad 1.01]$$

In computing the unit vector control vectors  $L$ ,  $G$  and  $H$  using the module REACH, the second transformation matrix  $M_2$  is selected as

$$M_2 = \left[ \begin{array}{c|c} I_4 & 0 \\ \hline F & I_1 \end{array} \right] = \left[ \begin{array}{ccccc} 1 & 0 & 0 & 0 & 0 \\ 0 & 1 & 0 & 0 & 0 \\ 0 & 0 & 1 & 0 & 0 \\ 0 & 0 & 0 & 1 & 0 \\ 0.041 & 4.98 & 2.62 & -1.79 & 1 \end{array} \right]$$

where the vector  $F$  has been determined above. In a similar manner to the previous section, the scalar  $\phi$  is chosen as



-1, thus giving the linear control vector  $L$  as

$$L = [-9.4 \quad -8.7 \quad -7.7 \quad 0.018 \quad -0.38]$$

while the non-linear control vectors  $G$  and  $H$  come out to be

$$G = [-0.12 \quad -1.2 \quad 0.1 \quad -0.03 \quad 0.84]$$

$$H = [4.9 \quad 5.5 \quad 2.45 \quad 0.07 \quad 2.5]$$

Figures 5.15 to 5.17 show the performance of the system under the controller synthesised above, for different values of the parameters  $D$  and  $R$ .

### 5.3.3 VSAGC Design For A Two-Area Interconnection

The block diagram representation of a two area interconnection is shown in Fig.5.11b. Subsystem  $i$  is dominated by hydro - generating plants while subsystem  $j$  is controlled by steam powered electric generators. Each area is assumed to be autonomous from the point of view of supplying its own load under normal operating conditions. When there occurs a load variation, resulting in deviations in frequency and scheduled tie-line power, the AGC equipment first detects whether the load variation is in its own area or in the neighbouring area (see Appendix A). The AGC equipment reacts only if the load variation is in its own area.

Against the above background, the block diagram of Fig.5.11b can be said to be inherently decoupled. It can

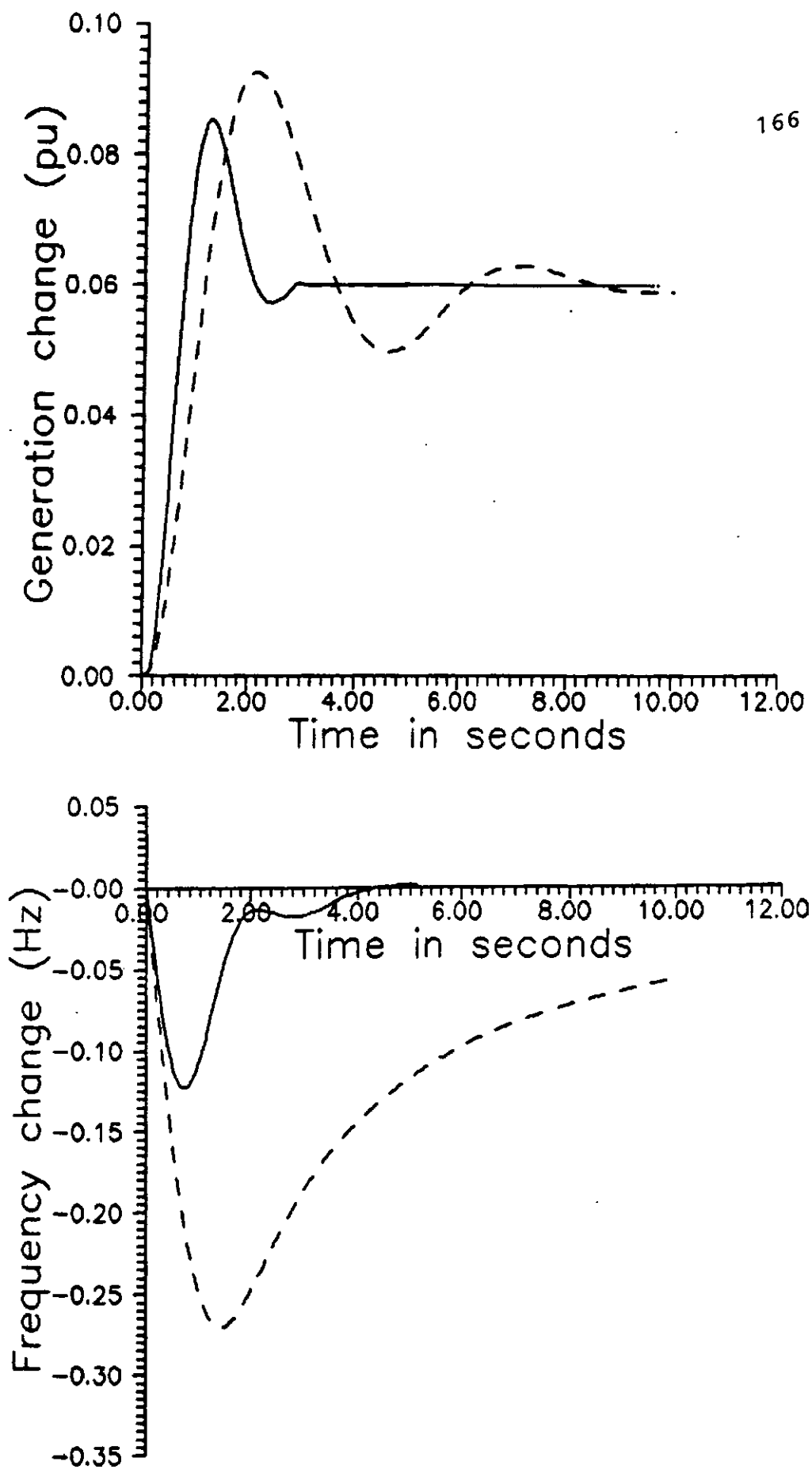


Fig.5.15 System responses for an area dominated by steam powered generators with  $D = 0.75$  pu,  $R = 0.04$  pu  
—— VSAGC ; ----- Int. Controller

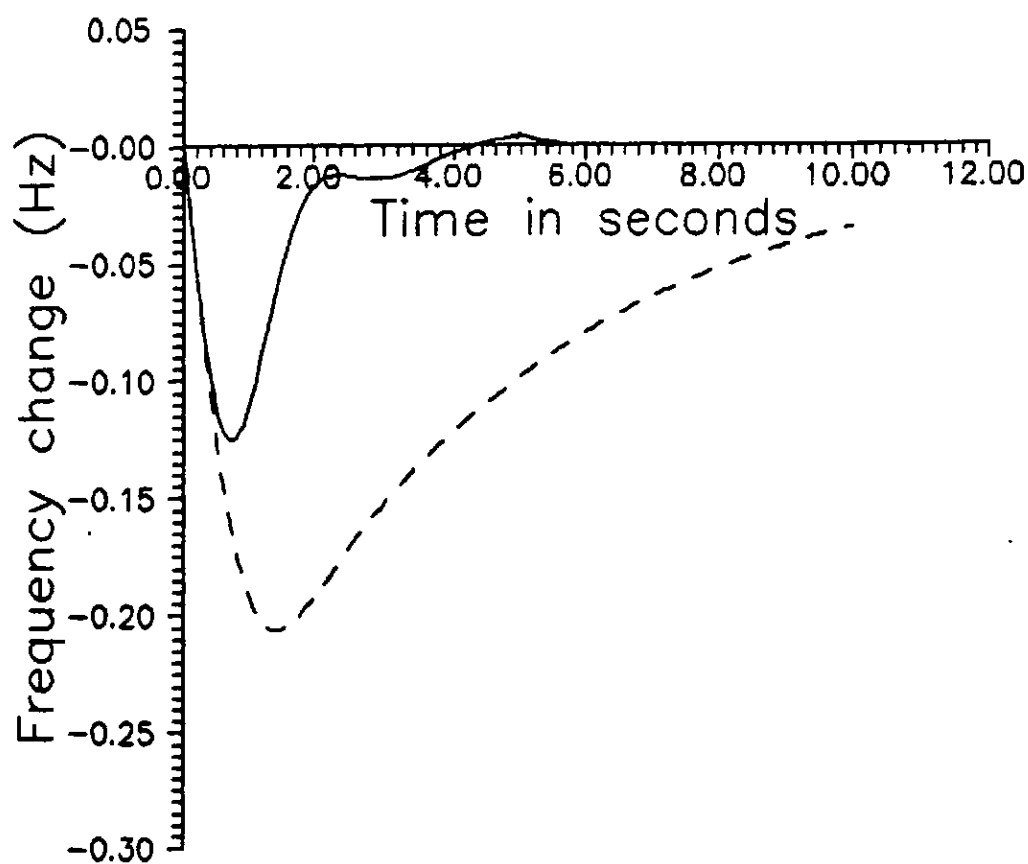
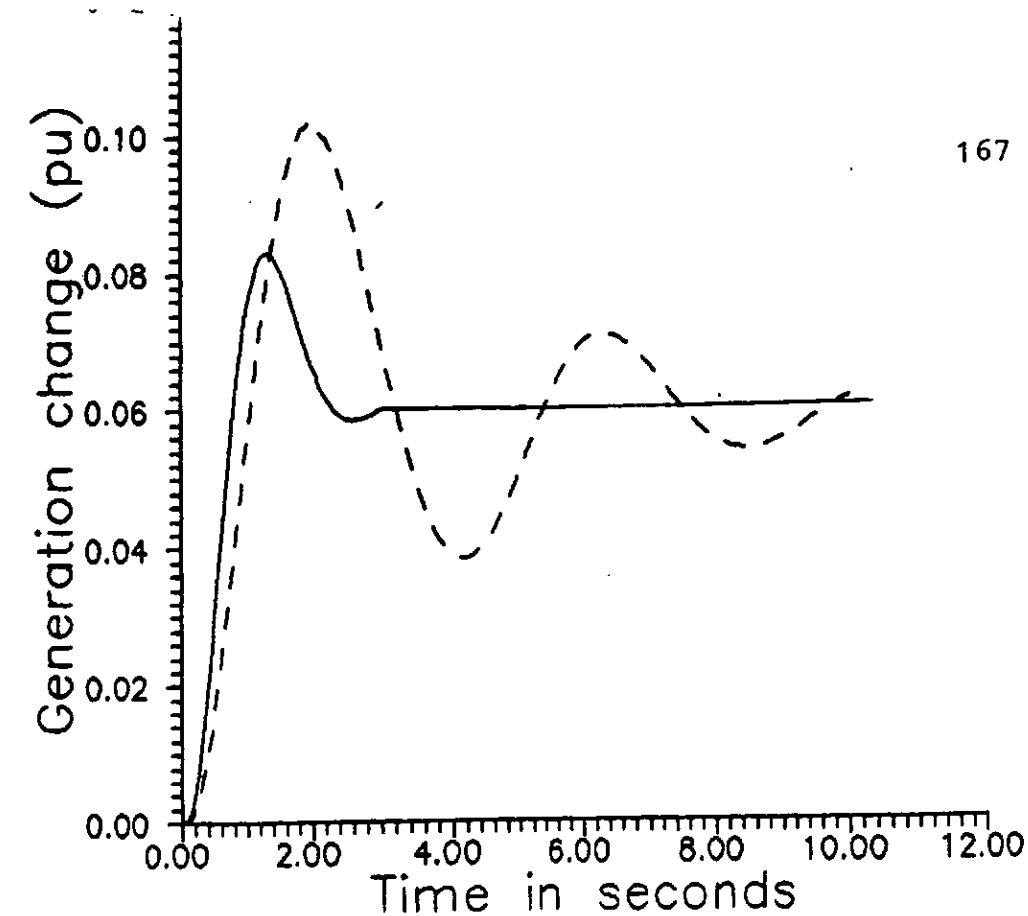


Fig.5.16 System responses for an area dominated by steam powered generators with  $D = 1.5$  pu,  $R = 0.167$ pu  
—VSAGC ; ----- Int. Controller.

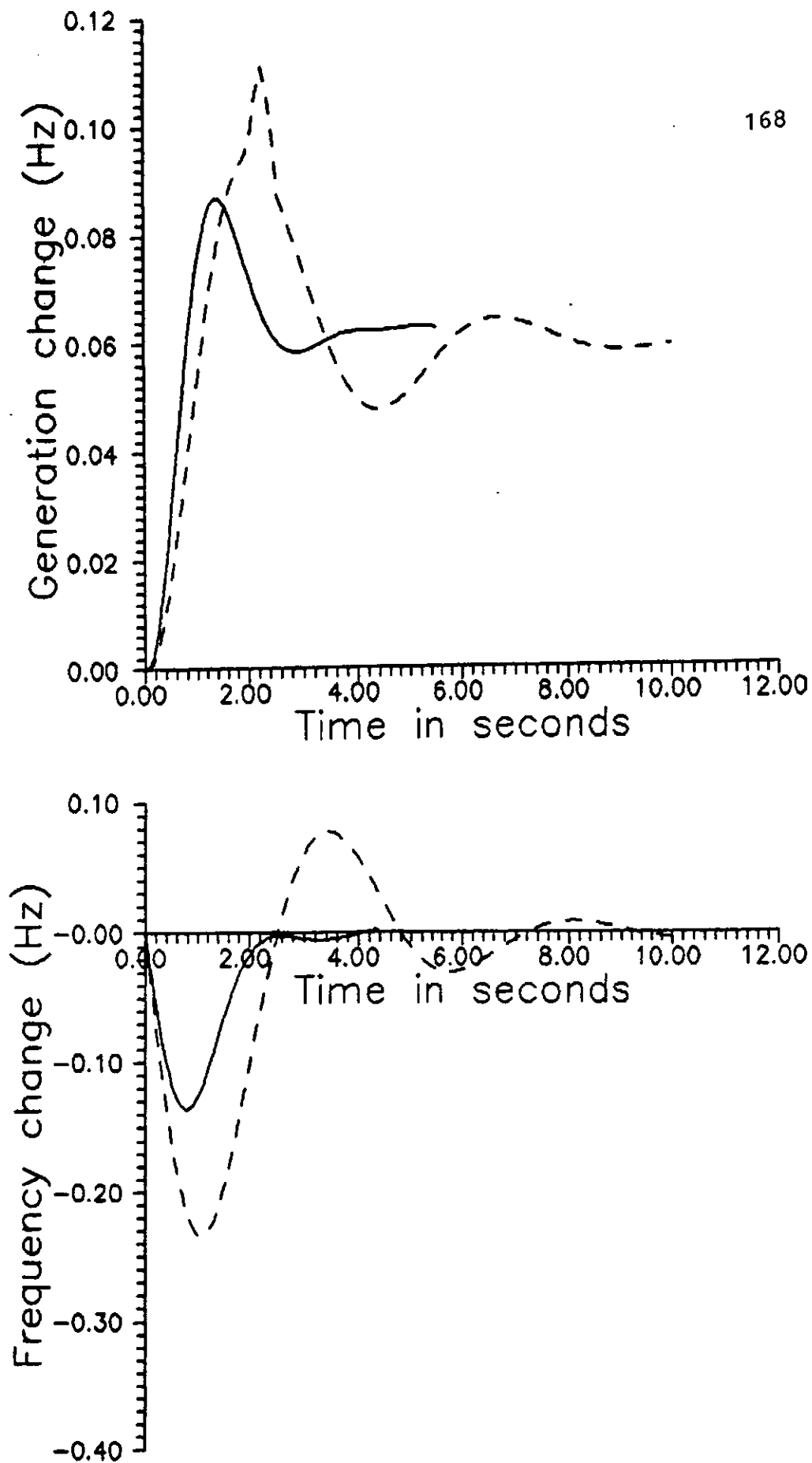


Fig.5.17 System responses for an area dominated by steam powered generators with  $D = 2$  pu,  $R = 0.04$  pu  
— VSAGC ; ----- Int. Controller.

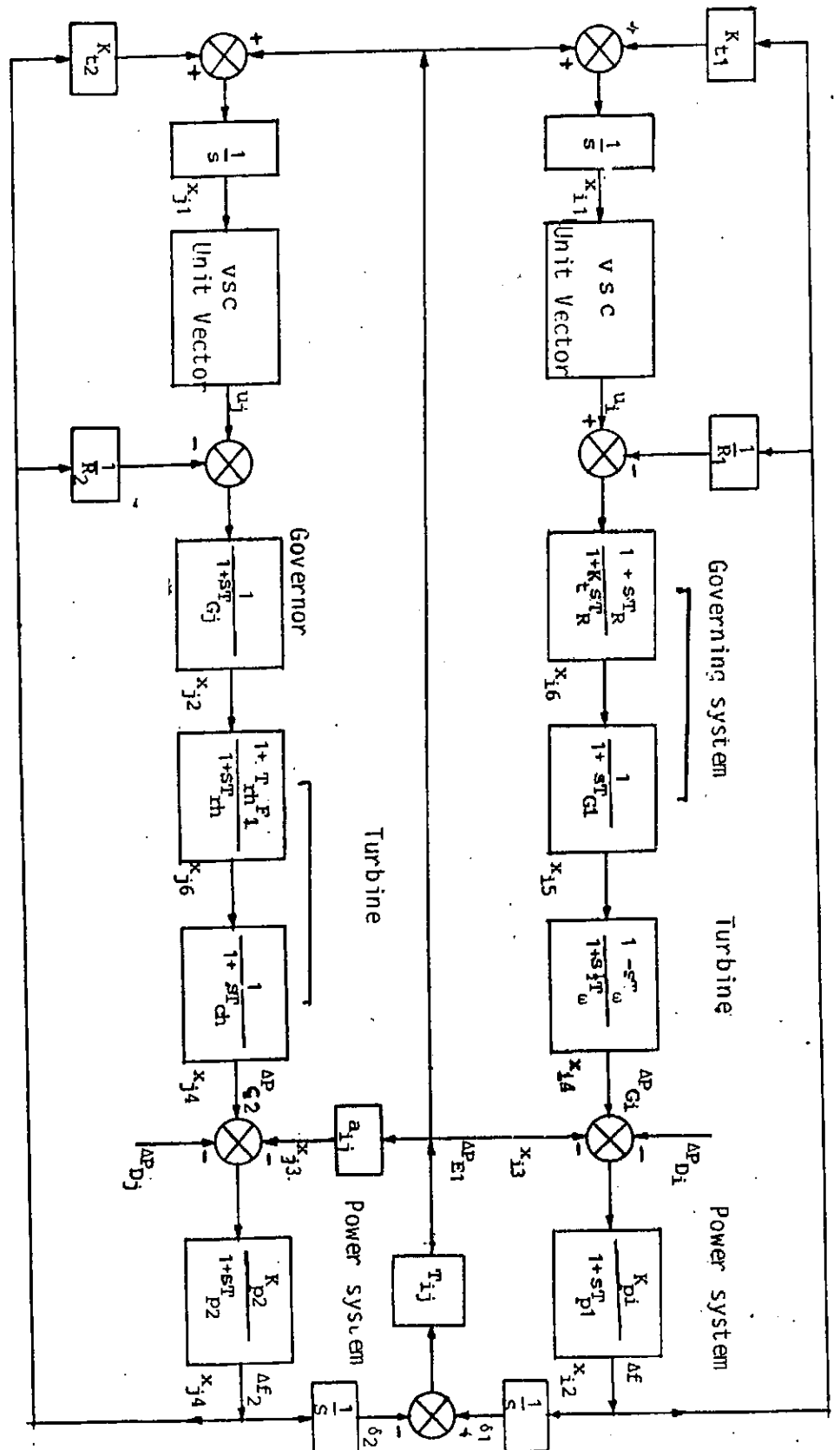


Fig: 5.11b : - Block Diagram of an Interconnected Area with Unit Vector VSC

therefore, be represented in the state variable form of eqn.(5.72) as a weakly coupled set of two subsystems viz:

$$\dot{x}_e(t) = A_e x_e(t) + B_e u_e(t) + \Gamma_e \xi_e(t) \quad (5.82)$$

where

$x_e = [x_i, x_j]'$  is the state vector

$u_e = [u_i, u_j]$  is the control vector

$\xi_e = [\xi_i, \xi_j]$  is the disturbance vector

$x_i$  is the state vector of subsystem i

$u_i$  is the control input vector of subsystem i and

$\xi_i$  is the disturbance vector of subsystem i.

The matrices  $A_e$ ,  $B_e$  and  $\Gamma_e$  are constant matrices defined as

$$A_e = \begin{bmatrix} A_{ii} & A_{ij} \\ A_{ji} & A_{jj} \end{bmatrix}$$

where  $A_{ii}$ ,  $A_{jj}$  are the system matrices of subsystems i and j respectively while  $A_{ij}$ ,  $A_{ji}$  are the respective inter-section matrices;

$$B_e = [B_i, B_j]'$$

$$\Gamma_e = [\Gamma_i, \Gamma_j]'$$

where  $B_i, \Gamma_i$  are the control and disturbance matrices of subsystem  $i$  while  $B_j, \Gamma_j$  are those of subsystem  $j$ .

The block diagram of Fig.5.11 can be reduced to the equation of eqn.(5.81) if:

$$A_{ii} = \begin{bmatrix} 0 & K_{fi} & 1 & 0 & 0 & 0 \\ 0 & -\frac{1}{T_{pi}} & -\frac{K_{pi}}{T_{pi}} & \frac{K_{pi}}{T_{pi}} & 0 & 0 \\ 0 & 0 & T_{ij} & 0 & 0 & 0 \\ 0 & 0 & 0 & -\frac{2}{T_{\omega}} & \frac{2}{T_{\omega}} + \frac{2}{T_{Gi}} & -\frac{2}{T_{Gi}} \\ 0 & 0 & 0 & 0 & -\frac{1}{T_{Gi}} & \frac{1}{T_{Gi}} \\ 0 & \left( \frac{1}{K_{RiT}} - \frac{1}{K_{TRi}} \right) \frac{K_{pi}}{K_{RiT}T_{pi}} & -\frac{K_{pi}}{K_{RiT}T_{pi}} & 0 & 0 & \frac{1}{K_{TRi}} \end{bmatrix} \quad \text{--- (5.83)}$$

$$A_{ij} = \begin{bmatrix} 0 & 0 & 0 & 0 & 0 & 0 \\ 0 & 0 & 0 & 0 & 0 & 0 \\ 0 & T_{ij} & 0 & 0 & 0 & 0 \\ 0 & 0 & 0 & 0 & 0 & 0 \\ 0 & 0 & 0 & 0 & 0 & 0 \\ 0 & 0 & 0 & 0 & 0 & 0 \end{bmatrix} \quad \text{-- (5.84)}$$

$$A_{jj} = \begin{bmatrix} 0 & 1 & K_{f2} & 0 & 0 & 0 \\ 0 & -\frac{1}{T_{Gj}} & 0 & -\frac{1}{R_j T_{Gj}} & 0 & 0 \\ 0 & 0 & 0 & a_{ij} T_{ij} & 0 & 0 \\ 0 & 0 & -\frac{K_{pj}}{T_{pj}} & -\frac{1}{T_{pj}} & \frac{K_{pj}}{T_{pj}} & 0 \\ 0 & 0 & 0 & 0 & -\frac{1}{T_{ch}} & \frac{1}{T_{ch}} \\ 0 & \left(\frac{1}{T_{rh}} - \frac{F_1}{T_{Gj}}\right) & 0 & \frac{-F_1}{R_j T_{Gj}} & 0 & -\frac{1}{T_{rh}} \end{bmatrix}$$

(5.85)

$$A_{ji} = \begin{bmatrix} 0 & 0 & 0 & 0 & 0 & 0 \\ 0 & -a_{ij} T_{ij} & 0 & 0 & 0 & 0 \\ 0 & 0 & 0 & 0 & 0 & 0 \\ 0 & 0 & 0 & 0 & 0 & 0 \\ 0 & 0 & 0 & 0 & 0 & 0 \\ 0 & 0 & 0 & 0 & 0 & 0 \end{bmatrix}$$

(5.86)

$$B_i = [0 \quad 0 \quad 0 \quad 0 \quad 0 \quad \frac{1}{K_t T_R}]' \quad (5.87)$$

$$B_j = [0 \quad \frac{1}{T_{Gj}} \quad 0 \quad 0 \quad 0 \quad \frac{F_1}{T_{Gj}}]' \quad (5.88)$$

$$\Gamma_i = [0 \quad -\frac{K_{pi}}{T_{pi}} \quad 0 \quad 0 \quad 0 \quad \frac{K_{pi}}{K_t T_{pi} R_i}]' \quad (5.89)$$



$$r_j = \begin{bmatrix} 0 & 0 & 0 & \frac{-K_{pj}}{T_{pj}} & 0 & 0 \end{bmatrix} \quad (5.90)$$

By substituting for the parameter values of the Nigerian power system (see Appendix E), eqns.(5.83) to (5.90) reduce to:

$$A_{ii} = \begin{bmatrix} 0 & 0.15 & 1.0 & 0 & 0 & 0 \\ 0 & -0.1415 & -4.717 & 4.717 & 0 & 0 \\ 0 & 0.1 & 0 & 0 & 0 & 0 \\ 0 & 0 & 0 & -0.5 & 3.83 & -3.33 \\ 0 & 6.925 & 4.718 & -4.718 & 0 & -0.0236 \\ 0 & 0 & 0 & 0 & -1.667 & 1.667 \end{bmatrix}$$

$$A_{ij} = \begin{bmatrix} 0 & 0 & 0 & 0 & 0 & 0 \\ 0 & 0 & 0 & 0 & 0 & 0 \\ 0 & 0.1 & 0 & 0 & 0 & 0 \\ 0 & 0 & 0 & 0 & 0 & 0 \\ 0 & 0 & 0 & 0 & 0 & 0 \\ 0 & 0 & 0 & 0 & 0 & 0 \end{bmatrix}$$

$$A_{jj} = \begin{bmatrix} 0 & 1 & 0.53 & 0 & 0 & 0 \\ 0 & -10. & 0 & -5. & 0 & 0 \\ 0 & 0 & 0 & 0.1 & 0 & 0 \\ 0 & 0 & -4.718 & -0.1415 & 4.718 & 0 \\ 0 & 0 & 0 & 0 & -3.846 & 3.846 \\ 0 & -4.9 & 0 & -2.5 & 0 & -0.1 \end{bmatrix}$$

$$A_{ji} = \begin{bmatrix} 0 & 0 & 0 & 0 & 0 & 0 \\ 0 & -0.1 & 0 & 0 & 0 & 0 \\ 0 & 0 & 0 & 0 & 0 & 0 \\ 0 & 0 & 0 & 0 & 0 & 0 \\ 0 & 0 & 0 & 0 & 0 & 0 \\ 0 & 0 & 0 & 0 & 0 & 0 \end{bmatrix}$$

$$B_i = [0 \quad 0 \quad 0 \quad 0 \quad 0.0236 \quad 0]'$$

$$B_j = [0 \quad 10 \quad 0 \quad 0 \quad 0 \quad 5]'$$

$$r_i = [0 \quad -4.718 \quad 0 \quad 0 \quad -4.717 \quad 0]'$$

$$r_j = [0 \quad 0 \quad 0 \quad -4.718 \quad 0 \quad 0]'$$

Now, if the load varies in area i, the EXIST and REACH modules of the computer aided design package VAGCD are invoked to design a VSAGC for subsystem i. In such a case, the procedure of the previous sections is followed to obtain the elements of the hyperplane matrix C as,

$$C_i = [5.06 \quad 1.09 \quad 0.627 \quad 5.32 \quad 1.0 \quad 4.58]$$

while the control vectors are computed to be

$$L_i = [10.7 \quad -12.7 \quad -8.64 \quad 20.2 \quad -10.3 \quad 14]$$

$$G_i = [-21.0 \quad -4.61 \quad -2.66 \quad -2.25 \quad -4.24 \quad 9.0]$$

$$H_i = [0.5 \quad 0.1 \quad 0.06 \quad 0.5 \quad 0.1 \quad 0.45]$$

Figures 5.18 and 5.29 show the performance of subsystems  $i$  and  $j$  respectively for a load variation in subsystem  $i$ .

Alternatively, if the load varies in subsystem  $j$ , the same approach as above is used to synthesize a VSAGC for area  $j$ . In such case, the elements of the sliding plane vector  $C$  are computed as

$$C = [12. \quad 102 \quad 9.87 \quad 0.278 \quad 0.005 \quad 205]$$

while the control vectors are obtained as

$$L = [-92.3 \quad -782 \quad -77.2 \quad 0.16 \quad -0.29 \quad 1560.]$$

$$G = [5.98 \quad -10.2 \quad -0.987 \quad -0.02 \quad -0.005 \quad 20.3]$$

$$H = [5.98 \quad 51.1 \quad 4.93 \quad 0.13 \quad 0.0026 \quad 102.]$$

The performance of subsystems  $i$  and  $j$  are respectively shown in Figs. (5.20) and (5.21) for a load variation in area  $j$ .

#### 5.4 Simulation Results

The performance of the Nigerian power system under VSAGC is investigated here using digital computer simulation. The simulation module described in section 4.7 is deployed to simulate the performance of the system under different

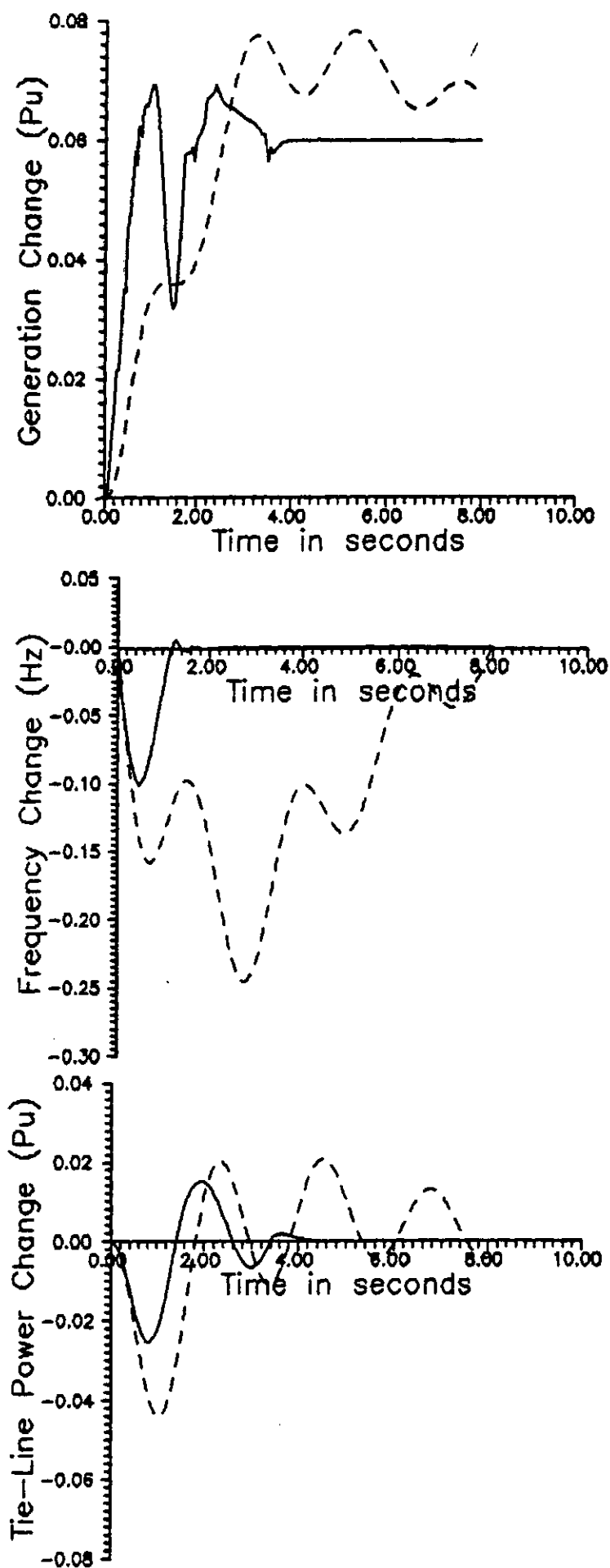


Fig.5.18 System Responses in area i for load variation in area i . — VSAGC; - - - Int. Controller

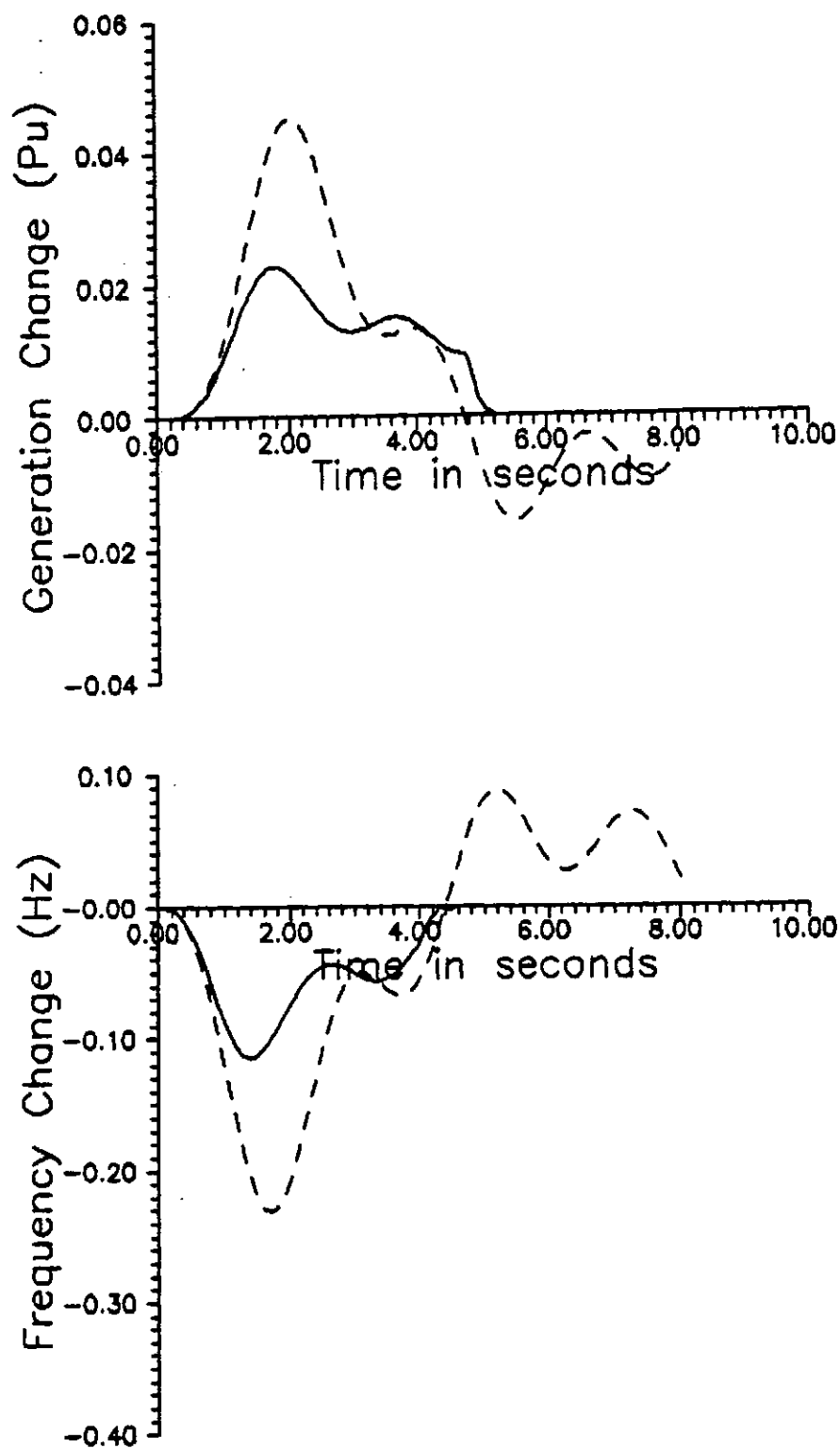


Fig.5.19 System responses in area j for load variation in area i: — VSAGC; - - - Int. Controller

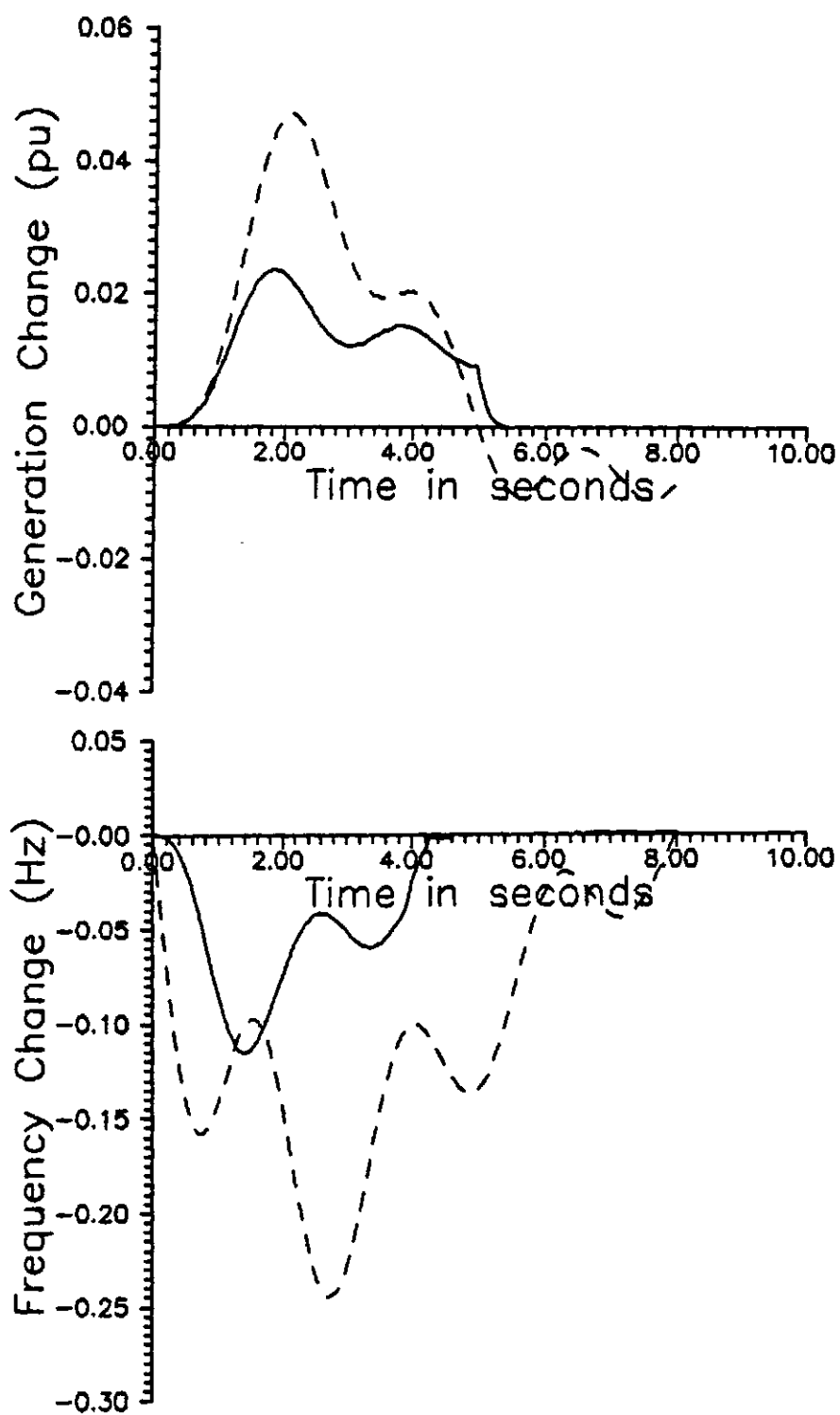


Fig.5.20 System responses in area  $j$  for load variation in area  $j$  : — VSAGC; --- Int. Controller.

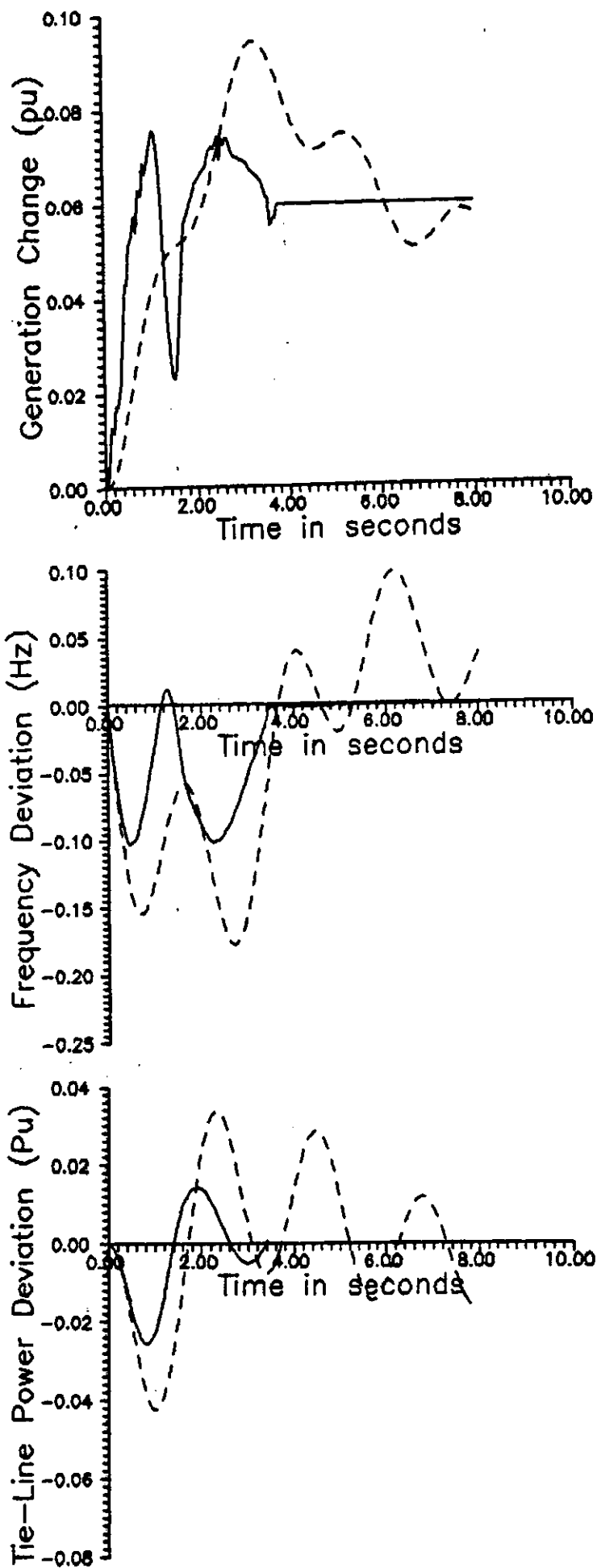


Fig.5.21 System responses in area j for load variation in area i : — VSAGC : ---- Int. Controller.

operating conditions. Four major operating conditions are investigated viz:

1. Absence of rate constraints
2. Presence of rate constraints
3. Presence of rate constraints and water hammer
4. Presence of rate constraints and deadband.

However, for each of the operating conditions, the permanent droop ( $R$ ), the temporary droop ( $r$ ) and the inherent load frequency characteristics ( $D$ ) are made to vary. This is necessitated by the need to determine which settings of  $r$  and  $R$  combine with a given value of  $D$  to give good performance. Such information is vital in deciding the  $r$  and  $R$  settings of all the electric generators employed for AGC.

Furthermore, under normal working conditions, the step change in load demand is not expected to exceed 0.01 pu. Although this standard is maintained by the power systems of industrialised nations, it can hardly exist in a developing country like Nigeria for the simple reason that the available generating/consumption capacity is low. For instance, if the available generating capacity in Nigeria is taken as 3000 Mw and two generators at Egbin power station supplying a total power of 180 Mw disengage from the grid, the change amounts to 0.06 pu. Therefore, the simulation studies carried out in this section considered 0.06 pu change in load demand.

#### 5.4.1 Absence Of Rate Constraints

Here, it is assumed that the maximum gate/valve opening position as well as the opening velocity are not



reached. The generators are also assumed to be operating at less than full load, so that any change in load demand can be absorbed. The change in load demand is also small enough not to force the rate of generation to get to maximum. For the hydro - generators, the blade angle motion varies linearly with the motion of the wicket gates.

Against the background of the above assumptions, the linear models of Figs. 5.9b, 5.10b and 5.11b are sufficient to describe the dynamics of the power system in the respective operating strategies. In other words, the linear equations developed in sections 5.3.1, 5.3.2 and 5.3.3 are used in the simulation studies discussed in this subsection.

The simulation results are shown in Figs. 5.12 - 5.14 for the hydro - dominated single area case, Figs 5.15 - 5.17 for the steam - powered plants dominated single area, while Figs. 5.18 - 5.21 depict the performance of the interconnected area. On each graph, the performance of the conventional integral controller is also super-imposed for ease of comparison. It is seen that the performance of the VSAGC is by far, superior to that of the conventional integral controller for a 0.06 pu step change in load demand in terms of lower overshoots and shorter settling time. Specifically, the settling time for the VSAGC is of the order of 2 - 3 seconds while that of the integral controller is above 10 seconds on the average for the transient frequency deviation. Also a combined setting of  $r = 1.0$  pu, and  $R = 0.1667$  pu with  $D = 2.0$  pu gives the best performance for the hydro - case while  $R = 0.04$  pu with  $D = 2$  gives the

best performance for the steam - area case, of all the combinations simulated. However, all the responses for different parameter variations are acceptable which goes to show that the VSAGC is a robust controller.

#### 5.4.2 Presence Of Rate Constraints

In practice, there is a limit to the amount of generation per second obtainable from a given generating plant. In a steam powered plant, this limit is imposed by the boiler characteristics and varies between 0.01 pu/min to 0.1 pu/min [74]. For the generators at Egbin power station in Nigeria, this limit is quoted as 0.01 pu/min.

The generators of interest at Kainji have a much higher generation rate than the steam plants. At the nominal water level, the maximum limit of generation rate is 0.05 pu/second.

In simulating for generation rate constraints in steam powered plants, the non-linear governing equation of section 5.2.3 [i.e eqn.(5.25)] is used instead of the linearised eqn.(5.68). The simulation result is shown in Fig.5.22 where it is seen that the settling time is doubled when compared with Fig.5.16 (e.g when we have a 0.06 pu step change in load)

In the case of the hydro-generating plants, both the non-linear hydro-governing equations of section 5.2.2 [ie eqns.(5.13) and (5.14)] and the hydro-turbine model of Fig.5.5 for the Kaplan turbine are used. The simulation

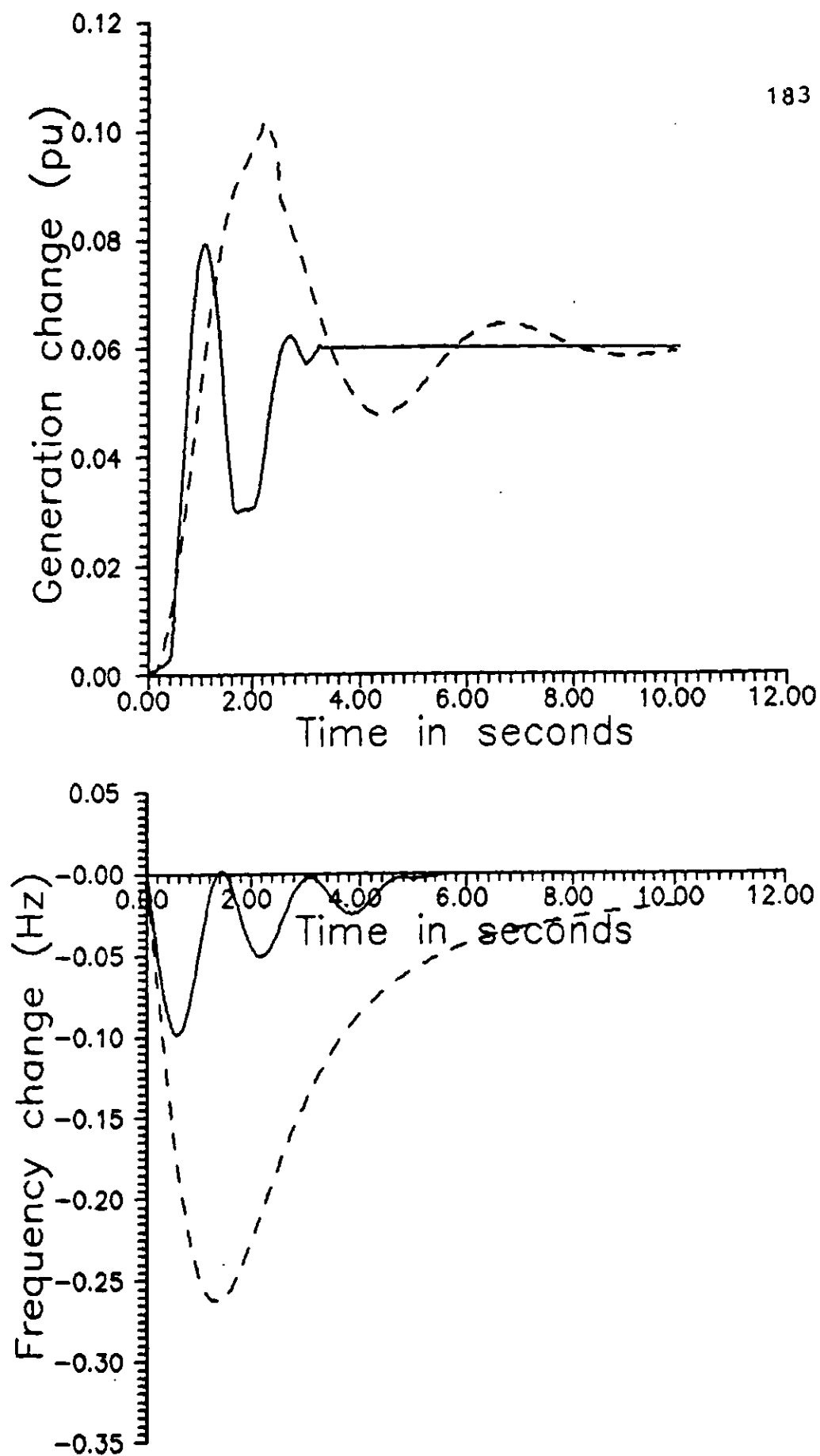


Fig.5.22 System responses in the presence of rate constraints (steam - area case): — VSAGC  
---- Int. Controller.

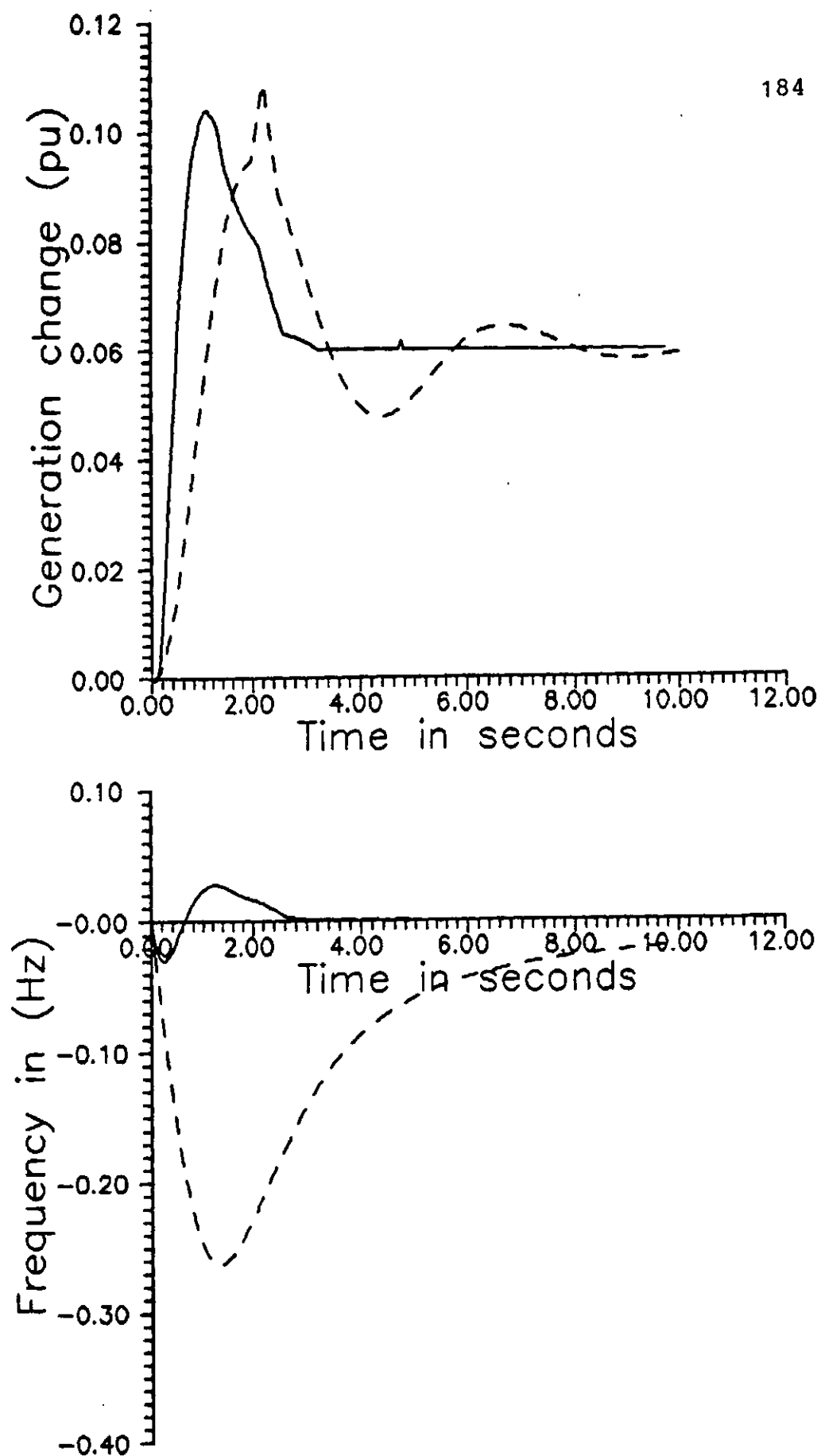


Fig.5.23 System responses in the presence of rate constraints (Hydro - area case) — VSAGC; ---- Int. Controller.

result is presented in Fig.5.23 where it is seen that for a 0.06 p.u change in load, the rate constraint has no significant effect on the performance of the hydro-plant. The fact is that the rate of 0.05 p.u/second could not even be attained during simulation. This fact must have informed the conventional use of such hydro - generating plants for the regulation of sustained load changes in power systems.

#### 5.4.3 Presence Of Rate Constraints And Water Hammer

Water hammer is a phenomenon that affects only the hydro - generating plants. The compressibility of water coupled with the elastic expansion of the conduit, gives rise to travelling pressure waves known as water hammer. It is shown in Appendix C that when water hammer effect is considered, the transfer function relating the turbine power with hydro-gate position is given by

$$\Delta P_m = \frac{M_\omega s^2 - T_\omega s + 1}{M_\omega s^2 + \frac{T_\omega}{2}s + 1} \Delta G \quad (5.91)$$

By assuming that the turbine power is proportional to the generated power,  $\Delta P_m$  in eqn.(5.90) can be replaced by  $\Delta P_G$  so as to conform with the block diagram of Fig.5.10b. By combining the non-linear hydro - governing equations with eqn.(5.91), a simulation study of the water hammer effect is performed on the single area power system dominated by

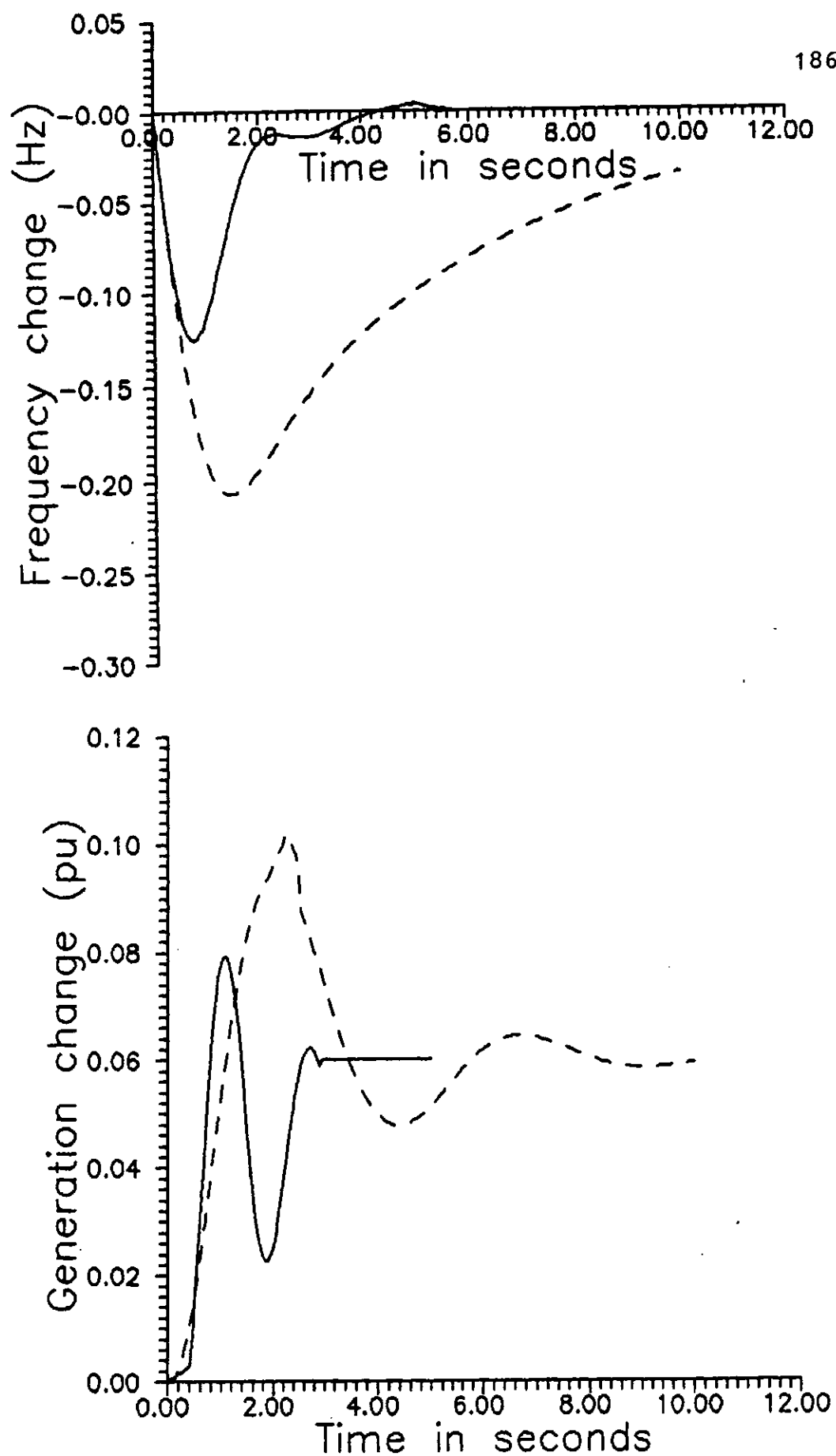


Fig.5.24 System responses in the presence of water hammer

— VSAGC    - - - - - Int. Controller.

hydro - generating plants. The value of  $M_w$  is taken to be 0.222 corresponding to a height of 200 feet (60.96 metres) and a length of 1000 feet (304.8 metres).

The result is presented in Fig.5.24 where it is easily observed that the effect of water hammer is minimal for 0.06 pu step change in load. This minimal effect is as a result of inherent robustness of variable structure controllers. The performance of the integral controller, which is shown in broken lines is seen to have deteriorated.

#### 5.4.4 Presence Of Rate Constraints And Deadband

In simulating for deadband effects in the presence of rate constraints, the non-linear equations are utilized. It is shown in Appendix D that the effect of deadband is to increase the effective speed regulation such that

$$R_e = R \left( 1 + \frac{2db}{R\Delta L} \right) \quad (5.92)$$

where  $R_e$  is the effective speed regulation in pu

$R$  is the governor droop setting

$db$  is the deadband in pu

$\Delta L$  is the per unit change in load demand.

The institute of Electrical and Electronic Engineers' (IEEE) standards allow for a maximum governor deadband of 0.06%, or 0.0006 pu. Then for a change in load demand of 0.06 pu and a droop setting of 4%, the simulation

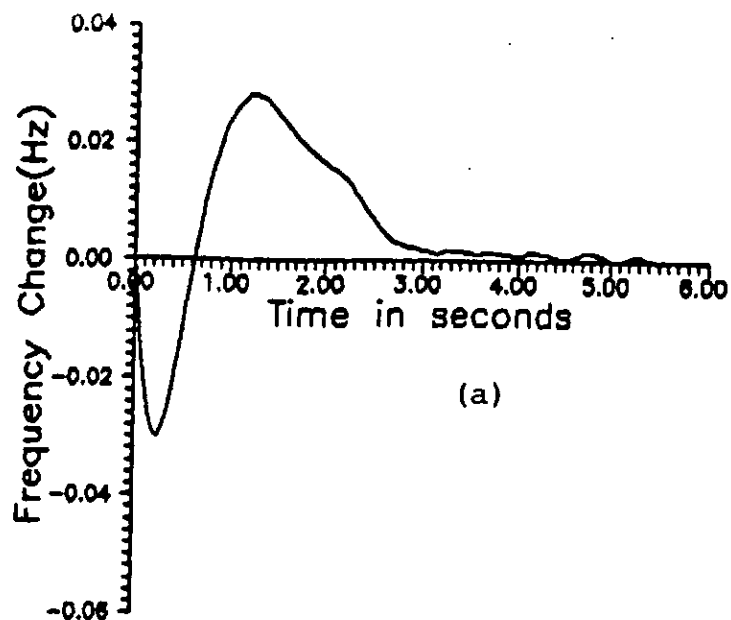
results are shown in Fig.5.25 for a hydro - dominated case and Fig.5.26 for an area dominated by steam powered plants. In each case, the system remains stable as confirmed by the phase plots of Figs.5.26b and 5.27b. This confirmation of system stability is necessary, since it is known that deadband effects can result in sustained system oscillation.

From all the results shown so far, it is clear that the VSAGC performance under deadband effects is acceptable from the point of view of the desired specifications listed in chapter one. However, it has to be observed that the maximum frequency and tie - line deviations have been increased by about 10% while the settling time has been increased by about 13%.

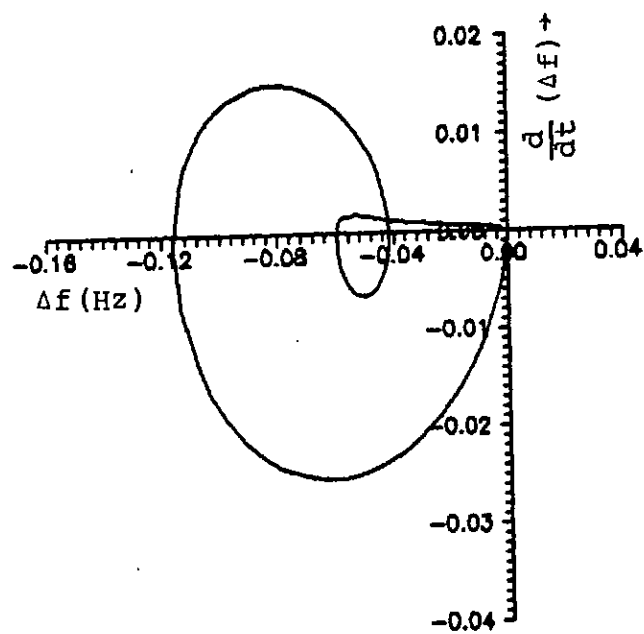
### 5.5 Conclusion:

This chapter has proposed three automatic generation control models of the Nigerian power system. Based on the linearised versions of these models, VSAGC schemes were synthesised for the power system plant using a design procedure proposed in chapter 3. Digital computer simulation studies were also deployed to evaluate the performance of the Nigerian power system under VSAGC for different operating conditions. Various linear and non-linear effects which affect practical power systems were also simulated so as to enhance the credibility of the results. Though a step change in load is assumed as the disturbance function, its magnitude is large enough to represent very closely the type of load

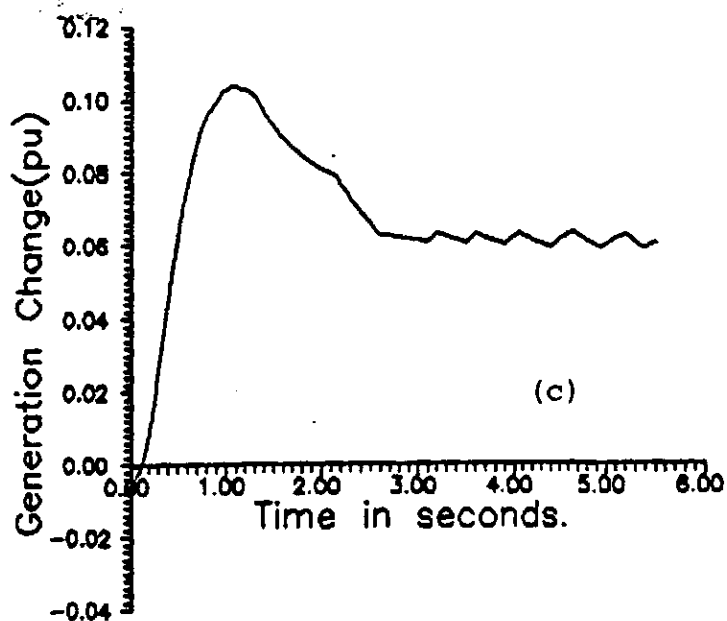




(a)

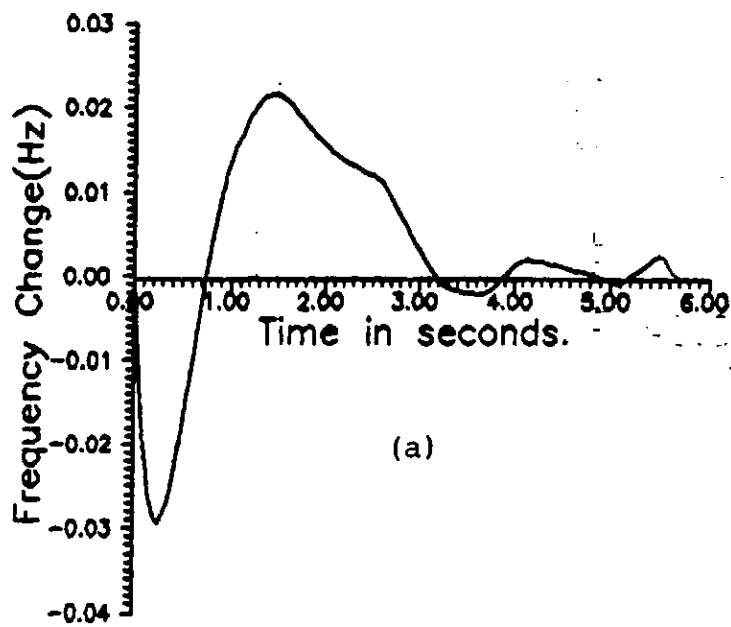


(b)

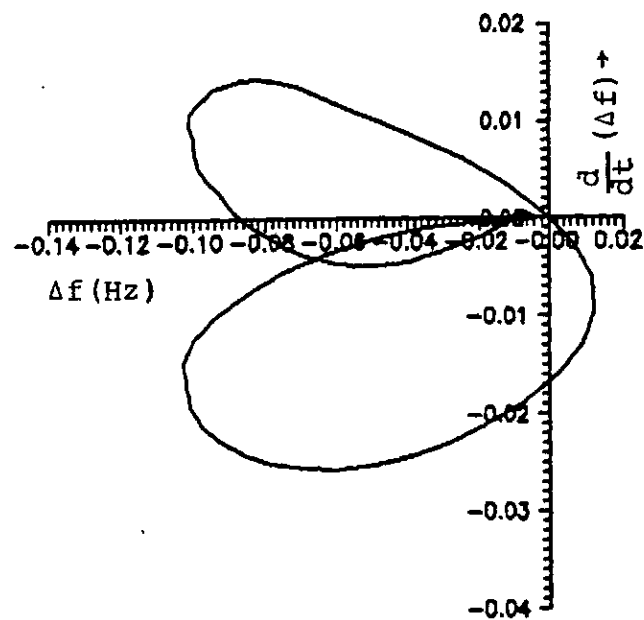


(c)

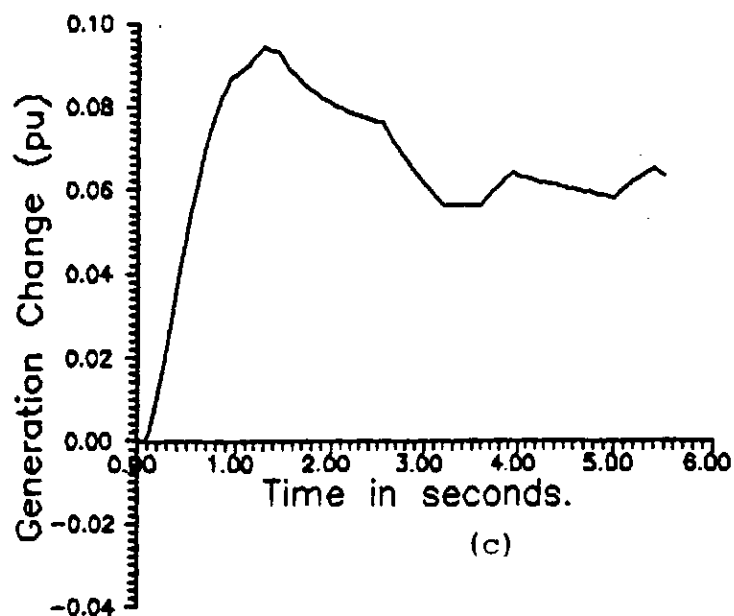
Fig.5.25 System responses in the presence of deadband  
(Hydro - dominated case)



(a)



(b)



(c)

Fig.5.26 System responses in the presence of deadband  
(Steam - dominated case).

variations prevalent in developing countries like Nigeria.

Based on the results obtained, it can be concluded that the VSAGC scheme possesses superior performance when compared with the conventional integral controller, in terms of shorter settling time and lower frequency, generated power and tie - line power deviations following a step change in load demand of 0.06 pu. Also, it has been shown that the VSAGC scheme is very robust, reacting minimally to system parameter variations and extraneous disturbances.

In the next chapter, the achievements of this thesis will be highlighted and appropriate conclusions drawn together with suitable recommendations. Suggestions are also advanced for further work.

## CHAPTER SIX

### CONCLUSIONS AND RECOMMENDATIONS

The work undertaken in this thesis has been motivated by the relatively poor performance of the Nigerian power system which is characterized by frequent power failures, as a result of which the Nation suffers huge economic loss. Having identified frequency and tie-line power transients as dangerous inputs to the power system plant, this thesis set out to develop a control scheme for the regulation of the everpresent mismatch between real power generation and consumption so as to maintain the frequency and tie-line power interchange within their scheduled limits. It has been revealed in chapter one that such an automatic generation control (AGC) scheme is currently implemented manually in most developing countries of the world including Nigeria. *Conclusion*

However, in developing a scheme for the AGC of electrical power systems, it has been found necessary to ensure such qualities as high speed of response represented by short settling time; minimal frequency and tie-line power deviations characterised by low overshoots and zero steady - steady error. Furthermore, the envisaged AGC scheme should be robust so as to withstand operating point variations as well as possess a simple structure in order to enhance practical implementation and reduce operating time lag, which, otherwise, will increase the system dead-

band. Above all, the scheme should be implementable on either a dedicated or general purpose digital computer to enable it form part of the present day energy management systems (EMS).

This thesis then, started in chapter two by reviewing the existing techniques for the AGC of electrical power systems. A scheme based on the classical control design approach which resulted in a proportional-plus-integral (PI) control action was shown to possess a simple structure, *shown where?* but exhibited poor dynamic performance in terms of large overshoots and relatively long settling time. Next to be investigated was a linear quadratic optimal control approach based on state space techniques. Though the dynamic performance of the system was greatly improved, the optimal control scheme for AGC was found to have a complex structure, *have it where?* requiring a lot of computer time and space. This has rendered its practical implementation rather costly. Also, the parameters of the optimal generation controller were found to be heavily dependent on the power system's operating point with the result that optimality became a temporary property of the system.

In order to minimise the short comings of the optimal control scheme for AGC, an alternative approach based on the variable structure systems (VSS) theory was investigated. It was discovered that the three key properties of fast response, structural simplicity and robustness were possessed by a variable structure control system. However, the design methodology for contemporary variable structure

automatic generation control (VSAGC) schemes reported in the technical literature had been largely a trial and error approach which was found to be time consuming. In addition, the control hierarchy algorithm which was employed for the synthesis of the nonlinear control function was discovered to be wasteful of control effort as well as requiring as many number of switchings as the system order.

Therefore, a new VSAGC design approach was proposed in chapter three. The proposed technique employs a systematic procedure based on the generalised eigen-structure assignment to compute the elements of the hyperplane matrix  $C$ . On the other hand, the synthesis procedure for the nonlinear control function is based on a design philosophy that the individual controls are continuous except on the final intersection of the switching hyperplanes where all the controls are discontinuous together. This approach ensures that the system motion is always towards the sliding manifold with the advantage that control effort is conserved and only two switchings are required. The superiority of the proposed VSAGC scheme over the existing one was amply demonstrated using digital computer simulation results. *how?  
data!*

In chapter four a computer aided design software package was developed for the synthesis and performance evaluation of the proposed VSAGC scheme on an industry standard PC-AT microcomputer. The package named "the Variable Structure Automatic Generation Control Design" (VAGCD)

was designed to have a modular structure as well as being fully interactive. The modular structure allowed for the use of the link-overlay facility whereby each module could be run as a stand alone system with the advantage that the working core memory requirement of the computer was minimised. The elaborate interactive capability of the package was meant to create a tool for both the novice and expert users so as to enhance the use of the package in education, research and industry environments. Simulation studies using the package were made to yield results in tabular or graphical form which could be observed on the video display unit or printed on paper.

The performance of the proposed VSAGC scheme was demonstrated in chapter five with application to Nigerian power system. Three AGC models of the Nigerian power system were proposed, each representing a possible operating strategy. The models, which were generally nonlinear, were developed from first principles, based on the real power balance equation, relating the mismatch in power generation and consumption to the changes in accelerating power and frequency. The first two models consisted of single control areas dominated by hydro and steam powered generators respectively. The third model was a two-area interconnection with one area dominated by hydro generating plants and the other by steam powered plants.

Then, the computer aided design package VAGCD was employed to synthesize an AGC scheme for each of the proposed

models. Simulation results were presented showing the proposed VSAGC performance for different operating conditions, including certain linear and nonlinear phenomena that occur in practical power systems. For ease of comparison, simulation results showing the PI controller performance for AGC were also presented. It was clear that the VSAGC performance was superior to that of the PI control scheme.

Specifically, the achievements of this thesis may be summarised as follows:-

1. An up-to-date survey of automatic generation control techniques reported in the technical literature is presented. These techniques have been classified into four main groups with the limitations of each group clearly pointed out. It is concluded that the deployment of variable structure controllers to the solution of the AGC problem holds substantial promise.
2. A new design approach for variable structure automatic generation control (VSAGC) schemes has been proposed. The proposed approach is based on the theory of variable structure systems (VSS) and it exploits the concepts of generalised eigenstructure assignment and unit-vector control, to synthesize a feedback control structure which guarantees the global reaching of the sliding mode and the preservation of motion on the sliding plane towards the origin of coordinates. The preserved motion must exhibit desired dynamic behaviour which is



determined by the appropriate selection of the eigen-structure spectrum. Simulation results are used in chapter three to demonstrate the superior performance of the proposed scheme in terms of speed of response, dynamic accuracy and robustness.

3. An interactive computer-aided design software package has been developed for the design and performance evaluation of the proposed VSAGC strategy as well as other existing AGC techniques, so as to enhance the use of the package for education and research. The package named VAGCD has the additional capability of providing the software part of a computerised control structure for the AGC of an electrical power system, in a power control centre environment. Hence, it can easily fit into the present day energy management systems (EMS). In order to reasonably predict the behaviour of any power system under AGC, the package has been provided with the means of simulating such nonlinear effects as generation rate limits, water hammer and deadband effects, which occur in practical power systems.
4. The operation of the Nigerian power system has been studied. From the data presented in chapter one, it is easily observed that the system performance is relatively poor. The trend of the yearly figures

further shows that the current efforts at increasing the generation capacity does not seem to have improved the system performance much. The study has also revealed that the generation control mechanism is completely manual, relying on telephone instructions from the National control centre (NCC) to the remote generating stations. Since pure time delay is known to cause instability in control systems, it can be concluded that the utter neglect of the AGC structure may have been partly responsible for the overall poor performance of the Nigerian power system.

5. Analytical models of the Nigerian power system suitable for the application of modern control theory to achieve generation control, have been proposed. Following the standard techniques of power system modelling for AGC, three models of the Nigerian power system are proposed, each representing a possible operating strategy. The models are useful in predicting the behaviour of the power system under different AGC schemes, via digital computer simulation, before deciding on which AGC strategy to adopt.
6. The proposed VSAGC scheme has been successfully applied to models of the Nigerian power system in chapter five. Simulation results show that the

performance of the system remains acceptable even in the presence of both nonlinear effects and relatively wide variations in load demand. For the sake of comparison, the system performance under the PI control action for AGC are also shown. The simulation results amply demonstrate the efficacy of the proposed scheme. The results in chapter five further demonstrate the applicability of the software package VAGCD.

Based on the achievements of this thesis listed above, it can be concluded that the thesis has attained its set objectives.

#### 6.1 Suggestions For Further Work

The work presented in this thesis has not considered some of the practical aspects of VSAGC implementation for a given electrical power system. These aspects include, the modalities for linking the VSAGC equipment to the remote generating stations, the distribution logic to be used and techniques of data acquisition. It is suggested that further work be done in this area before actual installation can commence.

Furthermore, it will not be very economical to dedicate one computer to AGC alone. It is therefore suggested that further work be done to incorporate other

functions like optimum power flow (OPF), economic load dispatch (ELD) and contingency analysis into the computer aided design package (VAGCD). Indeed VAGCD has been designed to allow for the addition of more modules that are not necessarily related to AGC.

# REFERENCES

- [1] IEEE Standard Definition of Terms in Automatic Generation Control of Electric Power Systems.
- [2] National Control Centre: "Annual grid operations report" 1985, 1986 - 1989.
- [3] Mortlock, J.R. and Humphrey Davies "Power system analysis" Chapman and Hall, London 1945.
- [4] Director, NCC Osogbo: "Day - to - day operational responsibilities and duties for joint working between NCC and area control centres" 1987.
- [5] NCC Osogbo "Reports of system disturbances of several dates" issued by NCC (random samples).
- [6] Brown Boveri Company "Procontrol: Functional description of the computer control system", BBC, Baden (Switzerland) 1985.
- [7] General Electric Company "Technical description of S/3 SCADA system" GEC Measurements March 1988.
- [8] Filippov, A.G. "Application of the Theory of Differential Equations to Non-linear Problems in Automatic Control" Proc. of 1st IFAC Congress, pp 923 - 927 Moscow, 1960.
- [9] Emelyanov, S.V. and Kostyleva, N.E. "Design of variable structure control systems with Discontinuous Switching Functions" Eng. Cybern. No.1, pp 156 - 160, 1964.
- [10] Itkis, U. "Control systems of Variable Structure" Wiley, New York 1976.
- [11] Utkin, V.I. "Sliding Modes and their Application in Variable Structure Systems", IEEE Trans. Vol.AC 22, No.2, April 1977.
- [12] Utkin, V.I. "Discontinuous Control Systems: The state of the Art in Theory and Practice" IFAC Congress, Munich, 1987, pp 75 - 94.
- [13] Utkin, V.I. and K.D. Yang, "Methods for Constructing Discontinuity Planes in VSS" Translated from *Automatika i Telemekhanika*, No. 10, pp. 72 - 77, October, 1978.
- [14] El-Ghezawi, O.M.E., et al "Analysis and Design of Variable Structure Systems using a Geometric Approach" INT. J. of Control. vol.38, No.3, pp 657 - 671 1983.
- [15] Dorling, C.M. and Zinober, A.S.I. "Two Approaches to Hyperplane Design in multivariable variable structure control systems".

- [16] Ryan, E.P. and Coreless, M. "Ultimate Boundedness and Asymptotic Stability of a Class of Uncertain Systems..." IMA Journal of Math. Control Information; Vol.1, No.3, pp.223 - 242, 1984.
- [17] Drazenovic, B. "The Invariance Conditions in variable structure systems" Automatica vol.5, pp 287-295
- [18] Ryan, E.P. "A Variable Structure Approach To Feedback Regulation of Uncertain Dynamical Systems". INT. J. Contr. vol.38, No.6 pp 1121 - 1134, 1983.
- [19] Kwakernaak, H and Sivan, R. "Linear Optimal Control Systems, Wiley, New York, 1972
- [20] Dorling, C.M. "Manual for VASSR CAD Package." Unpublished Report: Dept. of Applied and Computational Mathematics, University of Sheffield, 1985.
- [21] Concordia, C. and Kirchmayer, L.K. "Tie-line Power and Frequency Control of Electric Power Systems" AIEE Trans. Vol 72, Part III pp 562-572, 1953.
- [22] -Ibid - Part II, AIEE Trans, Vol.73 Part III-A pp 133 - 141, 1954.
- [23] Hovey, L.M. "Optimum Adjustment of Governors in Hydro Generating Stations", Engineering Journal (EIC) pp.64-71 November 1960
- [24] Undrill, J.M. and Woodward, J.L. "Nonlinear Hydro - Governing Model and Improved Calculation of Temporary Droop", IEEE Trans. vol. PAS-86, No.4, pp.443 - 452, April, 1967.
- [25] IEEE Committee Report. "Dynamic Models for Steam and Hydro Turbines in Power System Studies", IEEE Trans. vol PAS-92, pp.1904 - 1915, Nov/Dec.1973.
- [26] Demello F.P. et al "Automatic Generation Control, Part 1 - Process Modelling " IEEE Trans.vol PAS-92 pp 710 - 715, March/April 1973.
- [27] Taylor, C.W. and Cresap, R.Lee. "Real - Time Power System Simulation for Automatic Generation Control" IEEE Trans. vol PAS-95, no.1, pp 375 - 384; 1976
- [28] Elgerd, O.I. and Fosha, C.E. "Optimum Megawatt - Frequency Control of Multiarea Electric Energy Systems" IEEE Trans. vol. PAS-89, no.4, pp.556-563 April 1970.
- [29] Fosha, C.E. and Elgerd, O.I. "The Megawatt - Frequency Control Problem: A New Approach via Optimal Control Theory" IEEE Trans. vol -PAS-89, No.4, pp 563-577 April 1970.

- [30] Cavin, R.K. III et al "An Optimal Linear Systems Approach to Load-Frequency Control" IEEE Trans. vol. PAS-90, No.6, pp.2472-2482, 1971.
- [31] B.B.C. (Brown Boveri) "Manual For the Control Supervisor" Section on Automatic Generation Control pp.2 - 20, 1988.
- [32] Ontario Hydro "Production Manual" Bulletin, No. D-1, Section on Load-frequency Control 1972.
- [33] Elgerd O, I. "Electric Energy Systems Theory, An Introduction" TATA McGraw-Hill Publishing Company Ltd, New Delhi. India 1979 (Reprint) ,pp 315-389.
- [34] Kirchmayer, L.K. "Economic Control of Interconnected Systems" John Wiley and Sons N/Y, 1959.
- [35] IEEE Committee Report. "Power Plant Response" IEEE Trans. vol PAS-86, No.3, March 1967 pp.128-139
- [36] -Ibid- "Current Operating Problems Associated with Automatic Generation Control", IEEE Trans. vol. PAS -98, pp.88-96, 1979.
- [37] Hovey L.M. and Bateman, L.A. "Speed - regulation tests on a Hydro - Station supplying an isolated load" AIEE Trans. vol. PAS - 81, pp.364-368, October 1962.
- [38] Lawal, E.Y. "Duties of the National Control Centre" Proceedings of the Junior Staff Seminar NEPA, pp 1-15, May 1989.
- [39] Calovic, M. "Linear regulator design for a load and frequency control" IEEE Trans. vol PAS-91 No.6, pp 2271 - 2285, 1972
- [40] Calovic, M.S. et al, "Autonomous area generation control of interconnected power systems" Proc. IEEE, vol.124, No.4 April 1977
- [41] Tacker, E.C. et al "Design and simulation of an optimal stochastic controller for a composite two-area power system" Proc. IEEE Decision and Control Conference 1971
- [42] Miniesy, S.M. and Bohn, E.V. "Optimum load-frequency continuous control with unknown deterministic power demand" IEEE Trans. Vol. PAS-91, No.5 pp.1910 -1915 1972.
- [43] Glover, J.D. and Schweppe, F.C. "Advanced Load-frequency Control" IEEE Trans. vol. PAS-91, No.5, pp 2095-2103 Sept/Oct. 1972.
- [44] Williams, J.L. "Sensitivity analysis of the optimum Performance of conventional load-frequency control", IEEE Trans. vol. PAS-93, pp 1287-1291 1974.

- [45] Calovic, M.S. "Power system load and frequency control using an optimal linear regulator with integral feedback" 5th IFAC Congress, paper No.7.3 1972
- [46] Kwanty, H.G. et al "An optimal tracking approach to load-frequency control" IEEE Trans. vol.PAS-94, No.5, Sept/Oct. 1975.
- [47] Fosha, C.E.Jr. Elgerd, O.I. "Optimum linear control of the multivariate megawatt - frequency control problem" Proc. of JACC, Boulder - Colo, pp 471-472 1969
- [48] Young, K.D. et al "A singular perturbation analysis of high gain feedback systems" IEEE Trans. vol. AC-22, No.6, 1977 pp 931 - 937.
- [49] Slotine, J.J. and Sastry, S.S. "Tracking control of nonlinear systems using sliding surfaces, with application to robot manipulators". Int. J. of Control vol.38, No.2, 1978 pp 465 - 492.
- [50] Bengiamin, N.N. and Kauffmann, B. "Variable Structure position Control" Control Systems Magazine vol.4, No.3, pp 3-8, August 1984.
- [51] Young, K.D. "Controller design for a manipulator using theory of variable structure systems" IEEE Trans. vol.SMC-8, No.2 Feb.1978 pp.101-109.
- [52] Asada, H. and Slotine, J.J. "Robot analysis and control" Wiley - Interscience Publisher 1986
- [53] Harashima, F. et al. "Tracking Control of Robot Manipulator using sliding mode" Proc. of the 15th Inter. symposium on Industrial Robot. Sept 11-13, Tokyo 1985, pp 657 - 664.
- [54] Harashima, F. et al. "Practical robust control of robot arm using variable structure control". Proc. IEEE Intern. Conf. on Robotics and Automation, April 7 - 10, San - Francisco, USA, pp 532-539.
- [55] Hiroi, M. et al "Microprocessor based decoupled control of manipulator using modified model-following method with sliding mode" IEEE Trans. IE -33, No.2, pp 110 - 113 ,1986.
- [56] Hsu, Y.Y. and Chan, W.C. "Optimal variable structure controller for DC motor speed control" IEE Proc. vol.131 Pt.D No.6, Nov. 1984 pp 233 - 237.
- [57] Sabanovic, A. and Izosimov, D. "Application of sliding modes to Induction motor control" IEEE Trans IA-17 No.1, pp 41 - 49, 1983.



- [58] Dote, Y. and Hoft, R.G. "Microprocessor based sliding mode controller for DC motor control drives" IEEE IAS Conf. Record Cincinnati USA, 1980.
- [59] Harashima, F. et al. "MOSFET Converter - fed position servo system with sliding mode control" IEEE Trans. IE-32, No.3, pp 28 - 244 1985
- [60] Hashimoto, H. et al. "Brushless servomotor control using variable structure approach" IEEE - IA society annual meeting, Part 1, pp.72 - 79 1986
- [61] Matthews, G.P., Decarlo R, and Lifebvre "Towards a feasible variable structure control design for a synchronous machine connected to an infinite bus" IEEE Trans. AC-31, No.12, 1986.
- [62] Chan, W.C. and Hsu, Y.Y. "Stabilization of power systems using a variable structure stabilizer" Electrical power systems Res. vol.6, pp 129-139, 1983
- [63] -Ibid - "An optimal variable structure stabilizer for power system stabilization" IEEE Trans. PAS-102 pp 1738 - 1746, 1983
- [64] Panicker, K.S.M. et al "The transient stabilization of a synchronous machine using variable structure systems theory" Int.J. control, vol.42, No.3, pp 715-721, 1985.
- [65] Bengiamin, N.N. and Chan, W.C. "Variable structure control of electric power generation" IEEE Trans. PAS-101, pp.376-380, 1982
- [66] -Ibid - "Automatic generation control of interconnected power systems using variable structure controllers" Proc. IEE, vol.128, Pt.C, No.5, Sept.1981 pp 269 - 279.
- [67] Chan, W.C. and Hsu, Y.Y. "Optimal control of electric power generation using variable structure controllers" Electr. Power Syst. Res. vol.6, pp.269 - 278, 1983
- [68] Sivaramakrishnan, A.Y. et al. "Design of variable - structure load-frequency controller using pole assignment technique" Int.J. Contr. 40, No.3, pp.487-498, 1984.
- [69] Wollenberg, B.F. and Sakaguchi, T. "Artificial Intelligence in Power Systems Operations" Proc. of IEEE, vol.75, No.12, December 1987.
- [70] Schulte, R.P. et al. "Artificial intelligence solutions to power system operating problems" IEEE Trans. vol. PWR5 -2, No.4, Nov. 1987.

- [71] Kono, Y. et al. "Expert system Applications to power systems operations" 5th IEEE Int. Symposium on Intelligent control, Sept. 5-7 1990, Philadelphia USA, pp 1/6 - 6/6.
- [72] Kojima, Y. et al. "Development of a Guidance Method for Power System restoration" IEEE/PES Winter meeting New York, Jan. 29- Feb.3; 1989 pp 162 - 169.
- [73] Concordia, C. et al. "Effect of speed governor dead-band on tie-line power and frequency control performance" AIEE Trans. vol 76, Part III, pp.429-434 1957
- [74] Nanda, J. and Kaul, B.J. Proc. Institute of Electrical Engineers, No.125 Pt.D. pp 385 1978
- [75] "Recommended specifications for speed governing of steam turbines intended to drive electric generators rated 500kw and up" AIEE Standard No.600, May 1949.
- [76] Crouch, P.E. "Geometric structures in systems theory" IEE Proc. vol.128, Pt.D, No.5. Sept.1981.
- [77] Aström, K.J. "CAD Analysis and Modelling of Control Systems - a perspective" IEEE CSM vol.3, No.2, May 1983.
- [78] Martin James "Design of Man - Computer Dialogues" Prentice Hall, N.J. PP 3 - 25, 1973.
- [79] Lemmens, W.J. and Van - Den - Boom, A.J.W. "Interactive Computer Programs for Education and Research - a Survey" Automatica, Vol.15, pp - 113 -121 1979.
- [80] Denham, J.M. "Design issues for CACSD systems" Proc. of IEEE pp.1714 - 1731, Dec. 1984
- [81] Wieslander, J. "Design Principles for Computer Aided Design Software" Proc. IFAC Symposium on CACSD, Zurich, August 1979.
- [82] National Electric Power Authority, "Power System Development Plan" (1982 - 1990).

APPENDIX A

FREQUENCY AND TIE LINE POWER AS A FUNCTION OF AREA LOAD

In section 4.4.8, it is stated that the AGC equipment is able to determine whether the load changed in its own area or in the neighbouring area. By using certain derivations based on static conditions, it is shown here how the AGC equipment achieves this discrimination in practice [ ].

Consider Fig.2.5 under static conditions (ie  $s = 0$ ), the model equations reduce to:

$$\Delta P_{G1} = -\frac{1}{R_1} \Delta f_1 \quad (\text{AI})$$

$$\Delta P_{G2} = -\frac{1}{R_2} \Delta f_2 \quad (\text{AII})$$

$$D_1 \Delta f_1 + T_{12}(\delta_1 - \delta_2) = \Delta P_{G1} - \Delta P_{D1} \quad (\text{AIII})$$

$$D_2 \Delta f_2 + T_{12}(\delta_2 - \delta_1) = \Delta P_{G2} - \Delta P_{D2} \quad (\text{AIV})$$

Substituting eqns (AI) and (AII) into eqns. (AIII) and (AIV) respectively yields

$$(D_1 + \frac{1}{R_1}) \Delta f_1 + T_{12}(\delta_1 - \delta_2) = -\Delta P_{D1} \quad (\text{AV})$$

$$(D_2 + \frac{1}{R_2}) \Delta f_2 + T_{12}(\delta_2 - \delta_1) = -\Delta P_{D2} \quad (\text{AVI})$$

Adding eqns. AV and A VI gives

$$(D_1 + \frac{1}{R_1}) \Delta f_1 + (D_2 + \frac{1}{R_2}) \Delta f_2 = -\Delta P_{G1} - \Delta P_{G2} \quad (\text{AVII})$$

since, this is a synchronous system in steady state,

$$\Delta f_1 = \Delta f_2 = \Delta f \quad (\text{AVIII})$$

with the result the eqn. (A VII) becomes

$$[(D_1 + D_2) + (\frac{1}{R_1} + \frac{1}{R_2})] \Delta f = -\Delta P_{D1} - \Delta P_{D2}$$

or

$$\Delta f = \frac{-\Delta P_{D1} - \Delta P_{D2}}{(D_1 + D_2) + (1/R_1 + 1/R_2)} \quad (\text{AIX})$$

Hence, whether the load increased in area 1 (i.e.  $\Delta P_{D2} = 0$ ) or in area 2 (i.e.  $\Delta P_{D1} = 0$ ), the sign of the frequency deviation is negative.

On the other hand, by subtracting eqn. (A V) from eqn. (AVI) and solving for  $T_{12}(\delta_1 - \delta_2)$ , we obtain

$$T_{12}(\delta_1 - \delta_2) = \frac{-\Delta P_{D1}[D_2 + (1/R_2)] + \Delta P_{D2}[D_1 + (1/R_1)]}{[D_2 + (1/R_2)] + [D_1 + (1/R_1)]} \quad (\text{AX})$$

If the load varies in area 2, then  $\Delta P_{D1} = 0$  and eqn. (AX) reduces to

$$T_{12}(\delta_1 - \delta_2) = \Delta P_{t1} = \frac{\Delta P_{D2}[D_1 + (1/R_1)]}{[D_2 + (1/R_2)] + [D_1 + (1/R_1)]} \quad (\text{AXI})$$

Similarly, if the load varies in area 1,  $\Delta P_{L2} = 0$  and

$$T_{12}(\delta_1 - \delta_2) = \Delta P_{t1} = \frac{- \Delta P_{D1} [D_2 + (1/R_2)]}{[D_2 + (1/R_2)] + [D_1 + (1/R_1)]} \quad (\text{AXII})$$

It follows therefore, that when the load varies in the neighbouring area, the frequency and tie line power deviations in the own area have opposite signs. If, however, the load varies in the own area, the frequency and tie line deviations in the own area have the same sign. This sign variation is utilised by the AGC equipment to determine whether the load changed in the own area or in the neighbouring area.

Note that the tie line power is measured positive out of the area under consideration.

## APPENDIX B

### LINEARIZATION OF NONLINEAR MODELS

#### B.1 The Hydro - Governing System

From section 5.2.2.1, it was shown that at the instant when the rate constraints did not exist, the hydro-governing equations reduced to

$$\dot{c}_h = -\dot{b} - r\dot{g} - \frac{1}{T_R} (c_h + b) \quad (5.17)$$

$$\dot{g} = \phi_h (c_h - Rg) \quad (5.20)$$

where all the parameters are defined in section 5.2.2.1. Taking the Laplace transform of the above equations yield:

$$sc_h = -sb - rsg - \frac{1}{T_R} (c_h + b) \quad (B I)$$

$$sg = \phi_h c_h - \phi_h Rg \quad (B II)$$

Now solving for  $c_h$  in eqn. (BI) gives

$$c_h = -b - \frac{rsg}{s + \frac{1}{T_R}} \quad (BIII)$$

Substituting eqn. (B III) into eqn. (BII) and rearranging results in;

$$g(s + \phi_h R) \left( s + \frac{1}{T_R} \right) + \phi_h rsg = -\phi_h b \left( s + \frac{1}{T_R} \right) \quad (B IV)$$

or

$$g[s^2 + s(\phi_h R + \phi_h r + \frac{1}{T_R}) + \phi_h R \frac{1}{T_R}] = -\phi_h b(s + \frac{1}{T_R}) \quad (BV)$$

The quadratic term in the square bracket above is solved to give two approximate roots

$$s_1 = -\frac{1}{T_R} \text{ and } s_2 = \phi_h R + \phi_h r = \frac{r}{R} \phi_h (\frac{R^2}{r} + R)$$

which are substituted in eqn. (BV) to obtain:

$$g[(s + \frac{1}{T_R})(s + \{\phi_h R + \phi_h r\})] = -\phi_h (s + \frac{1}{T_R}) b \quad (BVI)$$

Since the bracketted term in  $s_2$  is a constant for any given setting of  $r$  and  $R$ , the hydro governing transfer function is approximated to

$$\Delta G = \frac{-\frac{sT_R + 1}{(sT_G + 1)(s\frac{r}{R}T_R + 1)}}{[\Delta P_C - \frac{1}{R} \Delta f]} \quad (B VII)$$

where  $T_G = \frac{1}{\phi_h R + \phi_h r}$  is the hydro-turbine governor time constant,  $\Delta G$  is the change in gate position  $g$  and the variable  $b$  has been replaced by eqn. (5.19).

## B.2 The Steam - Turbine Governing System

From section 5.2.2.2, the explicit form of the steam-turbine governing system model at the instant when none of the constraints exist takes the form:

$$\dot{g} = \phi_s (\Delta P_c - \frac{1}{R} \Delta f - Rg) \quad (5.26)$$

where all the parameters are as defined in that section. Taking the Laplace transform of the above equation and rearranging yields

$$g(s + \phi_s R) = \phi_s (\Delta P_c - \frac{1}{R} \Delta f) \quad (BVIII)$$

Now, if  $\Delta G$  represents the change in valve opening position due to a change in load demand, the steam governing system transfer function is given by

$$\Delta G = \frac{1}{sT_G + 1} (\Delta P_c - \frac{1}{R} \Delta f) \quad (BIX)$$

where  $T_G = \frac{1}{R\phi_s}$  is the governor time constant while any gain constant has been normalised to unity.

### B.3 The Hydro - Turbine System

In order to derive the linear form of the hydro-turbine system dynamic equations, the effect of servo control on the turbine blades is neglected. It is further assumed that; [22]

- i. The pipe and water are incompressible
- ii. The velocity of water varies directly with the gate opening and with the square root of the net head.



iii. The turbine output is proportional to the product of head and volume flow.

iv. The head losses in the conduit and gate may be neglected.

Hence the velocity of the water in the turbine and the conduit is given by

$$v = K G \sqrt{H_T} \quad (BX)$$

where  $G$  is the fractional gate opening;

$H_T$  is the effective head of water;

$v$  is the instantaneous velocity and

$K$  is the constant of proportionality.

For small displacements from an equilibrium position, eqn. (BX) is differentiated to obtain:

$$\frac{\Delta v}{v_0} = \frac{1}{2} \frac{\Delta H}{H_R} + \frac{\Delta G}{G} \quad (BXI)$$

where  $H_R$ ,  $v_0$  and  $G$  are the nominal head, velocity and fractional gate opening respectively. By Newton's second law, the acceleration due to the change in head at the turbine may be expressed as:

$$\rho LA \frac{d(\Delta v)}{dt} = -A \rho g_v \Delta H \quad (BXII)$$

where  $\rho$  is the mass density of water

$A$  is the cross-sectional of the pipe

$g_v$  is the acceleration due to gravity and

$L$  is the length of the conduit.

$\rho LA$  is the mass of water in the conduit while  $\rho g_v \Delta H$  is the incremental increase in pressure at the turbine. In normalised form, eqn. (BXII) becomes

$$\frac{Lv_O}{g_v H_R} s \left( \frac{\Delta v}{v_O} \right) = - \left( \frac{\Delta H}{H_R} \right) \quad (\text{BXIII})$$

where  $s = \frac{d}{dt}$  is the Laplace operator and  $s \left( \frac{\Delta v}{v_O} \right)$  is the normalised acceleration. Now the coefficient of the normalised acceleration can be expressed as a nominal starting time  $T_\omega$  so that

$$T_\omega = \frac{Lv_O}{g_v H_R} \quad (\text{BXIV})$$

The nominal starting time is the time required for a head  $H_R$  to accelerate the water in the conduit from standstill to the velocity  $v_O$ . By solving eqn. (BXI) for  $\left( \frac{\Delta H}{H_R} \right)$  and substituting the result in eqn. (BXIII), an expression relating the change in velocity to the change in gate opening is obtained as

$$\frac{\Delta v}{v_O} = \frac{1}{\frac{T_\omega}{2} s + 1} \frac{\Delta G}{G} \quad (\text{BXV})$$

where eqn. (BXIV) for  $T_\omega$  has been used.

The output of the turbine may be expressed as

$$P_m = (\text{Pressure}) (\text{flow}) = K_2 H v \quad (\text{BXVI})$$

where  $K_2 = \rho^2 L A g_v$  is a constant.

Differentiating eqn. (BXVI) yields

$$\frac{\Delta P_m}{P_m} = \frac{\Delta H}{H_R} + \frac{\Delta v}{v_o} \quad (\text{BXVII})$$

By substituting eqns. (BXIII) for  $(\frac{\Delta H}{H_R})$  and (BXV) for  $(\frac{\Delta v}{v_o})$  into eqn. (BXVII), the transfer function for turbine output is found as a function of gate position viz:

$$\frac{\Delta P_m}{P_m} = \frac{T_\omega s - 1}{\frac{T_\omega}{2} s + 1} \frac{\Delta G}{G} \quad (\text{BXVIII})$$

By expressing the values in per unit and noting that the turbine power  $P_m$  is directly proportional to the generated power  $P_G$ , eqn. (BXVIII) can be rewritten as

$$\Delta P_G = \frac{T_\omega s - 1}{\frac{T_\omega}{2} s + 1} \Delta G \quad (\text{BXIV})$$

which is the form used in eqn. (5.68).

## APPENDIX C

### WATER HAMMER EFFECT

The transfer function of hydro - gate position to turbine power, derived in chapter five, neglected the effect of compressibility of water. The following derivation incorporates this effect.

Assuming a uniform one-dimensional flow, the force equation may be written as

$$-\frac{1}{\rho} \frac{\partial p}{\partial x} = \frac{\partial u}{\partial t} + u \frac{\partial u}{\partial x} \approx \frac{\partial u}{\partial t} \quad (\text{CI})$$

where

$\rho$  is the density of water in  $\text{Kg/m}^3$

$p$  is the water pressure in  $\text{N/m}^2$

$u$  is the water velocity in  $\text{m/s}$

$t$  is time in seconds and

$x$  is the length of conduit (m)

The continuity equation is

$$\frac{\partial \rho}{\partial t} = - \frac{\partial}{\partial x}(\rho u) = - \rho \frac{\partial u}{\partial x} - \frac{u \partial \rho}{\partial x} \approx - \rho \frac{\partial u}{\partial x} \quad (\text{CII})$$

Now density can be eliminated in terms of pressure by the relation

$$\frac{\partial \rho}{\partial t} = \frac{\partial p}{\partial t} \times \frac{d\rho}{dp} = \frac{1}{v^2} \frac{\partial p}{\partial t} \quad (\text{CIII})$$

where  $v$  is the effective velocity of sound and it is assumed that the density  $\rho$  can be expressed as a function only of  $p$ . Then from Eqn. (CII) above,

$$\frac{\partial p}{\partial t} = -v^2 \rho \frac{\partial u}{\partial x} \quad (\text{CIV})$$

Equations (CI) and (CIV) may be expressed as difference equations in  $x$ , as

$$\frac{du_2}{dt} = \frac{1}{\rho \Delta x} (P_1 - P_3) \quad (\text{CV})$$

and

$$\frac{dP_3}{dt} = \frac{v^2 \rho}{\Delta x} (u_2 - u_1) \quad (\text{CVI})$$

where  $\Delta x = x_3 - x_1$  and 1, 2, 3 etc are the numbers of successive equally spaced sections. The simplest case is to consider the whole pipe as one section with half the storage volume on either end as shown in figure CI below. Thus the element of length of the pipe is  $L$  and the element of volume of the pipe is proportional to  $L/2$ , so that equations (CV) and (CVI) may be written as

$$\rho L \frac{d}{dt} \Delta u_2 = -\Delta P_3 \quad (\text{CVII})$$

$$\frac{L}{2} \frac{d}{dt} \Delta P_3 = v^2 \rho (\Delta u_2 - \Delta u_4) \quad (\text{CVIII})$$

noting that the variation of the reference head  $\Delta P_1$  is zero.

These may be combined as

$$\Delta P_3 = \frac{-\rho L s \Delta u_4}{\frac{L^2}{2v^2} s^2 + 1} \quad (\text{CIX})$$

where  $s = (d/dt)$

By combining equation (CIX) with the turbine flow equation [25]

$$\frac{\Delta u_4}{u_4} = \frac{1}{2} \frac{\Delta P_3}{P_3} + \frac{\Delta G}{G} \quad (\text{CX})$$

(where  $\Delta G$  is the change in gate position), yields

$$\frac{\Delta u_4}{u_4} = \frac{\frac{L^2}{2V^2} s^2 + 1}{\frac{L^2}{2V^2} s^2 + \frac{T_w}{2}s + 1} \frac{\Delta G}{G} \quad (\text{CXI})$$

where  $T_w$  is the water starting time or  $T_w = \frac{\rho L u_4}{P_3}$

In terms of the mechanical output power of the turbine  $P_m$ ,

where

$$\frac{\Delta P_m}{P_m} = \frac{\Delta P_3}{P_3} + \frac{\Delta u_4}{u_4} \quad (\text{CXII})$$

the transfer function of the hydro-gate position to the turbine power becomes

$$\Delta P_m = \frac{\frac{L^2}{2V^2} s^2 - \frac{T_w}{2} s + 1}{\frac{L^2}{2V^2} s^2 + \frac{T_w}{2} s + 1} = \frac{M_w - \frac{T_w}{2} s + 1}{M_w s^2 + \frac{T_w}{2} s + 1} \Delta G$$

where  $M_w = \frac{L^2}{2V^2}$  is the water compressibility factor.

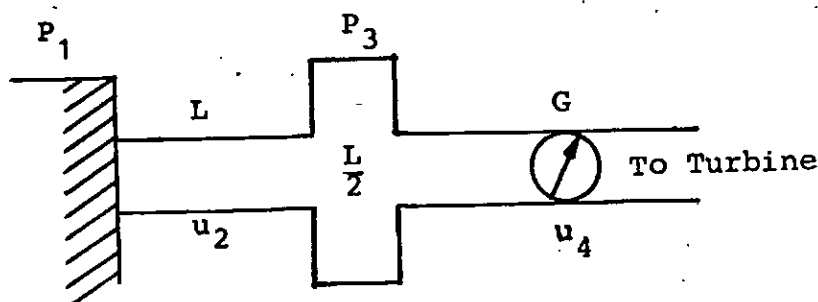


Fig. (CI) Simplest Lumped - Circuit representation of water compressibility.

# APPENDIX D

## ILLUSTRATION OF THE EFFECT OF DEADBAND

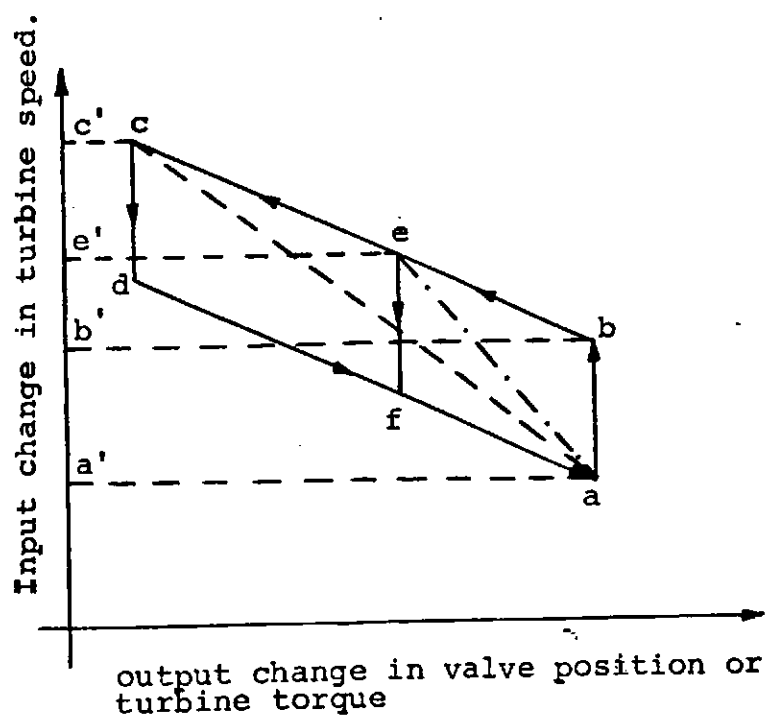


Fig.DI Illustration of Deadband Effect.

Fig.DI is a plot of the speed-deviation input signal to the governor over a small range as a function of turbine torque or control - valve position. If there were no deadband, variations in turbine speed, which is as a result of load demand changes, would cause the valves to move back and forth along the lines  $bc$  or  $ad$ , depending upon the governor setting. The governor speed regulation would be proportional to the slope of either line. In an actual governor, there exists a deadband represented by the vertical distance between lines  $ad$  and  $bc$ .

If the turbine speed varies between the limits  $a'$  and  $c'$ , the valve will not move until the speed has increased to  $b'$ ; thus, following the path  $abc$ . When the speed decreases again

to a', the valve will not move until the speed has changed by the amount of the deadband. Thus, the return trip will follow the path cda. The effective regulation, as far as the total steady state response is concerned, is proportional to the slope of the line ac, which is appreciably greater than the slope ad or bc with no deadband. For a smaller frequency excursion from a' to e', the valve will follow the path abefa and have an even greater regulation, as given by the slope of the line ae.

This analysis shows that the effective regulation of a governor with deadband will be greater for small load changes than for large load changes. As derived in reference 34, the effective speed regulation for a governor with deadband (db) is given by

$$R_e = R \left( 1 + \frac{2db}{R\Delta L} \right)$$

where

$R_e$  is the effective speed regulation in pu

$R$  is the governor droop setting

db is the deadband (pu) and

$\Delta L$  is the per unit change in load demand.



APPENDIX EPARAMETER VALUES OF THE NIGERIAN POWER SYSTEM

## I. Hydro - units 7 &amp; 8 at Kainji Power Station.

Rated Output MVA in continuous service	85.000 MVA
Power Factor	0.94
Rated output $M_w$ (approx)	80.000 $M_w$
Voltage rating	16Kv
Current rating	3070 A
No of poles	52
Speed	115.4 r.p.m
Frequency	50 Hz
Rated Head ( $H_T$ )	160 feet or 1.0pu

## - Model Parameter Values -

Governor time constant	$T_G$ = 0.6 seconds
Permanent speed droop	$R$ = 4 to 16.7%
Temporary speed droop	$r$ = 60 to 100%
Water starting time	$T_W$ = 4 seconds
Nominal frequency	$f_O$ = 50 Hz
Washout time constant	$T_R$ = 8 seconds
Rated gate opening position	$G$ = 1.0 pu
$\phi_h$ at rated gate opening	= 0.25 pu
$c_h$ at rated gate opening	= 0.15 pu
Rated blade velocity	$N$ = 1.0 pu
Rated turbine flow	$Q$ = 1.0 pu
Rated gate opening velocity	$\dot{g}$ = 0.1 pu /sec.
Maximum gate opening velocity	$\dot{g}_{max}$ = 0.2 pu/sec.
Maximum gate opening	$g_{max}$ = 1.25 pu
Effective head	$H_R$ = 0.56 - 0.81 pu
Blade angle at rated output	$\phi_{Brated}$ = 1.047 radians.
	$\phi_n$ = 1.308 rad.

Minimum blade angle  $\phi_{B_{min}}$  = 0.349 rad.  
 Blade servo time constant  $T_B$  = 0.08 seconds.

## II Steam Powered Generating Station (Egbin)

Rated MVA 245.8 MVA  
 Power Factor 0.9  
 Rated Real power 221.2  $M_w$   
 Voltage Rating 16 Kv  
 Speed (Nominal) 3000 r.p.m

### - Model Parameters -

Governor time constant  $T_G$  = 0.1 secs.  
 Permanent speed droop  $R$  = 0.04 pu  
 Nominal frequency  $f_O$  = 50 Hz  
 Valve opening at rated output = 1 pu  
 Valve opening velocity  $\dot{g}$  = 0.1pu/sec.  
 $\phi_s$  at rated output = 0.325 pu  
 Time constant of high pressure flow  $T_{CH}$  = 0.26 sec.  
 Reheat time constant  $T_{rh}$  = 10 sec.  
 High pressure constant  $F_1$  = 0.5 pu

## III. General Grid Data

Inherent load-frequency characteristics  $D = 0.75 - 2.0pu$

Inertia constant  $H$  = 5.0 secs  
 Model gain  $K_p$  = 1.33 - 0.5pu  
 Model time constant  $T_p$  = 5.3 - 14.13sec  
 Nominal frequency  $f_O$  = 50 Hz  
 Scheduled tie - line power  $P_E$  = 0.1 pu.

PROCEEDINGS OF THE INTERNATIONAL CONFERENCE  
ON DEVELOPING COUNTRIES AND THE NEW INFORMATION  
AGE - DECONIA '89

ON THE COMPUTER-AIDED DESIGN OF VARIABLE STRUCTURE CONTROL SYSTEMS  
WITH APPLICATION TO AUTOMATIC GENERATION CONTROL

J. KATENDE, F.N. OKAFOR and C.O.A. AWOSOPE  
Electrical Engineering Department University of Lagos,  
Lagos, Nigeria.

ABSTRACT

This paper presents an interactive computer-aided design (CAD) tool which has been developed by the authors, for the synthesis of non-linear control schemes in the form of variable structure systems. The use of the CAD tool is demonstrated by designing a variable structure automatic generation control (VSAGC) scheme for a typical single area network. Simulation results are presented to highlight the performance of the VSAGC scheme when regulating the mismatch between power generation and consumption during load demand variations.

LIST OF SYMBOLS

$x_1$	$\Delta f$	incremental frequency deviation in Hz.
$x_2$	$\Delta P_g$	incremental change in generator output power (pu Mw).
$x_3$	$\Delta X_g$	incremental change in governor valve position (p.u Mw).
$x_4$	$\int \Delta f dt$	incremental change in voltage angle (radians).
	$\Delta P_d$	load disturbance in p.u Mw.
	$\Delta P_c$	incremental change in speed-changer position (p.u Mw).
	$T_g$	governor time constant in seconds.

$T_t$	turbine time constant in seconds.
$T_p$	plant time constant in seconds.
$K_p$	plant gain
$R$	speed regulation due to governor action Hz pu Mw <sup>-1</sup>
$C$	switching vector
$s$	switching hyperplane
$\psi_{\alpha\beta}$	gains of the variable structure controller.

1. INTRODUCTION

A variable structure control (VSC) scheme is provided with a means of automatically switching from one control structure to another so as to exploit a combination of the useful properties of each of the structures as well as acquire new properties not present in any of the structures. One such property is referred to as the 'sliding mode'. Sliding modes, which are the basic motions in VSC systems, occur on one or more discontinuity surfaces deliberately created in the state space. Of particular significance is the fact that when the system is in the sliding mode it is insensitive to parameter variations and disturbances. This has put VSC schemes at the forefront of the field of robust control for uncertain dynamical systems (1, 2).

The development of VSC theory has been carried out, for scalar systems, over the past two decades and is mostly reported in the Russian technical literatures (3, 4, 5, 6). In recent years, VSC theory has attracted wide spread attention and has indeed been extended to include multi-variable systems (7, 8). The rapidly growing interest in VSC systems may be attributed to the following reasons: First of all, the advent of new design methods coupled with the advances in electronics has greatly facilitated the practical realization of sliding modes. Secondly, variable structure control seems to be a natural means of exploiting the use of the new power electronic elements which operate in a switching mode only. Finally, the practicability of VSC schemes has been amply demonstrated for a wide range of industrial plants which include among others, robots (9), metal cutting machine tools and electrical a.c. and d.c. drives (2).

The authors are currently investigating the use of VSC schemes in electrical power systems. For this purpose, a VSC system CAD tool has been developed. The CAD tool assists the user in designing the switching surfaces and in the choice of the switching control and the associated switching logic to yield sliding motion with prescribed dynamic behaviour.

The purpose of this paper therefore is to introduce the CAD tool together with a brief review of the concept of variable structure control systems theory. The usage of the CAD tool is demonstrated for the problem of designing a VSC automatic generation control scheme for a single area network.

## 2. VARIABLE STRUCTURE CONTROL SYSTEM THEORY.

Consider a multivariable plant described by

$$\dot{x} = Ax + Bu \quad (1)$$

where  $x \in \mathbb{R}^n$ ,  $u \in \mathbb{R}^m$ ,  $A \in \mathbb{R}^{n \times n}$  and  $B \in \mathbb{R}^{n \times m}$

In the usual state feedback controller design a fixed control structure is considered in the form

$$u = Kx \quad (2)$$

where the constant parameters of the  $m \times n$  matrix  $K$  are obtained using any of the control synthesis techniques such as those for pole assignment and optimal control. A VSC system incorporates a state feedback regulator of the form (2) with  $K$  replaced by  $\psi$  which is defined by

$$\psi = \hat{\psi} \text{diag} [\text{sgn } x_1, \text{sgn } x_2, \dots, \text{sgn } x_n] \quad (3)$$

where

$$\hat{\psi} = [\hat{\psi}_1, \hat{\psi}_2, \dots, \hat{\psi}_m]^t \quad (4)$$

$$\hat{\psi}_i = \begin{cases} 1, & \text{for } s_i(x) > 0 \\ -1, & \text{for } s_i(x) < 0 \end{cases} \quad (5)$$

$i = 1, 2, \dots, m; \alpha_i \neq \beta_i$

and  $\hat{\psi}_i$ ,  $\alpha_i$  and  $\beta_i$  are  $n$ -vectors while  $s_i(x)$  is a  $m$ -vector. Superscript  $t$  denotes vector or matrix transpose. Equation (5) indicates that vector  $\hat{\psi}_i$  is discontinuous on the switching hypersurface

$s_i(x) = 0$  in the  $n$ -dimensional state space. Hence the control  $u_i(x)$  can take on one of two structures depending on which side of  $s_i(x) = 0$  the state vector  $x$ , is located. In other words

$$u_i(x) = \begin{cases} u_i^+, & \text{for } s_i(x) > 0 \\ u_i^-, & \text{for } s_i(x) < 0 \end{cases} \quad (6)$$

The switching hypersurfaces are described by

$$s = Cx = 0 \quad (7)$$

where

$$s = [s_1, s_2, \dots, s_m]^t$$

and  $C \in \mathbb{R}^{m \times n}$  with full rank.

A state vector in the neighbourhood of the  $i$ -th switching hypersurface  $s_i = 0$  (on either side of it), will be directed towards the hypersurface provided the following 'reachability' condition is fulfilled (4).

$$s_i \dot{s}_i < 0 \quad (8)$$

When the state reaches a switching hypersurface it is required to slide along it toward the origin of the state space. When sliding occurs the equivalent control,  $u_{eq}$ , is obtained by solving for  $u$  in the algebraic equation

$$s = Cx = 0 \quad (9)$$

so that

$$u_{eq} = -(CB)^{-1}CAx \quad (10)$$

In other words, the equivalent feedback gain matrix is

$$\psi_{eq} = (CB)^{-1}CA \quad (11)$$

and the sliding mode is characterized by

$$\dot{x} = [A - B\psi_{eq}]x \quad (12)$$

Thus, when on the switching hyperplane, the state vector is determined merely by the properties of the controlled plant and the orientation of the switching hyperplane.

The VSC design objective is to find vectors  $\alpha_i$ ,  $\beta_i$  and matrix  $C$  so that the state vector reaches and slides on switching hyperplane  $s_i(x) = 0$ , toward the origin  $x = 0$ . The design may be in two stages:

(i) design of the switching hyperplanes through selection of matrix  $C$  so that the sliding mode is asymptotically stable with prescribed transients. This is often referred to as the 'existence' problem.

(ii) design of the switching control functions together with the switching logic to ensure that the state trajectory is steered toward the switching hyperplanes  $s = Cx = 0$ . This is also referred to as the 'reachability' problem.

## 2.1. DESIGN OF THE SWITCHING HYPERPLANES.

We consider the design of the switching hyperplanes which yield

prescribed closed-loop eigenvalues for the sliding mode [8].

Let  $n \times n$  orthogonal matrix  $T$  exist such that

$$TB = \begin{bmatrix} 0 \\ \text{---} \\ B_2 \end{bmatrix} \quad (13)$$

where submatrix  $B_2 \in \mathbb{R}^{m \times m}$  is non-singular.

Then we can effect the coordinate transformation

$$z = \begin{bmatrix} z_1 \\ \text{---} \\ z_2 \end{bmatrix} = Tx \quad (14)$$

where  $z_1 \in \mathbb{R}^{(n-m)}$  and  $z_2 \in \mathbb{R}^m$ .

Making use of eqns. (7), (8), and (14) it is possible to show that the equivalent closed-loop system in the sliding mode is described by the lower order system

$$\dot{z}_1 = [A_{11} - A_{12} C_1] z_1 \quad (15)$$

where  $A_{11}$ ,  $A_{12}$  and  $C_1$  are obtained from

$$TAT^t = \begin{bmatrix} A_{11} & : & A_{12} \\ \text{---} & & \text{---} \\ A_{21} & : & A_{22} \end{bmatrix}$$

$$\text{and } CT^t = [C_1 \ : \ C_2] \quad (16)$$

note that for an orthogonal matrix the inverse is the same as the transpose. The eigenvalues of

matrix  $[A_{11} - A_{12} C_1]$  can be placed arbitrarily by suitable choice of matrix  $C_1$ .

Matrix  $C$  is then given by

$$C = [C_1 \ : \ I] T \quad (17)$$

where  $C_2$  has been replaced by identity matrix  $I$  without loss of generality.

## 2.2. DESIGN OF THE CONTROL FUNCTIONS AND SWITCHING LOGIC.

The objective is to synthesize the control functions,  $u$ , which steer the state vector,  $x$ , towards the hyperplanes  $s = Cx = 0$  and hence yield a sliding motion simultaneously on all  $s = 0$ . Various design techniques have been proposed {3,6,5,7}. In this paper the hierarchy of controls method (5) is used to design the gains in the variable structure control law such that when the state vector eventually reaches the switching hyperplanes simultaneously, that is on the intersection manifold of all the planes. The design algorithm is summarized as follows:

Step 1. Suppose that the hierarchy of switching planes is

$s_1 \ s_2 \ s_3 \ \dots \ s_m$   
which means that sliding will occur on  $s_1$  first, then on the intersection of  $s_1$  and  $s_2$  and then on the intersection of  $s_1$ ,  $s_2$  and  $s_3$  etc.

Step 2. Let  $i = m$  thus specifying the bottom plane  $s_m = 0$ .

## PROCEEDINGS - DECONIA'89

Step 3. Suppose that sliding occurs on the first  $i-1$  switching hyperplanes and solve for the equivalent control

$$u_{eq}^{i-1} = [u_1 u_2 \dots u_{i-1}]^t$$

as a function of

$$u^{i+1} = [u_{i+1}, u_{i+2}, \dots, u_m]^t$$

from the equations

$$s_j = 0 \quad j = 1, 2, \dots, i-1$$

yielding

$$u_{eq}^{i-1} = P_{i-1} x + Q_{i-1} u^{i+1} + d_i u_i. \quad (18)$$

where matrices  $P_{i-1}$ ,  $Q_{i-1}$  and scalar  $d_i$  depend on the first  $i-1$  rows of matrices CA and CB

Step 4 Choose  $u_i^+$  and  $u_i^-$  in eqn (6)

to satisfy the reachability condition of eqn (8)

( $s_i s_i \leq 0$ ) on hypersurface  $s_i = 0$

Hence  $u_i$  must satisfy

$$\gamma_i u_i^+ \leq - \int_{u_i^-}^{u_i^+} \min_{u_i} [p_i^t x + q_i^t u^{i+1}] \quad (19)$$

$$\gamma_i u_i^- \geq - \int_{u_i^-}^{u_i^+} \max_{u_i} [p_i^t x + q_i^t u^{i+1}] \quad (20)$$

where  $\gamma_i \neq 0$  and vectors  $p_i$  and  $q_i$  depend upon

$P_{i-1}$ ,  $Q_{i-1}$  and  $d_i$ .

If  $u_i^+$  and  $u_i^-$  are linear in  $x$ , for example

$$u_i^+ = \psi_i^+ x = \alpha_i |x| \quad (21)$$

$$u_i^- = \psi_i^- x = \beta_i |x|$$

then the inequalities in eqns (19) and (20) can be evaluated component wise so that the bounds on  $\alpha_i$

and  $\beta_i$  can then be obtained to ensure sliding motion.

Step 5 Let  $i = i-1$ . If  $i > 0$  then go to step 3,

Else stop.

### 3. CAD TOOL FOR VSC SYSTEMS

When designing the CAD tool, the following specifications have been taken into consideration.

- (i) Ease of use (interactiveness)
- (ii) Flexibility, portability and modularity.
- (iii) Application in research/education and industry.

Interactiveness is implemented t

such a level as to accommodate a wide range of users from the novice to the expert. For portability, the programme code is in standard FORTRAN 77, which is transparent to the user. A modular structure was adopted to enhance flexibility and to allow for the use of link-overlay techniques enabling the economical use of the working core memory.

Fig. 1 shows the general structure of the CAD tool which consists of the main supervisor, 'VSC' and the four modules: MOD, EXIST REACH and SIMU.

If the diskette containing VSC is used to boot the computer, then the main supervisor is loaded and run automatically, otherwise the programme is invoked by entering the command 'VSC'. The menu of the supervisor is

```
HELP
MOD
EXIST
REACH
SIMU
DONE
```

which are the commands used to invoke each of the modules in the package. The HELP command is designed for the notice user and provides information on the usage of the CAD tool. The functions of the commands are summarized below:

**MOD** - loads the model matrices A and B into the main memory either interactively or from an existing file on the system's external store (diskette or hard disk).

Matrix T (eqn (13)) is determined together with its inverse,  $T^{-1}$

After computing  $TAT^{-1}$ , submatrices  $A_{11}$  and  $A_{12}$  (eqn. (16)) are extracted and converted into the standard controllable form using an  $(n-m) \times (n-m)$  transformation matrix  $T_c$ . All matrices are

stored into suitable files for future use or for use by other modules, and control is returned to the supervisor 'VSC'.

**EXIST** - is used to implement the solution of the existence problem using the matrices generated by MOD. It is provided with the set of desired closed-loop eigenvalues in the sliding mode and it computes the switching hyperplanes matrix C according to eqn. (17). Matrix C is saved in a file and control returns to VSC.

**REACH** - interactively determines the gains and for the discontinuous control functions which drive the state vector toward the switching planes in accordance with a user selected switching sequence. The default sequence used by REACH is that provided in the control hierarchy method algorithm of section 2.2. The program computes the bounds on the parameters  $\alpha_i$  and  $\beta_i$  which satisfy

$s_i \delta_i \leq 0$  for each of the switching

surfaces. The actual selected values are such that moderate control effort is used in the opinion of the user. By default REACH takes values which are double of the computed bounds. All parameters are saved in a file and control returns to the main supervisor.



SIMU - is used to effect the time simulation of the designed VSC system. A plot of the time response data is provided. It makes use of the result from the other modules, and when finished control is returned to VSC.

DONE - is used when the user wants to exit from the programme.

#### 4. AUTOMATIC GENERATION CONTROL EXAMPLE.

The problem of controlling the real power output of electric generators, in response to changes in system frequency and tie-line loading so as to maintain the scheduled system frequency and established tie-line interchange within prescribed limits is termed "automatic generation control" (AGC) or "load - frequency control" (LFC).

In this example the AGC problem for a single control area is considered. The power system is modelled by its power balance equation which relates the mismatch between power generation and consumption to the change in accelerating power and frequency (11). The control laws are then developed for the linearised model of the generally nonlinear system. For a system which is exposed to small changes in load during its normal operation, the linear model sufficiently represents its dynamics.

A block diagram representation of the AGC scheme for a single control area is shown in Fig. 2. The corresponding state variable formulation is given by

$$\dot{X} = AX + Bu + DAP$$

$$\text{where } A = \begin{bmatrix} -1/T_p & k_p/T_p & 0 & 0 \\ 0 & -1/T_p & 1/T_t & 0 \\ -1/T_g R & 0 & -1/T_g & 1/T_g \\ K & 0 & 0 & 0 \end{bmatrix}$$

$$B = \begin{bmatrix} 0 & 0 & 1/T_g & 0 \end{bmatrix}$$

$$\text{and } C = \begin{bmatrix} -K_p/T_p & 0 & 0 & 0 \end{bmatrix}$$

Other parameters are as defined in the list of symbols. Consider an AGC problem for a single area with the following parameter values (11).

$$T_p = 20 \text{ s} \quad K_p = 120 \text{ Hz p.u. MW}^{-1}$$

$$T_t = 0.3 \text{ s} \quad K = 0.6 \text{ p.u. MW rad}^{-1}$$

$$T_g = 0.08 \text{ s} \quad R = 2.4 \text{ Hz p.u. MW}^{-1}$$

Then matrices A, B, and D are given as

$$A = \begin{bmatrix} -0.05 & 6 & 0 & 0 \\ 0 & -3.33 & 3.33 & 0 \\ -5.208 & 0 & -12.5 & -12.5 \\ 0.6 & 0 & 0 & 0 \end{bmatrix}$$

$$B = \begin{bmatrix} 0 \\ 0 \\ -12.5 \\ 0 \end{bmatrix} \quad \text{and } D = \begin{bmatrix} -6 \\ 0 \\ 0 \\ 0 \end{bmatrix}$$

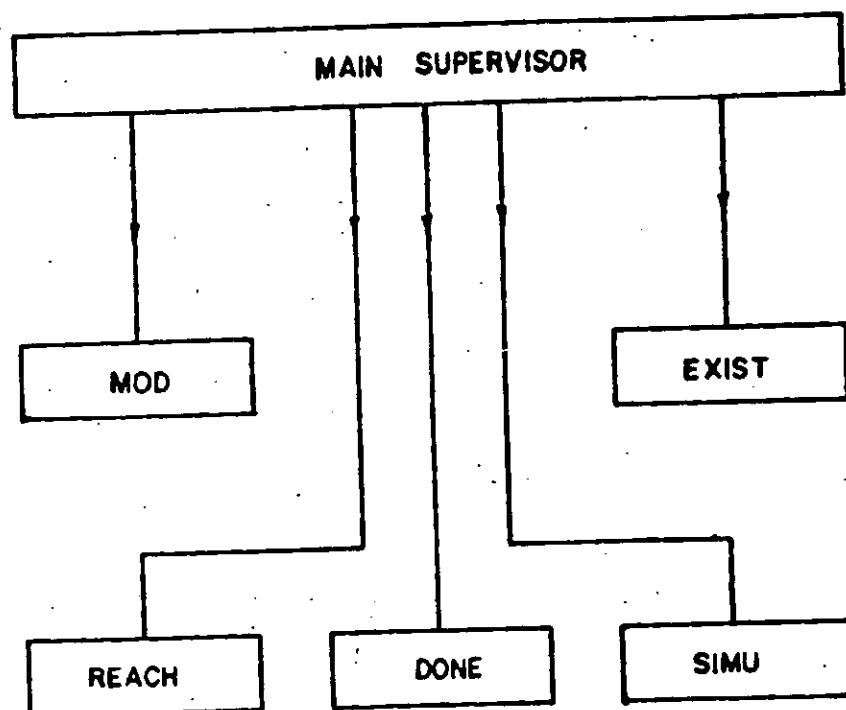


Fig. 1: General Structure of the CAD Tool.

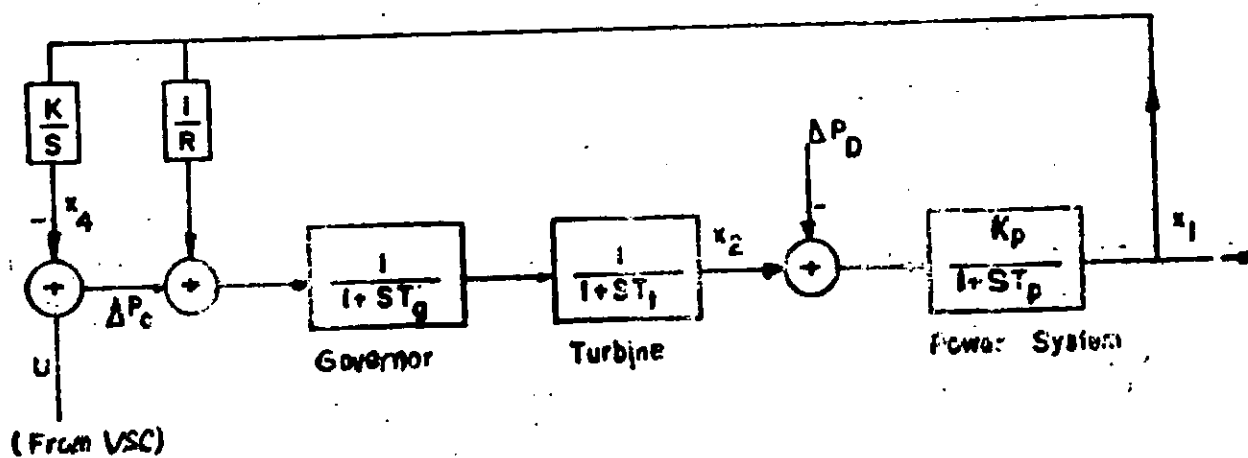


Fig. 2: Block Diagram of Single Control Area.

This is a single - input single - output system. The required orthogonal transformation matrix  $T$  is found to be

$$T = \begin{bmatrix} 1 & 0 & 0 & 0 \\ 0 & 1 & 0 & 0 \\ 0 & 0 & 0 & 1 \\ 0 & 0 & 1 & 0 \end{bmatrix}$$

The sliding modes are chosen to correspond to the eigenvalues of  $[A_{11} - A_{12}C_1]$  which are arbitrarily located at  $-3, -6, -9$ . The corresponding switching vector is obtained as

$$C = [4.905 \quad 4.385 \quad 1.0 \quad 13.501]$$

The bounds on the control gains which satisfy the reachability condition (eqn. (8)) are

$$\alpha_1 \geq 0.212 \quad ; \quad \beta_1 \leq 0.212$$

$$\alpha_2 \geq 1.186 \quad ; \quad \beta_2 \leq 1.186$$

$$\alpha_3 \geq 0.168 \quad ; \quad \beta_3 \leq 0.168$$

Subsequent simulation runs reveal that the gains which result in adequate dynamic accuracy with moderate control effort are

$$\alpha_1 = \alpha_2 = 5, \alpha_3 = 1, \alpha_4 = 0$$

$$\beta_1 = \beta_2 = -5, \beta_3 = -1, \beta_4 = 0$$

#### 4.1 SIMULATION RESULTS AND DISCUSSION.

Simulation results of  $P_G$  and  $f$  when the system is subject to a step load change of 0.03pu are

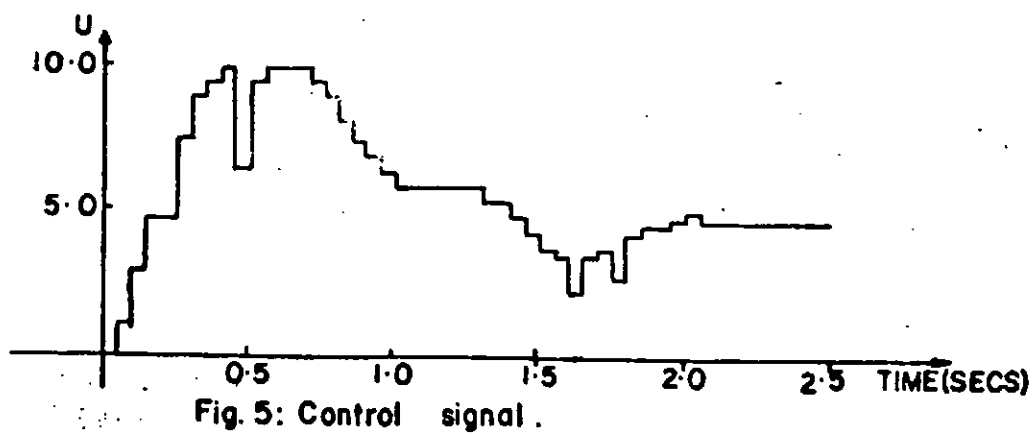
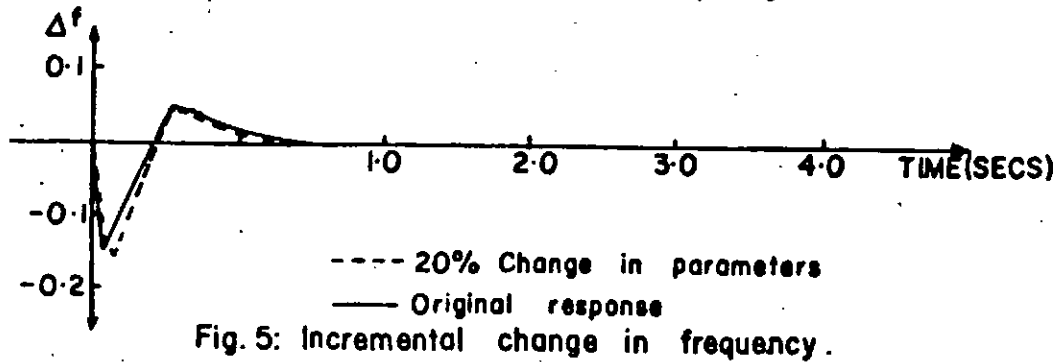
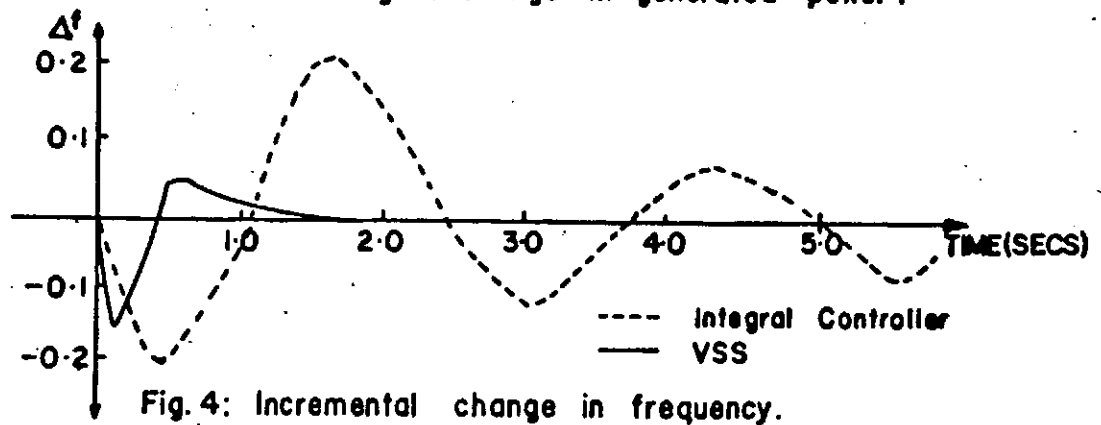
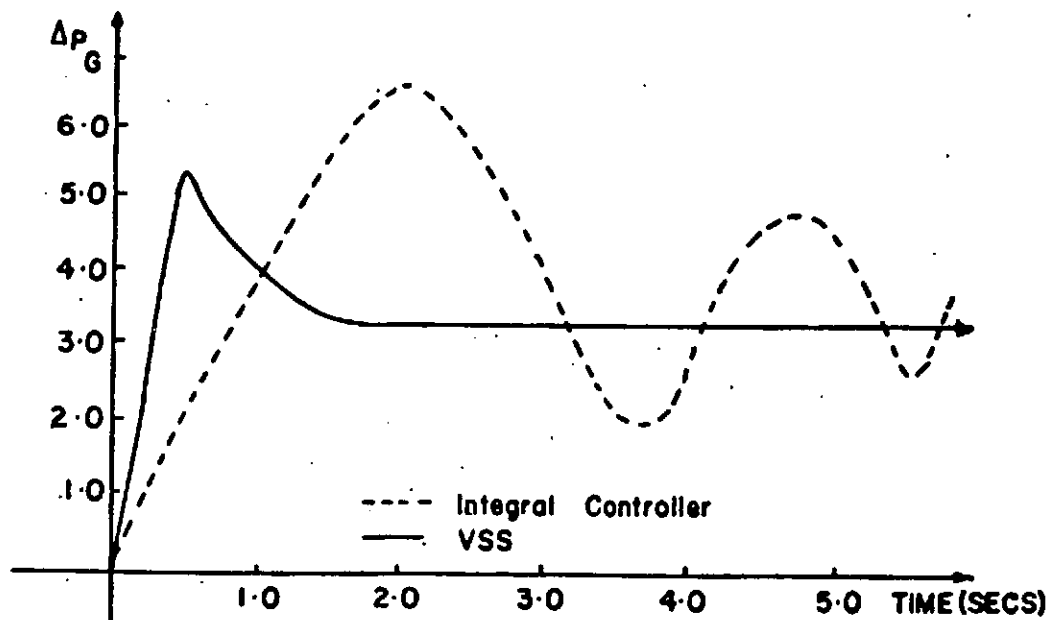
shown in Figure 3 and 4 respectively. Also shown (in broken lines) are similar results obtained using the integral controller alone, for the purpose of comparison. It is evident that the variable structure controller (VSC) greatly enhances the dynamic performance of the integral controller in terms of the maximum frequency deviation, rise and settling times. For instance, the settling time for  $f$  using the integral controller alone is of the order of 10 seconds for various values of gain -  $k$  while it is about 1.5 seconds for the VSC.

In figure 5, the broken lines represent the simulation results of  $f$  when the internal parameters of the system have changed by 20 percent. Since the system model is linear, it is meaningless to simulate for perturbations beyond first order. The two curves are almost similar showing the insensitivity of VSC to system parameter variations when operated on the sliding mode. Fig 4 depicts the variable structure control signal 'u'.

It should be noted however that the model used in the above example is presented in a generalised version. It typifies power systems on which operating records are regularly kept.

#### 5. CONCLUSION

This paper has presented an interactive CAD tool for the synthesis of variable structure controllers. The tool has a modular structure and its flexibility allows for the introduction of user-owned subroutines. Application of the tool to the AGC problem of a single control area was also discussed. Simulation results show that the VSC greatly enhances the dynamic performance of the



presently used integral controller. Further results also confirm the assertion that, when operated in the sliding mode, a VSC is insensitive to system parameter variations. This places VSC in the forefront of possible controllers for uncertain dynamical systems, such as interconnected power systems. This preliminary result informs the strategy of extending VSC to the NEPA - network, as is currently being investigated by the authors.

#### ACKNOWLEDGEMENTS

The financial support from the University of Lagos Central Research Committee (CRC) is gratefully acknowledged.

#### REFERENCES

1. E.P. RYAN: "A variable structure approach to feedback regulation of uncertain dynamical system", INT. J. Control, Vol. 38, No. 6, pp 1121 - 1134, 1983.
2. V.I. UTKIN: "Discontinuous Control Systems; State of the art in theory and applications". IFAC Congress, Munich, pp 75 - 94, 1987.
3. S.U. EMEL'YANOV: "Design of variable structure control systems with discontinuous switching functions", Engineering Cybernetics Vol. No. 1, pp 158 - 160, 1964.
4. U. ITKIN: "Control systems of variable structure", John Wiley & Sons, New York, 1976.
5. V.I. UTKIN: "Sliding modes and their applications in variable structure systems", MIR Publishers, Moscow (English translation) 1978.
6. A.F. FILLIPOV: "Applications of the theory of differential equations with discontinuous right-hand sides to non-linear control problems", Proc. 1st IFAC Congress, pp 923 - 925, 1960.
7. C.M. DORLING and A.S.I. ZINOBER: "Two approaches to hyperplane design in multivariable variable structure control systems", INT. J. CONTROL. Vol. 44, No. 1, pp 65 - 82, 1986.
8. V.I. UTKIN and K.D. YANG: "Methods for constructing discontinuity planes in multidimensional variable structure control systems, Automation and Remote Control, vol. 39, No. 10, pp 1466 - 1470, 1978.
9. K.K.D. YOUNG: "Controller design for a manipulator using theory of variable structure", IEEE Trans. Vol. SMS-8, pp. 101-109, 1977.
10. E.P. RYAN and M. CORLESS: "Ultimate Boundedness and Asymptotic Stability of a Class of uncertain dynamical systems via continuous and discontinuous feedback control", IMA Journal of Mathematical Control and Information, Vol. 1, pp 223 - 242, 1984.
11. O. I. ELGERD: "Electric Energy System Theory, An Introduction", Tata McGraw-Hill, New Delhi, 1973.

APPENDIX GTHE CODING OF VAGCD PROGRAMS

The design procedure for the proposed variable structure automatic generation control (VSAGC) scheme was presented in Chapter 3 while a computer aided design package named (VAGCD) was developed in chapter four, for the synthesis and performance evaluation of the proposed scheme. In this appendix, the structure and implementation of VAGCD are discussed in more detail. For ease of understanding, the design algorithm of chapter 3 is summarised and flow graphs are employed to demonstrate the coding sequence of the programs. Also included is a detailed block diagram representation of VAGCD structure.

G.1 STRUCTURE OF VAGCD

Basically, the process of designing and simulating the performance of a variable structure unit vector control system involves the following steps:

1. Input the system matrices and parameter values
2. Solve the existence problem by synthesizing the elements of the hyperplane matrix  $C$  which guarantee asymptotically stable sliding motion with prescribed transient behaviour.
3. Solve the reachability problem by synthesizing a unit vector control function which guarantees the hitting of the sliding plane and thereafter the continuity of motion along the sliding plane.

4. Simulate the performance of the designed system by solving the state equation using a fourth order Runge-Kutta integration algorithm and plotting/printing the state trajectories.
5. Output the results.

Computer codes are therefore written in standard FORTRAN 77 to accomplish each of the above steps. The programs are made to be interactive.

Each set of codes which implements one of the steps above is called a module. Each module is designed as a stand - alone system and does not interact with the other module except to the extent of generating results which are stored in specific files for any other module to access and use. This type of arrangement is called a modular structure. Note that each module consists of several other subroutines arranged in a hierarchical manner.

There is a main program named VAGCD which constitutes the main monitor while each module is run in a sub-monitor environment. When the package is started, the main monitor is invoked and from there other sub-monitors controlling each module can be invoked. The operating system environment is MS - DOS 3.2 or any other later version. The package is developed on an IBM PC - AT compatible with an 80386 processor which runs at 10 MHz and has 640 MB random access memory (RAM). Each module is link-overlaid with the main monitor in such a way that the module is loaded into the RAM only when invoked and put back into the read only memory (ROM) at the end of the session.

The AGC module incorporates subroutines for variable structure unit vector controller design as well as subroutines for computing the area control error ACE and for model testing. Note that for the AGC module to run on-line, other hardware such as supervisory control and data acquisition system (SCADA) must be in place to feed in the required power system data which are measured continually.

Finally, commercial application softwares for mathematical operations such as MATLAB was not used. Since the nature of the matrices are known, it was found easier to write sub-routines that perform matrix operations rather than using application programs that would demand for more of the limited working memory space. However, the simulation module (SIMU) incorporates a commercial graphics software GRAPHER for plotting the results. A detailed structure of VAGCD is shown in the block diagram of Fig.GI.

## G.2 Implementation Of VAGCD

The synthesis procedure for the switching hyperplane matrix  $C$ , starting from the canonical transformation may be summarised as follows:

1. Read matrices  $A$ , and  $B$
2. Test the pair  $(A,B)$  for controllability
3. Compute the transformation matrix  $M$  by inspection of eqn. (3.2)
4. Compute  $MAM'$
5. Partition  $MAM'$  to obtain  $A_4, A_{12}, A_{21}, A_{22}$



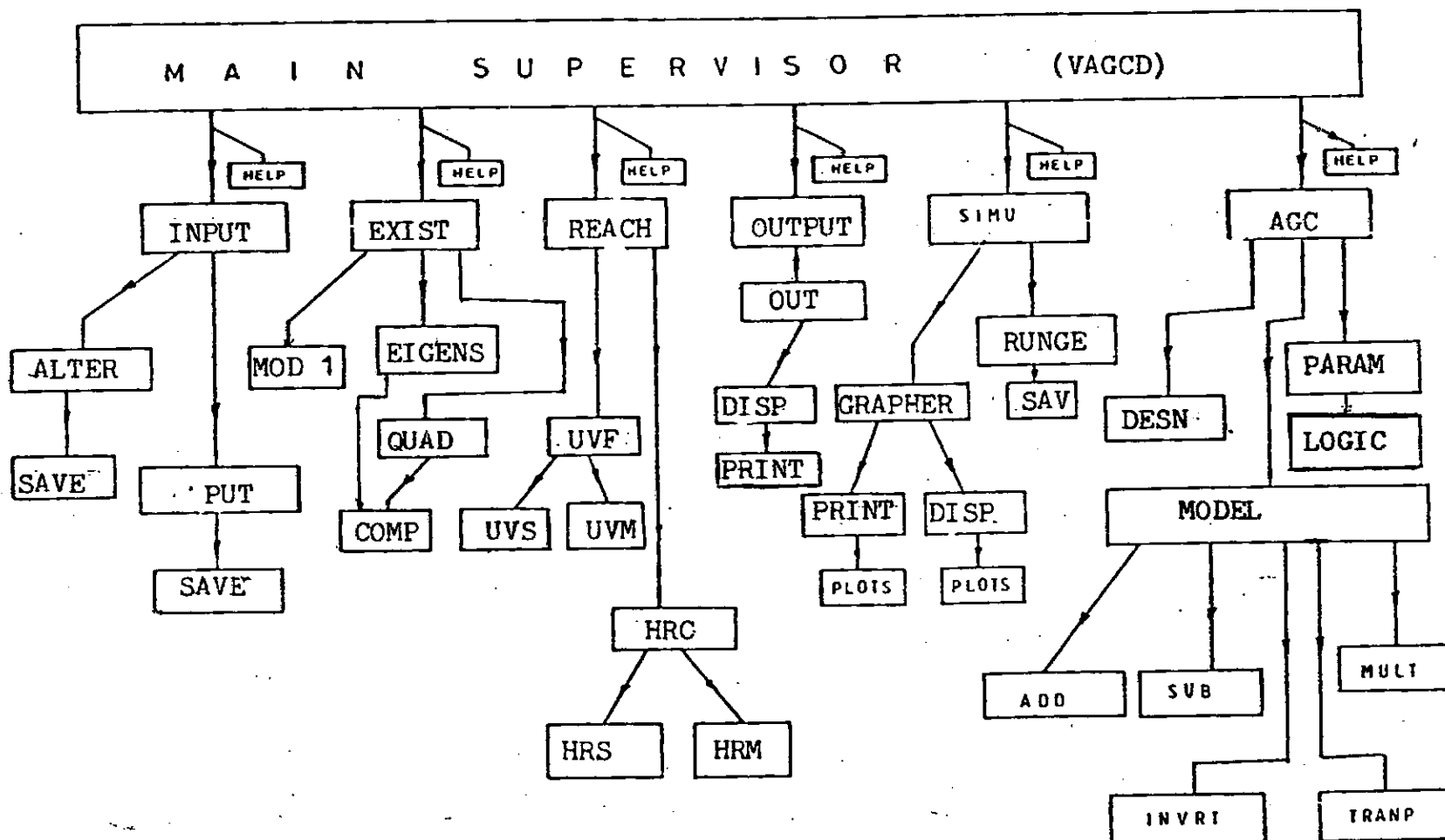


FIG. G.I DETAILED STRUCTURE OF VAGCD

6. Test  $A_{11}$ ,  $A_1$  for controllability
7. Transform  $A_{11}$  into the companion form
8. Enter the desired poles of the system  
(the number of poles =  $(n-m)$  and the poles must be distinct from the poles of matrix  $A$ )
- 9a. For  $m = 1$  (ie, single - input single - output system)  
Compute the intermediate matrix  $F$  using the conventional pole assignment algorithm
- 9bi. For  $m > 2$  (ie, multi-input system): compute the corresponding eigenvector matrix  $V$ .
- 9bii. Obtain the orthogonal matrix  $W$  by solving eqn. (3.24) and partition into  $W_1$ ,  $W_2$ .
- 9biii. Compute the intermediate matrix  $F$  by solving eqn. 3.26
10. Then compute the hyperplane matrix  $C$  from eqn. (3.27)

The flow graphs of Figs. G.2 and G.3 further illustrate the coding sequence for the solution of the existence problem.

Similarly, following the equations developed in section 3.4, the procedure for computing the parameters of the unit vector control function may be outlined as follows

1. Read matrices  $A$ ,  $B$ ,  $A_{11}$ ,  $A_{12}$ ,  $A_{21}$ ,  $A_{22}$ ,  $F$  and  $C$
2. Compute  $M_2$  and  $M_2^{-1}$  using equations (3.31) and (3.32) respectively.
3. Compute  $\phi_1$ ,  $\phi_2$  and  $\phi_3$  as defined in eqn. (3.35)
4. Enter the pole(s) of  $\phi$  while at the same time testing for validity of any chosen pole (a valid pole must be negative)
5. Enter the design parameter  $\rho$
6. Solve the Lyapunov equation (eqn. 3.39) for the positive definite matrix  $P_n$ .

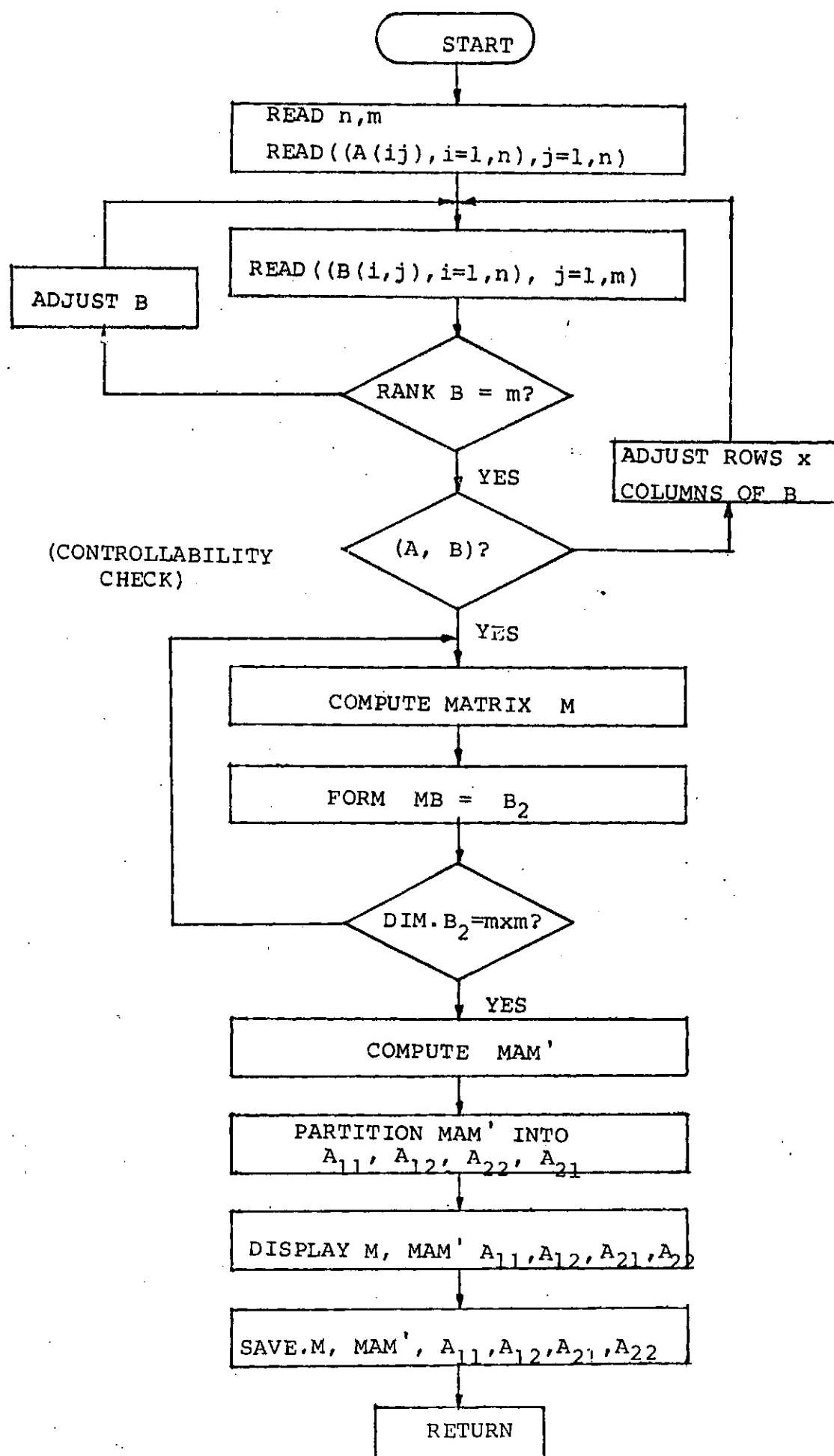


FIG.G2: FLOW CHART FOR CANONICAL TRANSFORMATION

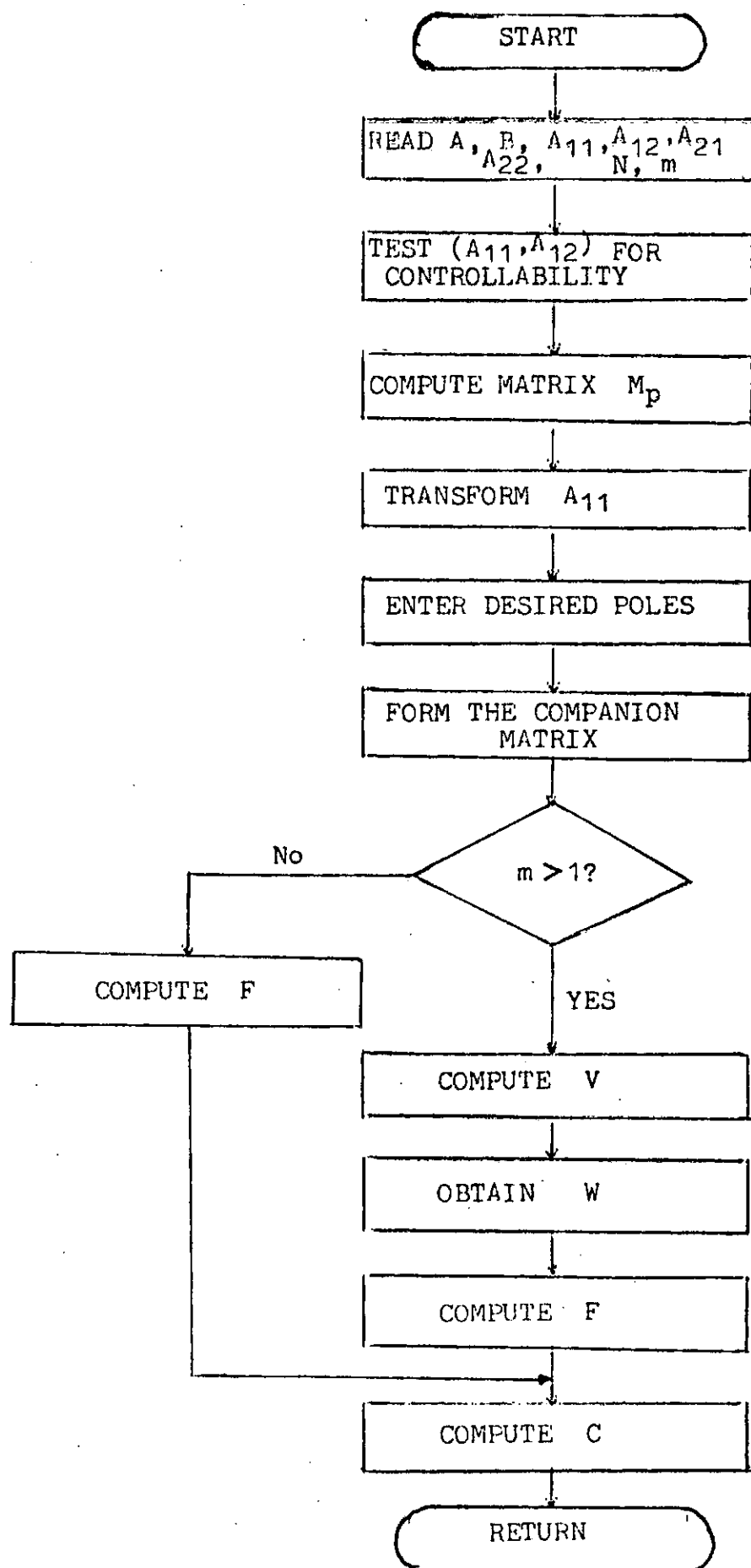


FIG. G.3 FLOW CHART FOR SOLVING THE EXISTENCE PROBLEM

7. Compute the coefficient 'L' of the linear control law using eqn. (3.38).
8. Compute coefficients G and H of the nonlinear control law using eqns. (3.42) and (3.43) respectively.

The flow graph of Fig.G.4 further illustrates the coding sequence.

The implementation of the simulation function follows the sequence outlined below:

1. Read matrices A, B, F, C, r, L, G, H and the system order N.
2. Enter the value of the change in load demand. (This value is in per unit of area capacity)
3. Enter the initial time (usually zero), the final time, the step size and the initial condition vector  $x(0)$
4. Solve for the nonlinearities present in the system. For instance eqn. (CXIII) is used for computing the water hammer effect while eqn. (DI) is used for dead-band effect.
5. Compute the variable structure unit vector control signal from eqn. (3.29)
6. Solve the state equation (a system of first order differential equations) eqn. (5.72) for the power system model of interest using the well known fourth order Runge-Kutta integration algorithm and determine the excursion of the system states as time goes from the initial to the final time.
7. Print and/or plot the results.

The flow graph of Fig.G.5 further elucidates the coding sequence of the simulation program.

Other modules implemented in VAGCD are either servicing or utilizing the three major functions described above. The flow charts for the implementation of the Input, Output and AGC Modules are respectively shown in figures G.6, G.7 and G.8

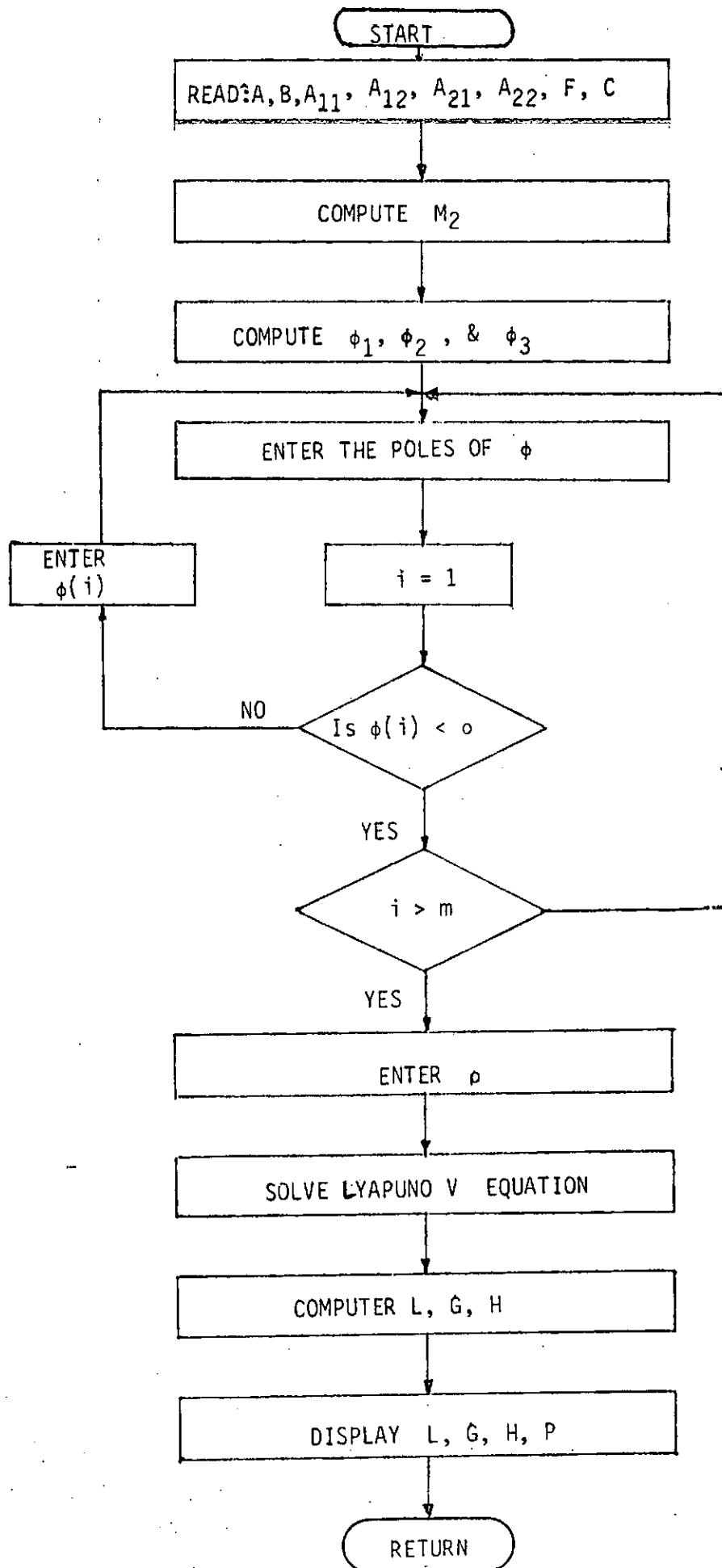


Fig. G.4: Flow Graph For Solving The Reachability Problem.

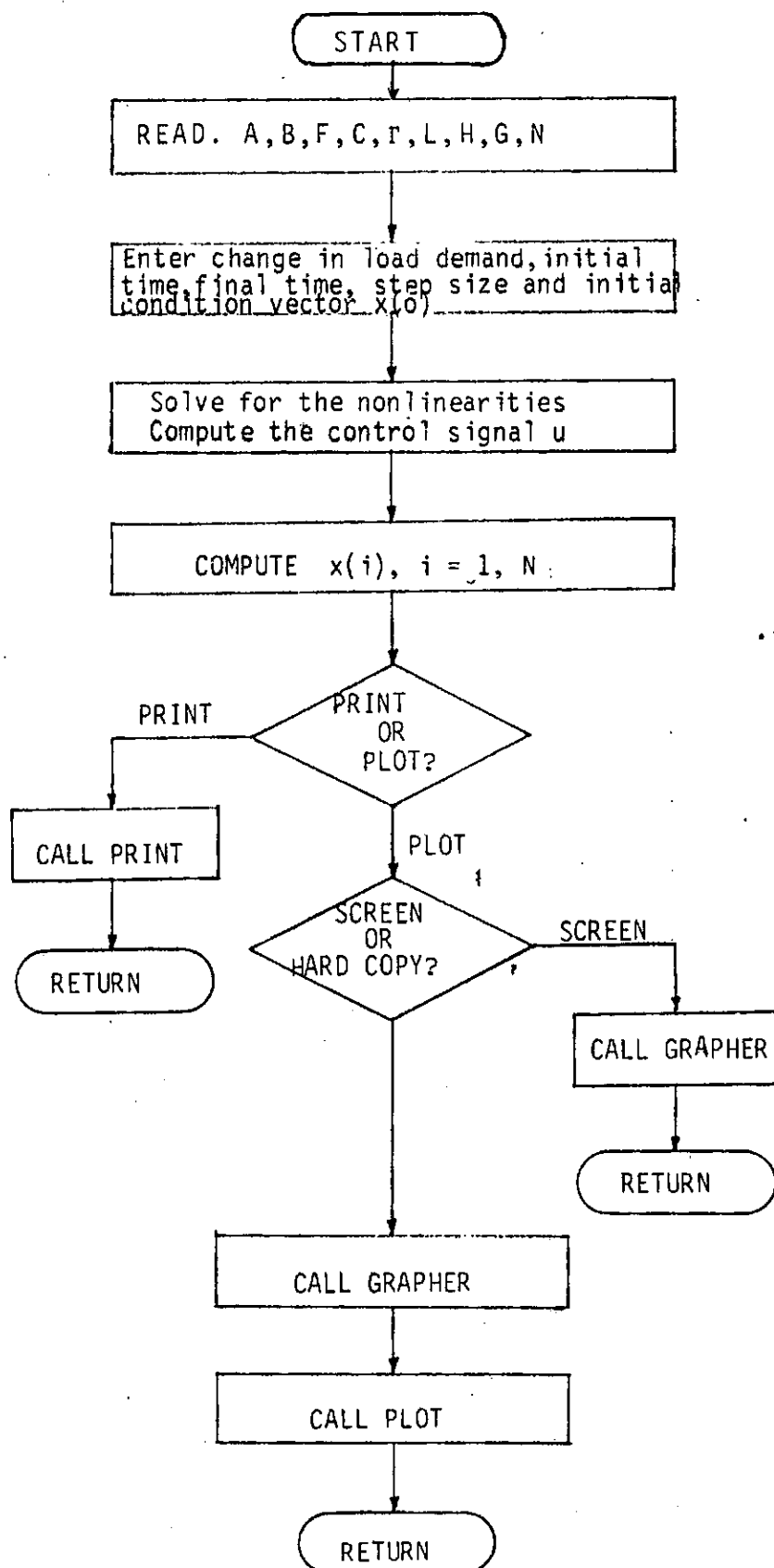


Fig. G.5 : Flow Chart For The Simulation Program.

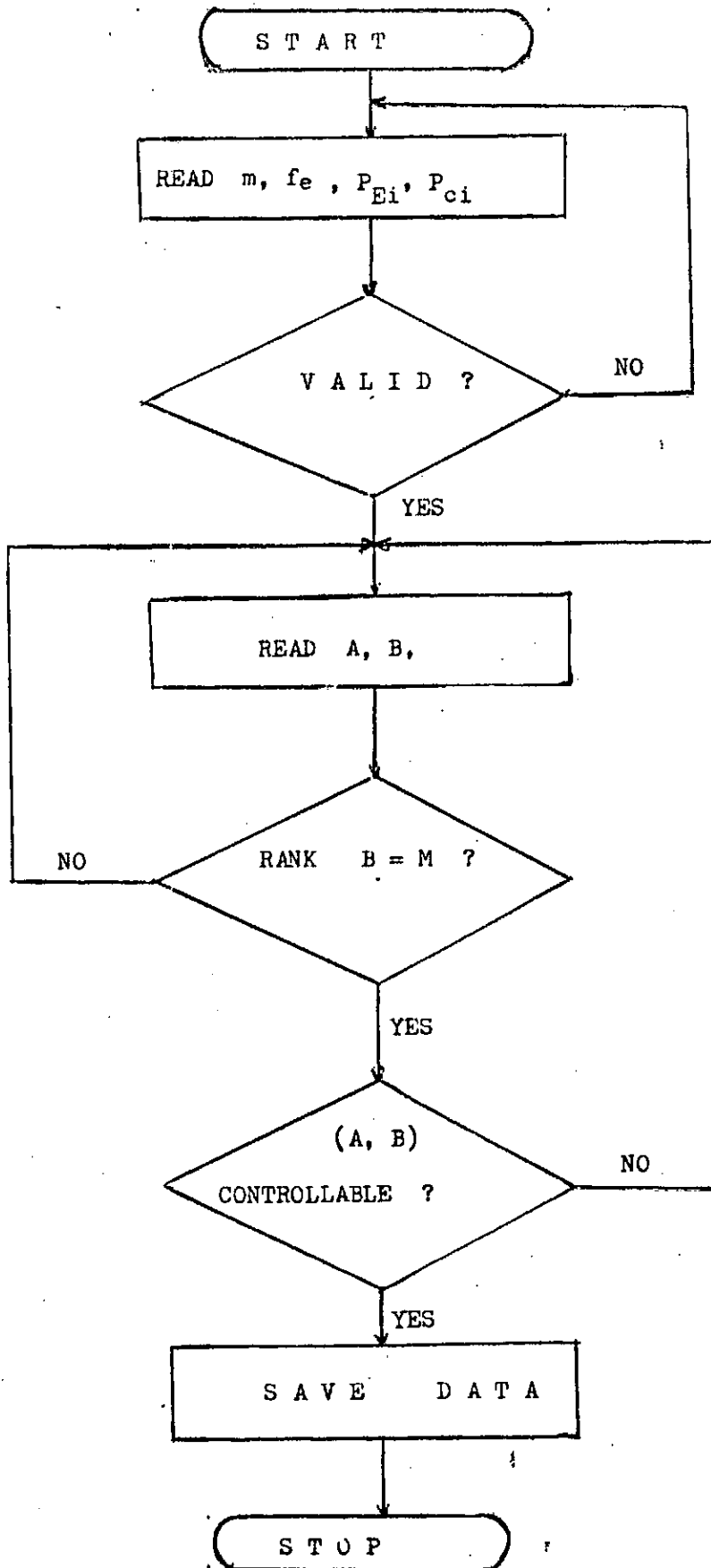


Fig. G.6 Flow Chart For The Input Module.



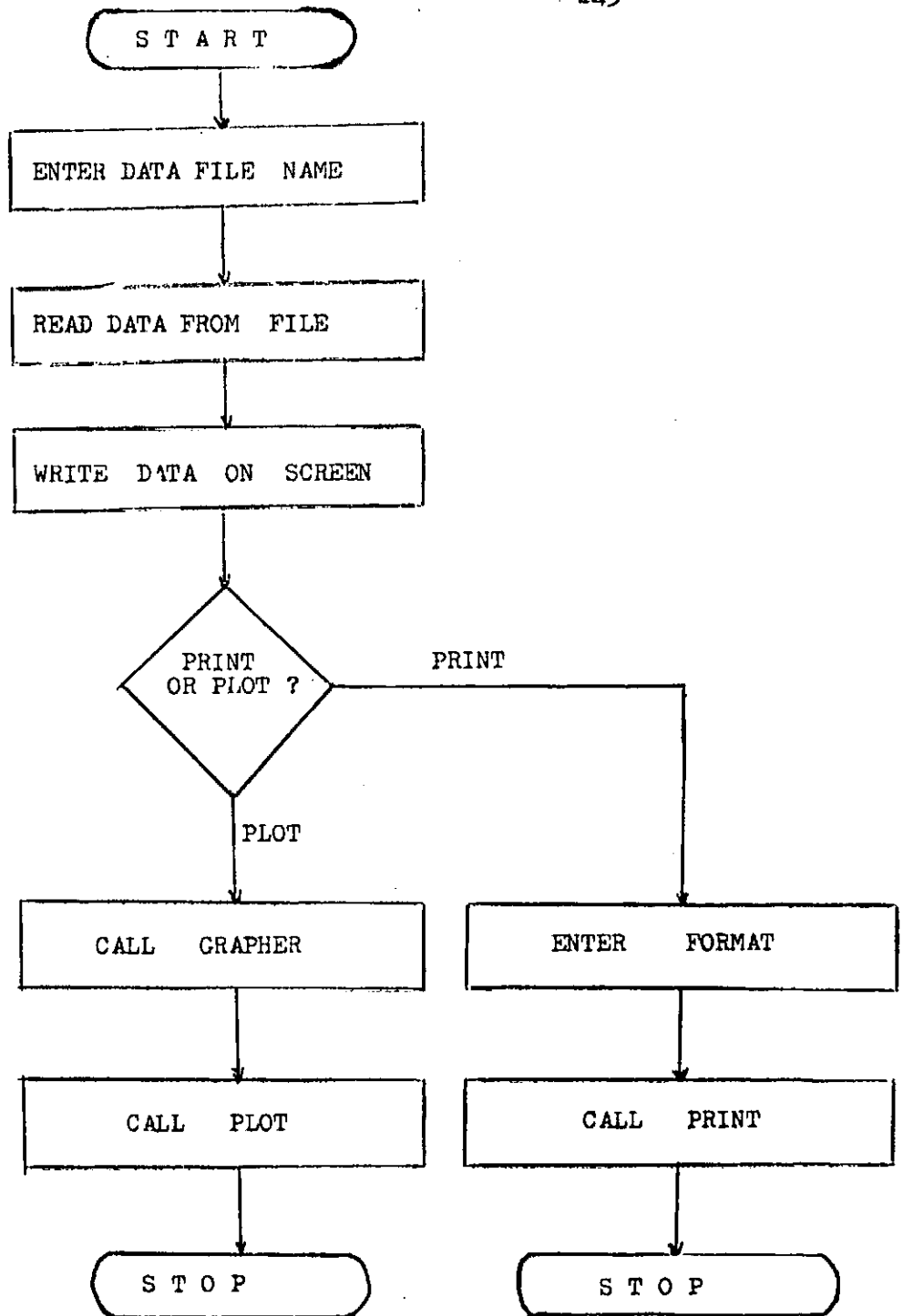


Fig. G.6 Flow Chart For Output Module.

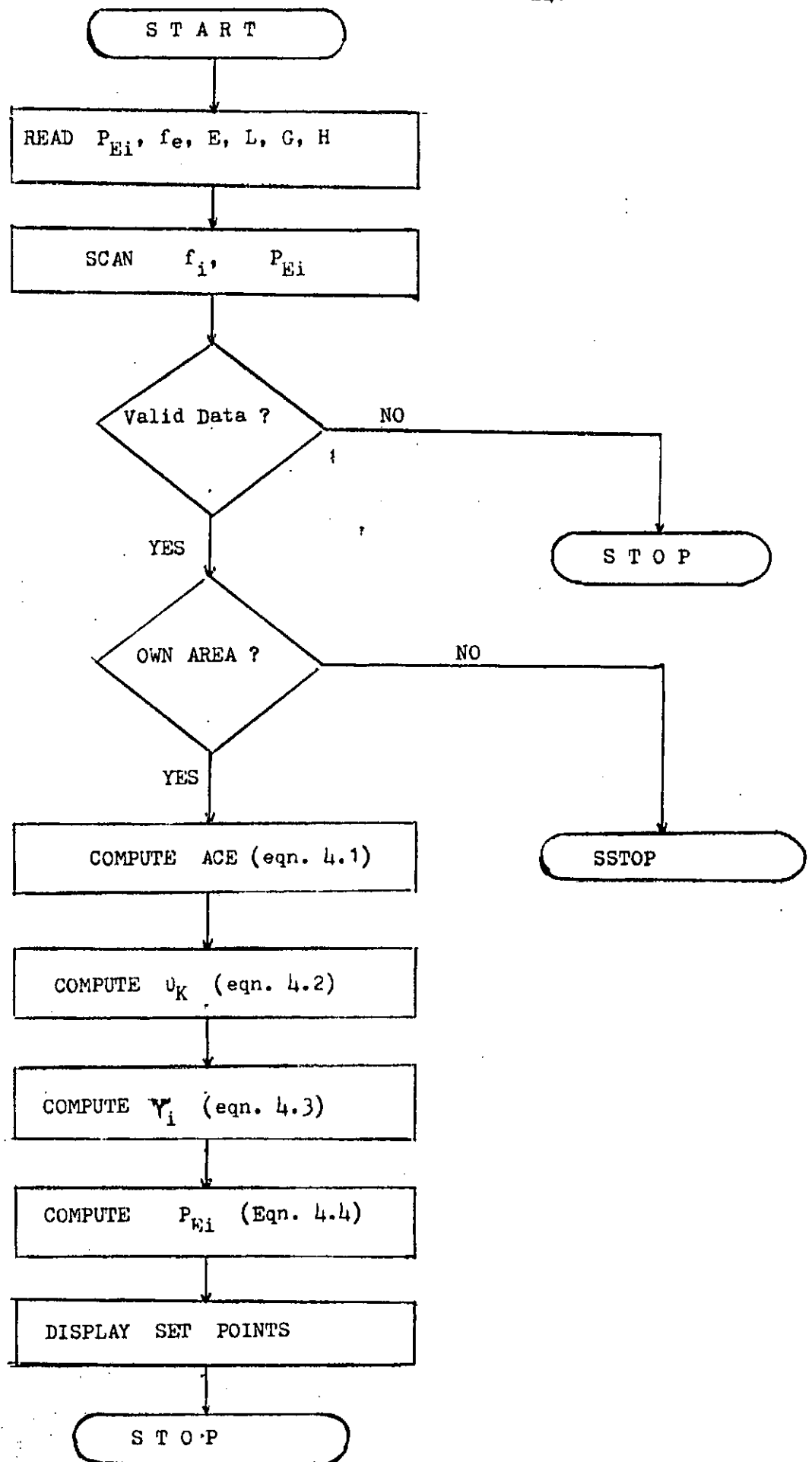


Fig. G.3 Flow Chart For The AGC Module.

```

/GRAPHER/FEEDBK.FOR DIMENSION B(5,5),R(5,5),T(5,5)B2(5,5),A(5,5)
DIMENSION B1(6),A12(5),AT(5,5),A11(5,5),C(5),B3(5,5)
DIMENSION A2(5,5)
CHARACTER FLAG1,FLAG2,FLAG3,FLAG4,FLAG5
OPEN(3, FILE = 'AB2.DAT')
OPEN(4, FILE = 'AFN2.DAT')
READ(3,'(2I1)') N,M
READ(3,'(5E10.3)') ((A(I,J),J=1,N),I=1,N)
READ(3,'(5E10.3)') (B1(I),I=1,N)
WRITE(*,'(A/)') ' MATRIX A'
WRITE(*,7) ((A(I,J),J=1,N),I=1,N)
WRITE(*,'(//A/)') ' MATRIX B TRANSPOSE '
WRITE(*,8) (B1(I),I=1,N)
7 FORMAT(3X,5E12.5)
8 FORMAT(3X,5E12.5)
WRITE(*,'(A)') 'TEST FOR CONTROLLABILITY?'
READ(5,'(A)') FLAG1
IF (FLAG1.EQ.'N') GO TO 567
CALL CONTRL(A,B1,A2,N)
WRITE(*,'(5E12.5)') ((A2(I,J),J = 1,N),I = 1,N)
PAUSE 'CONTROLLABILITY MATRIX'
567 WRITE(*,'(A)') ' TRANSFORMATION MATRIX AVAILABLE? Y/N '
2 READ(5,'(A)') FLAG3
IF(FLAG3.EQ.'N') GO TO 586
READ(3,'(5E10.3)') ((R(I,J),J = 1,N),I = 1,N)
WRITE(*,7) ((R(I,J),J = 1,N),I = 1,N)
GO TO 125
586 WRITE(*,'(A)') ' WANT TO USE ELEMENTARY MATRIX? Y OR N'
READ(5,'(A)') FLAG1
IF(FLAG1.EQ.'N') GO TO 111
CALL MENTARY(B1,R,N)
WRITE(*,'(A)') 'WISH TO CHANGE SOME VALUES?'
READ(5,'(A)') FLAG4
IF(FLAG4 .EQ. 'N') GO TO 125
124 WRITE(*,'(A)') 'ENTER THE VALUE OF I,J FOR R(I,J) ON 2I'
READ (5,'(2I1)') I,J
WRITE(*,'(A)') 'ENTER THE VALUE OF R(I,J) ON F10.3'
READ(5,'(F10.3)') YT
R(I,J) = YT
WRITE (*,'(A)') 'WANT TO CHANGE ANOTHER?'
READ (5,'(A)') FLAG5
IF(FLAG5.EQ.'Y') GO TO 124
GO TO 125
111 CALL ORTHO (B1,R,N)
C COMPUTE R INVERSE
125 CONTINUE
DO 1044 I = 1,N
DO 1044 J = 1,N
1044 T(I,J) = R(I,J)
CALL INVERT (T,N)
C FORM R X A X R-INVERSE
CALL PRODM (R,A,B2,N)
CALL PRODM (B2,T,B3,N)
N1 = N-M
DO 200 I = 1,N1
DO 200 J = 1,N1
200 A11(I,J) = B3(I,J)
DO 202 I = 1,N1
N2 = N1+1

```

```

4      AP = 0.
      AT = 0.
      DO 50 I = 1,N
      AT = AT + B(I,NN) * R(I,J)
50     AP = AP + R(I,J)*R(I,J)
      T(J,NN) = AT/AP
      NN = NN + 1
      IF(NN.LE.N) GO TO 45
C COMPUTE R(J) (COLUMN VECTORS)
      IC = J + 1
      DO 60 I=1,N
      AC = B(I,IC)
      DO 70 II = 1,J
      R(I,IC) = (R(I,IC) + AC - T(II,IC)*R(I,II))
70     AC = 0.
60     CONTINUE
40     CONTINUE
      WRITE(*, '(//,2X,A/)') 'MATRIX R'
      WRITE(*, '(5E10.3)') ((R(I,J),J=1,N),I=1,N)
      WRITE(*, '(A)') ' COLUMN CHANGE ,INPUT NCO,NDEST., ON 2I1 '
      READ(5, '(2I1)') NCO,ND1
      DO 401 JI = 1,N
      DY = R(JI,NCO)
      R(JI,NCO) = R(JI,ND1)
401    R(JI,ND1) = DY
C TRANSPOSE MATRIX R
      CALL INVERT (R,N)
c multiply R AND B MATRICES
      CALL PROD(R,B1,BT,N)
C IF BT IS NOT OF THE REQUIRED FORM,EXCHANGE ROWS OF R
      WRITE(*, '( ' DO YOU WANT TO EXCHANGE ROWS OF R? (Y/N) ' )')
      READ(5, '(A)') FLAG1
      IF(FLAG1.EQ.'N') GO TO 59
49     WRITE(*, '( ' INPUT THE ORIGINAL ROW ' )')
      READ(5, '(I2)') IG
      WRITE(*, '( ' INPUT DESTINATION ROW ' )')
      READ(5, '(I2)') ID
      DO 80 J=1,N
      GN = R(IG,J)
      R(IG,J) = R(ID,J)
80     R(ID,J) = GN
      WRITE(*, '( ' ( WANT TO REPEAT THE OPERATION? (Y/N) ' )')
      READ(5, '(A)') FLAG2
      IF(FLAG2 .EQ. 'Y') GO TO 49
C CHECK FOR ACCURACY
      WRITE (*, '(//A)') ' EXCHANGED R MATRIX '
      WRITE(*, '(//5E12.4)') ((R(I,J),J=1,N),I=1,N)
      CALL PROD(R,B1,BT,N)
59     RETURN
      END

SUBROUTINE TRANS (R,RT,N)
DIMENSION R(N,N), RT(5,5)
DO 10 I= 1,N
DO 10 J = 1,N
10    RT(J,I) = R(I,J)
      WRITE(*, '(//,2X,A/)') 'TRANSPPOSED MATRIX R'
      WRITE(*,7) ((R(I,J),J=1,N),I=1,N)
      FORMAT(/,4X,5E12.5)
      RETURN
      END

```

```

202  A12(I) = B3(I,N2)
      CALL LIRD (A11,A12,C1,N1)
      C1(N) = 1.
      DO 203 I = 1,N
      C(I) = 0.
      DO 203 J = 1,N
203  C(I) = C(I) + C1(J) * T(J,I)
      WRITE(*,'(5E12.5)') ((T(I,J),J = 1,N),I = 1,N)
      PAUSE 'INVERSE M MATRIX'
      WRITE(*,'(A)') ' ELEMENTS OF THE SLIDING PLANE VECTOR '
      WRITE(*,'(5E12.5)') (C(I),I = 1,N)
      WRITE(4,'(5E12.5)') (C(I),I = 1,N)
      STOP
      END

      SUBROUTINE MENTARY (B1,R,N)
      DIMENSION B1(6),R(5,5),BT(5)
      CHARACTER FLAG1,FLAG2
C FORM THE UNIT MATRIX
      DO 10 I = 1,N
      DO 10 J = 1,N
      R(I,J) = 0.
10    IF(I.EQ.J) R(I,J) = 1.
      WRITE(*,'(5E10.3)') ((R(I,J),J=1,N),I =1,N)
      CALL PROD(R,B1,BT,N)
      WRITE(*,'(A)') ' WANT TO EXCHANGE ROWS? Y/N '
      READ (5,'(A)') FLAG1
      IF(FLAG1.EQ.'N') GO TO 99
49    WRITE(*,'(A)') ' INPUT ROW NOS. TO BE EXCHANGED ON 2I1 '
      READ (5,'(2I1)') NI,ND
      DO 20 I =1,N
      GN = R(NI,I)
      R(NI,I) = R(ND,I)
20    R(ND,I) = GN
      WRITE(*,'(A)') ' WANT TO REPEAT THE OPERATION '
      READ(5,'(A)') FLAG2
      IF (FLAG2.EQ.'Y') GO TO 49
99    CALL PROD(R,B1,BT,N)
      WRITE(*,'(5E12.5)') ((R(I,J),J=1,N),I=1,N)
      RETURN
      END

      SUBROUTINE ORTHO (B1,R,N)
      DIMENSION B1(6),R(5,5),B(5,5),T(5,5),BT(5)
      CHARACTER FLAG1,FLAG2
      DO 5 I=1,N
      DO 5 J=1,N
      R(I,J) = 0.
      B(I,J)=0.
5      IF(I.EQ.J) B(I,J) = 1.
C COMPUTE R(1)
      DO 20 J=1,N
      R(J,1) = B1(J)
20    B(J,1) = B1(J)
      WRITE(*,'(A)') ' COMPOSITE B MATRIX***** '
      WRITE(*,'(5E12.3)') ((B(I,J),J = 1,N),I = 1,N)
C COMPUTE T(I,J)
      KT=N-1
      DO 40 J=1,KT
      NN=J+1
45    CONTINUE

```

```

SUBROUTINE LIRD (AP,BP,D,N)
DIMENSION AP(5,5),BP(5),AC(5,5),CMCP(5,5),CMCC(5,5),ALP(5,5)
DIMENSION D(5),BC(5),T(5,5),BK(5),POL(5,2),CCL(5,5),ML(5,5)
DIMENSION DIS(5)
REAL CCL,ML,DIS,LP
C READ(4,'(I2)') N
C READ(4,'(4E10.3)') ((AP(I,J),J=1,N),I=1,N)
C READ(4,'(4E10.3)') (BP(I),I=1,N)
C READ(4,'(4E10.3)') (DIS(I),I=1,N)
C READ(4,'(E10.3)') LP
WRITE(*,7)((AP(I,J),J=1,N),I=1,N)
WRITE(*,'(A)') 'MATRIX BP TRANSPOSE'
7 FORMAT(4X,4E10.3)
WRITE(*,7) (BP(I),I=1,N)
PAUSE 'MATRIX A11 AND BP'
WRITE(*,'(A)') ' TEST FOR CONTROLLABILITY ? ENTER FLAG = Y'
C FORM MCP
M1 = N+1
CALL CONTRL(AP,BP,CMCP,N)
WRITE(*,8) ((CMCP(I,J),J=1,N),I=1,N)
8 FORMAT(4X,4E10.3)
C PAUSE 'CMCP MATRIX,CHECK FOR CONTROLLABILITY'
CALL FADDEVA(AP,D,N,M1)
WRITE(*,'(//4E10.3)') (D(I),I = 1,M1)
PAUSE 'POLYM FROM FADDEVA'
NL1 = N-1
DO 10 I=1, NL1
DO 10 J=1, N
AC(I,J) = 0.
IK = I+1
10 IF(J .EQ. IK) AC(I,J) = 1.0
DO 33 J=1,N
ND = N - J + 2
33 AC(N,J) = -D(ND)
DO 20 I = 1, N
20 BC(I) = 0.
DO 123 I = 1,M1
123 D(I) = 1.
BC(N) = 1.
WRITE(*,'(//4E10.3)') ((AC(I,J),J=1,N),I = 1,N)
WRITE(*,'(//4E10.3)') (BC(I),I = 1,N)
PAUSE 'SYSTEM CLOSED LOOP MATRIX ABOVE'
CALL CONTRL(AC,BC,CMCC,N)
WRITE(*,'(A)') ' MCC MATRIX'
WRITE(*,7) ((CMCC(I,J),J=1,N),I=1,N)
PAUSE 'MCC MATRIX ABOVE'
C INVERT MCC
CALL INVERT (CMCC,N)
C COMPUTE T
CALL PRODM (CMCP,CMCC,T,N)
WRITE(*,'(//5E10.3)') ((T(I,J),J=1,N),I=1,N)
PAUSE 'MATRIX T'
C INVERT T
CALL INVERT(T,N)
WRITE(*,'(A)') ' T INVERSE'
WRITE(*,'(5E10.3)') ((T(I,J),J=1,N),I=1,N)
PAUSE 'T INVERSE'
C FORM THE CLOSED LOOP SYSTEM MATRIX
C READ THE DESIRED POLE LOCATION
WRITE(*,'(A)') ' INPUT DESIRED POLES ON 2E10.3 *****'
READ(5,'(2E10.3)') ((POL(I,J),J=1,2),I=1,N)

```

```

C   FORM QUADRATIC FACTOR FROM COMPLEX CONJUGATE POLE
      IF(POL(1,2) .EQ. 0.) GO TO 229
      D(3) = 1.
      D(2) = 2 * POL(1,1)
      D(1) = POL(1,1)**2 + POL(1,2)**2
      ND1 = 3
      IF(POL(3,2) .EQ. 0.) GO TO 25
      D(5) = 1
      D(4) = D(2) + POL(3,1)*2
      D(3) = D(1) + D(2) *POL(3,1)*2 + POL(3,1)**2 + POL(3,2)**2
      D(2) = D(2)*(POL(3,1)**2 + POL(3,2)**2) + D(1)*POL(3,1)*2
      D(1) = D(1)*(POL(3,1)**2 + POL(3,2)**2)
      ND1 = 5
      GO TO 25
229  D(3) = 1
      D(2) = POL(1,1) + POL(2,1)
      D(1) = POL(1,1)*POL(2,1)
      ND1 = 3
25   DO 40 I=ND1, N
      DO 50 J=1, ND1
      IN1 = ND1 - J + 1
      IF(IN1 .EQ. 1) GO TO 32
      D(IN1) = POL(ND1,1)*D(IN1) + D(IN1-1)
      GO TO 50
32   D(IN1) = POL(ND1,1)*D(IN1)
50   CONTINUE
      ND1 = ND1 + 1
      IF(ND1.GT.N) GO TO 400
40   CONTINUE
400  D(N+1) = 1.
      WRITE(*,'(//4E10.3)') (D(I), I = 1,M1)
      PAUSE 'POLYM COEFF'

C   FORM THE CLOSED LOOP A MATRIX
      DO 60 I=1, N-1
      DO 60 J=1, N
      ALP(I,J) = 0.
      KIK = I+1
60   IF(J .EQ. KIK) ALP(I,J)=1.
      DO 61 J=1,N
61   ALP(N,J) = -D(J)
      WRITE(*,'(A)') ' DESIRED CLOSED LOOP MATRIX'
      WRITE(*,'(//4E10.3)') ((ALP(I,J),J = 1,N),I = 1,N)
      PAUSE 'DESIRED CLOSED LOOP MATRIX'

C   COMPUTE THE FEEDBACK VECTOR K
      DO 70 I=1, N
70   BK(I) = AC(N,I) - ALP(N,I)
      WRITE(*,'(//4E10.3)') (BK(I),I = 1,N)
      DO 80 I=1, N
      D(I) = 0.
      DO 90 J=1, N
90   D(I) = D(I) + BK(J)*T(J,I)
80   CONTINUE
      WRITE(*,'(A)') ' ELEMENTS OF THE FEEDBACK VECTOR'
      WRITE(*,7) (D(I),I=1, N)
      PAUSE 'LEAVING LIRD'
      RETURN
      END

```

```

SUBROUTINE CONTRL (AT,BT,CMOC,N)
  DIMENSION AT(5,5),BT(5),CMOC(5,5),BOT(5),X(5,5)
  DIMENSION TAC(5,5),TBT(5,5)

```

```

CALL PROD(AT,BT,BOT,N)
DO 10 I=1, N
CMOC(I,1) = BT(I)
10 CMOC(I,2) = BOT(I)
DO 200 I = 1,N
DO 200 J=1,N
200 TBT(I,J) = AT(I,J)
I =3
213 CALL PRODM(AT,TBT,TAC,N)
WRITE(*,'(A)') ' TAC = AP SQUARED MATRIX '
WRITE (*,'(/SE10.3)') ((TAC(KI,J),J =1,N),KI = 1,N)
CALL PROD(TAC,BT,BOT,N)
DO 30 J=1, N
30 CMOC(J,1) = BOT(J)
DO 62 K=1,N
DO 62 J=1,N
62 TBT(K,J)= TAC(K,J)
I =I + 1
IF(I.LE.N) GO TO 213
RETURN
END

```

```

SUBROUTINE PROD (TN,BN,BOT,N)
DIMENSION TN(5,5),BN(5),BOT(5)
DO 20 I = 1,N
BOT(I) = 0.
DO 20 J = 1,N
20 BOT(I)= BOT(I) + TN(I,J) * BN(J)
RETURN
END

```

```

SUBROUTINE PRODM (AN,AM,TAC,N)
DIMENSION AN(5,5),AM(5,5),TAC(5,5)
WRITE (*,'(/SE10.3)') ((AM(I,J),J=1,N), I = 1,N)
DO 10 I= 1,N
DO 10 J =1,N
TAC(I,J) = 0.
DO 10 K = 1,N
10 TAC(I,J) = TAC(I,J) + AN(I,K)*AM(K,J)
WRITE(*,'(A)') ' TAC MATRIX INSIDE PRODM'
WRITE(*,'(/SE10.3)') ((TAC(I,J), J =1,N), I =1,N)
RETURN
END

```

```

SUBROUTINE INVERT(X,N)
DIMENSION A(5,5),X(5,5),C(5,10)
DATA EPS/1.0E-6/
WRITE(*,'(/SE10.3)') ((X(I,J),J =1,N),I =1,N)
C A = INPUT MATRIX, X = A-INVERSE, AND EPS IS THE TOLERANCE
N1 = 2*N
DO 10 I =1,N
DO 10 J = 1,N
10 C(I,J) = X(I,J)
DO 30 I =1,N
DO 30 J = 1,N
IF(I.EQ.J) GO TO 20
C(I,J+N) = 0.0
GO TO 30
20 C(I,J+N) = 1.0
30 CONTINUE
C

```



C INVERT MATRIX

```

C
DO 130 IP = 1,N
C FIND PIVOT ELEMENT IN COLUMN IP
IM = IP
IF(IP.GE.N) GO TO 50
IST = IP + 1
DO 40 I = IST,N
IF(ABS(C(IM,IP)).GE.ABS(C(I,IP))) GO TO 40
IM = I
40 CONTINUE
50 IF(ABS(C(IM,IP)).GE.EPS) GO TO 70
C NEAR ZERO DIAGONAL ELEMENT FLAG
WRITE(*,60) IP, C(IM,IP)
60 FORMAT(1H0,' DIAGONAL ELEMENT ',I2,'= ',1PE13.5)
IF(C(IM,IP).EQ.0.0) RETURN
70 IF(IM.EQ.IP) GO TO 90
C INTERCHANGING ROWS TO POSITION PIVOT ELEMENT
DO 80 J = IP,N1
CL = C(IP,J)
C(IP,J) = C(IM,J)
80 C(IM,J) = CL
C FIND MULTIPLICATION CONSTANT
90 CL = C(IP,IP)
C(IP,IP) = 1.0
DO 100 J = IST,N1
100 C(IP,J) = C(IP,J)/CL
C ZERO COLUMN OF PIVOT ELEMENT
DO 120 I = 1,N
IF(I.EQ.IP) GO TO 120
IP1 = IP + 1
CL = C(I,IP)
C(I,IP) = 0.
DO 110 J = IP1,N1
110 C(I,J) = C(I,J) - CL * C(IP,J)
120 CONTINUE
130 CONTINUE
M = N+1
DO 140 I = 1,N
DO 140 J = M,N1
K = J-N
140 X(I,K) = C(I,J)
WRITE(*,'(/SE10.3)') ((X(I,J),J = 1,N),I = 1,N)
RETURN
END

```

SUBROUTINE FADEVA (A1,D,N,M1)

```

C PROGRAM FOR INVERTING MATRICES A AND (SI-A) USING FADEVA,S
C METHOD.INPUT REAL ELEMENTS A(I,J) ROW WISE AND ORDER N.OUTPUT
C B MATRICES,A INVERSE AND CHARACTERISTIC EQUATION COEFFICIENTS D(M)
C IN DESCENDING ORDER. ORDER N MUST NOT BE MORE THAN 10.
C C: C MATRIX (TEMPORARY) AND CHECK MATRIX
C B: (N-1) B MATRICES ELEMENTS
C D: CHARACTERISTIC EQUATION COEFFICIENTS.
DIMENSION A1(5,5),D(5),B(5,5,5),C(5,5)
WRITE(*,'(/4E10.3)') ((A1(I,J),J = 1,N),I = 1,N)
PAUSE 'A MATRIX INSIDE FADEVA'
DO 10 I = 1,N
DO 10 J = 1,N
10 C(I,J) = A1(I,J)
D(1) = 1.0
DO 40 L = 1,N

```

```

      IT = L - 1
      M = L + 1
1C COMPUTE CHARACTERISTIC EQUATION COEFF. FROM TRACE
      D(M) = 0.
      DO 20 K = 1,N
20      D(M) = D(M) + C(K,K)
      D(M) = -D(M)/L
      IF(L.EQ.N) GO TO 50
C COMPUTE B(L) MATRICES FOR (SI-A) INVERSE
      DO 30 I = 1,N
      DO 30 J = 1,N
      B(I,J,L) = C(I,J)
30      IF(I.EQ.J) B(I,J,L) = C(I,J) + D(M)
C COMPUTE AB MATRIX
      DO 40 I = 1,N
      DO 40 J = 1,N
      C(I,J) = 0.0
      DO 40 IND = 1,N
40      C(I,J) = C(I,J) + A1(I,IND)*B(IND,J,L)
C COMPUTE A INVERSE
50      DO 60 I = 1,N
      DO 60 J = 1,N
60      C(I,J) = -C(I,J)/D(M)
      WRITE (*, '(//SE10.3)') (D(I), I = 1,M)
      PAUSE'D VECTOR INSIDE FADEVA'
      RETURN
      END

```

/GRAPHER/CONTROL.FORSC PROGRAM DESIGNS THE VSS CONTROLLER 'U' IN THE FORM  
C RELAYS WITH STATE DEPENDENTM GAINS.

```

      DIMENSION A(5,5),B(5),C(5),ALPHA(5),TEMP(5),ALPHAM(5)
      CHARACTER FLAG1,FLAG2,FLAG3,FLAG4
      OPEN(3,FILE = 'AB2.DAT')
      OPEN(2,FILE = 'AFN2.DAT')
      OPEN (9,FILE = 'CTR2.DAT')
      READ(3,'(I1)') N
      READ(3,'(5E10.3)') ((A(I,J),J = 1,N), I = 1,N)
      READ(3,'(5E10.3)') (B(I),I = 1,N)
      READ(2,'(5E12.5)') (C(I),I = 1,N)
      WRITE(*,'(5E12.5)') (C(I),I = 1,N)
      DO 10 I = 1,N
      TEMP(I) = 0.
      DO 10 J = 1,N
10    TEMP(I) = TEMP(I) + C(J) * A(J,I)
      PHA = 0.
      DO 20 I = 1,N
20    PHA = PHA + C(I)*B(I)
      DO 30 I = 1,N
30    ALPHA(I) = TEMP(I)/PHA
      PRINT '(/A,$)', 'MINIMUM ALPHA VALUES'
      WRITE(*,'(/5E10.3)') (ALPHA(I),I = 1,N)
      WRITE(*,'(A)') 'WISH TO MULTIPLY BY A FACTOR'
      READ(5,'(A)') FLAG1
      IF(FLAG1 .EQ. 'N') GO TO 45
      WRITE(*,'(A)') 'ENTER THE REAL NO. FACTOR'
      READ(5,'(E10.3)') FACTOR
      DO 40 I = 1,N
40    ALPHA(I) = ALPHA(I)*FACTOR
      GO TO 55
45    WRITE (*,'(A)') 'WISH TO CHANGE ALPHA VALUES'
      READ(5,'(A)') FLAG2
      IF (FLAG2 .EQ. 'N') GO TO 55
      WRITE(*,'(A)') 'ENTER THE VALUES OF ALPHA(I) ON (F10.3)'
      READ(5,'(E10.3)') (ALPHA(I),I = 1,N)
55    WRITE(*,'(A)') 'WISH TO ZERO SOME VALUES'
      READ(*,'(A)') FLAG3
      IF (FLAG3 .EQ. 'N') GO TO 65
70    PRINT '(A,$)', 'ENTER THE INTG. NO. (I) CORRESP. TO ALPHA(I)'
      READ(5,'(I1)') IK
      ALPHA(IK) = 0.
      WRITE(*,'(A)') 'WISH TO ZERO ANOTHER'
      READ(5,'(A)') FLAG4
      IF(FLAG4. EQ. 'Y') GO TO 70
65    WRITE(*,'(5E12.5)') (ALPHA(I), I= 1,N)
      WRITE(9,'(5E12.5)') (ALPHA(I),I = 1,N)
      END

```

```

/GRAPHER/RUNGA.FORC PROGRAM SOLVES THE STATE EQUATION USING FOURTH ORDER RUN
  DIMENSION A(5,5),AW(5,5),C(5),B(5),D(5),CB(5,5)
  DIMENSION CBIV(5,5),CT(5),UNIT(5,5),AT2(5,5)
  CHARACTER FLAG1,FLAG2
  OPEN (3,FILE = 'AB2.DAT')
  OPEN(4,FILE = 'AFN2.DAT')
  OPEN(8,FILE='RESULTS5.DAT')
  open(9,file='ctr2.dat',status='old')
  open(2,file='at2.dat',status='old')
  READ(3,'(2I1)') N,M
  READ(3,'(5E10.3)') ((A(I,J),J = 1,N),I = 1,N)
  READ(3,'(5E10.3)') (B(I),I=1,N)
  READ(3,'(5E10.3)') (D(I), I = 1,N)
  READ(4,'(5E12.5)') (C(I), I = 1,N)
  WRITE(*,'(5E10.3)') ((A(I,J),J= 1,N), I = 1,N)
  WRITE(*,'(5E10.3)') (B(I),I = 1,N)
C FORM UNIT MATRIX
  DO 10 I = 1,N
  DO 10 J = 1,N
  UNIT(I,J) = 0.
10 IF (I.EQ.J) UNIT(I,J) = 1.
  WRITE(*,'(5E10.3)') (D(I),I = 1,N)
  PRINT '(A,$) ', 'INPUT THE VALUE OF THE DISTURBANCE FUNCTION'
  READ(5,FMT='(E10.3)') DP
  DO 123 I = 1,N
123 D(I) = D(I) * DP
  WRITE(*,'(A)') ' INPUT THE VALUE OF UG FOR INT CONTROLLER'
  CALL RUNG (N,A,D,C,B)
999 STOP
  END
  SUBROUTINE RUNG(N,A,D,C,B)
C PROGRAM SOLVES THE STATE EQUATION
  DIMENSION XO(5),A(N,N),D(N),B(N),ALPHA(5),C(N)
  REAL H,TO,TF
  OPEN(7,FILE='AT2.DAT',status= 'old')
  OPEN(9,FILE='CTR2.DAT',STATUS='OLD')
  READ(9,'(5E12.5)') (ALPHA(I),I = 1,N)
  WRITE(*,'(A)') 'INPUT THE VALUE OF ALPHA ON F10.3'
  READ(5,'(F10.3)') (ALPHA(I),I=1,N)
  WRITE(*,'(5E12.5)') (ALPHA(I),I = 1,N)
  READ(2,'(3E10.3)') H,TO,TF
  WRITE(*,'(3E10.3)') H,TO,TF
  READ(2,'(5F10.5)') (XO(I),I = 1, N)
  WRITE(*,'(5F10.5)') (XO(I), I = 1, N)
  WRITE(*,'(5F10.5)') (D(I),I= 1,N)
  WRITE(*,'(5F10.5)') (C(I),I = 1,N)
  CALL RKAM(TO,XO,TF,H,N,A,D,C,B,ALPHA)
  RETURN
  END

  SUBROUTINE FUN(T,X,F,A,D,B,ALPHA,PSI,C,N)
  DIMENSION X(N),F(N),A(N,N),D(N),B(N),U(5),ALPHA(N),C(N)
  DIMENSION PSI(N)
  CALL CONTROL (T,F,X,A,ALPHA,PSI,C,B,U,N)
  DO 10 I = 1,N
  F(I) = 0.
  DO 20 L = 1,N
  F(I) = F(I) + (A(I,L) * X(L))
20

```

```

10      F(I) = F(I) + D(I) + U(I)
        RETURN
        END

```

```

        SUBROUTINE OUT(T,X,F,N)
        DIMENSION F(N),X(N)
        WRITE(*,'(6E10.3)') T,X(1),X(2),X(3),X(4),X(5)
        WRITE(*,'(6E12.5)') T,F(1),F(2),F(3),F(4),F(5)
        WRITE(8,'(E10.3,3X,E10.3,2X,E10.3,2X,E10.3,2X,E10.3,2X,E10.3)')
*      T,X(1),X(2),X(3),X(4),X(5)
        RETURN
        END

```

```

        SUBROUTINE RKAM(TO,XO,TF,H,N,A,D,C,B,ALPHA)
        DIMENSION XO(N),X(5),F(5),F3(5),F2(5),F1(5),A(N,N)
        DIMENSION FO(5),XK1(5),XK2(5),XK3(5),XK4(5),D(N)
        DIMENSION ALPHA(N),C(N),B(N),PSI(5)
        DO 56 I = 1,N
56      PSI(I) = ALPHA(I)
        IR = 0.
        T = TO
        DO 10 I = 1, N
10      X(I) = XO(I)
        CONTINUE
        CALL OUT (T,X,F,N)
        CALL FUN(T,X,F,A,D,B,ALPHA,PSI,C,N)
        DO 100 I = 1, N
100      F3(I) = F(I)
        CONTINUE
        DO 9 I = 1, N
9      XK1(I) = H*F(I)
201      CONTINUE
        T = TO + 0.5*H
        DO 202 I = 1, N
202      X(I) = XO(I) + 0.5*XK1(I)
        CONTINUE
        CALL FUN(T,X,F,A,D,B,ALPHA,PSI,C,N)
        DO 203 I = 1, N
203      XK2(I) = H*F(I)
        CONTINUE
        T = TO + 0.5*H
        DO 204 I = 1, N
204      X(I) = XO(I) + 0.5*XK2(I)
        CONTINUE
        CALL FUN(T,X,F,A,D,B,ALPHA,PSI,C,N)
        DO 205 I = 1, N
205      XK3(I) = H*F(I)
        CONTINUE
        T = TO + H
        DO 206 I = 1, N
206      X(I) = XO(I) + XK3(I)
        CONTINUE
        CALL FUN(T,X,F,A,D,B,ALPHA,PSI,C,N)
        DO 207 I = 1, N
207      XK4(I) = H*F(I)
        CONTINUE
        DO 208 I = 1, N
        RK = (XK1(I) + 2.*XK2(I) + 2.*XK3(I) + XK4(I))/6.
        X(I) = XO(I) + RK
        XO(I) = X(I)

```

```

208      CONTINUE
      TO = T
      CALL FUN(T,X,F,A,D,B,ALPHA,PSI,C,N)
      CALL OUT(T,X,F,N)
      CXDOT = 0.
      CDX = 0.
      DO 2008 I = 1,N
2008      CXDOT = CXDOT + C(I)* F(I)
      CDX = CDX + C(I) * X(I)
      PKD = CDX * CXDOT
      WRITE(*,'(2E12.5)') PKD,CDX
      IF(T-TF) 112,112,113
112      GO TO 9
113      RETURN
C      IR = IR + 1
C      IF(IR-2) 101,102,103
101      DO 1 I = 1, N
      F2(I) = F(I)
1      CONTINUE
      GO TO 9
102      DO 2 I = 1, N
      F1(I) = F(I)
2      CONTINUE
      GO TO 9
103      DO 3 I = 1, N
      FO(I) = F(I)
3      CONTINUE
300      T = T + H
      DO 301 I = 1, N
      AM = (55.*FO(I)-59.*F1(I)+37.*F2(I)-9.*F3(I))/24.
      X(I) = XO(I) + H*AM
301      CONTINUE
      CALL FUN(T,X,F,A,D,B,ALPHA,PSI,C,N)
      DO 302 I = 1, N
      AM = (9.*F(I)+19.*FO(I)-5.*F1(I)+F2(I))/24.
      X(I) = XO(I) + H*AM
      XO(I) = X(I)
302      CONTINUE
      CALL FUN(T,X,F,A,D,B,ALPHA,PSI,C,N)
      CALL OUT(T,X,F,N)
      IF(T-TF) 401,401,501
401      DO 402 I = 1, N
      F3(I) = F2(I)
      F2(I) = F1(I)
      F1(I) = FO(I)
      FO(I) = F(I)
402      CONTINUE
      GO TO 300
501      RETURN
      END

      SUBROUTINE CONTROL(T,F,X,A,ALPHA,PSI,C,B,U,N)
      DIMENSION C(N),U(N),ALPHA(N),X(N),CK(5),PSI(N),B(N),F(N)
      DIMENSION CJ(5),A(N,N)
      UJ = 0.
      RKT = 0.
      DO 10 I = 1,N
10      RKT = RKT +C(I)*X(I)
      DO 20 I = 1,N
20      CK(I) = X(I) * RKT
      DO 35 I =1,N
      CJ(I) = 0.

```

```

DO 35 J = 1,N
35 CJ(I) = CJ(I) + C(J) * A(J,I)
DO 36 I = 1,N
36 UJ = UJ + C(I) * B(I)
DO 30 I = 1,N
IF(CK(I).GT.0.10E-04) PSI(I) = ALPHA(I)
C BETA EQUALS NEGATIVE OF ALPHA
30 IF(CK(I).LT. -.10E-04) PSI(I) = -ALPHA(I)
C WRITE(*,71) (CK(I),I = 1,N)
71 FORMAT(/3(2X,E10.3))
C WRITE (9,71) T,PSI(1),PSI(3)
UK = 0.
DO 45 I =1,N
45 UK = UK -(PSI(I) * X(I))
DO 40 I = 1,N
40 U(I) = (B(I) * UK)
C WRITE(*,'(A,3E12.5)') ' ' U = ',T,U(2),U(5)
RETURN
END

```